

ISSN 1854-6250

APEM
journal

Advances in Production Engineering & Management

Volume 12 | Number 4 | December 2017



University of Maribor

Published by PEI
apem-journal.org

Advances in Production Engineering & Management

Identification Statement

	ISSN 1854-6250 Abbreviated key title: Adv produc engineer manag Start year: 2006 ISSN 1855-6531 (on-line)
	Published quarterly by Production Engineering Institute (PEI), University of Maribor Smetanova ulica 17, SI – 2000 Maribor, Slovenia, European Union (EU) Phone: 00386 2 2207522, Fax: 00386 2 2207990 Language of text: English APEM homepage: apem-journal.org University homepage: www.um.si

APEM Editorial

Editor-in-Chief

Miran Brezocnik

editor@apem-journal.org, info@apem-journal.org
University of Maribor, Faculty of Mechanical Engineering
Smetanova ulica 17, SI – 2000 Maribor, Slovenia, EU

Desk Editor

Tomaz Irgolic

desk1@apem-journal.org

Martina Meh

desk2@apem-journal.org

Website Technical Editor

Lucija Brezocnik

lucija.brezocnik@um.si

Editorial Board Members

Eberhard Abele, Technical University of Darmstadt, Germany
Bojan Acko, University of Maribor, Slovenia
Joze Balic, University of Maribor, Slovenia
Agostino Bruzzone, University of Genoa, Italy
Borut Buchmeister, University of Maribor, Slovenia
Ludwig Cardon, Ghent University, Belgium
Nirupam Chakraborti, Indian Institute of Technology, Kharagpur, India
Edward Chlebus, Wroclaw University of Technology, Poland
Franci Cus, University of Maribor, Slovenia
Igor Drstvensek, University of Maribor, Slovenia
Illes Dudas, University of Miskolc, Hungary
Mirko Ficko, University of Maribor, Slovenia
Vlatka Hlupic, University of Westminster, UK
David Hui, University of New Orleans, USA
Pramod K. Jain, Indian Institute of Technology Roorkee, India

Isak Karabegović, University of Bihać, Bosnia and Herzegovina
Janez Kopac, University of Ljubljana, Slovenia
Lanndon A. Ocampo, University of the Philippines Cebu, Philippines
Iztok Palcic, University of Maribor, Slovenia
Krsto Pandza, University of Leeds, UK
Andrej Polajnar, University of Maribor, Slovenia
Antonio Pouzada, University of Minho, Portugal
Rajiv Kumar Sharma, National Institute of Technology, India
Katica Simunovic, J. J. Strossmayer University of Osijek, Croatia
Daizhong Su, Nottingham Trent University, UK
Soemon Takakuwa, Nagoya University, Japan
Nikos Tsourveloudis, Technical University of Crete, Greece
Tomo Udiljak, University of Zagreb, Croatia
Ivica Veza, University of Split, Croatia

Limited Permission to Photocopy: Permission is granted to photocopy portions of this publication for personal use and for the use of clients and students as allowed by national copyright laws. This permission does not extend to other types of reproduction nor to copying for incorporation into commercial advertising or any other profit-making purpose.

Subscription Rate: 120 EUR for 4 issues (worldwide postage included); 30 EUR for single copies (plus 10 EUR for postage); for details about payment please contact: info@apem-journal.org

Cover and interior design: Miran Brezocnik

Printed: Tiskarna Koštomaj, Celje, Slovenia

Subsidizer: The journal is subsidized by Slovenian Research Agency

Statements and opinions expressed in the articles and communications are those of the individual contributors and not necessarily those of the editors or the publisher. No responsibility is accepted for the accuracy of information contained in the text, illustrations or advertisements. Production Engineering Institute assumes no responsibility or liability for any damage or injury to persons or property arising from the use of any materials, instructions, methods or ideas contained herein.

Copyright © 2017 PEI, University of Maribor. All rights reserved.

Advances in Production Engineering & Management is indexed and abstracted in the **WEB OF SCIENCE** (maintained by **Clarivate Analytics**): **Science Citation Index Expanded**, **Journal Citation Reports** – Science Edition, **Current Contents** – Engineering, Computing and Technology • **Scopus** (maintained by **Elsevier**) • **Inspec** • **EBSCO**: Academic Search Alumni Edition, Academic Search Complete, Academic Search Elite, Academic Search Premier, Engineering Source, Sales & Marketing Source, TOC Premier • **ProQuest**: CSA Engineering Research Database – Cambridge Scientific Abstracts, Materials Business File, Materials Research Database, Mechanical & Transportation Engineering Abstracts, ProQuest SciTech Collection • **TEMA (DOMA)** • The journal is listed in **Ulrich's** Periodicals Directory and **Cabell's** Directory



University of Maribor
Production Engineering Institute (PEI)

Advances in Production Engineering & Management

Volume 12 | Number 4 | December 2017 | pp 301–424

Contents

Scope and topics	304
A general approach to optimize disassembly sequence planning based on disassembly network: A case study from automotive industry Yu, B.; Wu, E.; Chen, C.; Yang, Y.; Yao, B.Z.; Lin, Q.	305
An integrated generalized discriminant analysis method and chemical reaction support vector machine model (GDA-CRSVM) for bearing fault diagnosis Nguyen, V.H.; Cheng, J.S.; Thai, V.T.	321
Improving workforce scheduling using artificial neural networks model Simeunović, N.; Kamenko, I.; Bugarski, V.; Jovanović, M.; Lalić, B.	337
Infrared temperature measurement and increasing infrared measurement accuracy in the context of machining process Masoudi, S.; Gholami, M.A.; Janghorban Iariche, M.; Vafadar, A.	353
Container assignment optimization considering overlapping amount and operation distance in rail-road transshipment terminal Wang, L.; Zhu, X.; Xie, Z.	363
Work sampling for the production development: A case study of a supplier in European automotive industry Martinec, T.; Škec, S.; Savšek, T.; Perišić, M.M.	375
An overview and evaluation of quality-improvement methods from the manufacturing and supply-chain perspective Radej, B.; Drnovšek, J.; Begeš, G.	388
Vehicle routing optimization with multiple fuzzy time windows based on improved wolf pack algorithm Cao, Q.K.; Yang, K.W.; Ren, X.Y.	401
Laser drilling of alumina ceramics using solid state Nd:YAG laser and QCW fiber laser: Effect of process parameters on the hole geometry Rihakova, L.; Chmelickova, H.	412
Calendar of events	421
Notes for contributors	423

Journal homepage: apem-journal.org

ISSN 1854-6250 (print)
ISSN 1855-6531 (on-line)

©2017 PEI, University of Maribor. All rights reserved.

Scope and topics

Advances in Production Engineering & Management (APEM journal) is an interdisciplinary refereed international academic journal published quarterly by the *Production Engineering Institute* at the *University of Maribor*. The main goal of the *APEM journal* is to present original, high quality, theoretical and application-oriented research developments in all areas of production engineering and production management to a broad audience of academics and practitioners. In order to bridge the gap between theory and practice, applications based on advanced theory and case studies are particularly welcome. For theoretical papers, their originality and research contributions are the main factors in the evaluation process. General approaches, formalisms, algorithms or techniques should be illustrated with significant applications that demonstrate their applicability to real-world problems. Although the *APEM journal* main goal is to publish original research papers, review articles and professional papers are occasionally published.

Fields of interest include, but are not limited to:

Additive Manufacturing Processes	Machine Learning in Production
Advanced Production Technologies	Machine Tools
Artificial Intelligence in Production	Machining Systems
Assembly Systems	Manufacturing Systems
Automation	Materials Science, Multidisciplinary
Big Data in Production	Mechanical Engineering
Computer-Integrated Manufacturing	Mechatronics
Cutting and Forming Processes	Metrology in Production
Decision Support Systems	Modelling and Simulation
Discrete Systems and Methodology	Numerical Techniques
e-Manufacturing	Operations Research
Evolutionary Computation in Production	Operations Planning, Scheduling and Control
Fuzzy Systems	Optimisation Techniques
Human Factor Engineering, Ergonomics	Project Management
Industrial Engineering	Quality Management
Industrial Processes	Risk and Uncertainty
Industrial Robotics	Self-Organizing Systems
Intelligent Manufacturing Systems	Statistical Methods
Joining Processes	Supply Chain Management
Knowledge Management	Virtual Reality in Production
Logistics in Production	

A general approach to optimize disassembly sequence planning based on disassembly network: A case study from automotive industry

Yu, B.^a, Wu, E.^a, Chen, C.^b, Yang, Y.^c, Yao, B.Z.^{b,*}, Lin, Q.^{a,*}

^aSchool of Transportation Science and Engineering, Beihang University, Beijing, P.R. China

^bAutomotive Engineering College, Dalian University of Technology, Dalian, P.R. China

^cTransportation Management College, Dalian Maritime University, Dalian, P.R. China

ABSTRACT

Disassembly sequences is a key element of products recycling or remanufacturing, and related with the recycling quality or maintenance cost. In order to improve the performance of the disassembly operation, this paper analyzes the disassembly information on automobile parts and draws the disassembly network graph by using evolution rules of the AND/OR graph. Then a disassembly model of automobile parts is established. Considering the mapping between the Floyd-Warshall algorithm and the automobile disassembly mode, we obtain the optimal disassembly sequence by solving the weighted disassembly model. Finally, a case study on automotive silicone oil fan clutch is given to illustrate the procedure. This approach could be used to obtain optimum disassembly routes of products containing complex AND/OR hierarchical relationships.

© 2017 PEI, University of Maribor. All rights reserved.

ARTICLE INFO

Keywords:

Automotive industry
Automotive parts
Disassembly sequence
Disassembly model
Disassembly network
Floyd-Warshall algorithm

*Corresponding author:

linqf@buaa.edu.cn
(Lin, Q.)
yaobaozhen@dlut.edu.cn
(Yao, B.Z.)

Article history:

Received 17 January 2017
Revised 21 July 2017
Accepted 19 September 2017

1. Introduction

Manufacturing industry has become a leading industry during the economy development, while manufacturing industry produces large amounts of waste, which causes heavy environment pollution [1]. In addition, improper use of industrial waste products (e.g. burying) aggravates the environment. The production of vehicles, as a mass consumer good, increases year by year, so does the number of scrapped cars. In one car, more than 70 % of the parts are made of metal, which belongs to renewable resources. If no appropriate action is taken for resource re-use, there will be a huge waste for the society. China and the European Union have introduced relevant laws and regulations which stipulate that the car manufacturers must recycle its own branded products. As the first step of automobiles recycling, how to determine the effective disassembly sequence has become one of the hot spots in the field of automobiles recycling.

The automobile disassembly sequence planning problem studies how to determine the optimal sequence based on assembly relations between different parts and techniques of process. A good disassembly sequence can reduce the time and cost of disassembly, which also improves the efficiency of disassembly and the recycling rate of waste products. For a long time, due to the

low level of technology for disassembly and recycling, the disassembly of automobile products are still mainly manual disassembly, which depends on the demolition skills of workers. Workers could find optimal disassembly sequence with their own experience when the size of disassembly is small. However, under the situation of the large disassembly size, finding an efficient disassembly sequence will become more difficult by only human experience. Thus finding an effective method for the disassembly sequence of the automobile product to make a reasonable planning will improve the efficiency of disassembly and the reuse rate of the product.

Two main steps are comprised in specifying the best disassembly sequence: (1) generating a set of feasible disassembly sequences, and (2) finding the most efficient sequence among these feasible solutions [2, 3]. Lambert conducted a brief survey on disassembly sequence planning problem [4]. In their paper, many solution methods have been introduced, including empirical methods, graphical methods, fuzzy method, e.g. simulated annealing [5], search algorithms and mathematical programming, e.g. linear programming [6], mixed integer programming.

The graph-based models, used to represent various disassembly sequences, includes undirected graphs, digraphs, AND/OR graphs, Petri nets, and so on [7-14]. In addition, most of researchers have concentrated on the second step that is to find the best disassembly sequence. Moore *et al.* discuss a Petri net-based method to generate disassembly process plans automatically for product with AND/OR disassembly precedence relationships [7]. De Mello and Sander-so solve the assembly problem using AND/OR graph theory [8]. But at the same time the disassembly operation is regarded as the inverse process of assembly. Zhang and Kuo and Zhang *et al.* use undirected graph theory to generate the model, while the depth and breadth is used for search algorithm to optimize the product disassembly sequence [9, 10]. Tiwari *et al.* use Petri net and cost evaluation parameters to study the disassembly sequence planning problem [11]. Zussman and Zhou use Petri net theory for product disassembly modelling, then apply adaptive algorithm to solve the model, and finally achieve the planning and optimization of product disassembly sequence [12]; Tang *et al.* further consider the disassembly uncertainty characteristic on the basis of the Petri net, and analyse the average time of the disassembly process [13].

Many heuristic algorithms have been applied in solving disassembly sequence planning problem, and achieved certain results. Li *et al.*, Kongar and Gupta set the remove time shortest and the times of disassembly direction changes least as the goal, and research the optimal disassembly sequence using the genetic algorithm [5, 15]. Adenso-Díaz *et al.* set the disassembly cost as the evaluation index, using a greedy randomized adaptive search algorithm to research the optimal disassembly sequence. At the same time, the paper also combines the path connection method in heuristic algorithms and the greedy random adaptive search algorithm, which obtains the optimization of the disassembly sequence with the double sides [16]. Failli and McGovern and Gupta Dini apply the ant colony algorithm to the disassembly sequence planning problems, and the disassembly sequence is optimized [17, 18]. Lye *et al.* establish a hierarchical product network that comprise different costs incurred during disassembly, and the multiple service action (MSA) algorithm then determines the minimum servicing cost based on Floyd's algorithm, a shortest path algorithm [19]. In addition, González and Adenso-Díaz apply the distributed search algorithm to the product disassembly sequence planning with a sequence dependent cost [20].

The purposes of disassembly are different. Some are for the maintenance or upgrade of the target component, and some are for recycling end-of-life products. As a result, there are three types of disassembly: complete, incomplete, and selective disassembly. Complete disassembly is a process that all subassemblies in a product are separated from each other, which is usually uneconomic. The incomplete disassembly, in which only part units are disassembled, aims to determine the appropriate disassembly level. According to Kang and Xirouchakis, most disassembly planning research has been concentrated on end-of-life products, which is incomplete disassembly planning. In the disassembly planning problem, part of the literatures works on the incomplete disassembly planning of abandoned products [21]. Behdad *et al.* study the incomplete disassembly planning, which applies mathematical model to obtain the optimal sequence of disassembly [22]. The purpose is to recycle the value of waste products. In contrast to incomplete disassembly, selective disassembly is for the purpose of maintenance or upgrade. It disassembles a determined component, which means that the target component is known. Srinivasan

and Gadh and Srinivasan *et al.* use wave propagation method to analyse and optimize the selective disassembly sequence [23, 24]. Since the set of products or components which needs to be disassembled has a topological structure, the selective disassembly sequence planning can be studied by using the wave level relation. Kara *et al.* propose a model for the selective disassembly sequence of the parts with a certain value for reusing, which can be used to reduce the disassembly time [25]. Chung and Peng point out that the wave propagation method can solve the selective disassembly sequence, but it can only solve products with a topological structure, ignoring the possibility of batch disassembly [26].

In this paper, based on the information of automobile parts, a reasonable product disassembly model is proposed using the network graph, which is used to express the relationship between the units [27-30]. This paper will transform the optimal disassembly sequence problem into the shortest path problem, aiming at planning and solving complete disassembly sequences, target (selective) disassembly sequences and economic optimal disassembly sequences (incomplete disassembly planning) combining with the Floyd-Warshall algorithm. The results show the validity of the model and algorithm.

The remaining of the paper is as follows: Section 2 proposes the disassembly sequence planning model on the basis of AND/OR graph. Section 3 combines the Floyd-Warshall algorithm with the disassembly sequence planning problem. In section 4, we analyse the disassembly sequence planning problem of the automotive silicone oil fan clutch, and test the proposed approach on silicone oil fan clutch disassembly network. Section 5 summaries the research of this paper, and the future research direction is pointed out.

2. Problem formulation

In the disassembly planning problem of automobile parts, the sequence is composed of four parts: the extraction of disassembly information, the establishment of the disassembly model, the generation of disassembly sequence, the evaluation and optimization of disassembly sequence. At present, the method based on graph theory is one of the methods for the generation and optimization of disassembly sequence [14, 31]. In the disassembly information model of the automobile parts, the parts in the process of disassembly are represented by a node, and the side is used to represent a disassembly operation. Through the processing and calculation of the graph, the corresponding disassembly sequence scheme is obtained. AND/OR graph has special advantages. In this section, we will introduce the extraction of disassembly information and the establishment of the model, respectively.

2.1 Disassembly network model

Disassembly network based on the AND/OR graph

In this paper, a disassembly model based on AND/OR graph is established. The node in the network represents the state of the parts in the disassembly process, and the side represents the operation process. And the main ideas of AND/OR graph is as follows:

In Fig. 1, assuming that "A" is the original problem, this problem can be decomposed into three sub problems: "A1", "A2", and "A3". If "A1, A2, A3" three sub problems can all be solved, then the original problem "A" can be solved too, which means "and relationship" exists between the three sub problems "A1, A2, A3". Node "A" is called "and node". As shown in Fig. 1(a), the tree constituted by "A, A1, A2, and A3" is called as "and tree". In the graph, to represent "And nodes", we use an arc to connect each edge which connects the AND node and its sub nodes. If there exist one solution between "A1, A2, A3", the original problem "A" is solvable, which is called an "or relationship" between the three sub problems "A1, A2, A3". Node "A" is called "or node". As shown in Fig. 1(b), the tree constituted by "A, A1, A2 and A3" is called as "or tree". If the above two trees are combined, the graph is called AND/OR graph. AND/OR graph contains and nodes and or nodes, as shown in Fig. 1(c).

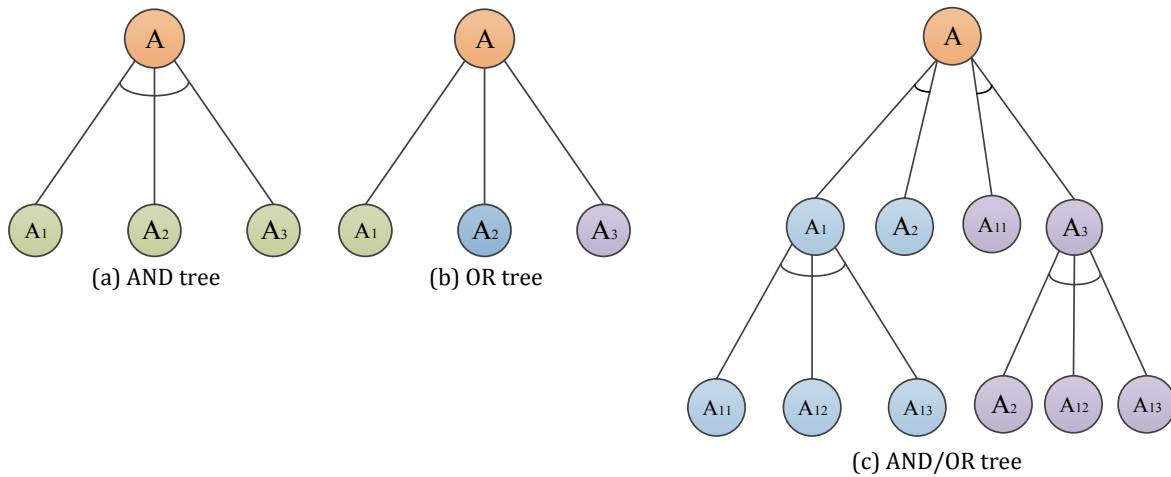


Fig.1 Graphical representation of the AND/OR tree

When using AND/OR graph to describe the disassembly sequence of the automobile product, node “A” represents the product, “A1, A2, A3, A11, A12 and A13” represent feasible subassemblies, and the edge indicates feasible disassembly operation. The process from the top node “A” to the bottom represents a product disassembly process. There are two ways for disassembling “A” product. In the first one we can disassemble “A” into “A1” and “A2”, then disassemble “A1” into “A11, A12 and A13”. In the other one “A” is first disassembled into “A3 and A11”, then “A3” is disassembled into “A2, A12 and A13”.

While the AND/OR graph cannot develop into the disassembly network directly. But we can design reasonable evolution rules to obtain the network diagram from the disassembly AND/OR graph. The corresponding evolution rules are defined as follows:

Rule 1: The establishment disassembly network is different from the top-down approach of AND/OR graph. It searches the entire possible disassembly paths from the bottom of the AND/OR graph to the top.

Rule 2: In a bottom-to-up search process, we store all the parts in the *and tree* at a node. If there is a relationship between all parts of an *and tree*, then find all possible disassembly ways. If there is no relationship between all parts of an *and tree*, set each part as an independent node. Connect all nodes with short lines without a specific order.

Rule 3: If there are more than one disassembly ways for a node in the graph. This node will be converted into different disassembly paths in the search progress.

In Rule 2, we connect the parts with short lines, but there is no disassembly relationship between parts. This paper simplifies the disassembly network graph based on the AND/OR graph. The simplified rules are as follows:

Rule 4: Delete all the individual parts of the transition graph, and reserve the part nodes, and connect them with short lines.

Rule 5: Define the node of part set. Connect the set of parts which can be disassembled into parts by one disassembly operation and the nodes of set of parts. The disassembly network will finally go into one node, representing the end of complete disassembly.

To illustrate the AND/OR graph and the model of disassembly graph, the analysis of the piston connecting rod unit (exclude piston part) in automobile is presented. Its assembly drawing is as shown in Fig. 2.

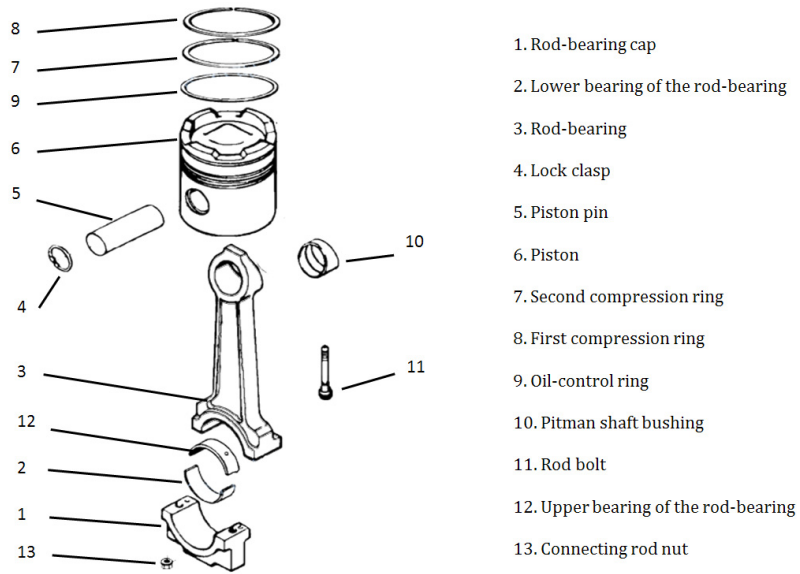


Fig. 2 Explosion diagram of piston connecting rod group

The AND/OR graph of rod-bearing part is shown in Fig. 3.

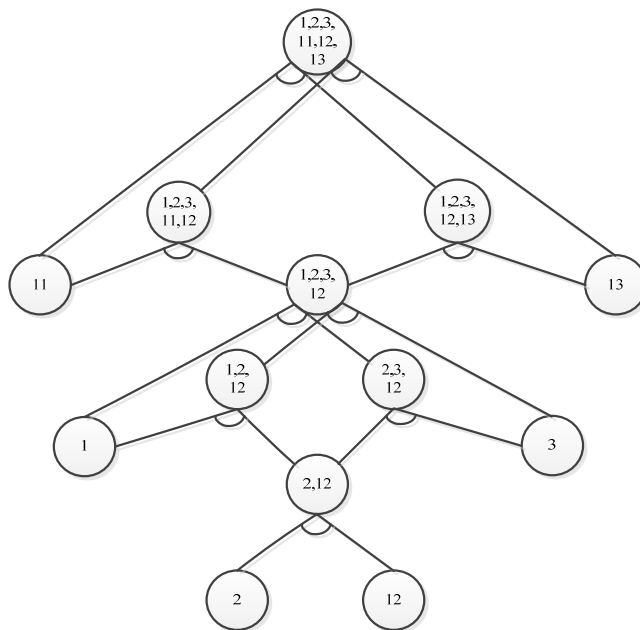


Fig. 3 The AND/OR graph model of the rod-bearing part

According to the rules described above, the AND/OR graph of the piston rod can be transformed into a graph, as shown in Fig. 4.

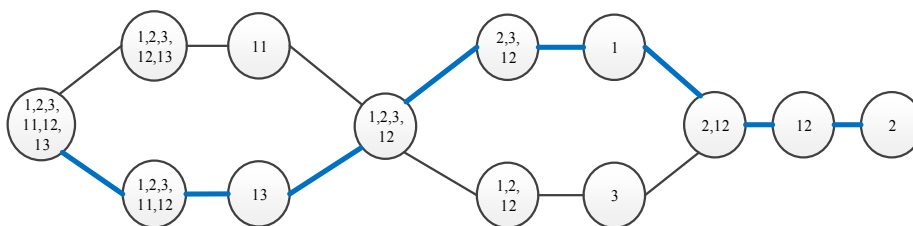


Fig. 4 The disassembly network graph of the rod-bearing part

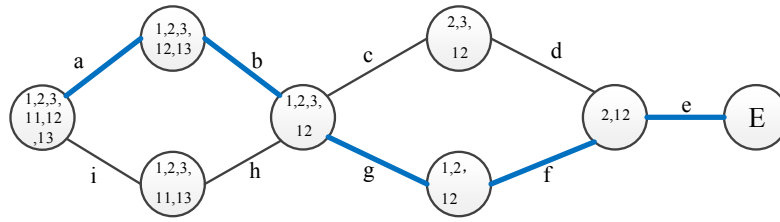


Fig. 5 Simplified graph of the disassembly network of the rod-bearing part

The disassembly network can be illustrated as Fig.4. The bold path represents a feasible disassembly sequence of piston group. According to Rules 4 and 5, the simplified graph is shown in Fig. 5.

The order of disassembly is from left to right in the simplified graph. The first point on the left side indicates the original product, that is, the starting point of the disassembly, while node “E” is the final disassembly state. The bold path is a disassembly sequence of piston connecting rod group. We take the piston connecting rod as an example to establish the transition matrix and the weighted adjacency matrix of the disassembly graph. In Fig. 6, numbers represent node and letters stand for disassembly steps.

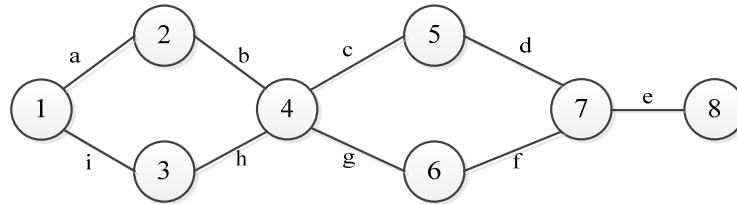


Fig. 6 The network graph of the rod-bearing part

Weight adjacency matrix of network

In order to formulate the disassembly process, this paper defines part set *S* and disassembly step set *A* to describe the states of parts and disassembly steps in the process of disassembly. Where *S* describes all possible parts that exist in the disassembly process (the original scrap product is also included in set *A*). Set *A* contains all the operation steps in the disassembly. Therefore, the simplified disassembly network can be represented by a *S* × *A* transition matrix *T*, and the elements in the matrix *T* are defined as follows:

$$a_{ij} \begin{cases} -1 & \text{Node } i \text{ is the starting point of } i \text{ to } j \\ 1 & \text{Node } i \text{ is the ending point of } i \text{ to } j \\ 0 & \text{Node } i \text{ is connected of } i \text{ to } j \end{cases} \quad (1)$$

Each row of the matrix corresponds to a part or a unit, and each column corresponds to an operation step. Matrix elements in the disassembly represent: if a disassembly step represents that a unit is disassembled, then the element is set as -1; if a disassembly step represents that the parts are assembled into a unit, then the element is set as 1, while the remaining elements in the matrix are 0.

This example illustrates the transition matrix of the network graph in Fig. 6 based on Eq. 1:

$$T = \begin{matrix} & \begin{matrix} a & b & c & d & e & f & g & h & i \end{matrix} \\ \begin{matrix} 1 \\ 2 \\ 3 \\ 4 \\ 5 \\ 6 \\ 7 \\ 8 \end{matrix} & \begin{vmatrix} -1 & 0 & 0 & 0 & 0 & 0 & 0 & 0 & -1 \\ 1 & -1 & 0 & 0 & 0 & 0 & 0 & 0 & 0 \\ 0 & 0 & 0 & 0 & 0 & 0 & 0 & -1 & 1 \\ 0 & 1 & -1 & 0 & 0 & 0 & -1 & 1 & 0 \\ 0 & 0 & 1 & -1 & 0 & 0 & 0 & 0 & 0 \\ 0 & 0 & 0 & 0 & 0 & -1 & 1 & 0 & 0 \\ 0 & 0 & 0 & 1 & -1 & 1 & 0 & 0 & 0 \\ 0 & 0 & 0 & 0 & 1 & 0 & 0 & 0 & 0 \end{vmatrix} \end{matrix}$$

Weight adjacency matrix of the directed graph: If each side has a value in directed graph $D = (V, E)$, then D is called weighted directed graph. If D is a simple weighted directed graph, the weight adjacency matrix of D is $W = (a_{ij})_{n \times n}$. The elements of matrix W are defined as follows:

$$a_{ij} = \begin{cases} w_{ij} & \text{if } (v_i, v_j) \in E \text{ and } w_{ij} \text{ is its weight} \\ 0 & \text{if } i = j \\ \infty & \text{if } (v_i, v_j) \notin E \end{cases} \quad (2)$$

Disassembly network graph is a directed graph, and different disassembly purposes correspond to different weights. For example, if the goal of the disassembly is to shorten the disassembly time, the weight given to each side of the directed graph is time [31-33]. If the goal of the disassembly is to obtain the maximum benefit, the weight given to each side is benefit.

2.2 Modelling develop

Because the disassembly process of auto parts is influenced by many factors, it is highly uncertain. In this paper, we put forward the following assumptions:

1. Non-destructive disassembly should be used to ensure the integrity of the parts.
2. The parts need to be disassembled are regarded as rigid bodies, which will not be damaged or deformed in the process of disassembly.
3. Use one part to represent several parts which have same purposes and functions. For example, bolts, etc.
4. When the part is removed through an operation, all the constraints associated with the part should be removed.
5. When a disassembly operation is carried out, at least one part of the product should be removed from the product.

According to the degree of disassembly, the disassembly can be divided into complete disassembly, target unit/part disassembly and economic disassembly sequence. Revenues and the costs of disassembly are considered in this paper. Through establishing the disassembly network graph and the adjacency matrix, we can clear the physical and mathematical meaning of the optimization model. Then we use the linear programming to solve the optimal disassembly sequence in three ways.

$x_i (i = 1, 2, 3, \dots)$ represents whether the disassembly operation step i is executed.

$$x_i = \begin{cases} 1, & \text{execute step } i \\ 0, & \text{otherwise} \end{cases} \quad (3)$$

For each step of operation, a parent part is disassembled into two or more than two sub parts. To ensure that only one of the ways is executed even the parent part can be disassembled in several ways, we give out the following constraints. As shown in Fig. 7, the unit "K" is obtained by disassembly operation "a", unit "K" has two disassembly ways: one is disassembled into part "U" and "V" through operation "b", unit "K" has two disassembly ways: one is disassembled into part "U" and "V" through operation "b".

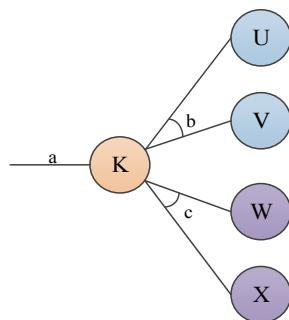


Fig. 7 Typical disassembly steps in disassembly network graph

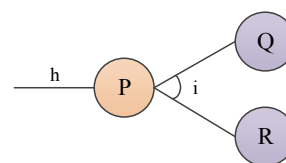


Fig. 8 Disassembly steps of unit P

So the constraint of the unit “K” is:

$$x_b + x_c \leq x_a, x_a = 1 \tag{4}$$

The sign \leq enables the occasion of “no disassembly” instead of “=”, which means that the complete disassembly sequences and selective disassembly sequences are both applied to this constraint. It is easy to conclude that for each subassembly; the node constraint can be generated, indicating that the sum of leaving flows \leq the sum of entering flows. As a result, a set of node constraints, that covers all feasible subassemblies except final subassemblies, is established. That is because final subassemblies are all single parts that need not to be disassembled further.

Once the disassembly network is established by the set of node constraints, the further task is to define the objective function. The economic benefits of the disassembly are considered in this paper. In Fig. 8, the parent subassembly “P” is obtained by operation “h” and the operation “i” is considered as an operation that destroys “P” and creates two parts “Q” and “R”. Thus the fits w_i brought by action “i”, is calculated as follows.

$$w_i = (r_r + r_q - r_p - c_i) \times x_i \tag{5}$$

where w_i is the benefits brought by operation “i”; r_r, r_q, r_p are the benefits of subassemblies “R, Q and P”, respectively. c_i is the cost of operation “i”; x_i is a binary variable that determines whether conduct the action “i”.

Thus, the objective function is the summation over all possible actions.

Model of complete disassembly

Complete disassembly is the complete decomposition of a complex product. That is, the product should be disassembled into individual part. In complete disassembly, regardless of the revenue of the disassembly, the disassembly will be carried out until the end. So the cost of disassembly is the only thing need to be considered. In this paper, the time cost of disassembly is considered as disassembly cost. So the objective of complete disassembly can be regarded as to minimize the time of disassembly:

$$\min \sum_j c_j x_j \tag{6}$$

$$s. t. \sum_j T_{ij} x_j \leq 0 \quad x_{j=1} = 1 \tag{7}$$

where c_j represents the time cost of the operation step j .

Model of optimal disassembly sequence

The disassembly for target units is carried out to obtain a certain part/unit. If removing the target parts is just to repair products, we just need to consider the disassembly time, rather than benefits. Then this optimization problem is similar to complete disassembly sequences. If the removal of waste products is to obtain the target parts, while the benefit of the other parts obtained from the disassembly process should be maximized. We need to consider the benefits and disassembly costs of the parts. Then the optimal sequence of the disassembly of the target parts can be expressed as the maximum benefit of disassembly. In the process of disassembly, the remaining parts may have lower reuse value than their disassembly costs. So in order to ensure the efficiency of disassembly, further disassembly should be stopped. We deal with the disassembly problem considering remaining values, and determine which removal steps can get the global maximum economic benefits.

$$\max \sum_i \sum_j (T_{ij} r_i - c_j) x_j \tag{8}$$

$$s. t. \sum_j T_{ij} x_j \leq 0 \quad x_{j=1} = 1 \tag{9}$$

where T_{ij} is the transition matrix; x_j is the binary variable; r_i is the benefits brought by subassembly i ; c_j is operation cost of j . $x_{j=1} = 1$ means the initial/first operation. The indexes i and j represent subassemblies and operations, respectively.

3. Floyd-Warshall algorithm

In this paper, the AND/OR graph is used to describe the disassembly process, and we make use of the conversion rules to convert the AND/OR graphs to disassembly network graphs. The process of searching for the path in the network is as same as the disassembly sequence planning.

Floyd-Warshall algorithm, which is one of the most commonly used algorithms to solve the shortest path, can find the shortest path between any two points. In Floyd-Warshall algorithm, the positive and negative values of weight w_{ij} are not limited to be positive numbers. Because of the disassembly cost is greater than the value that can be brought by the disassembly part, the benefit is negative, which means the weight of the disassembly network is negative too. So, it is feasible to use the Floyd-Warshall algorithm to solve the problem of disassembly sequences planning. The steps of the Floyd-Warshall algorithm are summarized as follows:

Step 1: Input weight matrix W , seek the shortest path from point v_r to point v_j ($j = 1, 2, 3 \dots$).

Step 2: Make $l_{rj}^{(k)}$ restore the shortest path from point v_r to point v_j within k steps. So $l_{rj}^{(1)} = w_{rj}$.

The path from v_r to v_j within k steps can be divided into two parts: from v_r to v_i within $k-1$ steps, the shortest path is $l_{ri}^{(k-1)}$; from v_r to v_j within one step, the shortest distance is w_{ij} .

$$l_{ij}^{(k)} = \min_{1 \leq i \leq n} \{l_{ri}^{(k-1)} + w_{ij}\} \tag{10}$$

$$l_k = (l_{r1}^{(k)}, l_{r2}^{(k)}, \dots, l_{rn}^{(k)})^T \quad (K = 1, 2, \dots) \tag{11}$$

According to the Eq. 11, the i^{th} element $l_{ri}^{(k)}$ in the column matrix l_k is the minimum of the sum of the i column $(w_{1i}, \dots, w_{ni})^T$ in the weight matrix W and the corresponding elements of row $l_{ri}^T (l_{r1}^{(k-1)}, l_{r2}^{(k-1)}, \dots, l_{rn}^{(k-1)})$.

$$l_k^T = l_{k-1}^T \times W \tag{12}$$

Step 3: When all $w_{ij} \geq 0$, the shortest path from v_r to v_i does not repeat (no circle). Since there are n nodes in the network, $n - 1$ steps are needed at most from v_r to v_i in the shortest path. If the shortest path contains n steps, we must repeat one step at a certain point, which makes it the same as the shortest path with $n - 1$ steps. So we have:

$$l_n = l_{n-1} \tag{13}$$

Step 4: After $n-1$ times multiplication of the matrixes, the shortest paths from v_r to each point can be found. When $l_k = l_{k-1}$ appears in the calculation process, we can find it consistent with the shortest distance of walking $k-1$ steps and k steps, then the calculation can be ended.

In this paper, the Floyd-Warshall algorithm is introduced to solve the problem of disassembly sequences planning for automotive products, and the optimal product disassembly sequence is obtained:

Step a: If the shortest time of disassembly is the target, the weight adjacency matrix W_t for the time of the disassembly should be put into the program. If obtaining maximum benefit of disassembly is the target, the weight adjacency matrix W for the benefit of disassembly should be put into the program.

Step b: Set $k = 1$, and the original vehicle as a starting point v_r of disassembly. Secondly, calculate the shortest distance $l_1^k = w_{r,j}$ from v_r to the disassembly state $v_j(j = 1,2,3, \dots, n)$ after one operation step.

Step c: Set $l_k^T = l_{k-1}^T \times W$ or $l_k^T = l_{k-1}^T \times -W$, $k = 2,3,4 \dots$ then calculate the shortest distance l_k^T to the disassembly state $v_j(j = 1,2,3, \dots, n)$ within at most k operation steps.

Step d: Confirm whether the equation $l_k^T = l_{k-1}^T$ is correct. If the equation is satisfied, then the algorithm ends, and we can get the product sequence. Otherwise, return to Step c.

In order to describe the application of the algorithm in this problem, the design procedure of the Floyd-Warshall algorithm is used to optimize the complete disassembly sequence of the piston connecting rod based on the benefit adjacency matrix in Sec. 2. The benefit adjacency matrix of the piston connecting rod group is assumed as follows:

$$W = \begin{matrix} & \begin{matrix} 1 & 2 & 3 & 4 & 5 & 6 & 7 & 8 \end{matrix} \\ \begin{matrix} 1 \\ 2 \\ 3 \\ 4 \\ 5 \\ 6 \\ 7 \\ 8 \end{matrix} & \begin{vmatrix} 0 & 7 & 6 & \infty & \infty & \infty & \infty & \infty \\ \infty & 0 & \infty & -2 & \infty & \infty & \infty & \infty \\ \infty & \infty & 0 & 1 & \infty & \infty & \infty & \infty \\ \infty & \infty & \infty & 0 & 2 & 3 & \infty & \infty \\ \infty & \infty & \infty & \infty & 0 & \infty & -1 & \infty \\ \infty & \infty & \infty & \infty & \infty & 0 & -4 & \infty \\ \infty & \infty & \infty & \infty & \infty & \infty & 0 & 3 \\ \infty & 0 \end{vmatrix} \end{matrix}$$

The optimized complete disassembly sequence is 1-3-4-5-7-8, as shown in bold path in Fig. 9. The maximum benefit of this disassembly sequence is 11.

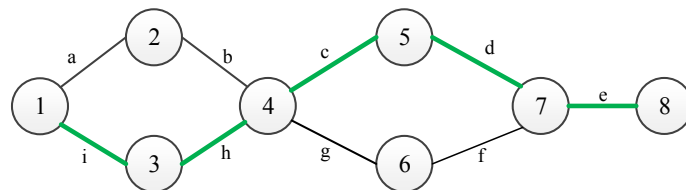
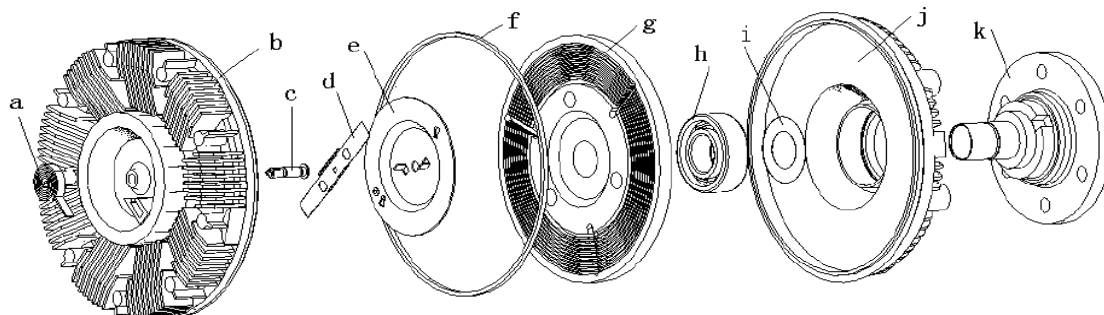


Fig. 9 The complete disassembly sequence of the piston connecting rod group

4. Case study

In order to verify the feasibility and effectiveness of the application of disassembly model based on the AND/OR graph in disassembly sequence planning, the silicon oil fan clutch is taken as an example depicted in Fig. 10. According to the connection relation and precedence relation between the silicone oil fan clutch parts, the disassembly AND/OR graph is obtained after analysis. As shown in Fig. 11.



a: Bimetallic strip temperature sensor; b: Clutch front cover; c: Valve shaft; d: Valve; e: Partition; f: Seal ring; g: Active plate; h: Bearing; i: Shim; j: Clutch rear cover; k: Drive shaft

Fig. 10 Silicon oil fan clutch assembly explosion diagram

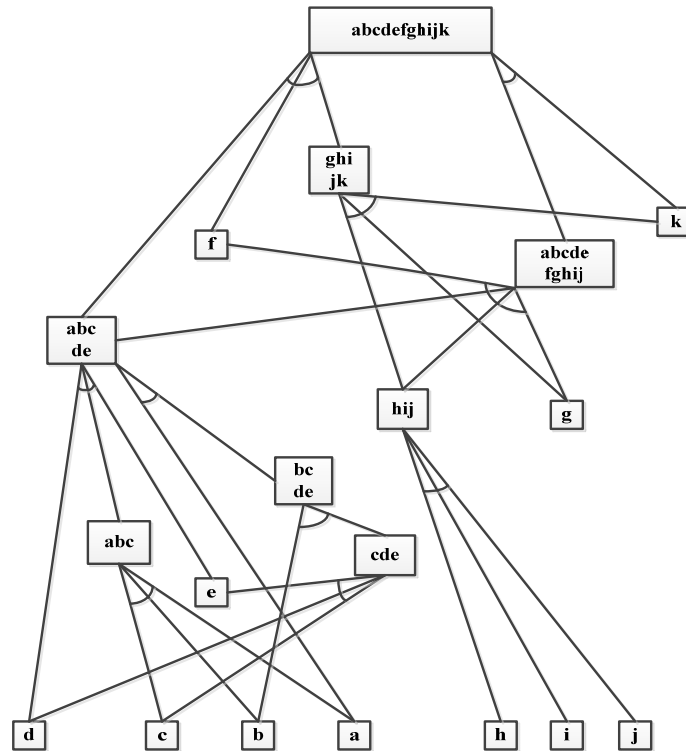


Fig. 11 The AND/OR graph model of silicon oil fan clutch disassembly

According to the rules between the disassembly AND/OR graph and the disassembly network graph, the AND/OR graph model of the silicon oil fan clutch are transformed and simplified to Fig. 12. The disassembly path of the silicon oil clutch is represented by the network.

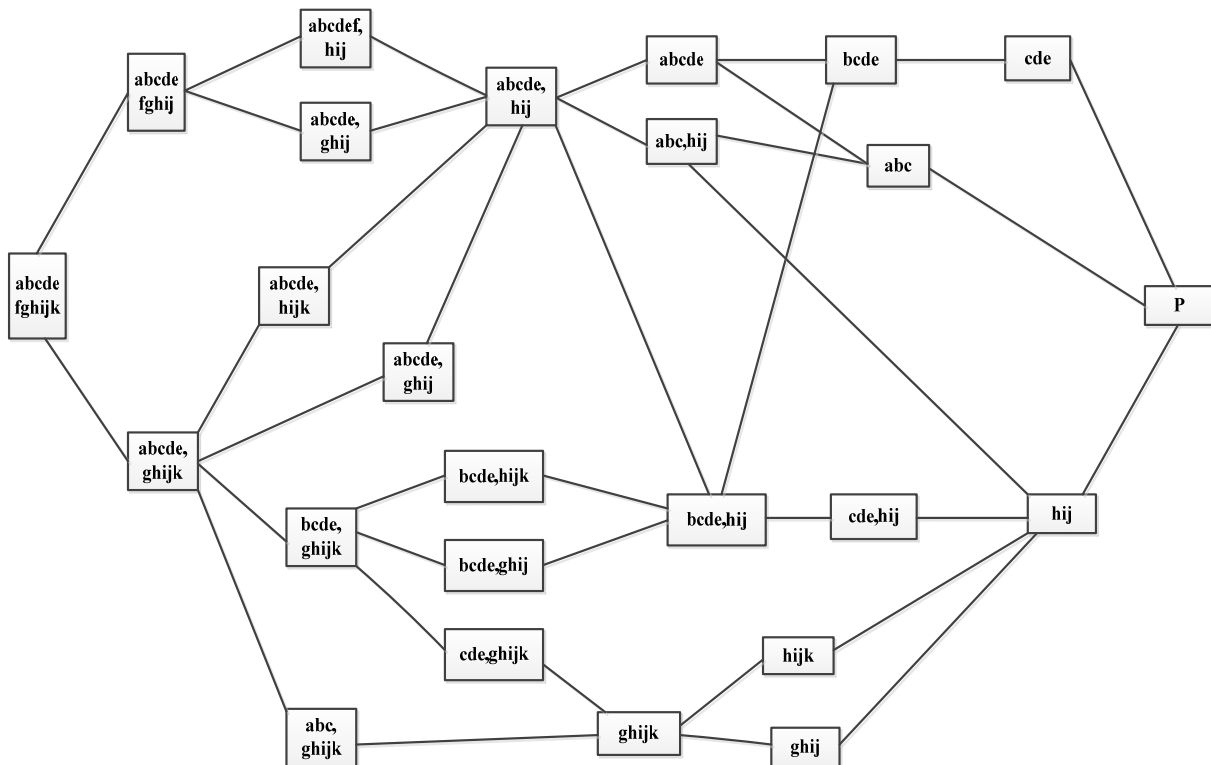


Fig. 12 The disassembly network diagram of silicone oil fan clutch assembly

The nodes in Fig. 12 are numbered for simplification as shown in Fig. 13. Number “1” is the original silicone oil clutch, while number “11” is the completely disassembly state of a silicon oil clutch. Other numbers are the states that may exist in the disassembly operation. Separate the different units in a node with a comma. For example, the node “bcde, hij” consists of two parts: the unit “bcde” and the unit “hij”.

Assume that the disassembly process of the silicon oil fan clutch is linear. In order to simplify the model, this paper only considers the time consumed by the disassembly process and the benefits of disassembly parts. The disassembly sequence planning is studied according to the disassembly network graph model.

First, we need to obtain the relevant data about the recovery value of all parts and units in disassembly operations. The relevant data is obtained according to the actual disassembly experience.

According to practical experience, the time adjacency matrix W_t of disassembly network graph is obtained. The demolition time for each disassembly operation and while the benefit adjacency matrix W of disassembly network graph can be attained accordingly.

Based on the data above, the Floyd-Warshall algorithm is used to solve the optimal sequence of the complete disassembly, the optimal sequence of the disassembly of the target unit, and the economic optimal disassembly sequence of the silicon oil fan clutch.

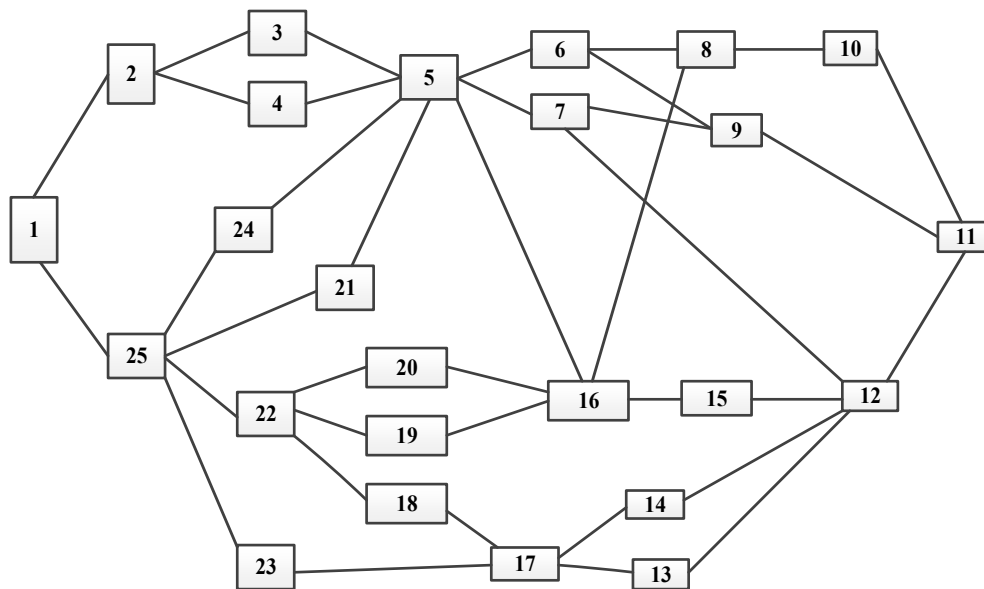


Fig. 13 The disassembly network diagram silicone oil fan clutch

4.1 The optimal sequence of the complete disassembly

We do not need to consider the effectiveness of the disassembly parts in complete disassembly, just need to consider the minimum disassembly cost. That is, the time of disassembly should be the least. Use the Floyd-Warshall algorithm to calculate the shortest path from node “1” to node “11”. The shortest time of complete disassembly is 32, corresponding to the complete disassembly is: 1-25-21-5-7-9-11 (Fig. 14).

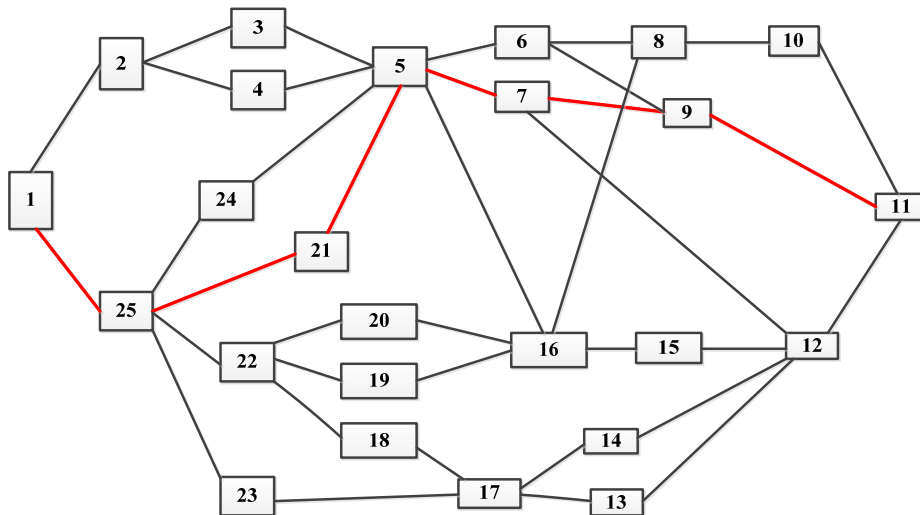


Fig. 14 The complete disassembly sequence path

4.2 Optimal sequence for disassembly of target units

Since the case is the disassembly of the target unit in the silicon oil fan clutch, and aim to maximize the benefits of disassembly while ensuring obtaining the target units successfully. Node “16” in Fig. 15 is the objective state. Calculate the shortest path from node “1” to node “16”. The optimal sequence is: 1-25-21-5-16 (Fig. 15), while the maximum benefit to the objective state is 81. The final state of disassembly is: part f, part k, part g, part a, unit “bcde”, unit “hij”.

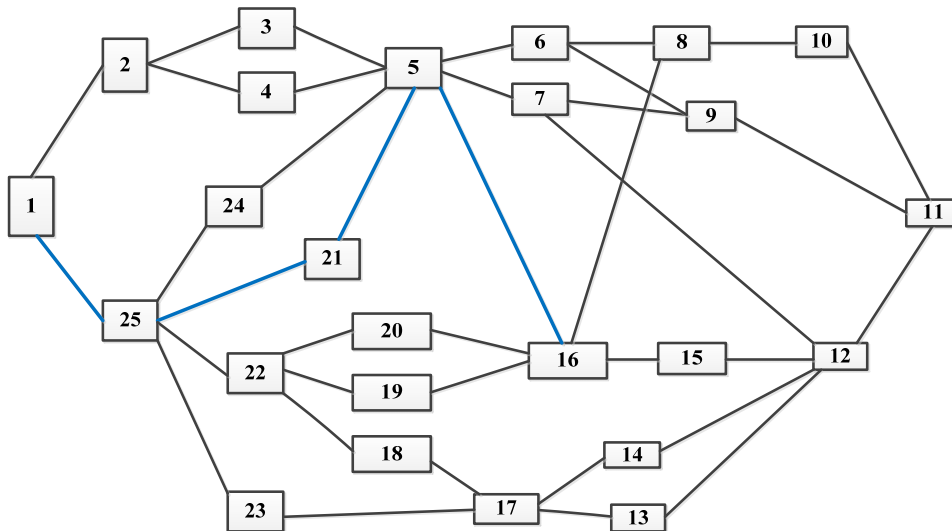


Fig. 15 Optimal sequence of disassembly of target units

4.3 Economic optimal sequence

The economic benefit of disassembly is the difference between the economic value of disassembled parts and the cost of disassembly process. While a products is disassembled to a certain extent, and the residual part recovery value is less than their disassembly cost, then further disassembly is unnecessary. In order to determine the economic optimal sequence of the silicon oil fan clutch, we need to calculate the benefits of node “1” to other nodes through the benefit adjacency matrix, and find the maximum benefits of them. The node of the maximum benefit is the end of the demolition operation. The benefit of node “1” to each node is shown in Fig. 16.

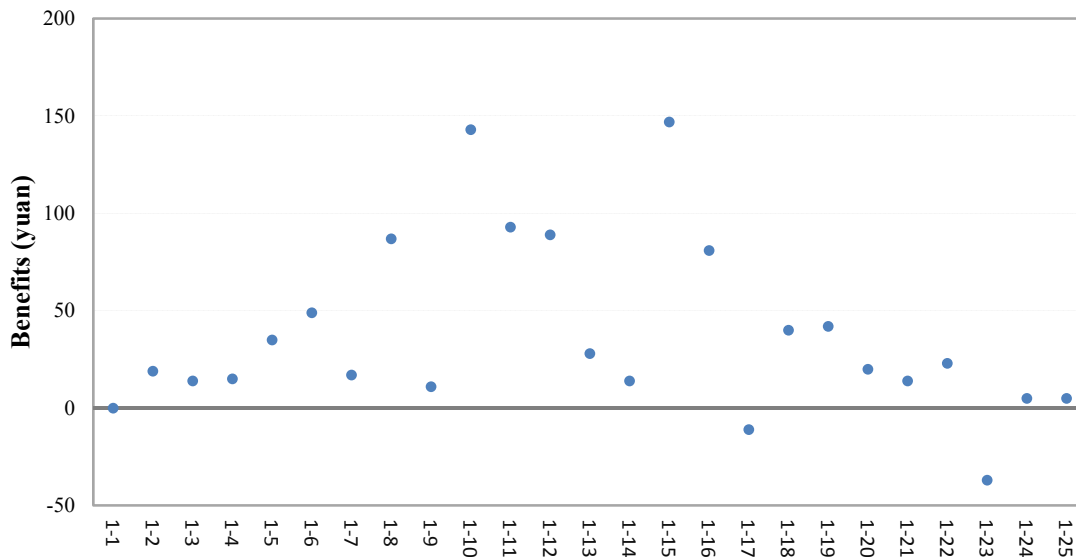


Fig. 16 Benefits of node 1 to each node

From Fig. 16 we can see that the maximum benefit appears at 1-15. That means when the silicon oil fan clutch is removed to the state of node “15”, the benefit of the whole disassembly is maximum, and the maximum benefit is 147. Economic optimal sequence is 1-25-21-5-16-15 (Fig. 17). The final state of disassembly is: part f, part k, part g, part a, part b, unit “cde”, unit “hij”.

By solving the optimal sequence of the above three kinds of disassembly methods, we verify the effectiveness of the disassembly network model and the Floyd-Warshall algorithm proposed in this paper for the disassembly sequence planning of silicon oil fan clutch. This paper improves the efficiency and efficiency of disassembly, and presents a new way of thinking for the disassembly sequence of automobile parts.

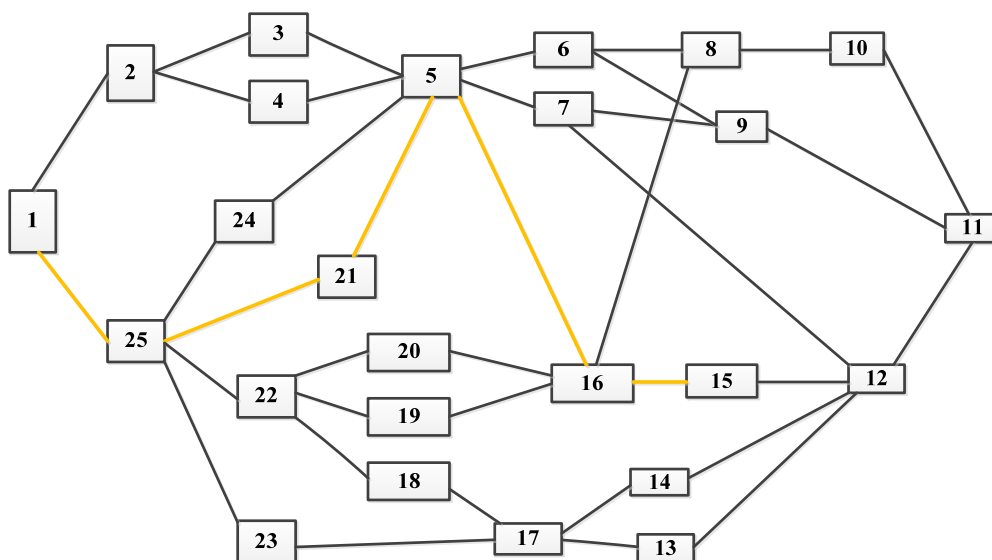


Fig.17 Economic optimal sequence

5. Conclusion

Disassembly and recycling of industrial products are one of the effective methods for resource conservation and environment protection. Reasonable disassembly planning helps to improve the disassembly efficiency and reduce the cost and time of disassembly. In this paper, the disas-

sembly sequence of automobile parts is studied. We propose the model of disassembly network based on the idea of the AND/OR graph. The transition matrix is used to describe the constraint relations between parts and units, while the weight adjacency matrix is used to describe the cost and benefit in disassembly operations. The disassembly sequence planning problem is solved by the classic Floyd-Warshall algorithm. The feasibility of the model and algorithm are verified by solving the optimal sequence of three different disassembly purposes. In this paper we consider the time and benefits of disassembly, but there are a lot of factors affect the disassembly efficiency in manufacturing. In the future, we will improve the model by considering more factors such as the direction of the demolition and the energy consumption. This approach could be applied to obtain optimum disassembly sequence of products containing complex AND/OR hierarchical relationships such as airplanes, automobiles and industrial machinery.

Acknowledgement

This work was supported in National Natural Science Foundation of China 71571026 and 51578112, Liaoning Excellent Talents in University LR2015008, and the Fundamental Research Funds for the Central Universities (YWF-16-BJ-J-40 and DUT16YQ104).

References

- [1] Yang, J., Sun, J. (2015). Vehicle path reconstruction using automatic vehicle identification data: An integrated particle filter and path flow estimator, *Transportation Research Part C: Emerging Technologies*, Vol. 58, 107-126, doi: [10.1016/j.trc.2015.07.003](https://doi.org/10.1016/j.trc.2015.07.003).
- [2] Behdad, S., Thurston, D. (2012). Disassembly and reassembly sequence planning tradeoffs under uncertainty for product maintenance, *Journal of Mechanical Design*, Vol. 134, No. 4, 169-184, doi: [10.1115/1.4006262](https://doi.org/10.1115/1.4006262).
- [3] Gerner, S., Kobeissi, A., David, B., Binder, Z., Descotes-Genon, B. (2005). Integrated approach for disassembly processes generation and recycling evaluation of an end-of-life product, *International Journal of Production Research*, Vol. 43, No. 1, 195-222, doi: [10.1080/00207540412331270414](https://doi.org/10.1080/00207540412331270414).
- [4] Lambert, A.J.D. (2003). Disassembly sequencing: A survey, *International Journal of Production Research*, Vol. 41, No. 16, 3721-3759, doi: [10.1080/0020754031000120078](https://doi.org/10.1080/0020754031000120078).
- [5] Li, J.R., Khoo, L.P., Tor, S.B. (2005). An object-oriented intelligent disassembly sequence planner for maintenance, *Computers in Industry*, Vol. 56, No. 7, 699-718, doi: [10.1016/j.compind.2005.03.005](https://doi.org/10.1016/j.compind.2005.03.005).
- [6] Lambert, A.J.D. (1999). Linear programming in disassembly/clustering sequence generation, *Computers & Industrial Engineering*, Vol. 36, No. 4, 723-738, doi: [10.1016/S0360-8352\(99\)00162-X](https://doi.org/10.1016/S0360-8352(99)00162-X).
- [7] Moore, K.E., Güngör, A., Gupta, S.M. (2001). Petri net approach to disassembly process planning for products with complex AND/OR precedence relationships, *European Journal of Operational Research*, Vol. 135, No. 2, 428-449, doi: [10.1016/S0377-2217\(00\)00321-0](https://doi.org/10.1016/S0377-2217(00)00321-0).
- [8] Li, D.Q., Fu, B.W., Wang, Y.P., Lu, G.Q., Berezin, Y., Stanley, H.E., Havlin, S. (2015). Percolation transition in dynamical traffic network with evolving critical bottlenecks, In: *Proceedings of the National Academy of Sciences*, Vol. 112, No. 3, 669-672, doi: [10.1073/pnas.1419185112](https://doi.org/10.1073/pnas.1419185112).
- [9] Zhang, H.C., Kuo, T.C. (1996). A graph-based approach to disassembly model for end-of-life product recycling, In: *Proceedings of the Nineteenth IEEE/CPMT International Electronics Manufacturing Technology Symposium*, Austin, USA, 247-254, doi: [10.1109/IEMT.1996.559739](https://doi.org/10.1109/IEMT.1996.559739).
- [10] Zhang, H.C., Kuo, T.C., Lu, H., Huang, S.H. (1997). Environmentally conscious design and manufacturing: A state-of-the-art survey, *Journal of Manufacturing Systems*, Vol. 16, No. 5, 352-371, doi: [10.1016/S0278-6125\(97\)88465-8](https://doi.org/10.1016/S0278-6125(97)88465-8).
- [11] Tiwari, M.K., Sinha, N., Kumar, S., Rai, R., Mukhopadhyay, S.K. (2002). A petri net based approach to determine the disassembly strategy of a product, *International Journal of Production Research*, Vol. 40, No. 5, 1113-1129, doi: [10.1080/00207540110097176](https://doi.org/10.1080/00207540110097176).
- [12] Zussman, E., Zhou, M.C. (2000). Design and implementation of an adaptive process planner for disassembly processes, *IEEE Transactions on Robotics Automation*, Vol. 16, No. 2, 171-179, doi: [10.1109/70.843173](https://doi.org/10.1109/70.843173).
- [13] Tang, Y., Zhou, M., Gao, M. (2006). Fuzzy-petri-net-based disassembly planning considering human factors, *IEEE Transactions on Systems, Man, and Cybernetics - Part A: Systems and Humans*, Vol. 36, No. 4, 718-726, doi: [10.1109/TSMCA.2005.853508](https://doi.org/10.1109/TSMCA.2005.853508).
- [14] Gao, J., Dong, X., Chen, H., Duan, G., Wang, J. (2003). Disassembly AND/OR graph model for "disassembly for recycling", In: *Proceedings of the IEEE International Symposium on Electronics and the Environment, 2003*, Boston, USA, 54-59, doi: [10.1109/ISEE.2003.1208047](https://doi.org/10.1109/ISEE.2003.1208047).
- [15] Kongar, E., Gupta, S.M. (2006). Disassembly sequencing using genetic algorithm, *The International Journal of Advanced Manufacturing Technology*, Vol. 30, No. 5-6, 497-506, doi: [10.1007/s00170-005-0041-x](https://doi.org/10.1007/s00170-005-0041-x).
- [16] Adenso-Díaz, B., García-Carbajal, S., Lozano, S. (2007). An efficient grasp algorithm for disassembly sequence planning, *OR Spectrum*, Vol. 29, No. 3, 535-549, doi: [10.1007/s00291-005-0028-x](https://doi.org/10.1007/s00291-005-0028-x).

- [17] Failli, F., Dini, G. (2001). Optimization of disassembly sequences for recycling of end-of-life products by using a colony of ant-like agents, In: *Proceedings of the 14th International Conference on Industrial and Engineering Applications of Artificial Intelligence and Expert Systems, IEA/AIE 2001, Budapest, Hungary*, 632-639, doi: [10.1007/3-540-45517-5_70](https://doi.org/10.1007/3-540-45517-5_70).
- [18] McGovern, S.M., Gupta, S.M. (2006). Ant colony optimization for disassembly sequencing with multiple objectives, *The International Journal of Advanced Manufacturing Technology*, Vol. 30, No. 5-6, 481-496, doi: [10.1007/s00170-005-0037-6](https://doi.org/10.1007/s00170-005-0037-6).
- [19] Lye, S.W., Lee, S.G., Khoo, M.K. (2000). An algorithm for optimizing the servicing of products with constrained, multiple defects, *International Journal of Production Research*, Vol. 38, No. 10, 2185-2200, doi: [10.1080/00207540050028043](https://doi.org/10.1080/00207540050028043).
- [20] González, B., Adenso-Díaz, B. (2006). A scatter search approach to the optimum disassembly sequence problem, *Computers Operations Research*, Vol. 33, No. 6, 1776-1793, doi: [10.1016/j.cor.2004.11.018](https://doi.org/10.1016/j.cor.2004.11.018).
- [21] Kang, J.-G., Xirouchakis, P. (2006). Disassembly sequencing for maintenance: A survey, *Proceedings of the Institution of Mechanical Engineers Part B Journal of Engineering Manufacture*, Vol. 220, No. 10, 1697-1716, doi: [10.1243/09544054JEM596](https://doi.org/10.1243/09544054JEM596).
- [22] Behdad, S., Kwak, M., Kim, H., Thurston, D. (2010). Simultaneous selective disassembly and end-of-life decision making for multiple products that share disassembly operations, *Journal of Mechanical Design*, Vol. 132, No. 4, doi: [10.1115/1.4001207](https://doi.org/10.1115/1.4001207).
- [23] Srinivasan, H., Gadh, R. (1998). A geometric algorithm for single selective disassembly using the wave propagation abstraction, *Computer-Aided Design*, Vol. 30, No. 8, 603-613, doi: [10.1016/s0010-4485\(98\)00009-8](https://doi.org/10.1016/s0010-4485(98)00009-8).
- [24] Srinivasan, H., Figueroa, R., Gadh, R. (1999). Selective disassembly for virtual prototyping as applied to de-manufacturing, *Robotics and Computer-Integrated Manufacturing*, Vol. 15, No. 3, 231-245, doi: [10.1016/S0736-5845\(99\)00023-X](https://doi.org/10.1016/S0736-5845(99)00023-X).
- [25] Kara, S., Pornprasitpol, P., Kaebnick, H. (2005). A selective disassembly methodology for end-of-life products, *Assembly Automation*, Vol. 25, No. 2, 124-134, doi: [10.1108/01445150510590488](https://doi.org/10.1108/01445150510590488).
- [26] Chung, C., Peng, Q. (2005). An integrated approach to selective-disassembly sequence planning, *Robotics and Computer-Integrated Manufacturing*, Vol. 21, No. 4-5, 475-485, doi: [10.1016/j.rcim.2004.11.008](https://doi.org/10.1016/j.rcim.2004.11.008).
- [27] Peng, Z., Shan, W., Guan, F., Yu, B. (2016). Stable vessel-cargo matching in dry bulk shipping market with price game mechanism, *Transportation Research Part E Logistics Transportation Review*, Vol. 95, 76-94, doi: [10.1016/j.tre.2016.08.007](https://doi.org/10.1016/j.tre.2016.08.007).
- [28] Yao, B., Chen, C., Cao, Q., Jin, L., Zhang, M., Zhu, H., Yu, B. (2016). Short-term traffic speed prediction for an urban corridor, *Computer-Aided Civil and Infrastructure Engineering*, Vol. 32, No. 2, 154-169, doi: [10.1111/mice.12221](https://doi.org/10.1111/mice.12221).
- [29] Yao, B., Hu, P., Lu, X., Gao, J., Zhang, M. (2014). Transit network design based on travel time reliability, *Transportation Research Part C Emerging Technologies*, Vol. 43, 233-248, doi: [10.1016/j.trc.2013.12.005](https://doi.org/10.1016/j.trc.2013.12.005).
- [30] Yu, B., Kong, L., Sun, Y., Yao, B., Gao, Z. (2015). A bi-level programming for bus lane network design, *Transportation Research Part C Emerging Technologies*, Vol. 55, 310-327, doi: [10.1016/j.trc.2015.02.014](https://doi.org/10.1016/j.trc.2015.02.014).
- [31] Tang, Y., Zhou, M., Zussman, E., Caudill, R. (2002). Disassembly modeling, planning and application, *Journal of Manufacturing Systems*, Vol. 21, No. 3, 200-217, doi: [10.1016/S0278-6125\(02\)80162-5](https://doi.org/10.1016/S0278-6125(02)80162-5).
- [32] Yao, B., Yu, B., Hu, P., Gao, J., Zhang, M. (2016). An improved particle swarm optimization for carton heterogeneous vehicle routing problem with a collection depot, *Annals of Operations Research*, Vol. 242, No. 2, 303-320, doi: [10.1007/s10479-015-1792-x](https://doi.org/10.1007/s10479-015-1792-x).
- [33] Yu, B., Wang, Y.T., Yao, J.B., Wang, J.Y. (2016). A comparison of the performance of ANN and SVM for the prediction of traffic accident duration, *Neural Network World*, Vol. 26, No. 3, 271-287, doi: [10.14311/NNW.2016.26.015](https://doi.org/10.14311/NNW.2016.26.015).

An integrated generalized discriminant analysis method and chemical reaction support vector machine model (GDA-CRSVM) for bearing fault diagnosis

Nguyen, V.H.^{a,b,c,*}, Cheng, J.S.^{a,b}, Thai, V.T.^{a,b,c}

^aState Key Laboratory of Advanced Design and Manufacturing for Vehicle Body, Hunan University, Changsha, China

^bCollege of Mechanical and Vehicle Engineering, Hunan University, Changsha, China

^cMechanical Engineering Department, Hanoi University of Industry, Hanoi, Vietnam

ABSTRACT

An expert technique in bearing fault diagnosis is proposed for the identification of actual status. A new diagnosis method based on a two-stage hybrid modality in integrating generalized discriminant analysis (GDA) with the chemical reaction support vector machine (CRSVM) classification model, named GDA-CRSVM, is proposed. The GDA reduces high-dimensional data to a more compact data, which serves an optimized CRSVM classification model with input data, in which a support vector machine (SVM) classifier model with the best parameters are selected by the meta-heuristic chemical reaction optimization algorithm (CRO) to build an optimized CRSVM classification model. The implementation of the new proposed method is based on a multi-aspect feature (MAF) set that presents most of the actual aspects of the complex vibration signal. The MAF set is collected from the statistical features in time-domain, frequency-domain, and time-frequency domain features are extracted by local characteristic-scale decomposition (LCD). Experiments have been conducted on two bearing vibration datasets by the expert technique in the bearing fault diagnosis. Results shown that the effectiveness of GDA-CRSVM in terms of classification accuracy and execution time.

© 2017 PEI, University of Maribor. All rights reserved.

ARTICLE INFO

Keywords:

Bearing fault
Expert fault diagnosis technique
Chemical reaction support vector machine (CRSVM)
Multi-aspect feature set
Generalized discriminant analysis (GDA)

*Corresponding author:

hung2009hau@gmail.com
(Nguyen, V.H.)

Article history:

Received 8 June 2017
Revised 23 October 2017
Accepted 26 October 2017

1. Introduction

The bearing is a key component of rotating machinery and is closely allied to system operation. Any failure of bearing may cause unsafe conditions for the operator and inefficient operation, stopping work may also affect associated systems. Hence, advanced fault diagnosis methods in the mechanical maintenance field are a focus of interest to many researchers. These methods can be summarized into several consecutive steps aimed at identifying patterns of fault status. The first step is acquisition vibration data, which may need pre-processing such as denoising or removing artefacts. The second step is feature extraction step to get the most important information. Then, these features are transformed into the pattern diagnosis model to classify patterns. Finally, the pattern diagnosis model determines the pattern type to which the particular fault signal belongs.

One the most important actions for fault diagnosis technique is feature extraction. An effectiveness feature set needs to contain the most salient features, beneficial features of the classification stage. This paper focuses on a multi-aspect feature extraction (MAF), which many actual

aspects of the complex vibration signal. MAF is based on statistical features in time-domain, frequency-domain, which directly represent the outward aspects of signal, and time-frequency domain features, which represent the intrinsic aspects deeply hidden in the vibration signal. Features in the time-frequency domain are especially extracted by local characteristic-scale decomposition (LCD), a method that becomes superior in running time, restraining the end effect and relieving mode mixing [1, 2]. The MAF set can be extracted from the original vibration signal as a high-dimensional feature vector including seven features that represent the aspect in the time-domain, eight features that represent the aspect in frequency-domain, and five features that represent the aspect in the time-frequency domain. The obtained MAF can provide extremely adequate information on various bearing conditions to make an effective diagnosis of performance.

Normally, a feature set of an original vibration signal can also provide more handy information. Increasing the problem of using these features efficaciously in a way that would interfere with the classification stage, such as the computational burden, the processing time is slower, the classification accuracy results are poorer. This paper aims at making classification performance more effective. The high-dimensional feature dataset that was extracted from vibration signals is mapped onto a new feature space to discover the intrinsic structure in these non-linear high-dimensional data and to obtain a more compact feature dataset in a lower dimension. Recently, dimensionality reduction approaches have aroused great interest in the fault diagnosis research field. Principal component analysis (PCA) [3, 4] is one of the most traditionally used, along with multi-dimensional scaling (MDS) [5] and linear discriminate analysis (LDA) [6, 7]. However, while these approaches are remarkably effective on linear data, they may not adequately handle complex non-linear data. This may be cause of low accuracy or misjudgement of a fault diagnosis with non-linear data. To expand the field of non-linear data of LDA, the generalized discriminant analysis (GDA) method was proposed by Baudat and Anouar (2000)[8]. The main idea is to project the input space into an advantageous feature space, where variables are nonlinearly related to the input space. According to the current literature, the GDA method has not been previously applied for fault diagnosis. In the case of medicine [9] and imaging [10], there are previous reference works. An important contribution in this study is the introduction of the GDA method in the discovery of the intrinsic structure of the non-linear high-dimensional feature dataset. Its combination with a classifier model make it effective for classification purposes.

Support vector machine (SVM) based on statistical learning theory is a new machine learning algorithm proposed by Vapnik *et al.* SVM is a powerful supervised machine learning tool and is used in a number of applications such as pattern recognition [11], time-series forecasting [12], robotics [13] and diagnostics [14]. When SVM is used, one should remark that the optimal parameters play a leading role for forming a classification model with high classification efficiency, thus creating something that has aroused the great interest of researchers for the selection of optimal parameters. Recently, several evolutionary based algorithms such as the genetic algorithm (GA) [15], particle swarm optimization (PSO) [16], ant colony optimization (ACO) [17], the simulated annealing algorithm (SA) [18] have been used to optimize the SVM parameters and have also shown promising ability as learning algorithms that can be utilized for diagnosis purposes [19]. However, their performance may vary from one object to another in fault diagnosis and may not be suitable for the different statuses of roller bearings. Besides, the efficiency of these optimization algorithms is characterized by the procedure used for selection the parameters, which requires a deep knowledge of the use of algorithms. The recent chemical reaction optimization (CRO) algorithm, which is a novel computational method, is one optimization of the found meta-heuristics introduced in 2010 [20]. CRO is an evolutionary optimization technique, which is comprehended from the nature of chemical reaction. It performs very well in solving optimization problems in a very short time. In a short period, there have been a few applications of CRO to the recognition field, data mining, classification rule [21, 22], and efficiency has been demonstrated. Indeed, CRO has been applied to solve complex problems successfully, has outperformed many existing evolutionary algorithms in most of the test cases. A guideline can be found in the tutorial introduced in [23] to help readers implement CRO for optimization problems. Motivated by the capability of CRO, an important contribution in this study is the authors' aim to use the CRO algorithm to select the best parameters of the SVM model, which is a fre-

quently used diagnosis technique called CRSVM. Then, the optimized CRSVM model is used for bearing fault diagnosis.

Finally, in this paper, a two-stage hybrid modality for integrating GDA with CRSVM is introduced, called GDA-CRSVM. The proposed GDA-CRSVM method is based on an expert technique that aims to exploit the highest identification accuracy in the fault diagnosis of roller bearings based on an MAF set. GDA is first used to reduce the high-dimensional feature set that acts as the data pre-processing for classifier model. Then, the obtained feature set provides the CRSVM model with input data. For exploration, experiments have been conducted on two bearing vibration datasets with different conditions based on the GDA-CRSVM method. Moreover, the acquired vibration signals have been analysed to extract the MAF set. It is remarkable that the performance of the GDA-CRSVM method is significantly better than that of the other methods and showed the most accurate results for classification purposes along with superior execution time.

The paper is constructed as follows. Section 2 presents materials and methods for bearing fault diagnosis. In Section 3, the GDA-CRSVM method is proposed by a two-stage hybrid modality by integrating the GDA method with the CRSVM classification model for the expert fault diagnosis technique. In Section 4, we present experiments for bearing fault diagnosis, where vibration data is acquired for roller bearings, MAF is used to extract vibration signals, and the actual fault statuses are identified by our proposed method. Section 5 is the conclusion. Acknowledgments and a list of references follow.

2. Materials and methods

2.1 Generalized discriminant analysis (GDA) method

Dimensionality reduction can be done by feature transformation to a low-dimensional data space once features have been extracted from the vibration signals. The purpose of the dimensionality reduction is to select the most superior features of the original feature set, which can provide dominant actuality-related information. Irrelevant or redundant factors must be discarded to improve classification performance, to avoid problems with dimensionality. Therefore, the GDA method is presented and used to select the superior features from the original feature set [8].

The objective of GDA is to find mapping for the input feature set into a lower dimensional space/ new space. The ratio of centre-class partner P_b to within-class partner P_w can be maximized [8]. A set of input patterns S of training features-set can be given as:

$$S = \sum_{c=1}^C S_c X_{ci} \quad c = 1, 2, \dots, C; i = 1, 2, \dots, S_c \quad (1)$$

This is a C-class problem, S_c is the number of samples in class c . The mapping $\psi: R^T \rightarrow T$ is non-linear for training patterns in the new space, thus $X \rightarrow \psi(X_{ci}), c = 1, 2, \dots, C; i = 1, 2, \dots, S_c$ is represented.

The center-class partner P_b to within-class partner P_w of the training feature set can be calculated as below:

$$P_w = \frac{1}{C} \sum_{c=1}^C \frac{1}{S_c} \sum_{i=1}^{S_c} \psi(X_{ci}) \psi^T(X_{ci}) \quad (2)$$

$$P_b = \frac{1}{C} \sum_{c=1}^C (\mu_c - \mu)(\mu_c - \mu)^T \quad (3)$$

We have to calculate the eigenvalues and eigenvectors $v, v \in T \setminus \{0\}$ to satisfy the equation:

$$\lambda P_w v = P_b v \quad (4)$$

$$\lambda = \frac{v'P_b v}{v'P_w v} \tag{5}$$

The eigenvectors v are combinations of $\psi(X_{ci})$ elements and the existing coefficients $f_{ci}, c = 1, 2, \dots, C; i = 1, 2, \dots, S_c$ such that:

$$v = \sum_{c=1}^C \sum_{i=1}^{S_c} f_{ci} \psi(X_{ci}) \tag{6}$$

To simplify, we can write the coefficient vector as below:

$$f = (f_{ci})_{\substack{c=1,2,\dots,C \\ i=1,2,\dots,S_c}} \tag{7}$$

Further, let us consider this vector. We used the kernel technique in the new space. Using the dot product of a sample m from class g and another sample n from class p , the dot product $(k_{mn})_{gp}$ gives the following:

$$(k_{mn})_{gp} = \psi(X_{gm}) \cdot \psi(X_{pn}) \tag{8}$$

First, let K be a $(N \times N)$ matrix defined in terms of the class elements by $(K_{gp})_{\substack{g=1,2,\dots,C \\ p=1,2,\dots,C}}$. In the new space, the K matrix is represented as below:

$$K = (K_{gp})_{\substack{g=1,2,\dots,C \\ p=1,2,\dots,C}} \tag{9}$$

where K_{gp} is a $(S_g \times S_p)$ matrix:

$$(K_{gp}) = (k_{mn})_{\substack{m=1,2,\dots,S_g \\ n=1,2,\dots,S_p}} \tag{10}$$

Then, a $(N \times N)$ matrix A is introduced, A is defined as:

$$A = (A_c)_{c=1,2,\dots,C} \tag{11}$$

where (A_c) is a $(S_c \times S_c)$ matrix with all terms equal to $1 / S_c$.

Finally, from the Eqs. 2, 3, 6 and 4, we found the inner product with vector $\psi(X_{ci})$ on both sides.

$$\lambda K K v = K A K v \tag{12}$$

There, v represents a column vector with values $v_{ci}, c = 1, 2, \dots, C; i = 1, 2, \dots, S_c$.

The solution of Eq. (12) is satisfactory when the eigenvectors of matrix $(K K)^{-1} K A K$ are calculated.

2.2 Optimal classification model

This section emphasizes the superiority of the CRO algorithm, which is then applied to select the best parameters of the SVM. These parameters play a leading role for building an optimal CRSVM classification model. The obtained CRSVM model can be used for fault diagnosis of bearing components, combining the input feature set to become the expert classifier model with high classification accuracy, stability and effectiveness of performance. Fig. 1 depicts the flowchart for using the CRO algorithm to select parameters of the SVM model.

Principle of SVM

Support Vector Machine (SVM) were introduced by Vapnik [24]. The SVM classifier is designed for classification tasks with two-class datasets. The data are separated by a hyperplane in order to maximize distance. The separating hyperplane is defined by the closest points of the training dataset, which are called support vectors. The details of SVM are presented in [14]. The parameter pair (C, γ) in the RBF kernel function (the penalty parameter of C and width parameter of γ) plays an important part in the classification purpose. The parameter pair values cover a broad

range and controls the generalization capability of SVM. The best selection of parameter pair is important and necessary to training the SVM classifier. In this work, values of C , γ are selected using the CRO algorithm for the best performance for accurate bearing fault diagnosis.

The optimized SVM model based on CRO

To fulfil the aim to build an optimal classification model, CRSVM, the CRO algorithm is used to exploit the best parameter pair (C , γ) of the SVM. The obtained classification model is employed to identify the bearing conditions.

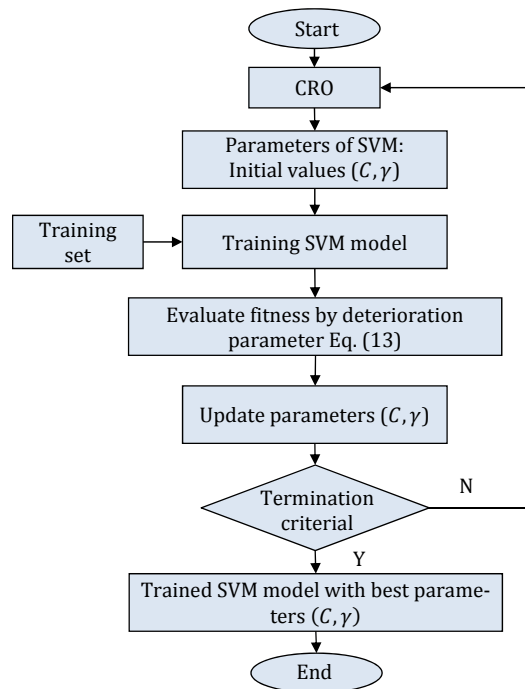


Fig. 1 The architecture of CRSVM classification model

Chemical reaction optimization algorithm

The CRO algorithm is introduced in 2010 [20] in the finding meta-heuristics of computational method which is the efficient optimization technique that enjoys the advantages of previous genetic algorithms and simulated annealing. This algorithm is not only inspired by the elementary chemical reactions, that is different from evolutionary algorithms motivated by biological evolution, but also easily constructed by defining the agents and the energy directional scheme. Consequently, algorithm has been deployed for different problems and has been successfully used to counteract complicated problems, outperforming other prevailing evolutionary algorithms in test conditions.

Furthermore, CRO algorithm carried out parallel of sub-reaction steps in the optimal process which benefits the minimizing for accomplishing time. Algorithm accomplishes local, global search with elementary reactions. In these, four types of elementary reactions are included: (1) on-wall ineffective collision, (2) decomposition, (3) inter-molecular ineffective collision, and (4) synthesis. In fact, each reaction is the interaction (the combination and variation) of molecules at a high energy level to become new products with a low energy level, in a stable status. The details of the CRO algorithm can be seen in [20, 23]. Motivated by the superior capability of CRO, the authors applied select parameters of the SVM model.

The solution to optimize the CRO algorithm involves using the natural chemical reaction of reactants to solve problems. The beginning of the algorithm establishes initial reactants, which play an important role in a solution. Then, the reactants react and produce four types of reactions. The algorithm is stopped when the termination criterion reaches final status, when no

more reactions can take place. In this work, the parameter pair (C, γ) of SVM is set as reactants in four types of reactions. According to this, the CRO algorithm consists of the following steps [21]:

- Step 1: Initialize the parameters.
- Step 2: Set the initial reactants and evaluate enthalpy.
- Step 3: Apply chemical reactions to reactants.
- Step 4: Update and select reactants.
- Step 5: Go to step 3 if termination criterion not satisfied.
- Step 6: Output reactant with best enthalpy.

Classification model CRSVM

The optimization parameter pair (C, γ) of the SVM can be obtained using the CRO algorithm. This CRO algorithm conducts stochastic searches using a population of molecules, each of which represents a possible solution to a problem. A population includes a finite number of molecules, with each molecule defined by an evaluating mechanism to obtain its potential energy.

The principled training phase of the CRSVM model includes seven main steps, which are implemented as follows:

- Step 1: Training and testing datasets are prepared after feature extraction from original vibration signals.
- Step 2: This is initialization step. The initial C, γ parameters are random for SVM. Set the maximum iteration number t_{max} . Set the iterative variable: $t = 0$ and perform the training process for the next steps. The parameters for this optimization algorithm are iteration $t_{max} = 50$, population size $pop = 5$, upper bound $u_p = 2^{12}$ and lower bound $l_p = 2^{-12}$.
- Step 3: Increase the iteration variable by set $t = t + 1$
- Step 4: Deterioration evaluation. The deterioration function is employed to evaluate the quality of every element. Eq. (13) shows the classification accuracy of an SVM classifier:

$$deterioration(\%) = \frac{N_{false}}{N_{\Sigma}} 100 \% \quad (13)$$

where N_{false} is false classified samples, N_{Σ} is total samples in the testing process. The desirable value is small for high classification accuracy.

- Step 5: Stop criteria checking. If the deterioration function satisfies Eq. (13) or iteration is maximal, go to step 7. If not, go to the next step.
- Step 6: Update the new C, γ parameters based on conditions. Go to step 3.
- Step 7: End of the training procedure. Fitting parameters are optimal output values.

The efficient search capability of the chemical reaction algorithm is incorporated with the generalization capability of SVM to bring out synergies of the classification accuracy. The architecture for CRSVM is presented in Fig. 1. Each reactant represents the candidate solution for the model, which includes the parameters C, γ .

3. An expert technique based on the proposed GDA-CRSVM method

In this section, the authors propose a new diagnosis method based on a two-stage hybrid modality for integrating GDA with the CRSVM, called the GDA-CRSVM. This takes special consideration of improved computational time, reduction of calculation memory and enhanced recognition accuracy of fault data. The methodology of dimensionality reduction (GDA) is close, which can obtain the total intrinsic emergent information of the original high-dimensional feature set. Combined, the optimized CRSVM model can obtain effective classification performance.

The process of the proposed method consists of two parts: dimensionality reduction and pattern recognition. First, the authors used the GDA method to reduce the high-dimensional fault feature dataset by taking out the most responsive features to produce a low-dimensional feature set. The obtained feature set increased the overall reliability of the fault diagnosis technique as well as the accuracy of diagnosis of an actual fault condition. Second, the reduced feature is

served as input to the optimized classification mode, which was elaborately optimized by the CRO algorithm based on the SVM, namely CRSVM.

Overall, the expert bearing fault diagnosis technique based on the GDA-CRSVM hybrid method aims to further improve fault diagnosis performance and ensure diagnosis reliability. It is presented in Fig. 2. From this figure, the technique includes four main steps as follows: Step 1 is vibration signal acquisition, Step 2 is MAF extraction, Step 3 is dimensionality reduction, Step 4 is pattern classification. The implementation process is described below:

Step 1: In the first step, the original vibration signals are acquired from acceleration sensors.

Step 2: Feature extraction is an urgent step of the diagnosis process. The extracted feature set represents important information about the actual bearing conditions, which governs the final results of the diagnosis process. This feature set contains the time-domain, frequency-domain features, and time-frequency domain features are extracted by the LCD method, which is used to form the MAF set of the original vibration signal.

Step 3: The GDA method is used to discover the intrinsic structure of the MAF set. The reduced feature set as a low-dimensional feature vector has more effective classification performance, such as reduced calculation memory, computational time, and the best classification accuracy results.

Step 4: The reduced feature set is divided into training set and testing set. Each low-dimensional training sample in its respective class labelled as the training set is used to discover the best parameter pair (C, γ) of the SVM by CRO. The obtained CRSVM classifier model is then used to recognize the samples in the testing set. For reliable diagnosis capability, the diagnosis technique based on this proposed GDA-CRSVM method is applied for bearing fault diagnosis.

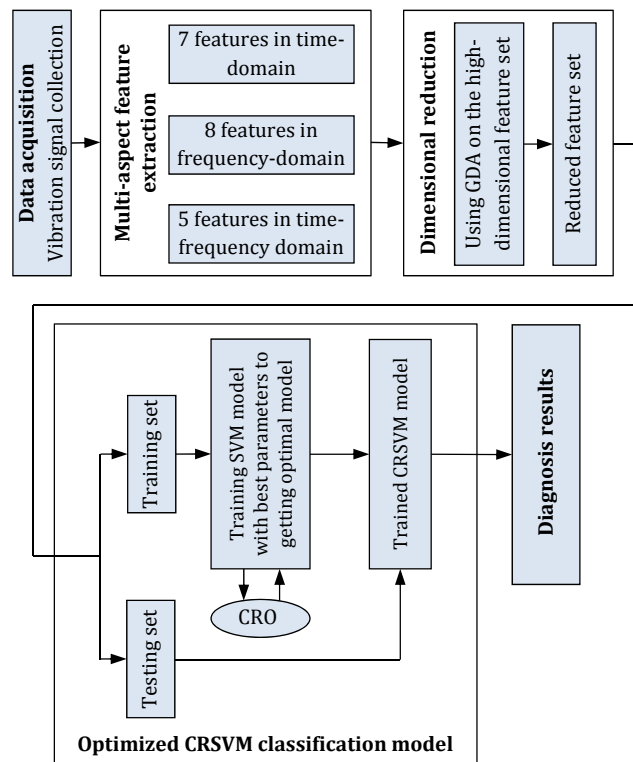


Fig. 2 Struct diagram of expert fault diagnosis technique

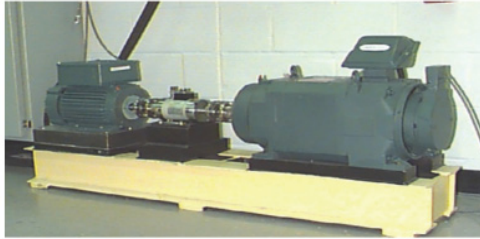


Fig. 3 Schematic of the experimental

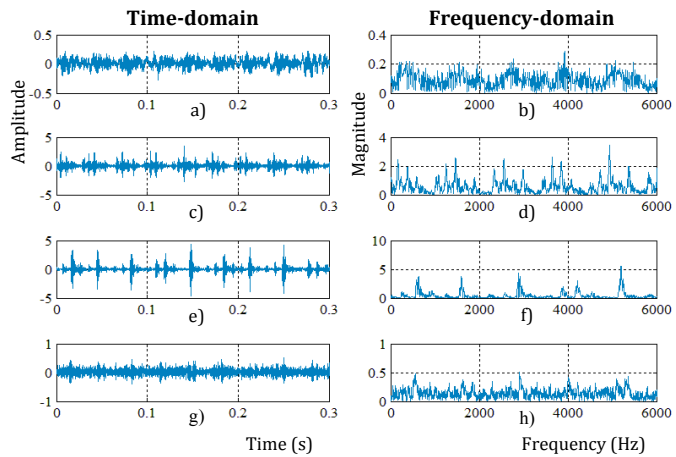


Fig. 4 The bearing conditions in the time domain and frequency domain

- a, b) Normal bearing
- c, d) Inner bearing fault
- e, f) Outer bearing fault
- g, h) Roller element fault

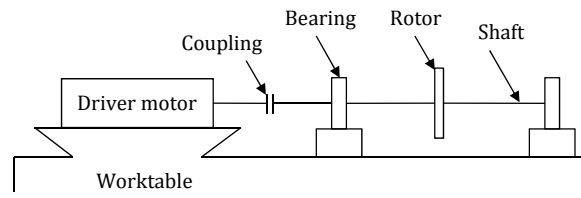


Fig. 5 The schematic drawing of test rig

4. Results and discussion for bearing fault diagnosis performance case study

In this section, two datasets of bearing conditions were collected. They are used for the experiments based on the proposal of proposed expert technique in actual status identification.

4.1 Data acquisition

The first dataset is vibration signals of bearing component fault cross from the Bearing Data Center at Case Western Reserve University (Loparo, 2013). Fig. 3 shows the experimental setup model, which consists of a two-HP reliance electric motor, a torque transducer and a dynamometer. The test bearings were installed on the motor shaft, which was loaded by dynamometer. The accelerometer data at DE were used as original signals for the detection of four bearing conditions: healthy bearing (HB), inner race (IR) fault, outer race (OR) fault, and rolling element (RE) fault. A defect was tested on the IR, OR, RE of test bearing using defect sizes 0.5334 mm (0.021 inches) in diameter with a depth of 0.2794 mm (0.011 inches) generated by electro-discharge machining. Four vibration signal datasets were acquired from the bearings with a sampling frequency of 12 kHz, tested under motor load of two-HP at a speed of 1750 RPM. Fig. 4 presents the vibration signals in time-domain, in frequency-domain from four signal samples of the bearing conditions. In each fault pattern, 25 samples were acquired from vibration signals. Each sample includes 4096 continuous data points in the time-domain. The results obtained groups with 100 vibration signals at various bearing conditions.

To further test the efficacy of the fault detection technique, the second dataset was acquired from test rig, as shown in Fig. 5 [25]. The bearing faults were introduced by laser cutting in the IR or RE with slot width of 0.15 mm and depth of 0.13 mm, respectively. The three experimental conditions tested were healthy bearing (HB), bearing with IR fault and bearing with RE fault. A total of 15 acceleration measuring signals with sampling frequency of 4096 Hz were acquired for each bearing condition.

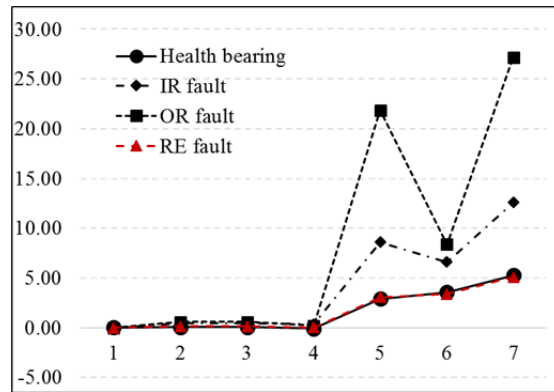


Fig. 6 The time-domain features of a bearing sample in different conditions

4.2 Multi-aspect feature extraction

The MAF set extracted from original vibration signals plays an important role for the achievement of the diagnosis model. The MAF includes time-domain features, frequency-domain features and features in the time-frequency domain, which are considered a high-dimensional feature vector.

- Time-domain features

The signal was analysed to extract seven time-domain statistical features TD_1 to TD_7 . Table 1 shows the seven feature definitions. In this table, the first five dimensions $TD_1 - TD_5$ reflect the vibration amplitude and energy in the time-domain, the last two dimensions TD_6, TD_7 are the crest factor and clearance factor, which represent the time-series distribution of the signals. Fig. 6 describes the time-domain features of the bearing samples in the different conditions.

Table 1 The feature definition equations in time-domain

No.	Time Domain (TD)		Remark
	Feature	Equation	
1	Mean	$TD_1 = \frac{1}{M} \sum_{i=1}^M x_i$	x_i is a vibration signal in time domain $i = 1, 2, \dots, M$, M is the number of data points.
2	Standard deviation	$TD_2 = \sqrt{\frac{1}{M-1} \sum_{i=1}^M (x_i - \bar{x})^2}$	
3	Root Mean Square	$TD_3 = \sqrt{\frac{1}{M} \sum_{i=1}^M x_i^2}$	
4	Skewness	$TD_4 = \frac{1}{TD_2^3(M-1)} \sum_{i=1}^M (x_i - \bar{x})^3$	
5	Kurtosis	$TD_5 = \frac{1}{TD_2^4(M-1)} \sum_{i=1}^M (x_i - \bar{x})^4$	
6	Crest factor	$TD_6 = \frac{\max x_i }{TD_3}$	
7	Clearance Factor	$TD_7 = x_{max} \left[\frac{1}{M} \sum_{i=1}^M \sqrt{ x_i } \right]^{-2}$	

- Frequency-domain features

Some signal information is also described in the frequency-domain and reveals information about the demodulation spectrum, amplitude frequency or distribution, which cannot be found in the time-domain. To extract these features, the Hilbert transform was first used to transform the vibration signals. Eight frequency-domain features FD_1 to FD_8 were then extracted from the

frequency spectrum of vibration signals, as shown in Table 2. The obtained features $FD_1 - FD_4$ describe the convergence or divergence of the spectrum power, FD_5, FD_6 indicate a change in position frequency. The spectrum power energy degree can centralize or de-centralize as described by parameter FD_7 and FD_8 can quantitatively measure disorder in the system. The frequency-domain features of the bearing conditions in an inner race fault, outer race fault, roller element fault and healthy fault are depicted in Fig. 7. The features of the conditional outer race fault and inner race fault are shown especially clearly.

- Time-frequency domain features

LCD is a self-adaptive method used in data decomposition. LCD has been successfully used to analyse non-linear, non-station signals, especially fault signals [2]. Obviously, LCD can extract the deeply hidden features in bearing fault data, as these features are very hard to distinguish only from the time-domain and frequency-domain statistical characteristics. In this study, the authors investigated the energy correlation coefficients between the first several intrinsic scale components (ISC), which were decomposed by the LCD method. These coefficients can reveal the original vibration signal in the time-frequency amplitude and distribution view, which is well and good for accurate diagnosis of a bearing fault. Further, any complex vibration signal $x(t)$ is decomposed into ISC and the residue by LCD, as in the equation below [1]:

$$x(t) = \sum_{i=1}^n ISC_i(t) + r_n(t) \tag{14}$$

where $ISC_i(t)$ is the i^{th} ICS of original signal obtained by LCD, the residue is $r_n(t)$.

Table 2 The feature definition equations in frequency-domain

No.	Frequency domain (FD)		Remark
	Feature	Equation	
1	Mean frequency	$FD_1 = \frac{1}{M} \sum_{i=1}^M p_i$	P_k is the energy probability distribution defined as: $P_k = p_i ^2 / \sum_{i=1}^M p_i ^2$
2	Standard deviation frequency	$FD_2 = \frac{1}{M-1} \sum_{i=1}^M (p_i - FD_1)^2$	
3	Skewness frequency	$FD_3 = \frac{1}{M} \frac{\sum_{i=1}^M (p_i - FD_1)^3}{\sqrt{\left(\frac{1}{M-1} \sum_{i=1}^M (p_i - FD_1)^2\right)^3}}$	where p_i is the spectrum of $x(i)$ vibration signal, $i = 1, 2, \dots, M$, M is the number of spectrum lines.
4	Kurtosis frequency	$FD_4 = \frac{1}{M} \frac{\sum_{i=1}^M (p_i - FD_1)^4}{\left(\frac{1}{M-1} \sum_{i=1}^M (p_i - FD_1)^2\right)^2}$	
5	Frequency centre	$FD_5 = \frac{\sum_{i=1}^M f_i p_i}{\sum_{i=1}^M p_i}$	f_i is the frequency value of the i^{th} spectrum line.
6	Root mean square frequency	$FD_6 = \sqrt{\frac{\sum_{i=1}^M f_i^2 p_i}{\sum_{i=1}^M p_i}}$	
7	Root variance frequency	$FD_7 = \sqrt{\frac{\sum_{i=1}^M (f_i - FD_5)^2 p_i}{M}}$	
8	Shannon Entropy	$FD_8 = - \sum_{i=1}^M p_k \log P_k$	

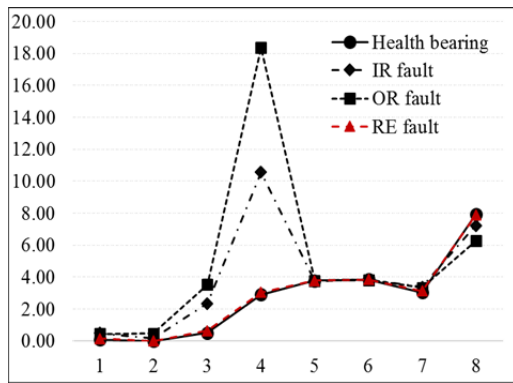


Fig. 7 The frequency-domain features of a bearing sample in different conditions

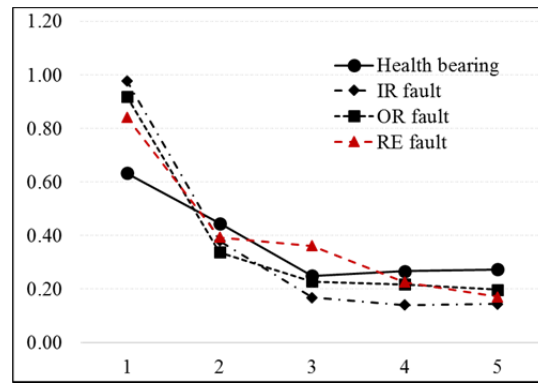


Fig. 8 Time-frequency domain features

The first several ISCs contain almost all valid fault information that characterizes the original signal. There, ISCs have higher energy than the rest. In this work, the first five ISCs were used to calculate the correlation of energy with the original vibration signal. These five energy correlation coefficients formed a feature subset representing the time-frequency domain features of bearing fault status. These following steps were taken:

- Step 1: The original vibration signals were collected from fault samples of the roller bearing.
- Step 2: The LCD method decomposed the vibration signals into ISCs. The first h ISCs were chosen.
- Step 3: The energy $E(ISC_i)$ of the first h ISCs was calculated, as related in Eq. 15 and Eq. 16:

$$E(ISC_i) = \sum_{n=1}^M a_k(t_n) \tag{15}$$

where $n = 1, 2, \dots, M$, M is data length of i^{th} ISC, t_n is the amplitude of point m in the ISC_i component, and $a_k(t)$ is the obtained amplitude of the i^{th} ISC by Hilbert transform:

$$ISC_i(t) = a_i(t)e^{i \int \omega_i(t) dt} \tag{16}$$

- Step 4: A feature vector F was constructed with the energy correlation coefficient as element:

$$F = [E'_1, E'_2, \dots, E'_k] \tag{17}$$

where $E'_i, i = 1, 2, \dots, k$ are the energy correlation coefficients.

$$E'_i = \frac{E_i}{\sum_{i=1}^m E_i} \tag{18}$$

Fig. 8 also shows time-frequency domain features of the bearing conditions. The deeply hidden features in the bearing fault signal were extracted by LCD. The feature values show that the energy level of ISCs gradually decreased.

The obtained time-frequency domain features were added into the feature set and thus the complete MAF was formed containing 20 features. The obtained MAF represents a bearing fault condition as a high-dimensional feature vector that serves the GDA-CRSVM method with input data.

4.3 Diagnosis analysis based on GDA-CRSVM

The high-dimensional MAF discovered non-linear characteristics by the GDA method as dimensionality reduction, which can be given as a low-dimensional feature set. The obtained low-dimensional feature set was then randomly divided into a training-testing partition, 70 % : 30 %. Finally, as mentioned in Section 3, the training set was used to train the optimal CRSVM diagnosis model in actual bearing conditions. The obtained optimal diagnosis model was employed to classify the samples in the testing set.

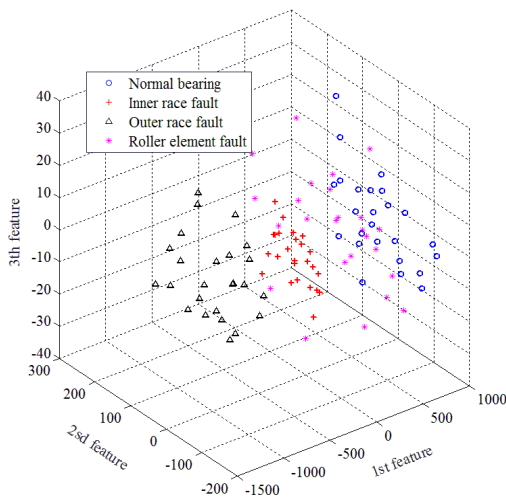


Fig. 9 Scatter plot for the reduced feature set by PCA

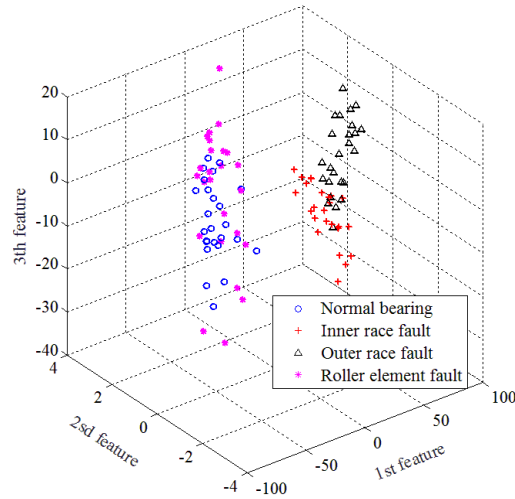


Fig. 10 Scatter plot for the reduced feature set by LDA

Feature-dimensional reduction by GDA method

Practically, the high-dimensional feature dataset involves too much memory for parameters, which results in a complicated and inefficient for classification model. For this goal, the extracted MAF of original vibration signals was reduced to three features using the GDA method mentioned in Section 2. To demonstrate the superiority of the introduced GDA dimensionality reduction method, when GDA is used in the process of the training pattern labelled into C classes, S_c number of samples in each class, C is set to 4, S_c is set to 25.

An experiment was conducted on the feature set, the authors explored this to evaluate the GDA method's dimensionality reduction performance on the sample feature set. We compared GDA with PCA and LDA as representative methods. The experimental results of the PCA, LDA and GDA methods are shown in Fig. 9 to Fig. 11, respectively, which show that PCA and LDA have dim pattern classification performance, with three classes of overlap. Compared with these, GDA can obtain a clearer separation on the mapping. Therefore, GDA can accurately separate the bearing fault status for the extracted MAF set. In fact, this is because the GDA has greater ability to discover the maximal ratio of centre-class partner to within-class partner in the multi-aspect data by employing class label information. Overall, the best GDA method is used for the high-dimensional MAF dataset to obtain the low-dimensional feature dataset with prominent features as a dimensionality reduction task.

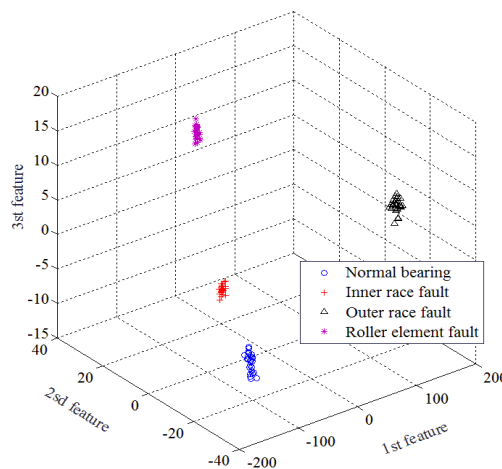


Fig. 11 Scatter plot for the reduced feature set by GDA

CRSVM training

In this study, CRSVM classifier models were designed to identify various bearing conditions. In fact, CRSVM1 was designed to identify normal bearing conditions, with normal bearing condition data assigned to $y = +1$, other data assigned to $y = -1$. CRSVM2 was designed to identify inner race faults of bearings, with inner race fault data assigned to $y = +1$, other data assigned to $y = -1$. CRSVM3 was designed to identify outer race faults, with outer race fault data assigned to $y = +1$, other data assigned to $y = -1$. In the same work, CRSVM4 was designed to identify roller element faults of bearings. To evaluate the performance of the diagnosis technique based on the proposed GDA-CRSVM method, the SVM was adopted to perform bearing condition diagnosis. This is a traditional model, with the parameter set selected to follow experience at $C = 200, d = 1$. These classifiers were trained on both the reduced feature set and the original MAF set to evaluate the recognition accuracy results and time of diagnosis.

Table 3 shows the MAF-GDA-CRSVM diagnosis techniques. They were designed to identify the different bearing conditions of the first dataset based on MAF and the proposed GDA-CRSVM method. In the experimentation in this dataset, these classifiers were trained with the reduced feature set, with 18 samples per class selected randomly as the training set, meaning 72 samples were collected as the training set. They were used to calculate the deterioration function Eq. (13) and construct the optimized classifiers. The seven rest samples per class were used to test the obtained classifier with the best parameters. The archived diagnosis results for bearing conditions are shown in Tables 4 and 5.

To demonstrate the effectiveness of the MAF-GDA-CRSVM diagnosis technique, we designed diagnosis models based on GDA-CRSVM to identify bearing conditions of the second dataset in Table 6. Similar to the process for the first dataset, the bearing fault diagnosis results are listed in Tables 7 and 8.

Table 3 The MAF-GDA-CRSVM diagnosis technique of the first dataset.

Bearing condition	A sample feature vector			Diagnosis technique			
				MAF-GDA-CRSVM1	MAF-GDA-CRSVM2	MAF-GDA-CRSVM3	MAF-GDA-CRSVM4
HB	-53.2173	0.2071	0.1407	(+1)	(-1)	(-1)	(-1)
IR fault	49.6764	8.0919	-0.2715	(-1)	(+1)	(-1)	(-1)
OR fault	35.4594	-8.7378	0.8780	(-1)	(-1)	(+1)	(-1)
RE fault	-31.0524	2.6843	-0.4135	(-1)	(-1)	(-1)	(+1)

Table 4 The diagnosis accuracy result (%) of first dataset with various feature sets

Bearing condition	Samples		Original feature set		Reduction feature set	
	Training	Test	SVM	CRSVM	GDA-SVM	GDA-CRSVM
HB	72	28	75	99.35	98.70	100
IR fault	72	28	75	97.08	92.85	99.03
OR fault	72	28	75	96.42	85.71	99.67
RE fault	72	28	75	88.63	96.42	98.70

Table 5 The time cost (s) of first dataset with various feature sets

Bearing condition	Original feature set		Reduction feature set	
	SVM	CRSVM	GDA-SVM	GDA-CRSVM
HB	1.3249	1.4095	1.2473	1.3035
IR fault	1.1137	1.4454	1.0277	1.0883
OR fault	0.9838	1.4490	0.9833	1.2997
RE fault	0.8671	1.5266	0.8869	1.5039

According to these results, the MAF set extracted from original vibration signals can cope well with both the SVM and CRSVM diagnosis models for all four bearing conditions. The use of all input features does not ensure an improvement in the classification accuracy results for the various classifiers. In fact, the diagnosis accuracy results in Tables 4, 7 shown that evaluation on the conventional SVM model with the high-dimensional feature set obtained the very poor accuracy, the accuracy is only 75 % in every bearing condition. Thus, this diagnosis technique usually tends to produce a rejection and not reuse the model. It should be emphasized that the low-

dimensional feature set gained from GDA generated the better results in comparison with high-dimensional feature set by the same SVM models, the accuracy got maximum of 98.70 % for the first dataset and getting maximum of 90 % for the second dataset.

Additionally, in this work, we explored the CRSVM model to exploit accuracy results for classification purpose. The CRSVM model has achieved good diagnosis accuracy result in the healthy bearing (HB) and inner race (IR) fault conditions even with using the high-dimensional feature set. Thus, this CRSVM model is more appropriate with diagnosis technique for individual condition of bearing. In particular, Table 4 and 7 also showed that the proposed GDA-CRSVM-based diagnosis technique provides the best results for most bearing conditions. Its meaning that GDA method generated the compact feature set that inputted the optimized CRSVM classification model in integrating to produce effectiveness. Consequently, this diagnosis technique can be more used in the mechanical engineering environment to satisfy with the expected results. Fig. 12, 13 presented the results in comparison the proposed method with the other methods.

Moreover, the execution time of the CRSVM classifier for bearing fault diagnosis is faster than other classifiers for both the original feature set and the reduced feature set, as the results show in Tables 5 and 8. The considerable usefulness of reducing the original input feature space defined by the GDA was combined with the optimal classifier CRSVM to build an expert bearing fault diagnosis technique.

Table 6 The MAF-GDA-CRSVM diagnosis technique of the second dataset

Bearing condition	A sample feature vector			Diagnosis technique		
				MAF-GDA-CRSVM1	MAF-GDA-CRSVM2	MAF-GDA-CRSVM4
HB	-52.6982	0.2977	-5.8266	(+1)	(-1)	(-1)
IR fault	15.0308	-2.0533	-1.4911	(-1)	(+1)	(-1)
RE fault	-25.3478	0.9476	9.9225	(-1)	(-1)	(+1)

Table 7 The diagnosis accuracy result (%) of second dataset with various feature sets

Bearing condition	Samples		Original feature set		Reduction feature set	
	Training	Test	SVM	CRSVM	GDA-SVM	GDA-CRSVM
HB	30	15	75	99.09	90	100
IR fault	30	15	75	95.45	86.81	96.82
RE fault	30	15	75	93.18	87.27	95

Table 8 The time cost (s) of second dataset with various feature sets

Bearing condition	Original feature set		Reduction feature set	
	SVM	CRSVM	GDA-SVM	GDA-CRSVM
HB	1.0190	1.0456	0.8793	1.0240
IR fault	1.0800	1.1376	0.9420	1.1522
RE fault	1.0495	1.1607	0.8901	0.9278

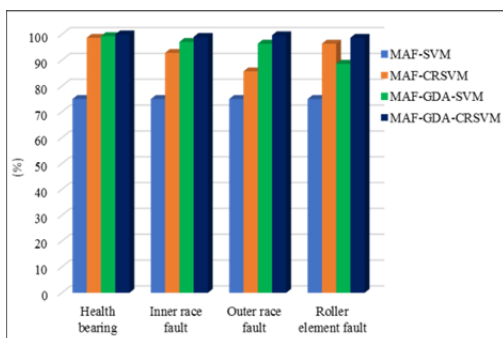


Fig.12 The classification accuracy of different diagnosis techniques for the first dataset

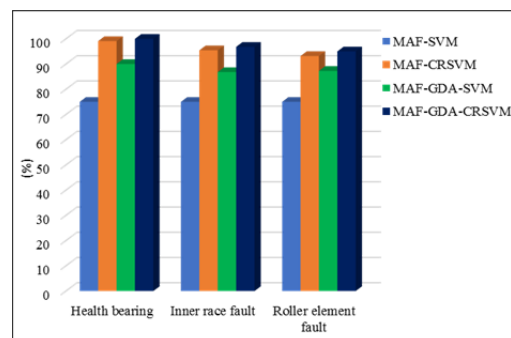


Fig.13 The classification accuracy of different diagnosis techniques for the second dataset

5. Conclusion

In this paper, a GDA-CRSVM-based expert fault diagnosis technique is proposed. The GDA-CRSVM method is a two-stage hybrid method that integrates GDA with CRSVM for an expert diagnosis technique. The original vibration dataset is firstly extracted the high-dimensional feature set by the MAF extraction. This feature set then provides GDA-CRSVM, in which the GDA method exploits to produce a reduced feature set which serves as input to the CRSVM classification model. The most of reduced feature set is used for training the optimized CRSVM classifier and the rest use for evaluation. The experimental results demonstrate the high efficiency of the proposed method and its expertness in bearing fault diagnosis.

In fact, the MAF extraction produces features in the different domain to represent the bearing status which can restrain the effect of proposed method. Furthermore, the proposed method capacity can be restricted due to the operating of GDA method depends on the classes label which reveals the non-objective condition in supervised feature learning. Thus, a feature reduction method is very useful and necessary for un-supervised feature learning in the future. Nevertheless, we have unshaken confidence that the GDA-CRSVM method can help to improve the fault classification performance of any diagnosis technique with different subjects. The practical applications of GDA-CRSVM is enquired and attached the most of features corresponding to the real subject status.

Acknowledgements

This research is supported by the National Key Research and Development Program of China (2016YFF0203400), and the National Natural Science Foundation of China (51575168 and 51375152). The authors would also like to thank the Collaborative Innovation Center of Intelligent New Energy Vehicles and the Hunan Collaborative Innovation Center for Green Car for support.

References

- [1] Zheng, J., Cheng, J., Yang, Y (2013). A rolling bearing fault diagnosis approach based on LCD and fuzzy entropy, *Mechanism and Machine Theory*, Vol. 70, 441-453, doi: [10.1016/j.mechmachtheory.2013.08.014](https://doi.org/10.1016/j.mechmachtheory.2013.08.014).
- [2] Liu, H., Wang, X., Lu, C. (2015). Rolling bearing fault diagnosis based on LCD-TEO and multifractal detrended fluctuation analysis, *Mechanical Systems and Signal Processing*, Vol. 60-61, 273-288, doi: [10.1016/j.ymssp.2015.02.002](https://doi.org/10.1016/j.ymssp.2015.02.002).
- [3] Chen, J., Liao, C.-M. (2002). Dynamic process fault monitoring based on neural network and PCA, *Journal of Process Control*, Vol. 12, No. 2, 277-289, doi: [10.1016/S0959-1524\(01\)00027-0](https://doi.org/10.1016/S0959-1524(01)00027-0).
- [4] Jolliffe, I.T. (2010). *Principal Component Analysis, Second Edition*, Springer, New York, USA.
- [5] Cox, T.F., Cox, M.A.A. (1994). *Multidimensional Scaling, Second Edition*, Chapman & Hall, London, UK.
- [6] Martinez, A.M., Kak, A.C. (2001). PCA versus LDA, *IEEE Transactions on Pattern Analysis and Machine Intelligence*, Vol. 23, No. 2, 228-233, doi: [10.1109/34.908974](https://doi.org/10.1109/34.908974).
- [7] Belhumeur, P.N., Hespanha, J.P., Kriegman, D.J. (1997). Eigenfaces vs. Fisherfaces: Recognition using class specific linear projection, *IEEE Transactions on Pattern Analysis and Machine Intelligence*, Vol. 19, No. 7, 711-720, doi: [10.1109/34.598228](https://doi.org/10.1109/34.598228).
- [8] Baudat, G., Anouar, F. (2000). Generalized discriminant analysis using a kernel approach, *Neural Computation*, Vol. 12, No. 10, 2385-2404, doi: [10.1162/089976600300014980](https://doi.org/10.1162/089976600300014980).
- [9] Dogantekin, E., Dogantekin, A., Avci, D. (2011). An expert system based on generalized discriminant analysis and wavelet support vector machine for diagnosis of thyroid diseases, *Expert Systems with Applications*, Vol. 38, No. 1, 146-150, doi: [10.1016/j.eswa.2010.06.029](https://doi.org/10.1016/j.eswa.2010.06.029).
- [10] Li, C.-H., Kuo, B.-C., Lin, L.-H., Wu, W., Lan, D. (2013). Apply an automatic parameter selection method to generalized discriminant analysis with RBF kernel for hyperspectral image classification, In: *2013 International Conference on Machine Learning and Cybernetics*, Tianjin, China, 253-258, doi: [10.1109/ICMLC.2013.6890477](https://doi.org/10.1109/ICMLC.2013.6890477).
- [11] Abbasion, S., Rafsanjani, A., Farshidianfar, A., Irani, N. (2007). Rolling element bearings multi-fault classification based on the wavelet denoising and support vector machine, *Mechanical Systems and Signal Processing*, Vol. 21, No. 7, 2933-2945, doi: [10.1016/j.ymssp.2007.02.003](https://doi.org/10.1016/j.ymssp.2007.02.003).
- [12] Lau, K.W., Wu, Q.H. (2008). Local prediction of non-linear time series using support vector regression, *Pattern Recognition*, Vol. 41, No. 5, 1539-1547, doi: [10.1016/j.patcog.2007.08.013](https://doi.org/10.1016/j.patcog.2007.08.013).

- [13] Pelossof, R., Miller, A., Allen, P., Jebara, T. (2004). An SVM learning approach to robotic grasping, In: *2004 IEEE International Conference on Robotics and Automation, 2004, Proceedings. ICRA '04.*, Vol. 4, 3512-3518, doi: [10.1109/ROBOT.2004.1308797](https://doi.org/10.1109/ROBOT.2004.1308797).
- [14] Gryllias, K.C., Antoniadis, I.A. (2012). A support vector machine approach based on physical model training for rolling element bearing fault detection in industrial environments, *Engineering Applications of Artificial Intelligence*, Vol. 25, No. 2, 326-344, doi: [10.1016/j.engappai.2011.09.010](https://doi.org/10.1016/j.engappai.2011.09.010).
- [15] Samanta, B. (2004). Gear fault detection using artificial neural networks and support vector machines with genetic algorithms, *Mechanical Systems and Signal Processing*, Vol. 18, No. 3, 625-644, doi: [10.1016/S0888-3270\(03\)00020-7](https://doi.org/10.1016/S0888-3270(03)00020-7).
- [16] Dou, D., Zhou, S. (2016). Comparison of four direct classification methods for intelligent fault diagnosis of rotating machinery, *Applied Soft Computing*, Vol. 46, 459-468, doi: [10.1016/j.asoc.2016.05.015](https://doi.org/10.1016/j.asoc.2016.05.015).
- [17] Zhang, X., Chen, W., Wang, B., Chen, X. (2015). Intelligent fault diagnosis of rotating machinery using support vector machine with ant colony algorithm for synchronous feature selection and parameter optimization, *Neurocomputing*, Vol. 167, 260-279, doi: [10.1016/j.neucom.2015.04.069](https://doi.org/10.1016/j.neucom.2015.04.069).
- [18] Gomes, T.A.F., Prudêncio, R.B.C., Soares, C., Rossi, A.L.D., Carvalho, A. (2012). Combining meta-learning and search techniques to select parameters for support vector machines, *Neurocomputing*, Vol. 75, No. 1, 3-13, doi: [10.1016/j.neucom.2011.07.005](https://doi.org/10.1016/j.neucom.2011.07.005).
- [19] Yang, D., Liu, Y., Li, S., Li, X., Ma, L. (2015). Gear fault diagnosis based on support vector machine optimized by artificial bee colony algorithm, *Mechanism and Machine Theory*, Vol. 90, 219-229, doi: [10.1016/j.mechmachtheory.2015.03.013](https://doi.org/10.1016/j.mechmachtheory.2015.03.013).
- [20] Lam, A.Y.S., Li, V.O.K. (2010). Chemical-Reaction-Inspired Metaheuristic for Optimization, *IEEE Transactions on Evolutionary Computation*, Vol. 14, No. 3, 381-399, doi: [10.1109/TEVC.2009.2033580](https://doi.org/10.1109/TEVC.2009.2033580).
- [21] Alatas, B. (2012). A novel chemistry based metaheuristic optimization method for mining of classification rules, *Expert Systems with Applications*, Vol. 39, No. 2, 11080-11088, doi: [10.1016/j.eswa.2012.03.066](https://doi.org/10.1016/j.eswa.2012.03.066).
- [22] Li, J.-Q., Pan, Q.-K. (2013). Chemical-reaction optimization for solving fuzzy job-shop scheduling problem with flexible maintenance activities, *International Journal of Production Economics*, Vol. 145, No. 1, 4-17, doi: [10.1016/j.ijpe.2012.11.005](https://doi.org/10.1016/j.ijpe.2012.11.005).
- [23] Lam, A.Y.S., Li, V.O.K. (2012). Chemical reaction optimization: A tutorial, *Memetic Computing*, Vol. 4, No. 1, 3-17, doi: [10.1007/s12293-012-0075-1](https://doi.org/10.1007/s12293-012-0075-1).
- [24] Vapnik, V.N. (1995). *The Nature of Statistical Learning Theory*, Springer, New York, USA, doi: [10.1007/978-1-4757-2440-0](https://doi.org/10.1007/978-1-4757-2440-0).
- [25] Yu, Y., YuDejie, Junsheng, C. (2006). A roller bearing fault diagnosis method based on EMD energy entropy and ANN, *Journal of Sound and Vibration*, Vol. 294, No. 1-2, 269-277, doi: [10.1016/j.jsv.2005.11.002](https://doi.org/10.1016/j.jsv.2005.11.002).

Improving workforce scheduling using artificial neural networks model

Simeunović, N.^a, Kamenko, I.^a, Bugarski, V.^a, Jovanović, M.^a, Lalić, B.^{a,*}

^aUniversity of Novi Sad, Faculty of Technical Sciences, Novi Sad, Serbia

ABSTRACT

This paper demonstrates a decision support tool for workforce planning and scheduling. The research conducted in this study is oriented on batch type production typical for smaller production systems, workshops and service systems. The derived model in the research is based on historical data from Public utility service billing company. Model uses Artificial Neural Networks (ANN) fitting techniques. A set of eight input indicators is designed and two variants were tested in the model with two different outputs. Several comprehensive parameter setting experiments were performed to improve prediction performances. Real case studies using historic data from public weather database and communal consolidated billing service show that it is difficult to predict the required number of servers-workers in front office. In a similar way, this model is adequate for complex production systems with unpredictable and volatile demand. Therefore, manufacturing systems which create short cycle products, typical for food processing industry, or production for inventory, may benefit of the research presented in this paper. ANN simulation model with its unique set of features and chosen set of training parameters illustrate that presented model may serve as a valuable decision support system in workforce scheduling for service and production systems.

© 2017 PEI, University of Maribor. All rights reserved.

ARTICLE INFO

Keywords:
Workforce scheduling
Production planning
ANN prediction
Operations management

**Corresponding author:*
blalic@uns.ac.rs
(Lalić, B.)

Article history:
Received 6 June 2017
Revised 15 September 2017
Accepted 8 November 2017

1. Introduction

In recent years artificial intelligence is increasingly used to solve optimisation problems in scheduling or timetabling [1]. The skilled Workforce Project Scheduling is a complex problem of resource assignments and task scheduling that are performed on daily bases in service centres [2]. Internal, as well as external, part of the service processes has to be performed as a whole with planned level of quality and efficiency. The aim of the paper is to demonstrate an example of workforce planning and scheduling, predicting the need of products and services, which has direct implication on operation manager's tasks such as: production process planning, design and management, logistics management, quality management and productivity improvement[3]. Chopra *et al.* defines the area of operational management as a planning and management of transformation processes which contribute to creation of social value [4]. Previous statements demonstrate that there is no strict limitation between production and service delivery [3], but is clear that efficient management of organizational resources have a positive effect on successfully reaching organizational goals.

Services are intangible and customers participate actively or passively in the service delivery process [5]. Waiting is inevitable in any service delivery process that involves some type of randomness like random arrival. Workforce management (WFM) systems are automated tools

which allow workforce to be managed more effectively and efficiently [6]. Workforce management systems may be observed as an IT systems driving the organizational innovation in workforce scheduling [7]. Workforce management tools enable the capability of the Company to increase the level of the productivity [8].

Experience based workforce scheduling is the simplest way of planning. In order to achieve flexibility and high responsiveness towards the client needs, different ways of planning methods and use of real time data may be used to improve the service process. Rather than solely plan driven approach, creating monthly or bi-annual plans of workforce scheduling, iterative and real time planning could be used as an alternative. Iterative planning is implemented through shorter iteration cycles (daily or weekly planning) and it requires a decision support system based on the real time data, predicting the estimation of the number of the clients to be attended by the production or service system, which is at the same time designed with satisfactory error level. Therefore, to able to plan more efficiently, and to be able to respond to unexpected changes in service demand, decision support tool should be developed and customized according to the Company needs. One way of achieving the solution for this problem is to develop Artificial Neural Network (ANN) prediction model to be used by workforce project scheduling manager.

Majority of demand prediction issues, especially in production systems oriented on lean approach and Just in Time (JIT) concept, may be resolved if the model proposed in this research would be used. Inputs for this kind of model may be multiple variables such as product demand, consumer income, product price range etc. These variables directly influence and should be incorporated in algorithm for product demand prediction. In this research study the focus is on product and service prediction which depend on seasonal parameters – weather condition. The model may be successfully used to reduce early risks in supply chain management. Early risks and uncertainties exists in demand prediction, capacity planning, time delivery estimation, and production cost estimation [9].

This study is motivated by the challenge to predict as accurately as possible the number of required servers in Public Billing Service Company, using weather forecast and historical transactions data, underlying on methodology of ANN. By predicting the expected number of servers on daily bases, management of the Company can direct and transfer employees from back-end to front-end office and vice versa. In this manner, operational efficiency would be improved and employees would be working with clients in the front-end office, or would be directed to the background activities.

The research objective of this paper was to explore if appropriate neural network decision support system could be developed for the needs of Public Utility Company billing department. Use of WFM system in a supermarket chain is presented by Mirrazavi and Beringer [10], and in their work system allowing the demand to be precisely estimated. Aicklein and Dowsland [1] used genetic algorithms for resolving scheduling problems in medical industry. Their intention was to develop a fast and flexible solution to nurse scheduling problem. Group of authors presented a hybrid genetic algorithm for solving scheduling problem in service centers with genetic algorithm as a decision support tool [2]. Application of Particle Swarm Optimization algorithm for scheduling of home care workers in UK showed promising results in terms of effective and efficient scheduling of employees [11]. Support Vector Machine may be used well to predict thermal comfort of visitors in public areas, and group of authors showed that certain climate factors can be well related to predict the comfort of visitors [12]. Rebai *et al.* [13] considered a problem of scheduling production jobs on parallel machines in production, and have minimized the job completion time with genetic algorithms. Nissen and Günther [14] also used Particle Swarm Optimization algorithm for day to day workforce scheduling, as the way to improve productivity. Workforce scheduling is very important part of operations management and a crucial for a good organization management [15]. As the reports suggest, in Germany (which is considered highly productive country) employees spend up to 36 % of their work time unproductively, depending on the branch [16]. In most cases the usual tools for planning are prior experience and spreadsheets [17]. Different decisions support models for the workforce scheduling are identified in the research literature but due to specificity of the observed system of the Pub-

lic Utility Company billing process it was necessary to develop a new customized solution to be used for this case.

Literature review

This section summarizes previous work scientific literature in the fields of: production and service systems, workforce scheduling and advanced technologies in workforce scheduling.

Production and service systems

In this paper we discuss workforce capacity management and operational distribution of the workforce in service and production systems. According the Schroeder production systems may be classified by the process type on: line systems, batch and project oriented production [18]. The research conducted in this study is oriented on batch type production which is typical for smaller production systems and workshops. Over the years there was a disagreement whether the service is a product or not and what is the difference between service and products [19]. According to the ISO 9001:2015 standard [20] service is defined as one of the four types of products, and their main characteristics are defined also. First characteristic is that service is intangible [21], although some authors tend to disagree with this [22]. Second characteristic is that services cannot be stock piled. Third characteristic states that it is impossible to separate the client getting the service and the service itself. Fourth characteristic is involvement of the client in the service process or the making of the service. Fifth characteristic is referred to as a service level quality in this paper, and it states that services are perishable goods, and they don't tolerate waiting [21]. If the service is received latter then expected the client will rate its quality lower, even if everything else was on the level that was expected by the client [23]. The quality of the service is correlated with the moment when the service is delivered [24]. Creating service experience-point of service starts at the first moment when the client gets in touch with service provider, interior of the place where service is provided, rules and terms of engagement [25], [26]. Numerous factors influence service experience such as interaction with employees [27], psychology and behavior of distribution personnel in direct contact with customers [28], and client waiting time in queue for the service [29].

Workforce scheduling

The impact of workforce scheduling system is very severe in terms of both quality of the service, and productivity [6], and not having a workforce scheduling system can be potentially disastrous for the company. In the transitional economies where Public Utility Companies are still self-centred instead of being client-centred, the inefficiency will signal for competition from private sector [30]. While having an workforce scheduling system based on experience can be appropriate prediction tool until certain extent, there are obviously limitations in terms of system size and ever-changing client demands [8]. Billing companies by the nature of their work have a negative connotation for the clients, service productivity should be in focus, while also having in mind clients waiting time [7]. Also there should be not worries about dip in productivity while rotation [31] as both front-end office and back-end office are equally demanding [2]. As with other service companies the key to successful work scheduling system is the prediction of client numbers [8] for each day in advance, and this is where artificial neural networks can help.

Advanced technologies in workforce scheduling

Soft computing methods such as artificial neural networks (ANN) have been successfully used for forecasting and decision-making [32]. In service systems, ANN have been applied mostly in simulation models [33]. Altiparmaket *at al.* [34] presented advantages of ANN metamodeling approach in modelling of asynchronous assembly systems. One good example of ANN application in predicting the accumulation of clients is published in [35] where ANN is used for forecasting patient length of stay in an emergency department. Not many cases of artificial neural networks (ANN) used as a decision support tool for short term planning in service systems can be found in research literature. Most of the research has been done in the field of medicine, specifically emergency medicine, where ANN was used to determine the length of stay of patients in

emergency departments. The model shows around 80 % of accuracy with 5 predictors. Gul *at al.* [35] also used ANN as a tool for predicting patient length of stay at intensive care. Candan *at al.* [36] used neuro-fuzzy ANN to create model that they used to predict demand in pharmaceutical industry. Milović *at al.* [37] used data mining to create decision support tool for hospital management. Different methods have been used for workforce scheduling such as PSO-based algorithm [11], indirect genetic algorithm [1], genetic algorithm [38] and others [8]. Other researchers used discreet event simulation model for capacity planning in emergency medical departments [39], [40]. All these researches create a prediction tool used for different goals like queue management, capacity management and workforce scheduling and rotation.

The rest of the paper is organized into seven sections. Section 2 defines the problem. Section 3 presents prior related research. Section 4 describes the research data. Section 5 discusses the ANN prediction model. In Section 6, the empirical results are summarized and discussed. Section 7 contains the concluding remarks and future work. Finally, references are listed in Section 8.

2. Problem definition

The problem to be tackled in this paper can be described as follows. The task is to create weekly schedule with daily updates if significant changes in input parameters are identified. The proposed schedule has to satisfy employee contracts and meet the forecasted demand of clients to be served by the Public Utility Company billing system. In other words, internal optimization of the systems (shifting employees between front-end and back-end office) should not decrease the expected service level quality measured by waiting time of the client, on the contrary, the service level quality level should be increased from the perspective of the client. When operating performance improved, sooner or later results are converted into profits [41]. In the Fig. 1 billing service process in the Public Utility Company is shown.

Scheduling manager should plan in the most efficient way the distribution of employees between the front-end office and back-end office. As the bills usually arrive in the first week of the month, the company can expect the most of the clients coming to their office to pay the bills at that time, and based on workers' previous experience workforce scheduling was planned based on this parameter. Bills are sent out on 6th or 7th of the month and majority of clients are expected to arrive in the front office around 15th of the month, therefore during those days' extra workers are allocated to the front-end office. However, many factors affect the behavior of clients coming to the front office to pay their bills. For instance, weather conditions, holidays, days of the week, are some of the most important factors affecting the clients. Research objective of this paper is to create a decision support tool, the artificial neural network system that would be able to predict the precise number of clients on daily bases (with acceptable error level) to be served in the billing process of Public Utility Company.

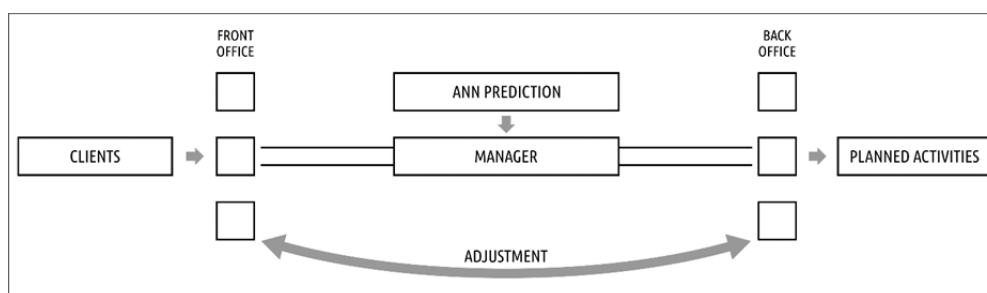


Fig. 1 Billing service process in the Company

Research data

This section presents the volume and origin of the research data and describes the selection of useful indicators for accurate prediction. The research data used in this study include publicly available daily weather information and historical transaction data from a Public Service Billing Company in period of one year (Fig. 2). The total number of cases is 393 days during one-year

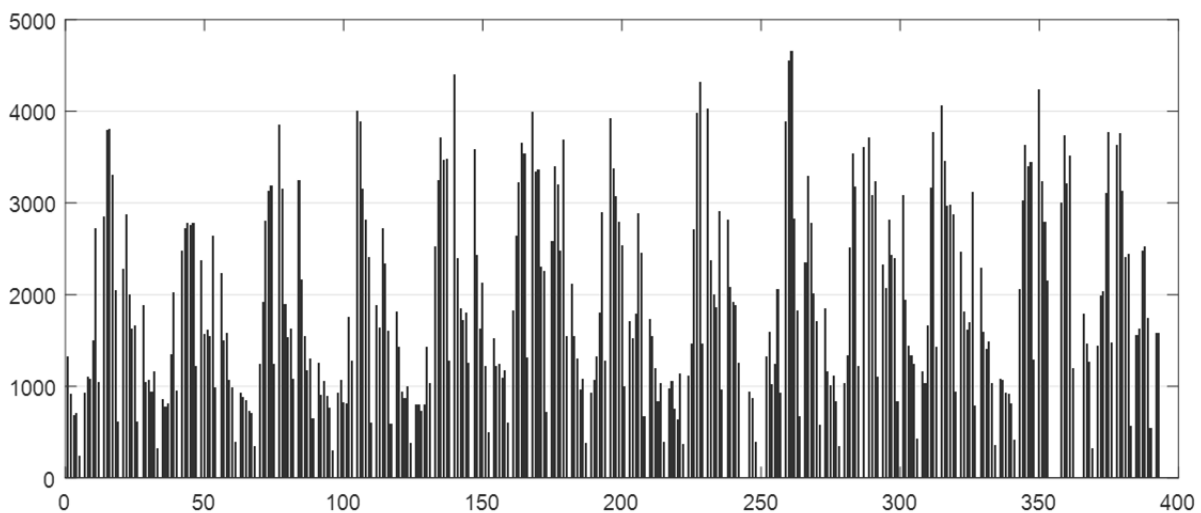
Table 1 Classification of the research data set

Subset	Time period (YYYY-MM-DD)	Number of days (samples)			Total	Percentage
		Full working time	Reduced working time	Nonworking day		
Training	2015-05-04 to 2016-03-31	235	45	52	332	84.48
Validation	2016-04-01 to 2016-05-08	22	5	11	38	9.67
Test	2016-05-09 to 2016-05-31	17	3	3	23	5.85
Total	2015-05-04 to 2016-05-31	274	53	66	393	100

period (from May 4 2015 to May 31 2016). Data set is classified on subsets (training, validation and test) and on type of working days in Table 1. The Public Billing Service Company operate in full working time (12.5 h) from Monday to Friday, in reduced working time (7 h) on Saturdays, while Sundays and National holidays are nonworking days.

From Fig. 2 it can be concluded that from there are very high oscillation on daily bases in number of transactions. Number of transactions per day ranges from to 245 to 4657 transactions per day. A lot of external factor affect the number of customers, and number of transactions in an observed day. The most influencing factor are weather conditions (rainfalls, very high and very low temperatures, thunderstorms etc.). The factor that has also very high influence is day in week, and day in month because payment deadline for communal bills is 20th in month, and during that period peak in number of customers can be expected. Training subset is presented to the network during training, and the network parameters are adjusted according to its error.

Validation subset is used to measure network generalization, and to halt training when generalization stops improving. Test subset has no effect on training and so provide an independent measure of network performance after training.

**Fig. 2** Number of transactions per day

Weather data

The weather conditions data are downloaded from the public historic weather data database. Data is derived from the nearest weather station for the same date range that fits date range used for number of transactions. Data of interests are temperature, relative humidity, pressure at sea level, wind speed and current weather events.

Data are measured eight times per day. Data about temperature, relative humidity, pressure at sea level and wind speed are averaged over working time for the day of interest. For weather event that describes observed day, the worst measured event is adopted.

Indicators

Indicators are calculated based on the number of transactions and weather conditions data. Indicators on the better way represent and emphasis characteristic of real data. Average number of transactions per day during week

$$\mu_j = \frac{1}{m} \sum_{i=1}^m TranNum_{i=j} \quad (1)$$

where j is an observed day in week, i is a current day in week and $TranNum_{i=j}$ is vector made up of m data samples of number of transactions where the current day in week is equals to the observed day in week.

Average number of transactions per day in month is calculated by Eq. 1 where j is an observed day in month, i is a current day in month and $TranNum_{i=j}$ is vector made up of m data samples of number of transactions where the current day in month is equals to the observed day in month.

Temperature index is calculated based on tree following equations that are proposed in [42]:

$$tempIndex = \begin{cases} 10 - heatIndex & T > 27 \\ 10 & 10 \leq T \leq 27 \\ 10 - windChill & T < 10 \end{cases} \quad (2)$$

$$heatIndex = -8.78 + 1.61T + 2.34H - 0.15TH - 1.23 \cdot 10^{-2}T^2 - 1.64 \cdot 10^{-2}H^2 + 2.21 \cdot 10^{-3}HT^2 + 7.25 \cdot 10^{-4}TH^2 - 3.58 \cdot 10^{-6}T^2H^2 \quad (3)$$

$$windChill = 13.13 + 0.62T - 13.95W_s^{0.16} + 0.486TW_s^{0.16} \quad (4)$$

where T is a temperature, H is a humidity and W_s is a wind speed.

Humidity index is calculated from relative humidity based on following equation.

$$humidityIndex = \begin{cases} H & P_{SL} < 40 \\ 40 & 40 \leq P_{SL} \leq 60 \\ 100 - H & T > 60 \end{cases} \quad (5)$$

Graphic representation of Eq. 5 is shown on Fig. 3:

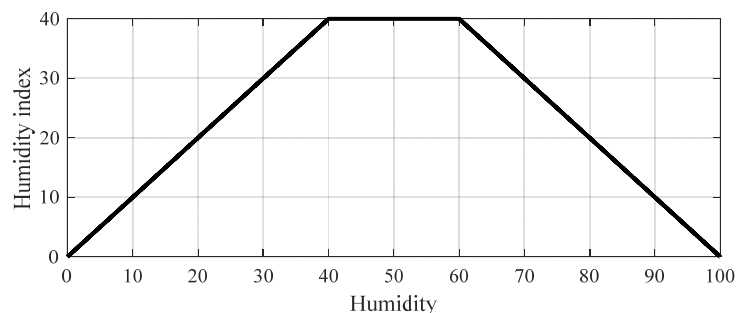


Fig. 3 Humidity index

Pressure index is calculated from pressure at sea level based on following equation:

$$pressureIndex = \begin{cases} 15 & P_{SL} > 1013.25 \\ P_{SL} - 1013.25 & 998.25 \leq P_{SL} \leq 1013.25 \\ 0 & T < 998.25 \end{cases} \quad (6)$$

Weather conditions are gradually coded starting with 1 representing the worst conditions (thunderstorms and rain) ending with 40 representing the good weather conditions (clear). Table 2 displays codes for particular weather conditions.

Table 2 Weather condition coding

Weather condition	Code
Thunderstorms and rain	1
Thunderstorm	2
Light thunderstorm	3
Light sandstorm	4
Light freezing rain	5
Heavy fog	6
Rain	10
Light rain showers	11
Light rain	12
Snow	13
Light snow	14
Light drizzle	15
Partial fog	20
Light fog	21
Mist	22
Overcast	30
Mostly Cloudy	31
Partly Cloudy	32
Scattered Clouds	33
Clear	40

Statistical parameters

Statistical parameters are calculated for all indicators and are presented in the Table 3.

Table 3 Statistical parameters of research data

Name of indicator	Min.	Max.	Mean	Std. dev.	Kurtosis	Skewness
Working hours	7.00	12.50	11.61	2.03	4.36	-1.83
Avg. trans. per day in week	812.51	2,276.34	1,886.60	481.54	4.12	-1.69
Avg. trans. per day in month	825.55	3,208.82	1,886.60	744.05	1.91	0.20
Temp. index	0.00	10.00	8.14	2.79	2.97	-1.18
Humidity index	1.00	40.00	29.29	11.12	2.25	-0.73
Pressure index	0.00	15.00	13.48	3.03	9.71	-2.57
Wind speed	0.72	32.40	8.31	5.17	5.83	1.52
Weather conditions	11.80	50.00	30.41	7.95	2.66	-0.24
Number of transactions	245.00	4,657.00	1,886.60	1,044.19	2.28	0.56
Number of servers	1.00	7.00	3.41	1.46	2.27	0.48

Mean value is calculated based on equation:

$$\mu = \frac{1}{n} \sum_{i=1}^n I_i \tag{7}$$

where I is vector made up of n data samples of observed indicator.

Standard deviation is calculated based on equation:

$$\sigma = \frac{1}{n} \sqrt{\frac{1}{n-1} \sum_{i=1}^n |I_i - \mu|^2} \tag{8}$$

where I is vector made up of n data samples of observed indicator and μ is mean value of I .

Kurtosis is a measure of how outlier-prone a distribution is and is calculated based on equation:

$$k = \frac{E(I - \mu)^4}{\sigma^4} \quad (9)$$

Skewness is a measure of the asymmetry of the data around the sample mean and is calculated based on equation:

$$S = \frac{E(I - \mu)^3}{\sigma^3} \quad (10)$$

In both equations (Eq. 9 and 10) I represents vector made up of n data samples of observed indicator, μ is mean value of I , σ is standard deviation of I and $E(t)$ represents the expected value of the quantity t .

3. ANN prediction model

Neuron is the basic process element of ANN. Model of one neuron can be seen in Fig. 4. Generally speaking neuron has n inputs labeled with x_i ($i = 1, 2, 3, \dots, n$) that represents source of input signal. Every inputs are weighted with w_i before reach the body of process element. In process element all weighted inputs and bias w_0 are summarized. Activation signal R_i gets a value of summation if a sum is greater than threshold θ_i otherwise activation signal becomes zero. Activation signal R_i further leads to nonlinear function f_i . The output of nonlinear function is the output of neuron O_i . The functional depending from input to output for one neuron is given in following equation:

$$O_i = f_i \left(\sum_{j=1}^n w_{ij} x_{ij} + w_0 \right) \quad (11)$$

$$\sum_{j=1}^n w_{ij} x_{ij} + w_0 \geq \theta_i$$

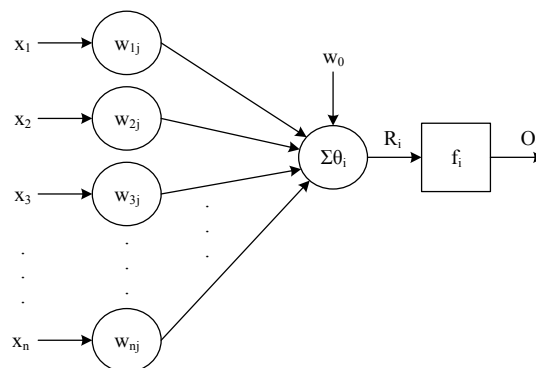


Fig. 4 A model of one neuron

In this research, two-layer feed-forward Artificial Neural Network with sigmoid hidden neurons (white circles in Fig. 6) and linear output neurons (gray circles in Fig. 6) is composed for prediction of required number of servers in billing service. Network inputs are carefully designed as eight indicators with greatest impact on prediction performance.

Two different training sets are created for ANN training experiments. First training set is created to train the network to predict the number of transactions, from which is later calculated the number of required servers. This calculation takes into consideration the number of working hours (the next working day) and statistical average number of transactions per server. One server can process up to 55 transactions per hour. Statistical average number of transactions per server is calculated as 688 (55×12.5) transactions for full working time (12.5 h) and 385 (55×7) transactions for reduced working time (7 h). The correlation between number of transactions and number of servers is given in following equation:

$$\text{ServNum} = \begin{cases} 1, & 1 \leq \text{TranNum} \leq 688 \text{ (385)} \\ 2, & 689 \text{ (386)} \leq \text{TranNum} \leq 1375 \text{ (770)} \\ 3, & 1376 \text{ (771)} \leq \text{TranNum} \leq 2063 \text{ (1155)} \\ 4, & 2064 \text{ (1156)} \leq \text{TranNum} \leq 2750 \text{ (1540)} \\ 5, & 2751 \text{ (1541)} \leq \text{TranNum} \leq 3438 \text{ (1925)} \\ 6, & 3439 \text{ (1926)} \leq \text{TranNum} \leq 4125 \text{ (2310)} \\ 7, & 4126 \text{ (2311)} \leq \text{TranNum} \leq 4813 \text{ (2695)} \end{cases} \quad (12)$$

where *ServNum* is calculated number of servers and *TranNum* is number of transactions. Graphical representation of this equation is shown in Fig. 5. In brackets is given number of transactions for day with reduced working time (Saturdays).

The second idea was to train the network to predict the number of required servers directly. For that case, desired output column of training set was recalculated using Eq. 11.

The architecture of the prediction model is illustrated in Fig. 6. The number of neurons in hidden layer is determined empirically. The output layer consists of just one neuron with a purpose to return the predicted number of transactions that will occur next day. Prediction model uses the output of the ANN to calculate the required number of servers for the next working day.

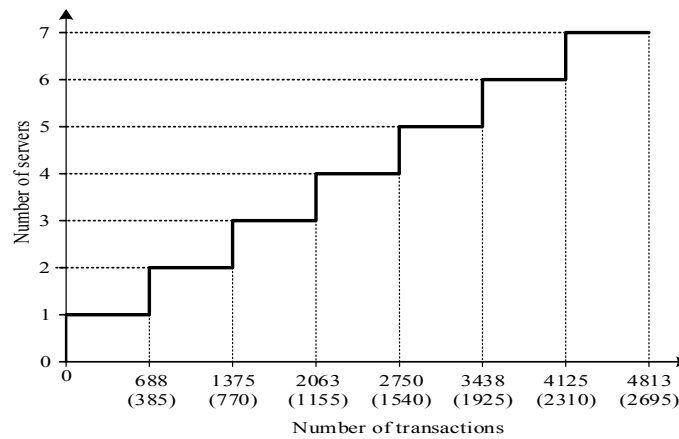


Fig. 5 Ceiling function

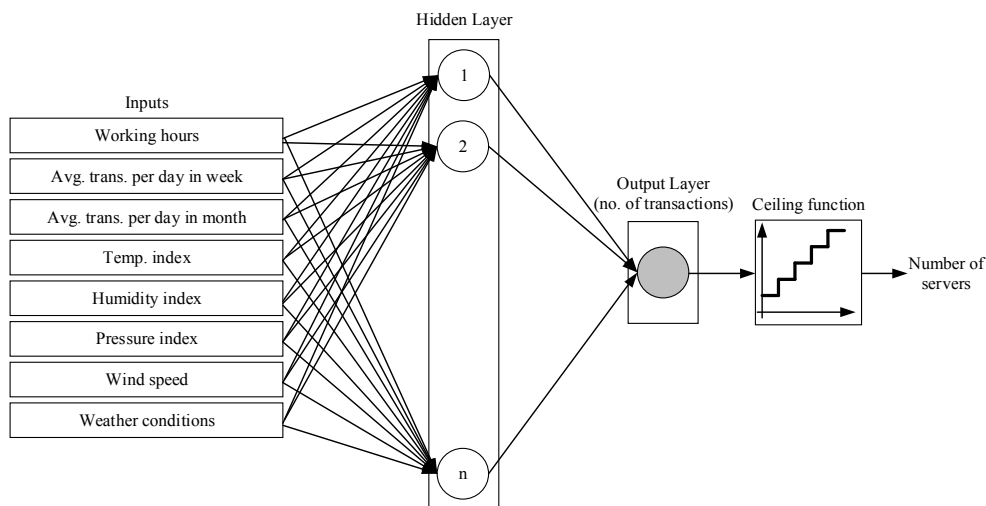


Fig. 6 The architecture of prediction model

The backpropagation learning algorithm was used for training the proposed ANN. Three different training functions Levenberg-Marquard, Bayesian regularization and Scaled conjugate gradient algorithm. Levenberg-Marquard algorithm typically requires more memory but consume less time. Training automatically stops when generalization stops improving, as indicated

by an increase in the mean square error of the validation samples. One example of convergence graph can be seen in Fig. 7. Bayesian regularization typically requires more time, but can result in good generalization for difficult, small or noisy datasets. Training stops according to adaptive weight minimization (regularization). Scaled conjugate gradient algorithm requires less memory. Training automatically stops when generalization stops improving, as indicated by an increase in the mean square error of the validation samples.

Fifty-one different values of neurons in hidden layer (n) were tested for both training sets. Number of neurons is ranging from 8 to 58 neurons in experiments. ANN has 8 inputs and it is not recommended to use number of neurons in hidden layer smaller than number of inputs. Also very large number of neurons often leads to network overfitting and can be time consuming during training process. Training was repeated thirty times for each combination of parameters (2 training sets, 3 training functions and 51 different number of neurons in hidden layer). That yield 9.180 ($2 \times 3 \times 51 \times 30$) treatments for ANN. The best training function, the most appropriate number of neurons in hidden layer and the best combination of both are determined in these experiments. Table 4 summarizes ANN parameters and their values used in experiments.

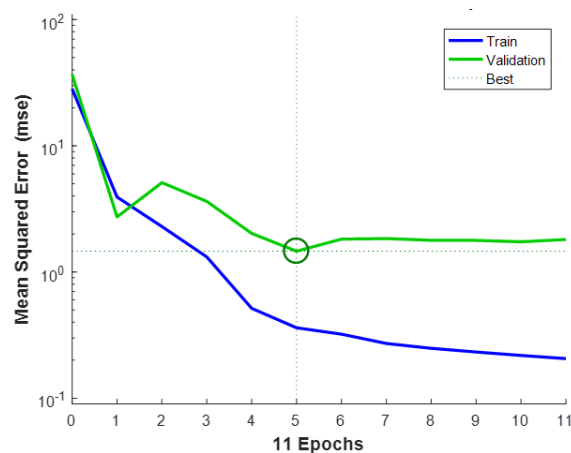


Fig. 7 Convergence graph

Table 4 ANN parameter values tested in experiments

Parameters	Level(s)
Backpropagation training function	Levenberg-Marquard, Bayesian regulation, Scaled conjugate gradient
Number of neurons in hidden layer	8, 9, 10, ... , 58
Maximum number of epochs to train	1000
Maximum validation failures	6
Minimum performance gradient	1e-6
Performance goal	0

4. Results and discussion

The aim of this study was to demonstrate a decision support tool for Public Billing Service company that would help them schedule the workforce with better accuracy, leaving them time for planning work in the back office. The presented prediction tool is intended to be used by the company to improve the operational efficiency with rotation of employees between back-end and front-end while both improving the workforce efficiency and service experience for the customers. We've presented decision support system that is based on the predictions made by artificial neural networks that take in account different variables and put out a number of servers needed (workers in front office) for the day ahead. It is suitable for single or small batch production for products that cannot be stored for a long time (such as food), and demand prediction is very important for these systems. Each product or line of products is produced in a different manner. Advantage of batch production is its flexibility to accommodate specific requests of customers. In this production type products are frequently changed and tasks for workforce are

varying significantly. Different simulation models used in production systems are customized for service management and vice versa. McDonald's Company, or similar fast food production systems where food is prepared in the back office in accordance with all the organization principles in industrial production may serve as a good example of production and service systems analogy. Similarly, workshop for pastry and ice cream production where product offer directly depends on weather circumstances. Workforce in this production type have to be more qualified than workforce in line production systems, which increases labour costs and total cost of production process. Due to this reason, well performed demand estimation is very important to distribute resources in production process. Artificial intelligence and neural networks application brings better consumer behaviour estimation. By using the proposed model, demand planning and production process improvement and optimization is expected.

The major contributions of this study was to explore, demonstrate and verify the predictability of required number of servers (front office workers) for the next working day in real billing service institution in Novi Sad (Serbia). Using historical and forecast data, the proposed methodology gives very encouraging results. The number of required servers, which in real cases varied from one to seven, is predicted exactly in most test cases, while the worst cases were very rare and with maximal error of two servers. This effectiveness proved that presented ANN model could be a valuable decision support in workforce scheduling system. With the help of the prediction tool, employees in billing department can be assigned with proper tasks (in front-end or back-end) resulting with increased productivity.

For ANN trained with first training set, mean error between target (real) and output (predicted) number of transactions is shown on Fig. 8. For the same ANN mean error between target (real) and output (predicted) number of servers expressed through number of transactions is shown on Fig. 9. On both figures (Fig. 8 and Fig. 9) error obtained with Levenberg-Marquard algorithm is displayed with dash-dotted line, error achieved with Bayesian regularization algorithm is displayed with dashed line and error achieved with Scaled conjugate gradient algorithm is displayed with dotted line. Best mean error in number of transactions is obtained when ANN with 26 neurons is trained with Bayesian regularization algorithm. In that case mean error was 429.17 transactions. When number of transactions is expressed in number of servers best mean error is achieved when ANN with 21 neurons is trained with Bayesian regularization algorithm. In that case mean error has value 0.55 servers.

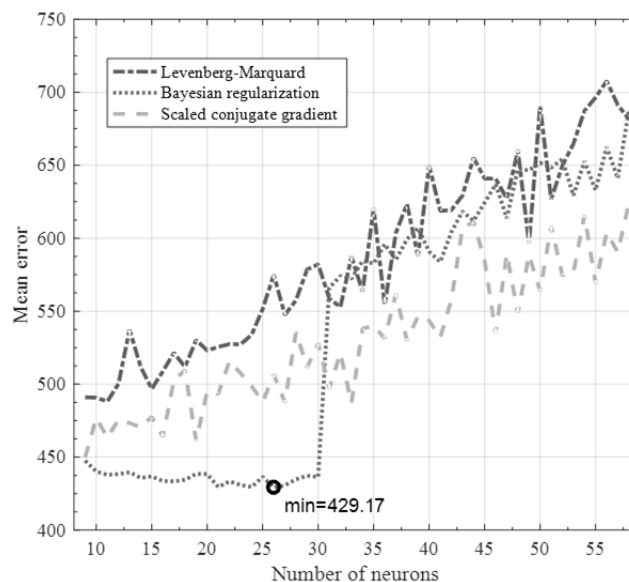


Fig. 8 Mean error between target and output number of transactions for first training set

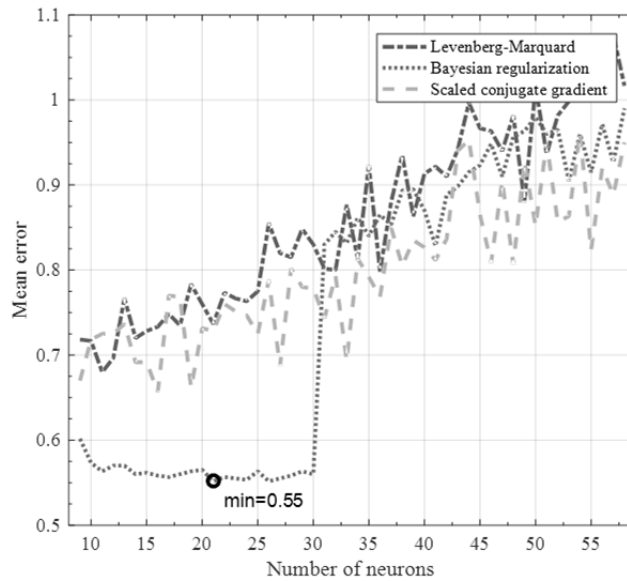


Fig. 9 Mean error between target and output number of servers for first training set

For ANN trained with second training set mean error between target (real) and output (predicted) number of servers is shown on Fig. 10. Error obtained with Levenberg-Marquard algorithm is displayed with dash-dotted line, error achieved with Bayesian regularization algorithm is displayed with dashed line and error achieved with Scaled conjugate gradient algorithm is displayed with dotted line. Best mean error in number of servers is obtained when ANN with 43 neurons is trained with Bayesian regularization algorithm. In that case mean error has value 0.83 servers.

For ANN trained with first training set, minimum error in number of transactions is obtained with 17 neurons and Scaled conjugate gradient algorithm, Fig. 11(a). In that case mean error was 295.87 transactions, Fig. 11(b). For the same ANN minimum error in number of servers is obtained with 14 neurons and Scaled conjugate gradient algorithm, Fig. 11(c). In that case mean error was 0.3 servers, Fig. 11(d).

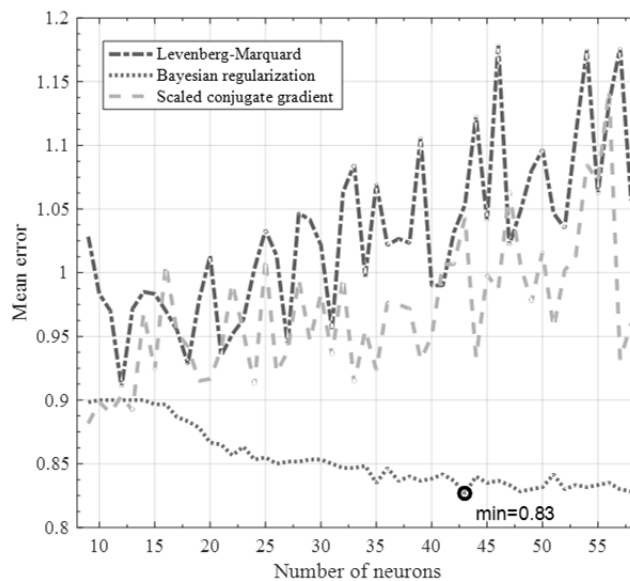


Fig. 10 Mean error between target and output number of servers for second training set

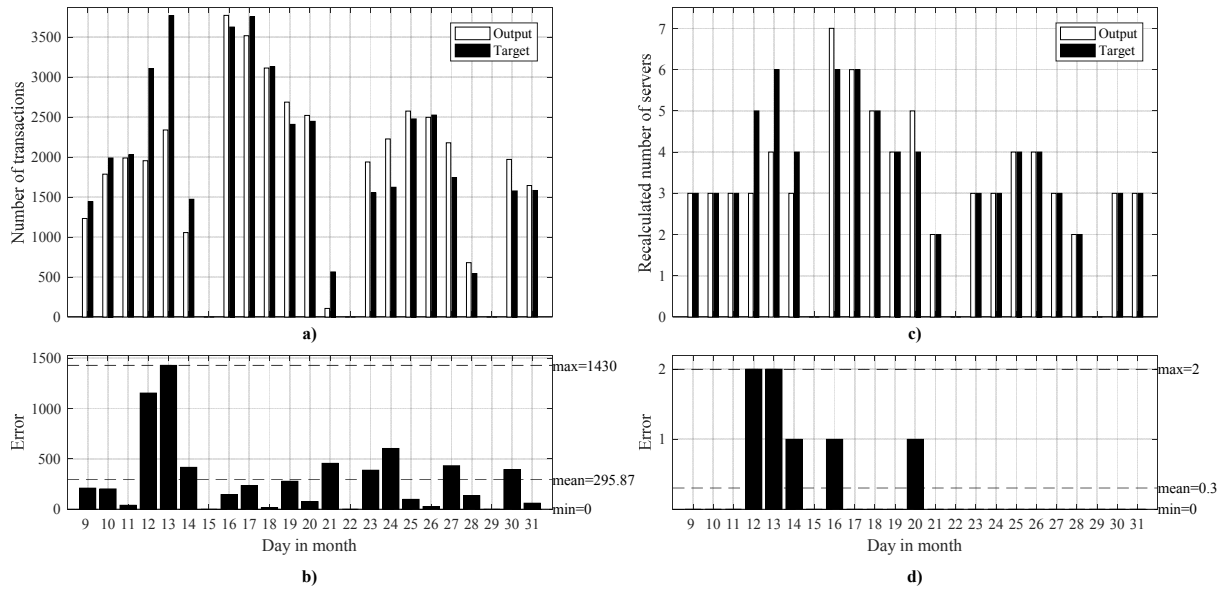


Fig. 11 Target and output number of transactions for first training set (a), error between them (b), target and output number of servers for first training set (c), error between them (d)

For ANN trained with second training set, minimum error in number of servers is obtained with 28 neurons and Levenberg-Marquard algorithm, Fig. 12(a). In that case mean error was 0.57 servers, Fig. 12(b).

In Table 5 is presented summarized view of obtained errors for ANN tested with train and test subset of both training set.

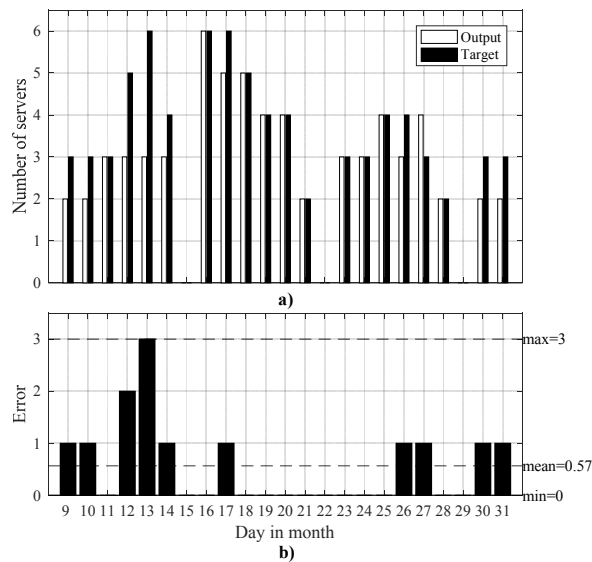


Fig. 12 Target and output number of servers for second training set (a), error between them (b)

Table 5 Results review

Training set	Min	Max	Mean	Err = 0 (%)	Err = 1 (%)	Err > 2 (%)
First training set (training subset)	0.00	2.00	0.12	88.34	11.38	0.28
First training set (test subset)	0.00	2.00	0.30	78.26	13.05	8.69
Second training set (training subset)	0.00	3.00	0.18	84.28	13.82	1.90
Second training set (test subset)	0.00	3.00	0.57	56.52	34.79	8.69

4. Conclusion

In this paper we have presented a decision support tool to be used in Public Utility Service Company. Primary objective was to improve efficiency of workforce scheduling which was successfully achieved with use of prediction system. With use of presented decision support system management can plan workforce rotation and optimize both the front-end office workers and back-end office workers and synchronize activities. Another objective was to improve quality and reduce waiting times for clients, and with proper workforce scheduling there should be a minimum of ad-hoc situations demanding additional counter to reduce the waiting lines. ANN prediction model estimating number of expected clients on daily bases was key to achieving the predefined research objectives. Estimation error is satisfactory and proposed model could be applied in the real system with minor changes in the work system. By using the model presented in the paper, unpredictability can be reduced since ANN prediction model improves demand estimation, which helps in real time workforce distribution and thus reduces supply chain management risks.

Improving waiting times is one way of improving the customer service, and secondary focus of this research paper was on this parameter. Adequate and timely response have become a prerequisite for good business results in industrial production and service management. Due to frequent product or service demand changes it is important to be capable to adapt the rearrange distribution of machines/servers or workforce to accommodate the market expectations. As this is the Public Utility company case, the queuing policy is that there should always be minimum number of servers available. With that in mind, an average error of 0.3 servers per day would be major increase both in company's productivity in back-end office (primary focus) and in customer satisfaction due the minimized waiting time. In current working conditions, with minimum number of servers needed the waiting time is around 2.3 minutes, and the average error of 0.3 servers would not have significant impact on waiting time. However, having extra workers in the front-end office on less crowded days is not needed (frequent scenario with current workforce scheduling), and their assignment to the back-end office would greatly improve the operational efficiency. Data used in the ANN prediction model were historical daily transaction information on transactions and publicly available weather conditions during that period, summing up to 8 parameters in total.

In the future research additional historical data about transaction or influence of e-commerce should be taken into account. Improving other dimensions of the customer service (apart from reduction of waiting time which was focus of this research) should also be taken in account for future research. Adding the historical data of transactions would improve the ANN training. In this research one year of data was used, but with further data we could expect to reduce the error present in the current model due the nature of moving holidays (mainly religious holidays), that are specific for this region. As it was seen in the results, major error in the prediction model was tied to the case of moving holiday.

References

- [1] Aickelin, U., Dowsland, K.A. (2004). An indirect genetic algorithm for a nurse-scheduling problem, *Computers & Operations Research*, Vol. 31, No. 5, 761-778, doi: [10.1016/S0305-0548\(03\)00034-0](https://doi.org/10.1016/S0305-0548(03)00034-0).
- [2] Valls, V., Pérez, Á., Quintanilla, S. (2009). Skilled workforce scheduling in service centres, *European Journal of Operational Research*, Vol. 193, No. 3, 791-804, doi: [10.1016/j.ejor.2007.11.008](https://doi.org/10.1016/j.ejor.2007.11.008).
- [3] Bayraktar, E., Jothishankar, M.C., Tatoglu E., Wu, T. (2007). Evolution of operations management: Past, present and future, *Management Research News*, Vol. 30, No. 11, 843-871, doi: [10.1108/01409170710832278](https://doi.org/10.1108/01409170710832278).
- [4] Chopra, S., Lovejoy, W., Yano, C. (2004). Five decades of operations management and the prospects ahead, *Management Science*, Vol. 50, No. 1, 8-14, doi: [10.1287/mnsc.1030.0189](https://doi.org/10.1287/mnsc.1030.0189).
- [5] Sandmann, W. (2013). Quantitative fairness for assessing perceived service quality in queues, *Operational Research*, Vol. 13, No. 2, 153-186, doi: [10.1007/s12351-011-0111-9](https://doi.org/10.1007/s12351-011-0111-9).
- [6] Calabrese, A., Capece, G., Costa, R., Di Pillo, F., Paglia, D. (2013). The impact of workforce management systems on productivity and quality, *Knowledge and Process Management*, Vol. 20, No. 3, 177-184, doi: [10.1002/kpm.1417](https://doi.org/10.1002/kpm.1417).
- [7] Calabrese, A. (2012). Service productivity and service quality: A necessary trade-off?, *International Journal of Production Economics*, Vol. 135, No. 2, 800-812, doi: [10.1016/j.iipe.2011.10.014](https://doi.org/10.1016/j.iipe.2011.10.014).

- [8] Van den Bergh, J., Beliën, J., De Bruecker, P., Demeulemeester, E., De Boeck, L. (2013). Personnel scheduling: A literature review, *European Journal of Operational Research*, Vol. 226, No. 3, 367-385, doi: [10.1016/j.ejor.2012.11.029](https://doi.org/10.1016/j.ejor.2012.11.029).
- [9] Taylor, D.L., Brunt, D. (2001). *Manufacturing operations and supply chain management: The LEAN approach*, Thomson Learning, London, UK.
- [10] Mirrazavi, S.K., Beringer, H. (2007). A web-based workforce management system for Sainsburys supermarkets Ltd., *Annals of Operations Research*, Vol. 155, No. 1, 437-457, doi: [10.1007/s10479-007-0204-2](https://doi.org/10.1007/s10479-007-0204-2).
- [11] Akjiratikarl, C., Yenradee, P., Drake, P.R. (2007). PSO-based algorithm for home care worker scheduling in the UK, *Computers & Industrial Engineering*, Vol. 53, No. 4, 559-583, doi: [10.1016/j.cie.2007.06.002](https://doi.org/10.1016/j.cie.2007.06.002).
- [12] Mladenović, I., Sokolov-Mladenović, S., Milovančević, M., Marković, D., Simeunović, N. (2016). Management and estimation of thermal comfort, carbon dioxide emission and economic growth by support vector machine, *Renewable and Sustainable Energy Reviews*, Vol. 64, 466-476, doi: [10.1016/j.rser.2016.06.034](https://doi.org/10.1016/j.rser.2016.06.034).
- [13] Rebai, M., Kacem, I., Adjallah, K.H. (2000). Scheduling jobs and maintenance activities on parallel machines, *Operational Research*, Vol. 13, No. 3, 363-383, doi: [10.1007/s12351-012-0130-1](https://doi.org/10.1007/s12351-012-0130-1).
- [14] Nissen, V., Günther, M. (2009). Staff scheduling with particle swarm optimisation and evolution strategies, In: *EvoCOP, Evolutionary Computation in Combinatorial Optimization*, Tübingen, Germany, 228-239, doi: [10.1007/978-3-642-01009-5_20](https://doi.org/10.1007/978-3-642-01009-5_20).
- [15] Pinedo, M., Chao, X. (1998). *Operations scheduling with applications in manufacturing and services*, Irwin/McGraw-Hill, Boston, USA.
- [16] Bakhrankova, K. (2008). Production planning in continuous process industries: Theoretical and optimization issues, In: *Operations Research Proceedings 2008*, University of Augsburg, Augsburg, Germany, 67-72.
- [17] ATOSS Software AG, Standort Deutschland 2006: Zukunftssicherung durch intelligentes personal management, from: <https://www.atoss.com/en-gb/Workforce-Management>, accessed October 13th, 2016.
- [18] Schroeder, R.G. (1989). *Operations management: Decision making in the operations function*, McGraw-Hill, New York, USA.
- [19] Solomon, M.R., Surprenant, C., Czepiel, J.A., Gutman, E.G. (1985). A role theory perspective on dyadic interactions: The service encounter, *Journal of Marketing*, Vol. 49, No. 1, 99-111, doi: [10.2307/1251180](https://doi.org/10.2307/1251180).
- [20] ISO – International Organization for Standardization, ISO 9000:2015, from: <https://www.iso.org/standard/45481.html>, accessed October 13th, 2016.
- [21] Slack, N., Brandon-Jones, A., Johnston, R. (2014). *Operations Management, 7th Edition*, Pearson, London, UK.
- [22] Vargo, S.L., Lusch, R.F. (2004) The four service marketing myths: Remnants of a goods-based manufacturing model, *Journal of Service Research*, Vol. 6, No. 4, 324-335, doi: [10.1177/1094670503262946](https://doi.org/10.1177/1094670503262946).
- [23] Tom, G., Lucey, S. (1995). Waiting time delays and customer satisfaction in supermarkets, *Journal of Services Marketing*, Vol. 9, No. 5, 20-29, doi: [10.1108/08876049510100281](https://doi.org/10.1108/08876049510100281).
- [24] Zemke, R. (2002). Managing the employee connection, *Managing Service Quality: An International Journal*, Vol. 12, No. 2, 73-76, doi: [10.1108/09604520210421374](https://doi.org/10.1108/09604520210421374).
- [25] Aaker, D.A., Biel, A.L. (1993). Converting image into equity, In: *Brand Equity & Advertising: Advertising's Role in Building Strong Brands*, Hillsdale, New York USA, 67-82.
- [26] Kerin, R.A., Ambuj, J., Howard, D.J. (1992). Store shopping experience and consumer price-quality-value perceptions, *Journal of Retailing*, Vol. 68, No. 4, 376-397.
- [27] Grace, D., O'Cass, A. (2004). Examining service experiences and post-consumption evaluations, *Journal of Services Marketing*, Vol. 18, No. 6, 450-461, doi: [10.1108/08876040410557230](https://doi.org/10.1108/08876040410557230).
- [28] Ren, X.Y., Kong, Z.F., Liang W.C., Li, H.C., Zhou, X.Y. (2017). Vehicle scheduling based on plant growth simulation algorithm and distribution staff behaviour, *Advances in Production Engineering & Management*, Vol. 12, No. 2, 173-184, doi: [10.14743/apem2017.2.249](https://doi.org/10.14743/apem2017.2.249).
- [29] Bielen, F., Demoulin, N. (2007). Waiting time influence on the satisfaction-loyalty relationship in services, *Managing Service Quality: An International Journal*, Vol. 17, No. 2, 174-193, doi: [10.1108/09604520710735182](https://doi.org/10.1108/09604520710735182).
- [30] Yang, Y., Hou, Y., Wang, Y. (2013). On the development of public-private partnerships in transitional economies: An explanatory framework, *Public Administration Review*, Vol. 73, No. 2, 301-310, doi: [10.1111/j.1540-6210.2012.02672.x](https://doi.org/10.1111/j.1540-6210.2012.02672.x).
- [31] Thompson, G.M., Goodale, J.C. (2006). Variable employee productivity in workforce scheduling, *European Journal of Operational Research*, Vol. 170, No. 2, 376-390, doi: [10.1016/j.ejor.2004.03.048](https://doi.org/10.1016/j.ejor.2004.03.048).
- [32] Hill, T., Marquez, L., O'Connor, M., Remus, W. (1994). Artificial neural network models for forecasting and decision making, *International Journal of Forecasting*, Vol. 10, No. 1, 5-15, doi: [10.1016/0169-2070\(94\)90045-0](https://doi.org/10.1016/0169-2070(94)90045-0).
- [33] Sundari. M.S., Palaniammal, S. (2015). Simulation of M/M/1 queuing system using ANN, *Malaya Journal of Matematik*, Vol. 3, No. 1, 279-294.
- [34] Altıparmak, F., Dengiz, B., Bulgak, A.A. (2007). Buffer allocation and performance modeling in asynchronous assembly system operations: An artificial neural network metamodeling approach, *Applied Soft Computing*, Vol. 7, No. 3, 946-956, doi: [10.1016/j.asoc.2006.06.002](https://doi.org/10.1016/j.asoc.2006.06.002).
- [35] Gul, M., Guneri, A.F. (2015). Forecasting patient length of stay in an emergency department by artificial neural networks, *Journal of Aeronautics and Space Technologies*, Vol. 8, No. 2, 43-48, doi: [10.7603/s40690-015-0015-7](https://doi.org/10.7603/s40690-015-0015-7).
- [36] Candan, G., Taşkin, M.F., Yazgan, H.R. (2014). Demand forecasting in pharmaceutical industry using artificial intelligence: Neuro-fuzzy approach, *Journal of Military and Information Science*, Vol. 2, No. 2, 41-49.
- [37] Milovic, B., Milovic M. (2012). Prediction and decision making in health care using data mining, *International Journal of Public Health Science*, Vol. 1, No. 2, 69-78, doi: [10.11591/ijphs.v1i2.1380](https://doi.org/10.11591/ijphs.v1i2.1380).

- [38] Asensio-Cuesta, S., Diego-Mas, J.A., Canós-Darós, L., Andrés-Romano, C. (2012). A genetic algorithm for the design of job rotation schedules considering ergonomic and competence criteria, *The International Journal of Advanced Manufacturing Technology*, Vol. 60, No. 9-12, 1161-1174, doi: [10.1007/s00170-011-3672-0](https://doi.org/10.1007/s00170-011-3672-0).
- [39] Carmen, R., Defraeye, M., Van Nieuwenhuysse, I. (2015). A decision support system for capacity planning in emergency departments, *International Journal of Simulation Modelling*, Vol. 14, No. 2, 299-312, doi: [10.2507/IJSIMM14\(2\)10.308](https://doi.org/10.2507/IJSIMM14(2)10.308).
- [40] Baesler, F., Gatica, J., Correa, R. (2015). Simulation optimisation for operating room scheduling, *International Journal of Simulation Modelling*, Vol. 14, No. 2, 215-226, doi: [10.2507/IJSIMM14\(2\)3.287](https://doi.org/10.2507/IJSIMM14(2)3.287).
- [41] García-Alcaraz, J.L., Maldonado-Macías, A.A., Alor-Hernández, G., Sánchez-Ramírez, C. (2017). The impact of information and communication technologies (ICT) on agility, operating, and economical performance of supply chain, *Advances in Production Engineering & Management*, Vol. 12, No. 1, 29-40, doi: [10.14743/apem2017.1.237](https://doi.org/10.14743/apem2017.1.237).
- [42] Oliver, J.E. (2005). *Encyclopedia of world climatology*, Springer, Dordrecht, The Netherlands.

Infrared temperature measurement and increasing infrared measurement accuracy in the context of machining process

Masoudi, S.^{a,*}, Gholami, M.A.^b, Janghorban Iariche, M.^c, Vafadar, A.^d

^aYoung Researchers and Elite Club, Najafabad Branch, Islamic Azad University, Najafabad, Iran

^bDepartment of Mechanical Engineering, Shiraz Branch, Islamic Azad University, Shiraz, Iran

^cAbadan School of Medical Sciences, Abadan, Iran

^dSchool of Engineering, Edith Cowan University, Perth, Australia

ABSTRACT

One of the major challenges in the machining process is measuring the temperature accurately which has a considerable importance in calibrating finite element models and investigating thermodynamic of machining process. In the present paper, one of the effective methods for measuring temperature in the machining processes – i.e. infrared imaging – is used and effective parameters which increase measurement accuracy are investigated. One of the most effective parameter in the temperature measurement accuracy of infrared imaging is extracting and calibrating the emissivity coefficient for different temperature ranges. The obtained results show that the lack of precision calibration of the emissivity for different temperature ranges may cause high error in the measurement results. To measure temperature, several experiments are performed for turning a thin walled workpiece which is made of aluminium alloy Al-7075 and the effects of the machining parameters and tool material – polycrystalline diamond (PCD) and cemented carbide – are studied. Based on the achieved results, it can be concluded that the generated temperature in the cutting area can be decreased significantly by using PCD tools and selecting appropriate machining parameters.

© 2017 PEI, University of Maribor. All rights reserved.

ARTICLE INFO

Keywords:

Machining
IR temperature measurement
Emissivity
PCD tool
Carbide tool
Al-7075

*Corresponding author:

smasoudi86@gmail.com
(Masoudi, S.)

Article history:

Received 25 June 2017
Revised 14 October 2017
Accepted 20 October 2017

1. Introduction

In metal machining processes, the majority of the applied energy in metal deformation and the friction between tool and workpiece appear to enhance heat at the cutting area [1]. The heat generated at this area causes numerous economic and technical problems in the machining process. Some of these problems include rapid wear of the tool due to diffusion acceleration inducing of residual stresses and structural changes in the machined surface and the tool due to exerted thermal gradients, and also thermal distortion and deformation of the work piece, especially in thin-walled workpieces [2]. In order to attain optimal process outputs, it is important to identify creation manner, intensity, and heat distribution in the cutting area precisely. Despite many research projects done in this area; it is difficult to present a perfect theory of the heat generation mechanism and also to predict heat intensity and distribution in the machining process, due to the thermodynamic and nonlinear complex nature of this process, which also involves high pressure and strain in a small area [3].

Recently, there have been lots of unsolved issues in this area and some contradictory results have been reported from research projects. However, the influence of machining different pa-

rameters, material, and the geometry of the tool on the heat in the cutting area has been proved by many researchers [4-6]. Tool material is one of the effective parameters in cutting process efficiency and generated heat in the cutting area. In the machining of high strength aluminium alloys, cemented carbide tools are the most widely used tools. Among different metals, aluminium alloys have a suitable machinability due to a low machining force and low generated heat. Using common tool for machining these alloys creates built-up edge (BUE) which decreases tool-life and process efficiency especially in dry machining [7]. Therefore, using cutting tools with low friction and high hardness may lead to heat and BUE reduction and ultimately the tool's life, and process efficiency increase. Polycrystalline diamond (PCD) cutting tools are one of the most effective tools in aluminium alloys machining. PCD tools consist of an artificial diamond layer which is constructed at very high pressure and temperature and is brazed on a base of cemented carbide. These tools have unique characteristics including very high hardness, Young's modulus, and thermal conductivity, and a low friction coefficient of their surface which leads to enhance in cutting process effectiveness [8].

Experimental measurement and studying temperature in the cutting area are another challenge in machining science, and numerous methods have been developed for this. Several important methods use a thermocouple, infrared radiation (IR) measurement, measurement of hardness, and study of metal's microstructure changes which may provide some advantages or disadvantages [9]. One of the effective techniques of measuring temperature is infrared radiation measurement, which is a non-contact method. In this method, the temperature of the body is measured by considering the thermal energy or infrared radiation which is radiated from the body [10].

This research is aimed to study the effect of cutting parameters and tool material on the temperature of cutting area in turning of a thin walled workpiece which is made of aluminium alloy Al-7075. To measure temperature, a thermal infrared camera (IR) was used, and factors affecting the accuracy of measurements were evaluated.

2. Materials and methods

2.1 Infrared temperature measurement principle

Each hot object with a temperature higher than absolute zero (Kelvin's zero or $-273.15\text{ }^{\circ}\text{C}$) radiates an infrared radiation according to its temperature. The relation between radiated energy q_e , and an object's temperature is defined by Stefan Boltzmann law:

$$q_e = \varepsilon\sigma T^4 \quad (1)$$

Where σ is the Stefan Boltzmann constant and is equal to $\sigma = 5.67 \cdot 10^{-8} \left(\frac{\text{W}}{\text{m}^2\text{K}^4} \right)$. T is the thermodynamic temperature of an object in terms of K and ε is the emissivity coefficient of the object's surface. ε is defined as the emitted energy of a body at a specific temperature divided by the emitted energy of a black body, which is a dimensionless quantity. A black body is an object or material which absorbs the all existing radiations with any wave length and does not reflect any radiation [11]. An ideal black body theoretically has an emissivity coefficient of 1, but in practice, the emissivity coefficient of all objects is less than 1. When the thermal radiation collapses onto an object, it may be absorbed, reflected, or transmitted. The relation between absorptivity α , reflectivity ρ and transmissivity τ is defined as below

$$\alpha + \rho + \tau = 1 \quad (2)$$

In fact, the effective radiation received by the infrared detectors of an infrared thermal camera consists of three parts: (1) the object's radiation; (2) the radiation caused by light and the reflection of environmental heat on the object's surface and (3) atmospheric transmission radiation. Infrared detectors integrate radiation energy received in their working wavelength range, and then create its corresponding electrical signal $f(T_r)$:

$$f(T_r) = \tau_\alpha \varepsilon f(T) + \tau_\alpha (1 - \varepsilon) f(T_\mu) + (1 - \tau_\alpha) f(T_a) \quad (3)$$

This relation is a general equation for temperature measurement in a thermal camera in which τ_α is atmospheric transmissivity. T , T_r , T_μ and T_a are the measured temperature of the object, temperature shown by camera, environment temperature, and temperature of atmosphere respectively. The three right-hand side terms of the above equation define the object's radiation, the radiation caused by the reflection of object and radiation of atmospheric transmission, respectively. If the object is a black body, then: $\tau_\alpha = 1$ and therefore: $f(T_r) = f(T)$, meaning the temperature shown by the camera equals the object's temperature. But for any other object except a black body and especially for any metal with a high reflection and low absorptivity, there is a significant variation between $f(T_r)$ and $f(T)$. When the distance between the target object and the camera is small, then the effect of atmospheric radiation is negligible [12]. Thus, the accuracy of emissivity coefficient is the most important parameter in the accuracy of temperature measurement with an infrared thermal camera, since this parameter will fully specify the surface's characteristics in regard to absorptivity or the reflection of infrared radiation [13].

The IR method has many advantages; first, the IR method is a non-contact method and does not create any interference with heat flow in the cutting area. Also, the IR method has a very fast response. However, the IR technique has restrictions, such as the high dependency of measurement accuracy on the precise determination of the emissivity coefficient [14]. In some of the research performed on heat measurement with the IR technique, the emissivity coefficient of the tool and the workpiece is not mentioned, or the emissivity coefficient change of the machined surface and chip is not considered [15-17]. Some researchers have covered the surface of the workpiece or the tool with a material with a specific emissivity coefficient, to decrease the errors due to the determination of the emissivity coefficient [18, 19]. This method is applicable in the measurement of a fixed surface, but in machining, due to material removal, a new surface with a different emissivity coefficient will be created, and the reflection of the new surface on the covered surface and the chip surface decreases the effectiveness of this method.

2.2 Experimental procedure

Several different experiments were carried out on a thin-walled parts of Al-7075 alloy by a computer numerical control (CNC) machine (Tabriz TC50 model), to study the effects of various machining parameters on the heat generated in the cutting area. To evade the pressure of chuck jaws on the workpiece and its subsequent deformation, the workpiece was bolted on a fixture which was fastened into a chuck. Fig. 1 shows the geometry of the fixture, the workpiece and the assembled workpiece on the fixture.

The temperature was measured by using an IR camera (Dali DL700 model). The camera was mounted on a sheet which was linked to the turret, so that by using tool feed on the workpiece, the gap between the cutting area and the infrared camera remained constant. Fig. 2 shows the setup for performing the experimental case studies.

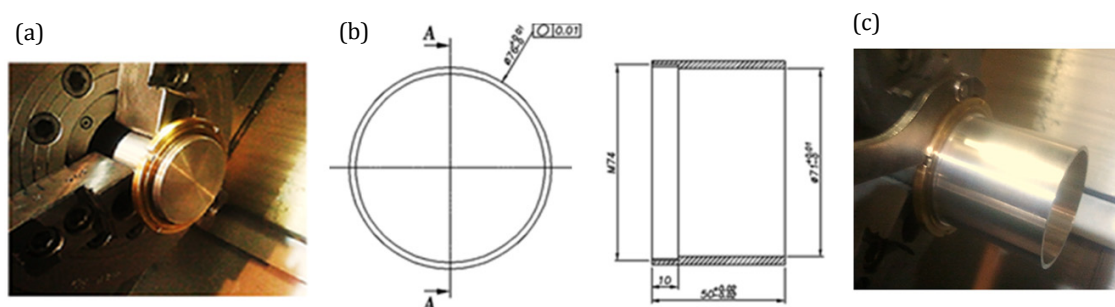


Fig. 1 The geometry of (a) the fixture, (b) the workpiece, (c) and the assembled workpiece on the fixture

The conditions of machining process

To study the effects of different conditions of the cutting process on the temperature, and the effect of various parameters on each other, a full factorial design was used for experimental case studies. This study investigates the effects of feed rate, cutting speed, and tool material.

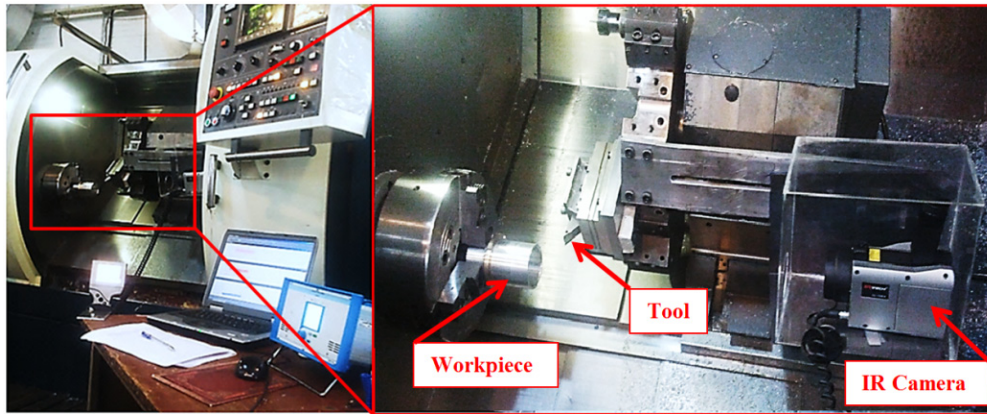


Fig. 2 The setup for measurement of the machining temperature in the CNC machine

Table 1 Machining parameters and required levels

Parameters	Level			
	A	B	C	D
Feed rate (mm/min)	60.0	120.0	180.0	-
Cutting speed (m/min)	230.0	350.0	470.0	590.0
Cutting tool	Polycrystalline diamond	Cemented carbide	-	-

Table 1 presents various levels for cutting parameters which were applied in case studies. Therefore, 24 tests were machined by using a CNC lathe machine. In order to validate the experimental results, each test was repeated three times. Moreover, in order to study the effect of the tool material on the temperature, two type of cutting insert with various materials of cemented carbide (Sandvik-VCGX160404-AL) and PCD (Sandvik-VCMW160404FP) were utilized. In the all experiments, the cutting depth equalled 1 mm in dry cutting condition.

Emissivity calibration and temperature measurement

To measure the heat in the cutting area, a thermal infrared camera was applied. The camera had a spectral range of 8-14 μm, a frame rate of 50/60 Hz and a temperature resolution of 0.05 °C. The camera’s detector was uncooled amorphous Silicon and sensitivity of 0.08 °C in 30 °C. The calibration of the camera’s detector was performed in different temperature ranges, using a black body (Optikos-model BBS-200). The black body’s emissivity was 0.994. Since, the 3.4 μm to 5 μm wavelength bandwidth provides higher accuracy in the machining process [20, 21], 4 μm wavelength bandwidth was adjusted in the camera. The camera lens which show a 15mm × 20 mm window were located on the cutting area to reach a 320 × 256 pixels resolution.

Emissivity is a function of temperature, wavelength, surface characteristics, and emission direction. However, the temperature is the most important factor influencing the emissivity as the luminance of a black body (L_{λ}^0) is a function of wavelength (λ) and temperature (T) in the Plank’s law:

$$L_{\lambda}^0 = \frac{C_1 \lambda^{-5}}{\pi \left[\exp\left(\frac{C_2}{\lambda T}\right) - 1 \right]} \tag{4}$$

C_1 and C_2 are constant parameters. In fact, the emissivity (ε) is defined as the ratio between the real monochromatic luminance and the luminance of a black body as below:

$$\varepsilon = \frac{L_{\lambda}(\lambda, T, \Delta)}{L_{\lambda}^0(\lambda, T)} \tag{5}$$

$L_{\lambda}(\lambda, T, \Delta)$ is defined as value of luminance for wavelength λ , at temperature T and direction Δ . The relation between luminance with wavelength and temperature is shown in Fig. 3(a). As this figure shows temperature is the most important factor which influences the emissivity coefficient [22]. Accurate determination of emissivity is the most important parameter in temperature

measurement accuracy with an infrared camera. The emissivity coefficient of a chip surface changes by varying temperature during machining. Since the aim of this research is measuring the temperature of the chip, to increase the accuracy, the precise determination of the chip's emissivity for different temperature ranges is necessary. Therefore, a part of the chip, were heated to different temperature ranges from 50-310 °C by using a tungsten element device which creates a controlled temperature by utilizing specified voltage and current. The exact value of chip's temperature was determined via a contact thermocouple (Testo model 925-T/C Type) and the chip's temperature was measured using the IR camera simultaneously. The emissivity of the IR camera was calibrated and defined so that the camera's apparent temperature was precisely identical with the thermocouple's measured temperature. Fig. 3(b) shows the results of experimentally emissivity extracted curve in different temperature ranges for Al-7075 according to above instruction. Results showed that by changing temperature from 50-310 °C the emissivity coefficient values were varied between 0.136 and 0.254. By following this instruction, the accurate emissivity of the chip for different temperature was extracted. Since the reflection of emitted radiation in the measurement environment on the desired object leads to an increase in its emitted radiation and therefore a decrease in measurement accuracy, the present research tried to eliminate all light and heat sources in the measurement area during the experiments.

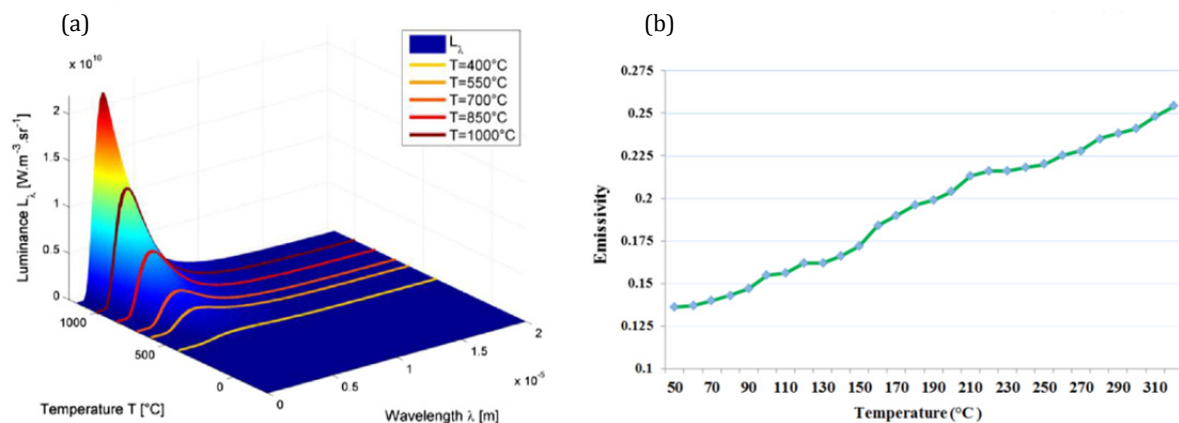


Fig. 3 (a) Luminance as a function of wavelength and temperature [22], (b) Experimental emissivity curve which is extracted for different temperatures for Al-7075

3. Results and discussion

Fig. 4 shows two thermal images of the cutting area which were achieved through experiments. Fig. 4(a) shows that the chips gather around the cutting area and the tool, while Fig. 4(b) indicates that the produced chips get away from cutting area. By comparing these two images, it can be observed how the increase of the emitted energy from a body is affected by reflection. Fig. 4(a) shows that due to the chip warping and aggregation around the tool, the camera's measured temperature increases significantly, so that in the same machining conditions, due to chip aggregation, 90 °C temperature difference was occurred. The reason is that each chip acts as a thermal radiation energy resource due to its high temperature. While hot chips are aggregated in a small area, reflected energy is emitted from every part of the chip to the other chips and continuing this procedure leads to an intensive and exponential increase of the infrared radiation emitted from the chip and ultimately increases the camera's calculated temperature.

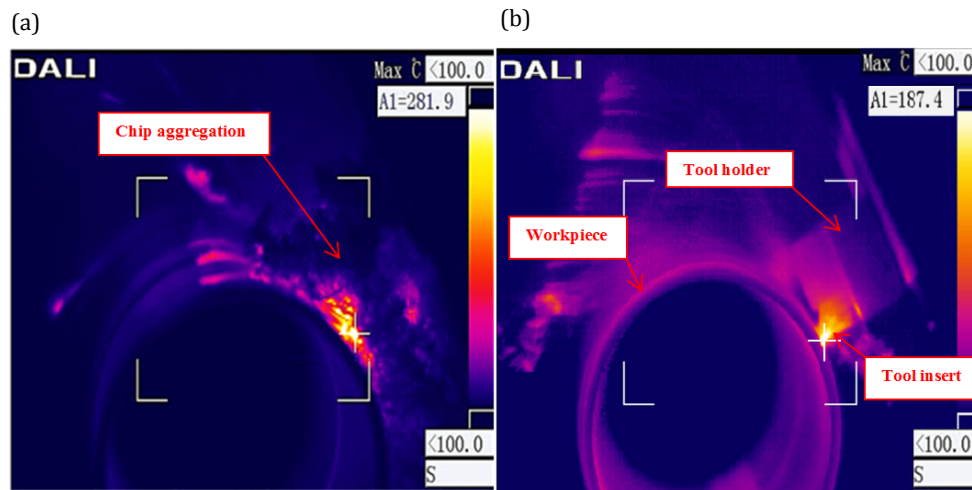


Fig. 4 Thermal infrared image in two cases of (a) chip aggregation and (b) appropriate expulsion of chip from cutting area

This process ultimately increases the camera's calculated temperature. Indeed, in the Eq. 3, $\tau_{\alpha}(1 - \varepsilon)f(T_{\mu})$ significantly increases which is related to the radiation reflected on the surface. Chip aggregation occurs for continues chips, especially in the soft material and aluminium alloys machining. This issue was considered in the temperature measurement of the experimental case study to prevent inaccurate measurement. During the experiments, the temperature measured and recorded in the first 10 mm part of workpiece from starting point to prevent the possible errors due to the reflected energy emitted from the machined surface.

In the machining process, a part of the heat generated is transferred to the machined surface and the tool and makes a thermal gradient in the workpiece and tool which causes micro-structural changes in the metal, partial expansion, and induces residual stresses [2]. Fig. 5 shows that the thermal gradient applied to the workpiece. As this figure shows, in both image (a) and image (b), the cross-hair indicates a thermal gradient in the inner surface of the workpiece and the region of tool contact with the workpiece. In these areas, the temperature in a thin band is significantly superior to the other sections. This phenomenon is more intensive in metals such as aluminium with higher heat transfer coefficient; because heat transfers to beneath the surfaces of the workpiece rapidly. This intensive thermal gradient is created in some seconds in a section of the workpiece which leads to partial expansion and residual stresses in the workpiece. This effect is especially important in thin-walled workpieces as the induced residual stresses lead to dimensional instability and distortion.

Fig. 5 indicates that by increasing the temperature of the cutting area, a thermal gradient be transferred to the workpiece increases. Image (a) corresponds to an experiment when feed rate and cutting speed are 180 mm/min and 590 m/min respectively, for the carbide tool. The measured temperature in this test was 202 °C. Image (b) for the PCD tool corresponds to an experiment when the feed rate and cutting speed are 120 mm/min and 590 m/min, respectively. The reported temperature in this case was 132 °C. Due to the greater heat generation in Fig. 5(a) in comparison with (b), the heat transferred to the surface of the workpiece is much higher.

Figs. 6(a) and (b) indicate the experimental results which show the effect of feed rate and cutting speed on the measured temperature of chip for carbide and PCD tools in 2D and 3D plots, respectively. The temperature of the chip in the PCD tool is significantly lower than in the carbide tools. Nevertheless, by increasing feed rate and cutting speed the temperature increases and the heat increase slope becomes steeper as the cutting speed raises for both PCD and Carbide tools. For instance, when feed rate and cutting speed are 180 mm/min and 590 m/min, respectively, the maximum temperature for the PCD insert is 149 °C, while maximum measured temperature for the carbide insert is 203 °C.

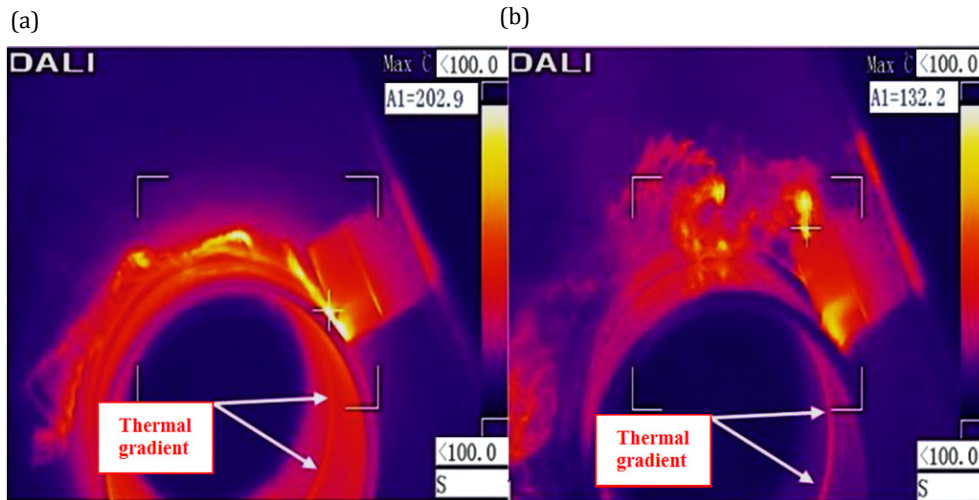


Fig. 5 The transmission of the generated heat from cutting zone to the workpiece, and the creation of a thermal gradient in a section of the workpiece

Generally, PCD insert has lower friction coefficient in comparison to carbide tools [23]. Therefore, heat caused by friction in rake and flank surfaces will be lower. Moreover, due to the friction being lower the required forces to form chips decrease and thus less heat is generated in the cutting area. Fig. 7 shows the microscopic images of the rake surfaces of two PCD and carbide tools at a magnification of 400 times. As seen in this figure, the surface of PCD tools has a more uniform structure and fewer ups and downs than the surface of carbide tools, which reduce the coefficient of friction in PCD tools.

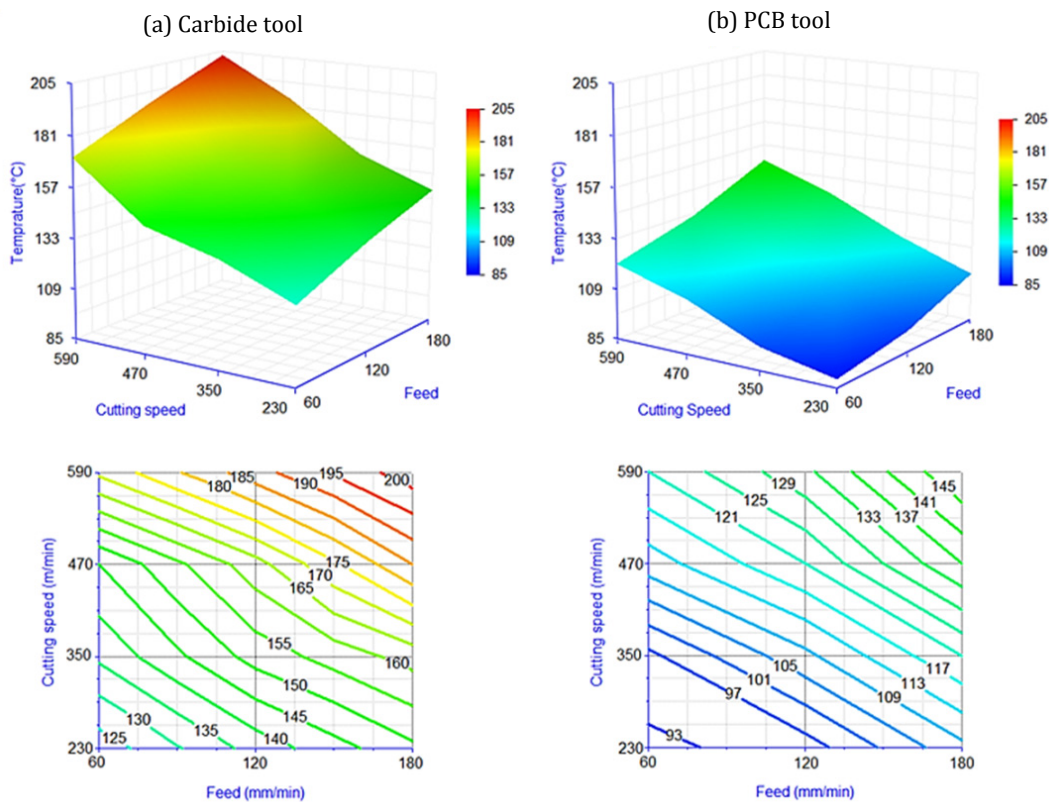


Fig. 6 Experimental results of measured chip temperature for carbide tool (a) and PCD tool (b) versus feed rate and cutting speed changes

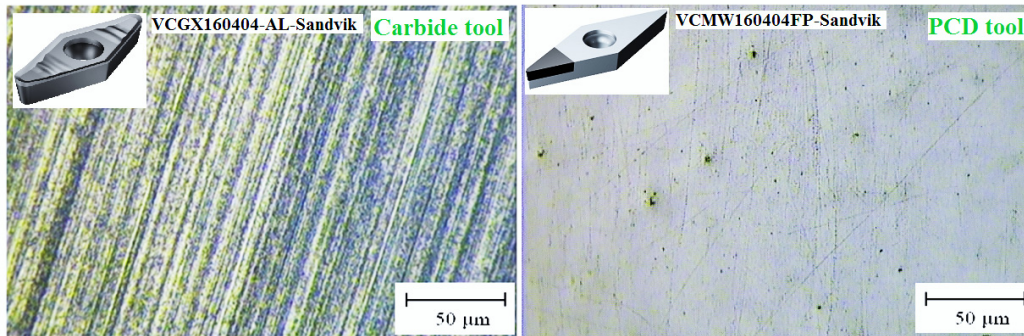


Fig. 7 Microscopic image: Rake surface of PCD and carbide tools in experiments with a magnification of 400×

Another characteristic of PCD tools is a higher thermal conductivity in comparison with carbide tools, which leads to more heat transfer from the cutting area and thus a decrease in the temperature of the chip and workpiece [23]. On the other hand, because less heat and a lower machining force are applied to the tool, and because of the high strength and hardness of PCD tools, the rate of wear is much slower than it is for carbide tools. Therefore, the temperature increase of the cutting area due to tool wear in these tools is much lower than that of carbide tools. In general, using PCD tools in high-strength aluminium alloys machining is preferable to using carbide tools and increases cutting efficiency.

Fig. 8 shows that to study the effect of emissivity coefficient on the accuracy of the temperature measurement value. In this figure the measured temperature values with calibrated emissivity are compared to the temperature values with a constant emissivity, 0.11, according to reference [24]. As can be seen, by increasing temperature, the difference between the measured values increases. The reason for this result is that in the high measured temperature, the difference between the constant and calibrated emissivity coefficients is more. By using the constant emissivity, 0.11, which is less than all the calibrated emissivity values, the measured temperature by IR camera increases, which is in accordance with Eq. 3. Based on the achieved results, the lowest and highest difference values which are measured at the same condition are 5 °C and 45 °C, respectively, and the average temperature difference is 20.5 °C. These results clearly show the importance of precise calibration of chip’s emissivity for different temperature ranges in temperature measurement by infrared imaging in machining processes.

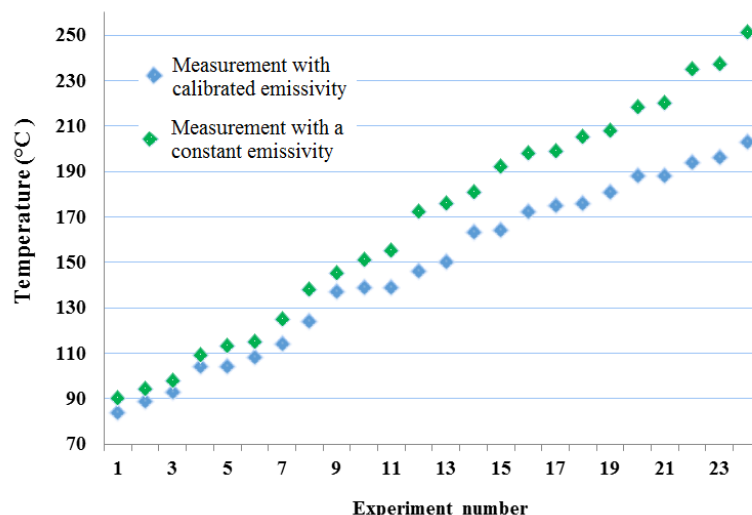


Fig. 8 Comparison between the measured temperatures values with the calibrated emissivity and a constant emissivity (0.11)

4. Conclusion

In the present study, the influence of cutting parameters and tool material on the temperature of the cutting area in the turning of an Al-7075 alloy thin-walled workpiece were investigated. To measure temperature, a thermal infrared camera (IR) was used, and factors affecting the accuracy of measurements were evaluated. The results showed that using IR camera is one of the effective methods for temperature measurement in machining processes. However, due to limitations in the IR method, some remarks should be considered to increase the validity and accuracy of temperature measurement in the machining processes. One of the effective parameters in the temperature measurement by using thermal imaging is defining and calibrating a precise emissivity for different ranges of temperature which are investigated in the present paper by performing experimental tests. The achieved results indicate that the lack of calibration of emissivity coefficient cause a considerable difference between the measured values and leads to errors as high as 24 % in temperature measurement.

The results also showed that chip aggregation in the cutting area due to the reflection of emitted energy between hot chips can cause huge errors in temperature measurement which should be considered. The studied experiments that used the IR camera clearly indicated the transition a portion of the generated heat to the workpiece and consequently forming a thermal gradient on it. The thermal gradient created in the thin-walled workpiece can cause various problems such as metal micro-structural change, partial expansion, residual stresses, and distortion which may be prevented by using temperature-reducing techniques.

According to the results obtained in the cutting process with the PCD insert, due to the low friction coefficient and improved cutting conditions of this tool, the temperature in cutting areas was much lesser than that of the carbide insert. In cutting experiments with the PCD insert, the average temperature was 71 % lesser than in the carbide insert. Therefore, PCD inserts are an appropriate substitute for carbide inserts in the cutting of high-strength aluminium alloys. From the results of this research, it can be concluded that the temperature generated in the cutting area can be lowered significantly by using PCD tools and selecting appropriate machining parameters. Therefore, the results of this research create a more comprehensive perception of the operation and effectiveness of PCD tools in machining of different alloys.

References

- [1] Wang, Z., Basu, S., Saldana, C. (2017). Low-temperature machining in a fully submerged cryogenic environment, *Machining Science and Technology*, Vol. 21, No. 1, 19-36, doi: [10.1080/10910344.2016.1260428](https://doi.org/10.1080/10910344.2016.1260428).
- [2] Masoudi, S., Amirian, G., Saeedi, E., Ahmadi, M. (2015). The effect of quench-induced residual stresses on the distortion of machined thin-walled parts, *Journal of Materials Engineering and Performance*, Vol. 24, No. 10, 3933-3941, doi: [10.1007/s11665-015-1695-7](https://doi.org/10.1007/s11665-015-1695-7).
- [3] Riou, O., Guiheneuf, V., Delaleux, F., Logerais, P.-O., Durastanti, J.-F. (2016). Accurate methods for single-band apparent emissivity measurement of opaque materials, *Measurement*, Vol. 89, 239-251, doi: [10.1016/j.measurement.2016.04.006](https://doi.org/10.1016/j.measurement.2016.04.006).
- [4] Thepsonthi, T., Özel, T. (2015). 3-D finite element process simulation of micro-end milling Ti-6Al-4V titanium alloy: Experimental validations on chip flow and tool wear. *Journal of Materials Processing Technology*, Vol. 221, 128-145, doi: [10.1016/j.jmatprotec.2015.02.019](https://doi.org/10.1016/j.jmatprotec.2015.02.019).
- [5] Heigel, J.C., Whinton, E., Lane, B., Donmez, M.A., Madhavan, V., Moscoso-Kingsley, W. (2017). Infrared measurement of the temperature at the tool-chip interface while machining Ti-6Al-4V, *Journal of Materials Processing Technology*, Vol. 243, 123-130, doi: [10.1016/j.jmatprotec.2016.11.026](https://doi.org/10.1016/j.jmatprotec.2016.11.026).
- [6] Jiang, F., Liu, Z., Wan, Y., Shi, Z., Zhang, H. (2016). Experimental investigation of cutting tool temperature during slot milling of AerMet 100 steel, *Proceedings of the Institution of Mechanical Engineers, Part B: Journal of Engineering Manufacture*, Vol. 230, No. 5, 838-847, doi: [10.1177/0954405414563421](https://doi.org/10.1177/0954405414563421).
- [7] Tabei, A., Shih, D.S., Garmestani, H., Liang, S.Y. (2016). Micro-texture evolution in aggressive machining of al alloy 7075, *Materials and Manufacturing Processes*, Vol. 31, No. 13, 1709-1717, doi: [10.1080/10426914.2015.1090597](https://doi.org/10.1080/10426914.2015.1090597).
- [8] Amini, S., Khosrojerdi, M.R., Nosouhi, R., Behbahani, S. (2014). An experimental investigation on the machinability of Al₂O₃ in vibration-assisted turning using PCD tool, *Materials and Manufacturing Processes*, Vol. 29, No. 3, 331-336, doi: [10.1080/10426914.2013.864411](https://doi.org/10.1080/10426914.2013.864411).
- [9] Davoodi, B., Hosseinzadeh, H. (2012). A new method for heat measurement during high speed machining, *Measurement*, Vol. 45, No. 8, 2135-2140, doi: [10.1016/j.measurement.2012.05.020](https://doi.org/10.1016/j.measurement.2012.05.020).

- [10] Yashiro, T., Ogawa, T., Sasahara, H. (2013). Temperature measurement of cutting tool and machined surface layer in milling of CFRP, *International Journal of Machine Tools and Manufacture*, Vol. 70, 63-69, doi: [10.1016/j.ijmachtools.2013.03.009](https://doi.org/10.1016/j.ijmachtools.2013.03.009).
- [11] Svetlitzka, A., Slavenko, M., Blank, T., Brouk, I., Stolyarova, S., Nemirovsky, Y. (2014). THz measurements and calibration based on a blackbody source. *IEEE Transactions on Terahertz Science and Technology*, Vol. 4, No. 3, 347-359, doi: [10.1109/TTHZ.2014.2309003](https://doi.org/10.1109/TTHZ.2014.2309003).
- [12] Quan, Y., Xu, H., Ke, Z. (2011). Research on some influence factors in high temperature measurement of metal with thermal infrared imager, *Physics Procedia*, Vol. 19, 207-213, doi: [10.1016/j.phpro.2011.06.150](https://doi.org/10.1016/j.phpro.2011.06.150).
- [13] Liu, D., Wang, G., Nie, Z., Rong, Y.K. (2016). An in-situ infrared temperature-measurement method with back focusing on surface for creep-feed grinding, *Measurement*, Vol. 94, 645-652, doi: [10.1016/j.measurement.2016.09.013](https://doi.org/10.1016/j.measurement.2016.09.013).
- [14] Müller, B., Renz, U. (2003). Time resolved temperature measurements in manufacturing, *Measurement*, Vol. 34, No. 4, 363-370, doi: [10.1016/j.measurement.2003.08.009](https://doi.org/10.1016/j.measurement.2003.08.009).
- [15] Hou, J., Zhao, N., Zhu, S. (2011). Influence of cutting speed on flank temperature during face milling of magnesium alloy, *Materials and Manufacturing Processes*, Vol. 26, No. 8, 1059-1063, doi: [10.1080/10426914.2010.536927](https://doi.org/10.1080/10426914.2010.536927).
- [16] Hamlaoui, N., Azzouz, S., Chaoui, K., Azari, Z., Yaltese, M.-A. (2017). Machining of tough polyethylene pipe material: Surface roughness and cutting temperature optimization, *The International Journal of Advanced Manufacturing Technology*, Vol. 92, No. 5-8, 2231-2245, doi: [10.1007/s00170-017-0275-4](https://doi.org/10.1007/s00170-017-0275-4).
- [17] Cuesta, M., Aristimuño, P., Garay, A., Arrazola, P.J. (2016). Heat transferred to the workpiece based on temperature measurements by IR technique in dry and lubricated drilling of Inconel 718, *Applied Thermal Engineering*, Vol. 104, 309-318, doi: [10.1016/j.applthermaleng.2016.05.040](https://doi.org/10.1016/j.applthermaleng.2016.05.040).
- [18] Vitkovskii, V.V., Gorshenev, V.G., Potapov, Y.F. (2009). Measurement of spectral directional emissivity of materials and coatings in the infrared region of spectrum, *Thermal engineering*, Vol. 56, No. 3, 245-248, doi: [10.1134/S0040601509030100](https://doi.org/10.1134/S0040601509030100).
- [19] Armendia, M., Garay, A., Villar, A., Davies, M.A., Arrazola, P.J. (2010). High bandwidth temperature measurement in interrupted cutting of difficult to machine materials, *CIRP Annals, Manufacturing Technology*, Vol. 59, No. 1, 97-100, doi: [10.1016/j.cirp.2010.03.059](https://doi.org/10.1016/j.cirp.2010.03.059).
- [20] Meca Meca, F.J., Rodríguez Sanchez, F.J., Sanchez, P.M. (2002). Calculation and optimisation of the maximum uncertainty in infrared temperature measurements taken in conditions of high uncertainty in the emissivity and environment radiation values, *Infrared Physics & Technology*, Vol. 43, No. 6, 367-375, doi: [10.1016/S1350-4495\(02\)00125-1](https://doi.org/10.1016/S1350-4495(02)00125-1).
- [21] Boué, C., Holé, S. (2012). Infrared thermography protocol for simple measurements of thermal diffusivity and conductivity, *Infrared Physics & Technology*, Vol. 55, No. 4, 376-379, doi: [10.1016/j.infrared.2012.02.002](https://doi.org/10.1016/j.infrared.2012.02.002).
- [22] Valiorgue, F., Brosse, A., Naisson, P., Rech, J., Hamdi, H., Bergheau, J. M. (2013). Emissivity calibration for temperatures measurement using thermography in the context of machining, *Applied Thermal Engineering*, Vol. 58, No. 1-2, 321-326, doi: [10.1016/j.applthermaleng.2013.03.051](https://doi.org/10.1016/j.applthermaleng.2013.03.051).
- [23] Li, G., Rahim, M.Z., Ding, S., Sun, S. (2016). Performance and wear analysis of polycrystalline diamond (PCD) tools manufactured with different methods in turning titanium alloy Ti-6Al-4V, *The International Journal of Advanced Manufacturing Technology*, Vol. 85, No. 1-4, 825-841, doi: [10.1007/s00170-015-7949-6](https://doi.org/10.1007/s00170-015-7949-6).
- [24] Wen, C.-D., Mudawar, I. (2006). Modeling the effects of surface roughness on the emissivity of aluminum alloys, *International Journal of Heat and Mass Transfer*, Vol. 49, No. 23-24, 4279-4289, doi: [10.1016/j.ijheatmasstransfer.2006.04.037](https://doi.org/10.1016/j.ijheatmasstransfer.2006.04.037).

Container assignment optimization considering overlapping amount and operation distance in rail-road transshipment terminal

Wang, L.^{a,*}, Zhu, X.^a, Xie, Z.^{a,b}

^aSchool of Traffic and Transportation, Beijing Jiaotong University, Beijing, P.R. China

^bState Key Laboratory of Rail Traffic Control and Safety, Beijing Jiaotong University, Beijing, P.R. China

ABSTRACT

Container assignment strategy is crucial to the operation efficiency of rail-road container transshipping system. An effective container assignment approach can markedly improve integral operation efficiency of rail-road container transshipping system. In this paper, the container assignment problem in rail-road transshipment terminal was described and formulated as a two-stage optimization model considering overlapping amount and operation distance of crane. The first stage optimization model was to optimize container assigning positions for minimizing the total overlapping amount caused by container assigned in the considered block at one planning period, and an iterative solution procedure was proposed to obtain container assignment sets. Based on the container assignment sets obtained by the first stage, the second stage optimization model was to optimize the container assigning sequence for decreasing the total operation distance of crane, and a genetic algorithm was designed to obtain the optimal container handling sequences in container assignment process. Computational experiments on the data from a rail-road transshipment terminal in China were implemented to test efficiency of the proposed approach. Computational results showed that the proposed approach was effective to reduce overlapping amount and operation distance in container assignment process. The proposed approach is significant for the production and management of rail-road container transshipping terminals.

© 2017 PEI, University of Maribor. All rights reserved.

ARTICLE INFO

Keywords:

Intermodal transportation
Container assignment
Terminal scheduling
Rail-road transshipment terminal
Optimization
Genetic algorithms

*Corresponding author:

liwang@bjtu.edu.cn
(Wang, L.)

Article history:

Received 25 January 2017
Revised 21 October 2017
Accepted 26 October 2017

1. Introduction

Intermodal transportation is defined as the successive use of various modes of transportation (road, rail, air and water) without any handling of the goods themselves during transfers between modes [1]. In rail-road intermodal transshipping system, massive quantities of containers are carried by railway for long distances, and short distance transshipping and delivery are undertaken by container trucks. To enable containers efficiently transferred between trains and trucks, modern rail-road transshipment terminals are required, which have advanced modern handling resources and efficient scheduling strategies.

As a key resource of rail-road transshipment terminals, storage space is used for temporarily stockpiling inbound and outbound containers unloaded from container trains and trucks. Storage space allocation is a critical scheduling strategy defined as the temporary allocation of the inbound/outbound containers to the storage blocks at each period with aim of balancing the

workload between blocks in order to minimize the storage/retrieval times of containers [2]. Container assignment is an important decision making problem in storage space allocation strategy, which is a vital constraint for other strategies. Therefore, it is necessary for rail-road transshipment terminals to optimize their container assignment.

Outbound containers assignment problem was formulated as a mixed-integer linear programming model, whose objectives were to utilize space efficiently and make loading operations more efficient [3]. The location assignment for arriving outbound containers during container-receiving stage was formulated as two novel dynamic programming models, and compared with existent model on small-scale instances [4]. A novel mixed-integer programming model was developed to integrate storage space allocation and ship scheduling for achieving high space utilization, low material loss, and low transportation costs [5]. For improving the operations efficiency for retrieving inbound container in container terminal, three optimization models under different strategies of storing containers were proposed, namely, a non-segregation model, a single-period segregation model, and a multiple-period segregation model [6]. An ant-based model was present for the storage space allocation problem to balance operational quantities among different blocks, and minimize the moving distance of internal trucks between container yards and berths [7].

For solving container assignment problem, several heuristic algorithms were developed. An efficient GA was proposed to solve the extensional container assignment problem in container terminal [2]. For large-scale SSAP instances, a two-stage heuristic was proposed. For the first stage, a neighborhood searching heuristic was present to generate the priority sequence; a rollout-based heuristic was developed to improve the incumbent solution in the second stage [8]. An outer-inner cellular automaton algorithm (CAOI) was developed to solve SSAP, using YBAP and SAP as an integrated optimization process [9].

According to the literature review above, most of studies focused on container assignment problem in maritime container terminals. These studies generally decomposed the problem into two stages, and developed different heuristic algorithms to solve the problem. By contrast, specific literature on rail-road transshipment terminal is scarce. A two-stage optimization model was proposed to balance operational quantities and reduce overlapping amount of inbound containers [10]. A container slot allocation model based on mixed storage mode was present to minimize container overlapping amounts and a heuristic algorithm was designed for solving the model [11]. These studies only focused on decreasing the overlapping amounts, and did not consider the crane operation distance together in container assignment optimizing process. The operation distance is also an important indicator for storage space allocation in rail-road transshipment terminals. Some studies focused on crane operation optimization without considering container overlapping amount [12, 13].

Therefore, we simultaneously consider overlapping amount and operation distance in container assignment process. The main contributions of this paper are as follows. First, we present a two-stage approach for formulating the container assignment problem to minimize overlapping amount and total operation distance of crane. Second, a rolling horizon implement strategy is designed for obtain an approximate optimal solution. The proposed approach is effective for different size of planning periods.

The remainder of this paper is organized as follows. The container assignment problem in rail-road transshipment terminals is described in Section 2, and formulated in Section 3. A rolling horizon implement strategy is developed in Section 4. Computational results are discussed in Section 5. Section 6 covers the conclusion.

2. Problem description

A typical container transshipping system of rail-road transshipment terminals is mainly composed by three subsystems, including loading-unloading subsystem, storage space allocation subsystem and transport subsystem, which is shown in Fig. 1.

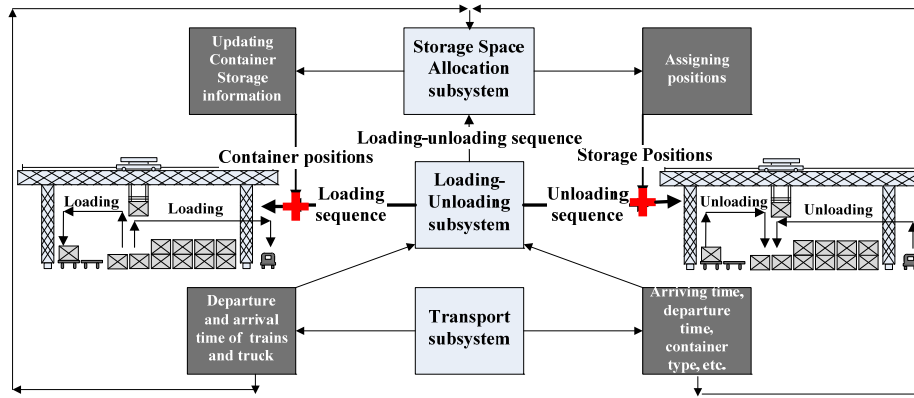


Fig. 1 A typical container transshipping system in rail-road transshipment terminals

These three subsystems ensure outbound and inbound containers can be quickly transferred in rail-road transshipment terminals. The main mission of storage space allocation subsystem is to assignment containers to the suitable positions. The assignment processing has two tasks, first is to allocated containers to blocks, and the other is to assign container to slots. Our study only focuses on the second task to assign containers in considered block.

As observed in Fig. 1, assigned containers in rail-road transshipment terminals can be classified into the following two kinds.

- Rail vehicle unloading containers (RVUC): inbound containers are on rail vehicles before unloaded and assigned to container yard.
- Truck unloading containers (TRUC): outbound containers are on trucks before unloaded and assigned to container yard.

The operations of two type assigned containers are shown in Fig. 2.

By simultaneously considering overlapping amount and operation distance, we can decompose the container assignment problem into two stages.

- First stage: Assign optimal positions for TRUCs and RVUCs to minimize overlapping amount and obtain container assignment sets.
- Second stage: Optimize assigning sequence to minimize the total operation distance of crane based on assignment sets obtained in the first stage. Because arriving time of TRUC is uncertain and discrete, TRUC assigning sequence cannot be optimized. Therefore, this stage optimization is only for the RVUCs, and TRUCs are assigned according to arriving sequence.

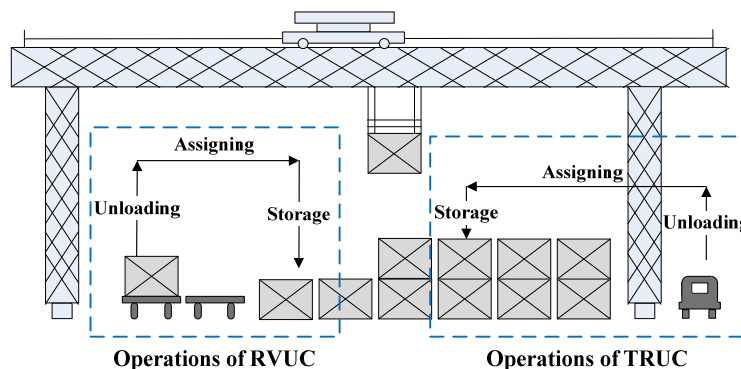


Fig. 2 Operations of two type allocated containers

3. Problem formulation

Based on the problem described above, the container assignment problem in rail-road transshipment terminal is formulated as two-stage optimization model.

3.1 Assumptions

The problem is formulated based on the following assumptions.

- 1) Initial assigning amount of RVUCs and TRUCs are assumed to be known at beginning of each planning epoch.
- 2) Arrival and departure time of containers are got beforehand and no delay happens at planning period.
- 3) There are enough resources, i.e., gantry cranes, container slots, to assign containers to the considered block.
- 4) Containers in the model are the same size.

3.2 Notations and variables

The notations and variables of two-stage optimization model are shown in Table 1.

Table 1 Notations and variables

Indexes	
$q, r :$	row index, $1 \leq q \leq R, 1 \leq r \leq R$
$a, b :$	bay index, $1 \leq a \leq B, 1 \leq b \leq B$
$e, l :$	layer index, $1 \leq e \leq L, 1 \leq l \leq L$
$(r, b, l) :$	container slot (r row, b bay, l layer)
$i, j :$	assigning index
Parameters	
$N :$	total amount of RVUCs and TRUCs
$B :$	bay amount in considered block
$R :$	row amount in considered block
$L :$	maximum layer height
$det_{(r,b,l)} :$	departure time of container in (r, b, l)
Sets	
$\tilde{S}_{RV} :$	container set of RVUCs
$\tilde{S}_{TR} :$	container set of TRUCs
$\tilde{S}_b :$	container slots set in considered block
Variables	
$S_{(r,b,l)} :$	1, if (r, b, l) has container; 0, otherwise.
$S_{(r,b,l)}^i :$	1, if assigning the i^{th} container to (r, b, l) ; 0, otherwise.
$K_{(r,b,l),(r,b,l-e)}^{RVUC} :$	overlapping of $(r, b, l-e)$ generated by RVUC assigned to (r, b, l) . 1, if $det_{(r,b,l)} < det_{(r,b,l-e)}$; 0, otherwise.
$K_{(r,b,l),(r,b,l-e)}^{TRUC} :$	overlapping of $(r, b, l-e)$ generated by TRUC assigned to (r, b, l) . 1, if $det_{(r,b,l)} < det_{(r,b,l-e)}$; 0, otherwise.
$CW_i :$	1, if the i^{th} container is RVUC; 0, otherwise.
$d_{(r,b,l)}^i :$	operation distance of the i^{th} container
$X_{(q,a,e),(r,b,l)}^j :$	1, if the j^{th} container assigned immediately begins after the i^{th} container assignment has been finished; 0, otherwise.

3.3 First stage optimization model

In the first stage, RVUCs and TRUCs are assigned to optimal container slots in each planning period. The optimization model is written as follows.

$$\min \sum_{i=1}^N [CW_i \sum_{e=1}^{l-1} K_{(r,b,l),(r,b,l-e)}^{RVUC} + (1 - CW_i) \sum_{e=1}^{l-1} K_{(r,b,l),(r,b,l-e)}^{TRUC}] \quad (1)$$

$$S_{(r,b,l)}^i - S_{(r,b,l-1)} \leq 0, \forall i \in \tilde{S}_{RV} \cup \tilde{S}_{TR}, \forall (r, b, l), (r, b, l-1) \in \tilde{S}_b \quad (2)$$

$$(1 + \sum_{e=1}^{l-1} S_{(r,b,l-e)}^i) \sum_{n=1}^{i-1} S_{(r,b,l)}^n - 1 \leq 0, \forall i \in \tilde{S}_{RV} \cup \tilde{S}_{TR}, \forall (r, b, l), (r, b, l-e) \in \tilde{S}_b \quad (3)$$

$$\sum_{i=1}^N \sum_{r=1}^{R/2-1} (1 - CW_i) S_{(r,b,l)}^i - \sum_{i=1}^N \sum_{r=R}^{R/2+1} (1 - CW_i) S_{(r,b,l)}^i \geq 0, \forall (r, b, l) \in \tilde{S}_b \quad (4)$$

$$\sum_{i=1}^N \sum_{r=1}^{R/2-1} CW_i S_{(r,b,l)}^i - \sum_{i=1}^N \sum_{r=R}^{R/2+1} CW_i S_{(r,b,l)}^i \geq 0, \forall (r, b, l) \in \tilde{S}_b \quad (5)$$

The objective function (Eq. 1) is to minimize the total overlapping amount in considered block at one planning period. The first part is the overlapping amount caused by RVUCs, and the other part is the overlapping amount caused by TRUCs. Constraint (Eq. 2) indicates that position upon empty container slot cannot be assigned. Constraint (Eq. 3) means that the subsequent operation container does not allow to be assigned below the previous operation containers. Constraint (Eq. 4) is assignment preferences of TRUCs, which ensures assigning positions of TRUCs should be near to rail handling tracks in order to decrease loading time of container trains. Constraint (Eq. 5) is assignment preferences of RVUCs, which ensures assigning positions of RVUCs should be near to truck lane for reducing loading time of trucks.

3.4 Second stage optimization model

In the second stage, based on container assignment sets obtained from the first stage, RVUCs assigning sequence will be optimized to decrease the total operation distance of crane. The optimization model is written as follows.

$$\min \sum_{i=1}^N S_{(r,b,l)}^i d_{(r,b,l)}^i \quad (6)$$

$$d_{(r,b,l)}^i = (|b-i|+r) + (|b-j|+r) X_{(q,a,e),(r,b,l)}^{ji}, \forall i, j \in \tilde{S}_{RV} \cup \tilde{S}_{TR}, \forall (r, b, l), (q, a, e) \in \tilde{S}_b \quad (7)$$

$$\sum_{j=1}^N X_{(q,a,e),(r,b,l)}^{ji} \leq 1, \forall i \in \tilde{S}_{RV} \cup \tilde{S}_{TR}, \forall (r, b, l), (q, a, e) \in \tilde{S}_b \quad (8)$$

$$\sum_{i=1}^N X_{(q,a,e),(r,b,l)}^{ji} \leq 1, \forall j \in \tilde{S}_{RV} \cup \tilde{S}_{TR}, \forall (r, b, l), (q, a, e) \in \tilde{S}_b \quad (9)$$

$$\frac{S_{(r,b,l)}^i \cdot S_{(r,b,e)}^j}{(i-j)(l-e)} \geq 0, \forall i, j \in \tilde{S}_{RV} \cup \tilde{S}_{TR}, \forall (r, b, l), (r, b, e) \in \tilde{S}_b \quad (10)$$

The objective function (Eq. 6) is to minimize RVUCs operation distance in considered block at one planning period. Constraint (Eq. 7) represents operation distance calculation of each RVUCs. The distance includes two parts. The first is loaded moving distance between the initial and final position of RVUC. The other is the unloaded moving distance from the final position of one operation to the initial position of its subsequent operation. Constraint (Eq. 8) and constraint (Eq. 9) are assigning sequence constraints, which ensure that each RVUC assigning operation at most has one pre-order operation and one subsequent operation. Constraint (Eq. 10) indicates that the assigned RVUCs must be operated in well-defined sequence.

4. Solution algorithm

For solving the two-stage optimization model present above, a rolling horizon implement strategy is developed in this section. The two-stage optimization model is solved in each planning period based on RVUCs and TRUCs initial information at beginning of each planning epoch. The implement process is shown in Fig. 3.

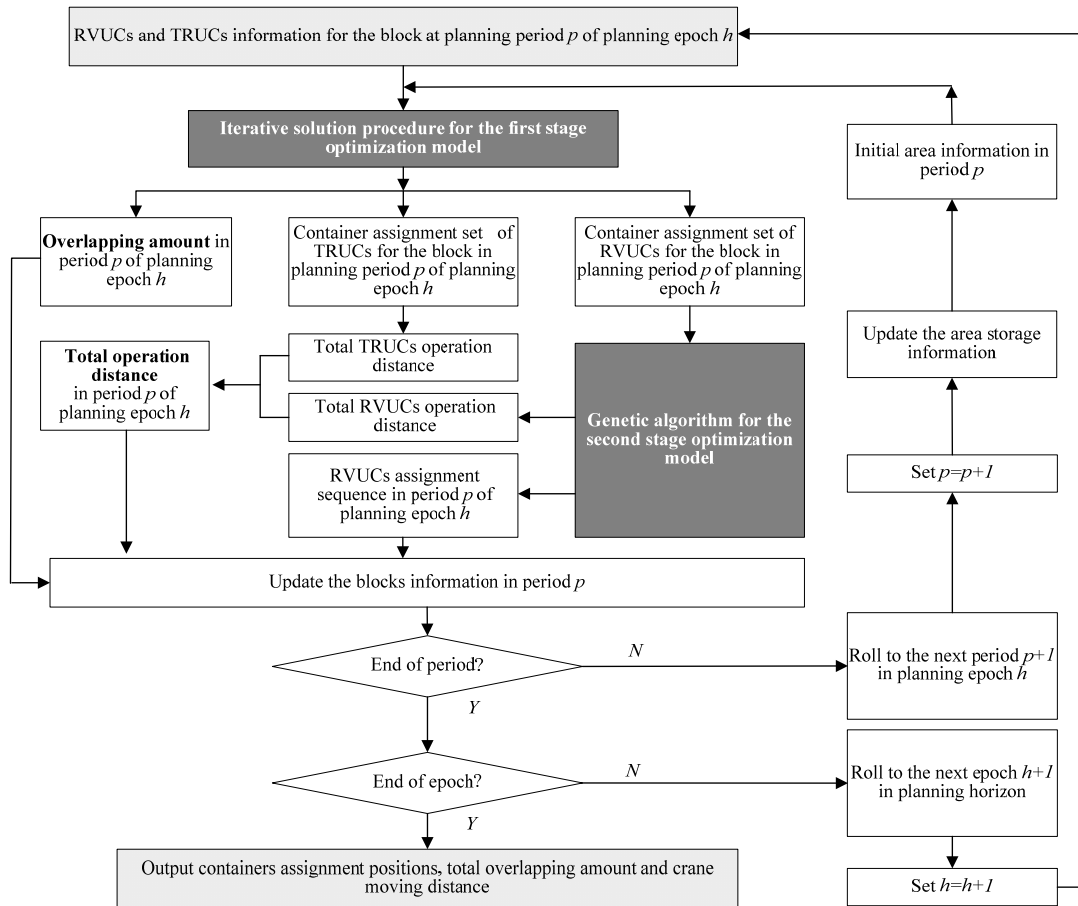


Fig. 3 A rolling horizon implement process

4.1 Iterative solution procedure for the first stage

In implement process, we introduce an iterative solution procedure for the first stage optimization model to minimize overlapping amount and obtain container assignment sets at one planning period. The related notations are described in Table 2.

In iterative solution procedure, for the i^{th} container, we firstly need distinguish the container type. For TRUC, we search the optimal assigning positions from the row near the loading-unloading track, and for RVUC, the search begins at the row near the truck operation lane. After the iterative solution procedure, we can obtain container assignment set for the i^{th} container. The details of iterative solution procedure are shown in Table 3.

Table 2 Notations of iterative solution procedure

n :	solution index
\tilde{K} :	overlapping amount sets
\tilde{F}_i :	feasible assigning set of the i^{th} container
\tilde{A}_i :	minimum overlapping amount set of the i^{th} container which belongs to RVUCs
\tilde{B}	TRUCs assignment set with minimum overlapping amounts
\tilde{S}_{ss}	optimal RVUCs assignment set with minimum total overlapping amounts
K_i^{RVUC}	overlapping amount of the i^{th} container belongs to RVUCs
K_i^{TRUC}	overlapping amount of the i^{th} container belongs to TRUCs
K_n^{VU}	overlapping amounts generated by the n^{th} feasible solution of RVUCs
K_n^{RU}	overlapping amounts generated by the n^{th} feasible solution of TRUCs
I	an arbitrary positive big number

Table 3 Iterative solution procedure

Iterative solution procedure	
Step 1:	Parameter initialization. Set $i = 1, r = 1, b = 1, \tilde{K} = \phi, \tilde{S}_{ss} = \phi, \tilde{A}_i = \phi, \tilde{B} = \phi, \tilde{F}_i = \phi, K_i^{RVUC} = I, K_i^{TRUC} = I$, go to step 2.
Step 2:	Distinguish type of the i^{th} container, get \tilde{F}_i based on the constraint (2) and (3). If the i^{th} container belongs to TRUC, go to step 3. Otherwise, let $r = R$, then go to step 6.
Step 3:	If $(r, b, l) \notin \tilde{F}_i$, go to step 4. Otherwise, assign the i^{th} container to (r, b, l) , calculate K_n^{RU} , and compare with K_i^{TRUC} . If $K_n^{RU} > K_i^{TRUC}$, go to step 4. Otherwise, let $K_i^{TRUC} = K_n^{RU}, \tilde{B} = \{S_{(r,b,l)}^i\}$, and go to step 4.
Step 4:	Let $b = b + 1$. If $b \leq B$, go to step 3. Otherwise, let $r = r + 1$, then go to step 5.
Step 5:	If $r \leq R$, go to Step 3. Otherwise, let $\tilde{K} = \tilde{K} \cup \{K_i^{TRUC}\}, \tilde{B} = \tilde{B} \cup \{S_{(r,b,l)}^i\}$, then go to step 10.
Step 6:	If $(r, b, l) \notin \tilde{F}_i$, go to step 7. Otherwise, assign the i^{th} container to (r, b, l) , calculate K_n^{VU} , and compare with K_i^{RVUC} . If $K_n^{VU} > K_i^{RVUC}$, go to step 7. Otherwise, go to step 9.
Step 7:	Let $b = b + 1$. If $i - 3 \leq b \leq i + 3$, go to step 6. Otherwise, let $r = r - 1$, then go to step 8.
Step 8:	If $r \geq 1$, go to step 6. Otherwise, let $\tilde{K} = \tilde{K} \cup \{K_i^{RVUC}\}, \tilde{A}_i = \tilde{A}_i \cup \{S_{(r,b,l)}^i\}$, then go to step 10.
Step 9:	If $K_n^{VU} = K_i^{RVUC}$, let $\tilde{A}_i = \tilde{A}_i \cup \{S_{(r,b,l)}^i\}$, then go to step 7. Otherwise, let $K_i^{RVUC} = K_n^{VU}, \tilde{A}_i = \{S_{(r,b,l)}^i\}$, and go to step 7.
Step 10:	The i^{th} container assignment is finished. Let $r = 1, b = 1, i = i + 1$. If $i > N$, go to step 11, otherwise, go to step 2.
Step 11:	Procedure terminates. Obtain overlapping amount of the period p based on \tilde{K} , get \tilde{S}_{ss} based on the constraint (3) and the mapping relationship of \tilde{A}_i .

4.2 Genetic algorithm for the second stage

Based on the optimal container assignment sets obtained from the first stage, a genetic algorithm is developed for optimizing assigning sequences to minimize total RVUCs operation distance at one planning period. Main steps of genetic algorithm implementation are introduced in the following subsections.

Chromosome representation

Two-dimensional encoding is employed for chromosome representation in this paper. Each chromosome represents a possible assigning sequence of RVUCs at one planning period, and includes genes are RVUCs amount in considered block at one planning period. Each gene includes five parts, which are RVUC index, row, bay and layer index of assignment slot, and arrival period of RVUC. The sequence of gene from the left to right represents the assigning sequence. A sample of chromosome representation is shown in Fig. 4. In the sample, there are 6 RVUCs to be assigned, gene1 represents the 5th RVUC arriving at the second period is assigned to the container slot (5,7,1), and the whole chromosome means the six RVUCs are assigned according to the sequence of 5-(5,7,1)-1-(2,9,1)-4-(4,6,2)-6-(1,11,1)-2-(6,9,2)-3-(4,10,2).

	Gene 1	Gene 2	Gene 3	Gene 4	Gene 5	Gene 6
RVUC index	5	1	4	6	2	3
Row index of assignment slot	5	2	4	1	6	4
Bay index of assignment slot	7	9	6	11	9	10
Layer index of assignmet slot	1	1	2	1	2	2
Arrival period of RVUC	2	2	2	2	2	4

Fig. 4 A Sample of chromosome representation

Evaluation of fitness value

Some of chromosomes generated by the genetic operators do not violate constraint (10). Therefore, every chromosome must be verified whether its corresponding sequence satisfies the constraint. If it satisfies constraints (10), calculate the chromosome fitness value based on Eq. (11). Otherwise, set its fitness value to zero.

$$Fitness\ value = \frac{1}{\sum_{i=1}^N S_{(r,b,l)}^i d_{(r,b,l)}^i} \tag{11}$$

Genetic operators design

In the developed GA, initial generation is randomly generated, and tournament selection is employed as selection operator.

- **Crossover operator**

Based on constraints (Eq. 8) to (Eq. 10), the values of RVUC index cannot to be lost and repeated in offspring, so the order crossover operator is employed in this paper. The crossover operator works as follows, and a sample of crossover operating is shown in Fig. 5.

Step1: Randomly select a substring from each parent.

Step2: Copy the selected substring into the front of other parent to produce a proto-child.

Step3: Scan the first layer of proto-child from left to right, and delete repeated gene values behind the substring. An offspring is produced.

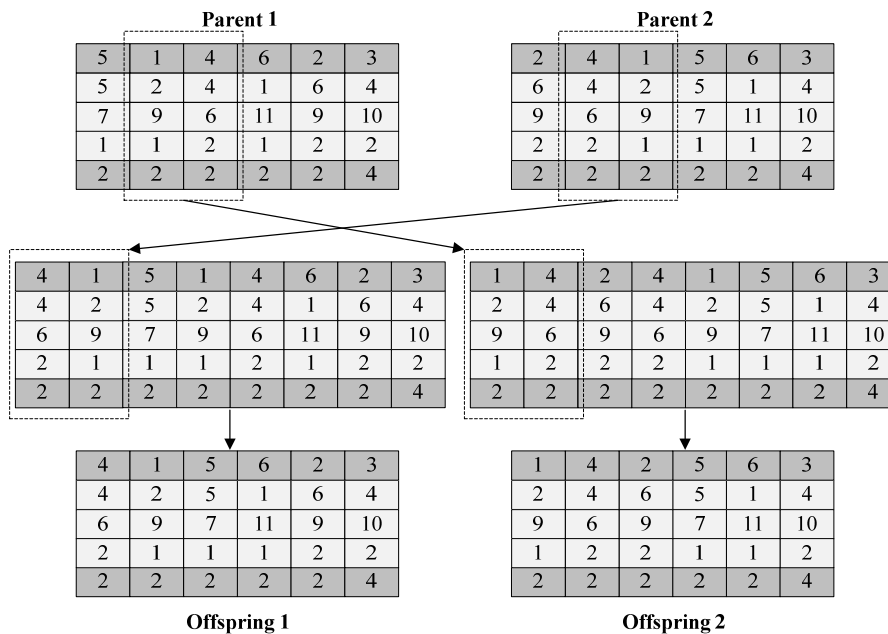


Fig. 5 A sample of crossover operating

- **Mutation operator**

To avoid losing and repeating of RVUC index in offspring, we use the inversion mutation operator, which firstly chooses two mutation points randomly, then inverts two points genes. A sample is shown in Fig. 6.

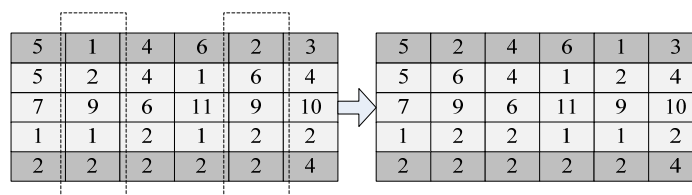


Fig. 6 A sample of mutation operating

5. Computational experiments: Results and discussion

To illustrate the approach proposed above, computational experiments are conducted by using the data from a rail-road transshipment terminal in China. For evaluating efficiency of the proposed approach, some comparisons are made. All experiments are implemented based on a personal computer with Intel Core(TM) i5-2450M @ 2.50GHz processors and 4 GB RAM.

Parameters related to the rail-road transshipment terminal are introduced as follows. The container yard of terminal has four blocks. Each block includes 20 bays, 6 rows and 2 layers. Most of RVUCs and TRUCs are handled no more than two days after they assigned to blocks, so we set two days as a planning horizon, one day as a planning epoch and six hours as a planning period. Therefore, each planning horizon has two planning epochs or eight planning periods.

Firstly, we choose a planning epoch to implement the proposed approach. The initial information of RVUCs and TRUCs in considered block at one planning epoch is shown in Table 4.

Based on the initial information in Table 4, the iterative solution procedure for the first stage is conduct to obtain RVUCs and TRUCs assignment sets with minimum overlapping amount. For evaluating improvement of the proposed approach (PA), we make a comparison with random search algorithm (RSA) which is used in rail-road transshipment terminals. Computational results of the first stage are shown in Table 5.

Table 4 Initial information at one planning epoch

Planning period 1				Planning period 2				Planning period 3				Planning period 4			
No.	T	At	Dt												
1	I	2	34	1	I	6	38	1	II	13	26	1	II	18	72
2	I	2	19	2	I	6	32	2	II	13	26	2	II	18	72
3	I	2	17	3	I	6	20	3	II	15	26	3	II	20	48
4	I	2	32	4	I	6	32	4	II	15	48	4	II	20	72
5	I	2	38	5	I	6	40	5	II	17	72	5	I	21	55
6	I	2	32	6	I	6	40	6	I	17	34	6	I	21	55
7	I	2	34	7	I	6	40	7	I	17	56	7	I	21	64
8	I	2	32	8	I	6	38	8	I	17	37	8	I	21	45
9	I	2	38	9	I	6	32	9	I	17	37	9	I	21	58
10	I	2	20	10	II	7	26	10	I	17	38	10	I	21	40
11	I	2	20	11	II	7	26	11	I	17	32	11	I	21	67
12	I	2	35	12	II	9	26	12	I	17	32	12	I	21	62
13	I	2	22	13	II	9	48	13	I	17	44	13	I	21	38
14	I	2	38	14	II	9	48	14	I	17	36	14	I	21	38
15	I	2	56	15	II	10	48	15	I	17	36	15	I	21	62
16	I	2	15	16	II	10	48	16	I	17	36	16	I	21	59
17	I	2	34	17	II	10	48	17	I	17	40	17	II	22	48
18	I	2	38	18	II	10	48	18	I	17	40	18	II	22	48
19	I	2	63	-	-	-	-	19	I	17	34	19	II	23	48
20	I	2	20	-	-	-	-	20	II	18	48	20	II	23	72
21	I	2	36	-	-	-	-	21	II	18	72	21	II	23	72
22	II	4	26	-	-	-	-	22	II	18	72	-	-	-	-
23	II	6	26	-	-	-	-	-	-	-	-	-	-	-	-
24	II	6	48	-	-	-	-	-	-	-	-	-	-	-	-

Notes: T denotes Type (I—RVUC, II—TRUC); At denotes the arrival period of containers in a planning horizon; Dt denotes the departure period of containers in a planning horizon.

Table 5 Comparison between PA and RSA in the first stage at one planning epoch

Planning period	Overlapping amount (PA)	Overlapping amount (RSA)	GAP ¹
1	4	9	55.6 %
2	2	5	60.0 %
3	3	7	57.1 %
4	2	4	50.0 %
Total amount	11	25	56.0 %

Notes: GAP¹= (overlapping amount obtained by RSA - overlapping amount obtained by PA) · 100/ overlapping amount obtained by RSA.

As observed in Table 5, the overlapping amount has been decreased in each planning period. Based on RVUCs assignment sets obtained by the first stage, genetic algorithm for the second stage is conducted to optimize assigning sequence. For 50 independent runs, the average time consumption of each planning period is 2.3 min, the average time consumption of each planning epoch is 11.7 min, which can meet requirement of practical operations in rail-truck transshipment terminals. In order to evaluate our approach, we compare the operation distance obtained by our approach with average operation distance of RVUC assignment sets (AOD). The computational results of the second stage are shown in Table 6.

As shown in Table 6, operation distance has been reduced by optimizing assigning sequence at each planning period. The decrease of operation distance can directly improve container assignment efficiency. For further evaluating performance of the proposed approach, computational experiments on 30 days are implemented. The experimental results are shown in Fig. 7.

Table 6 Comparison between PA and AOD in the second stage at one planning epoch

Planning period	Operation distance (PA) (m)	Operation distance (AOD) (m)	GAP ²
1	836.4	875.5	4.5 %
2	340.6	356.5	4.5 %
3	597	622	4.0 %
4	476.4	507.5	6.1 %
Total amount	2250.4	2361.5	4.7 %

Notes: $GAP^2 = (\text{operation distance obtained by AOD} - \text{operation distance obtained by PA}) \cdot 100 / \text{operation distance obtained by AOD}$.

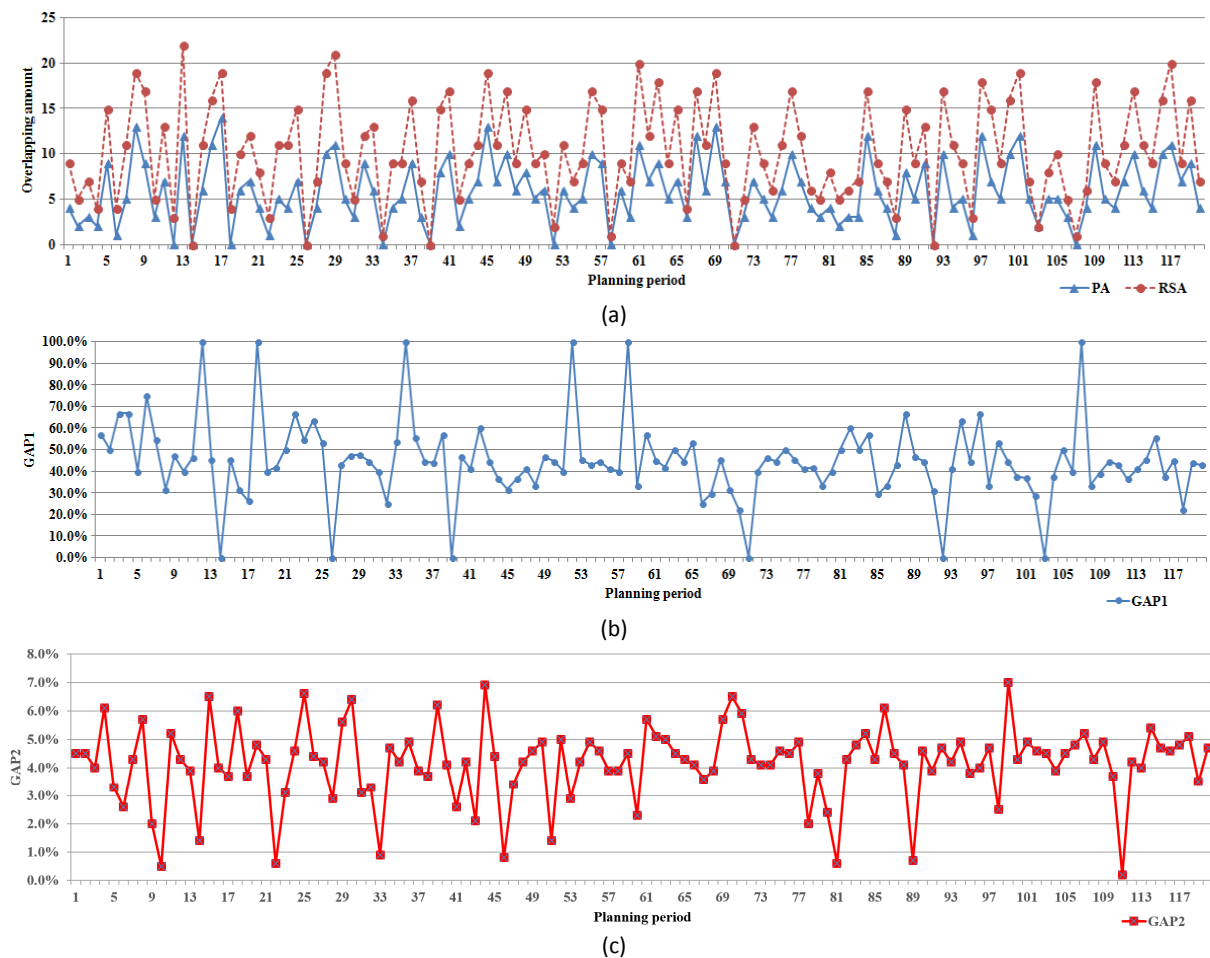


Fig. 7 Overlapping amount in 30 days: (a) overlapping amount comparison between PA and RSA in 30 days; (b) GAP¹ in 30 days; (c) GAP² in 30 days

As observed in Fig. 7(a) and (b), the overlapping amount caused by RVUCs and TRUCs assigned are prominently reduced at each period of 30 days, and average of GAP¹ is 44.8 %. Almost half of container re-handling operations have been eliminated by optimizing assignment of RVUCs and TRUCs. On the basis of minimum overlapping amount, RVUC assignment sequences are optimized to minimize the operation distance at each period, and the average of GAP² is 4.1 % shown in Fig. 7(c). The decreases of overlapping amount and operation distance can directly improve container loading-unloading operation and cranes utilization efficiency. The experimental results of different size planning periods indicate that the proposed approach is effective and efficient for container assignment in rail-road transshipment terminals.

6. Conclusion

In this paper, container assignment problem of rail-road transshipment terminals was considered and formulated as a two-stage optimization model. The first stage was to optimize assignment positions to minimize overlapping amount, and the second stage was to optimize assigning sequence to minimize the operation distance. For solving the model, an iterative solution procedure was proposed to minimize overlapping amount in the first stage, and a genetic algorithm was developed to minimize operation distance in the second stage. Computational experiments were conducted by using real-life data, and results showed that our approach could reduce overlapping amount and operation distance while containers assigning, and remarkably improve efficiency of containers storage allocation.

The proposed approach cannot be directly used to optimize other container logistics system, etc. water-rail and water-road transshipment system. Because each system has its specific container assignment rules, optimization problem has different constraints. These logistics processes optimization can draw on our problem solving procedure, and proposed similar approach based on these characteristics. Our approach can serve as an important reference for container assignment problem.

In future, considering the uncertainty of container arrival-departure time which caused by the delay of trains and trucks, to propose the automatic container assignment optimization model under uncertainty is a possibility for further research.

Acknowledgement

This work was supported by the Major Program of National Natural Science Foundation of China (grant number 71390332), Specialized Research Fund for the Doctoral Program of Higher Education (grant number 20130009110001), Fundamental Research Funds for the Central Universities (grant number 2015JBM056), Talented Faculty Funds of Beijing Jiaotong University (Grant no. 2016RC045) and China Postdoctoral Science Foundation (grant number 2015M570925).

References

- [1] Boysen, N., Flidner, M. (2010). Determining crane areas in intermodal transshipment yards: The yard partition problem, *European Journal of Operational Research*, Vol. 204, No. 2, 336-342, doi: [10.1016/j.ejor.2009.10.031](https://doi.org/10.1016/j.ejor.2009.10.031).
- [2] Bazzazi, M., Safaei, N., Javadian, N. (2009). A genetic algorithm to solve the storage space allocation problem in a container terminal, *Computers & Industrial Engineering*, Vol. 56, No. 1, 44-52, doi: [10.1016/j.cie.2008.03.012](https://doi.org/10.1016/j.cie.2008.03.012).
- [3] Kim, K.H., Park, K.T. (2003). A note on a dynamic space-allocation method for outbound containers, *European Journal of Operational Research*, Vol. 148, No. 1, 92-101, doi: [10.1016/S0377-2217\(02\)00333-8](https://doi.org/10.1016/S0377-2217(02)00333-8).
- [4] Zhang, C., Wu, T., Zhong, M., Zheng, L., Miao, L. (2014). Location assignment for outbound containers with adjusted weight proportion, *Computers & Operations Research*, Vol. 52, 84-93, doi: [10.1016/j.cor.2014.06.012](https://doi.org/10.1016/j.cor.2014.06.012).
- [5] Tang, L., Sun, D., Liu, J. (2016). Integrated storage space allocation and ship scheduling problem in bulk cargo terminals, *IIE Transactions*, Vol. 48, No. 5, 428-439, doi: [10.1080/0740817X.2015.1063791](https://doi.org/10.1080/0740817X.2015.1063791).
- [6] Yu, M., Qi, X. (2013). Storage space allocation models for inbound containers in an automatic container terminal, *European Journal of Operational Research*, Vol. 226, No. 1, 32-45, doi: [10.1016/j.ejor.2012.10.045](https://doi.org/10.1016/j.ejor.2012.10.045).
- [7] Sharif, O., Huynh, N. (2013). Storage space allocation at marine container terminals using ant-based control, *Expert Systems with Applications*, Vol. 40, No. 6, 2323-2330, doi: [10.1016/j.eswa.2012.10.032](https://doi.org/10.1016/j.eswa.2012.10.032).
- [8] Hu, W., Wang, H., Min, Z. (2014). A storage allocation algorithm for outbound containers based on the outer-inner cellular automaton, *Information Sciences*, Vol. 281, 147-171, doi: [10.1016/j.ins.2014.05.022](https://doi.org/10.1016/j.ins.2014.05.022).

- [9] Boysen, N., Fliedner, M., Jaehn, F., Pesch, E. (2013). A survey on container processing in railway yards, *Transportation Science*, Vol. 47, No. 3, 312-329, doi: [10.1287/trsc.1120.0415](https://doi.org/10.1287/trsc.1120.0415).
- [10] Wang, L., Zhu, X., Xie, Z. (2014). Storage space allocation of inbound container in railway container terminal, *Mathematical Problems in Engineering*, Vol. 2014, 1-10, doi: [10.1155/2014/956536](https://doi.org/10.1155/2014/956536).
- [11] Wang, L., Zhu, X.-N., Yan, W., Xie, Z.-Y., Li, Q.-B. (2013). Optimization Model of Mixed Storage in Railway Container Terminal Yard, *Journal of Transportation Systems Engineering and Information Technology*, Vol. 2, 172-178, doi: [10.3969/j.issn.1009-6744.2013.02.026](https://doi.org/10.3969/j.issn.1009-6744.2013.02.026).
- [12] Guo, P., Cheng, W., Zhang, Z., Zhang, M., Liang, J. (2013). Gantry crane scheduling with interference constraints in railway container terminals, *International Journal of Computational Intelligence Systems*, Vol. 6, No. 2, 244-260, doi: [10.1080/18756891.2013.768444](https://doi.org/10.1080/18756891.2013.768444).
- [13] Wang, L., Zhu, X., Xie, Z. (2016). Rail mounted gantry crane scheduling in rail-truck transshipment terminal, *Intelligent Automation & Soft Computing* Vol. 22, No. 1, 61-73, doi: [10.1080/10798587.2015.1041764](https://doi.org/10.1080/10798587.2015.1041764).
- [14] Tang, M., Gong, D., Liu, S., Zhang, H. (2016). Applying multi-phase particle swarm optimization to solve bulk cargo port scheduling problem, *Advances in Production Engineering & Management*, Vol. 11, No. 4, 299-310, doi: [10.14743/apem2016.4.228](https://doi.org/10.14743/apem2016.4.228).
- [15] Grubišić, N., Dundović, Č., Žuškin, S. (2016). A split task solution for quay crane scheduling problem in mid-size container terminals, *Tehnički vjesnik - Technical Gazette*, Vol. 23, No. 6, 1723-1730, doi: [10.17559/TV-20150914110215](https://doi.org/10.17559/TV-20150914110215).
- [16] Rajkovic, R., Zrnic, N. Stakic, D. (2016). Application of a mathematical model for container transport flow of goods: From the Far east to Serbia, *Tehnički vjesnik - Technical Gazette*, Vol. 23, No. 6, 1739-1746, doi: [10.17559/TV-20140629203730](https://doi.org/10.17559/TV-20140629203730).

Work sampling for the production development: A case study of a supplier in European automotive industry

Martinec, T.^a, Škec, S.^a, Savšek, T.^b, Perišić, M.M.^a

^aUniversity of Zagreb, Faculty of Mechanical Engineering and Naval Architecture, Zagreb, Croatia

^bTPV d.d., Novo Mesto, Slovenia

ABSTRACT

Effective development of production processes within modern engineering projects requires project management to take into consideration the socio-technical project aspects, such as insights into individual and team work, including how much time team members spend on different activities, how they communicate, within what context and in what manner. The paper reports on a self-reporting work sampling approach developed and tailored for the production development and the application of the approach in an automotive industry supplier company. A case study was conducted in a Tier 1 development and manufacturing supplier for the automotive industry in EU. Although the approach requires a significant amount of preparation efforts to configure the tools and reduce participants self-reporting bias, it is less intrusive during data collection as it does not require the presence of researchers. Results provide insights into team members' work type engagement and how their activity was coupled with the context, the manner and the nature of information transaction utilized. Project managers can use these insights to tailor workloads and modify team composition to improve collaboration, coordination and information exchange.

© 2017 PEI, University of Maribor. All rights reserved.

ARTICLE INFO

Keywords:

Automotive industry
Production development
Project management
Teamwork
Work sampling

*Corresponding author:

tomislav.martinec@fsb.hr
(Martinec, T.)

Article history:

Received 24 February 2017
Revised 23 October 2017
Accepted 26 October 2017

1. Introduction

Product realization can be defined as a set of activities integrating product design and production development to deliver products that meet the needs of customers [1]. The benefits of the integrated development are particularly manifested within the narrow time frame of modern engineering projects. The integrated approach to development of new products has been well embraced, with automotive industry being the front-line example. To provide short time-to-market, automotive original equipment manufacturers (OEMs) are forced to integrate product- and production-related activities [2] and involve suppliers from early phases of the product development [3]. Nevertheless, the activities of production development are often ignored within product development models even though it provides crucial steps in delivering marketable products [4].

Production development can be perceived as a concept related to development of effective production processes and improvement of production ability [1]. Activities of production development start at the very beginning of product realization (product conception and design), when important aspects of manufacturing technologies and materials are defined. Successful integration and efficient development rely mostly on well-established coordination and cooperation [5] and resource allocation by the management [1] in both OEMs and supplier organizations. More-

over, the increasing need for organizational innovation as a source of competitive advantage asks for new managerial practices not only to cope with development of complex products but also to reduce administrative costs and improve workplace satisfaction [6].

Traditionally, the management approaches in product and production development context are often focused solely on the technical aspects of project management [7], such as planning, scheduling, risk management, cost control, etc. Recently, the progress of information technology has significantly advanced these technical aspects of project management and made them more efficient [7]. Despite the availability of different tools, effective project management needs to take into consideration also the socio-technical perspective [8], since it is the people that are the centre of projects. Project managers thus require understanding and timely insight into the working processes, the teamwork and the working environment in which the developers are engaged.

To better understand the socio-technical aspects of production development, there is a need to collect data for the activity of each participant in the development process. Such data collection often implies logbooks and retrospective interviews or questionnaires. However, in recent years, the number of new data gathering approaches significantly increased by using digital technologies such as the use wearable recording equipment (photo, video and audio) and tracking software [9]. Building on these premises, a self-reporting approach for work sampling has been developed and tailored for the production development context. Work sampling is a methodical approach used for measuring the timeshare individuals spend performing different activities, based on collecting data at specific time intervals. In comparison to other work measurement methods, work sampling is perceived as a more reliable, valid and practical approach [10].

Several aspects of scientific contribution have been identified within the extent of this paper. Firstly, a methodology for a longitudinal work sampling research in organizational environment has been developed to allow conducting this type of research in production development context. Work sampling in production context tends to be applied mainly for shop floor workers [11], whereas in presented research it is introduced within the development environment. Secondly, insights from the literature and organizational settings have been applied to develop comprehensive self-reporting menu structures for the production development context, which were then validated in a case study. Thirdly, the paper reports on a unique empirical study of work measurement conducted in production development, at a supplier level in automotive industry, and reveals rich insights on working in that context. Besides the analysis of individual work, the presented study includes the team perspective of production development activities which was neglected in previous research. Finally, the paper describes a more efficient method of self-report work sampling and, as such, allows the transition from research to practical use in organizations.

2. Methodology

The implementation of the work sampling approach required the development of a methodology for longitudinal work sampling research in organizational environment. The methodology consists of five main steps as illustrated in Fig. 1. The first step combines literature review and discussion with representatives of the organization in which the case study takes place. In the second step the work sampling method is adapted based on the insights obtained from the literature and the organizations. The adaptation of the method is followed by the development of a mobile application tool which simplifies and speeds up the self-reporting approach. After the work sampling application's functionality is verified, it is introduced within the case study organization, as the fourth methodology step. At last, the validation of the collected data and obtained insights can be performed by means of interviews and questionnaires performed on study participants.

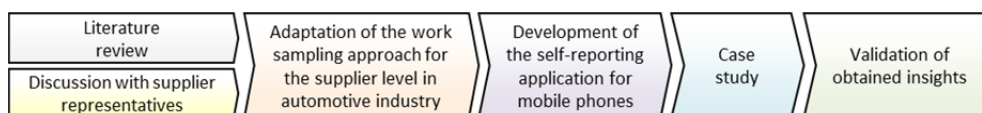


Fig. 1 An overview of the research methodology

2.1 Insights from the literature and the discussions with supplier representatives

Current trends of mass vehicle customization demand an ongoing improvement of efficiency and flexibility of production processes of both the OEMs and their suppliers [2]. Modular designs allow automotive OEMs to shift from outsourcing single components to more valuable and physically larger independent modules [3, 12]. Following this, parts of design and production are outsourced to suppliers. The competitiveness of OEMs thus depends largely on the performance of suppliers and their production development teams.

To increase understanding on activity of production development teams, researchers have been studying the process using approaches such as observations, interviews, document studies and surveys [13, 14]. Besides measuring the work of individual team members, a special importance has been put on teamwork aspects of development activities. Recent studies thus emphasize that collaborative performance should not be overlooked when teams are composed [15]. Therefore, to understand better how production development is conducted, participants of the process must be observed within the team and teamwork context.

In the context of product realization, a team is defined as a small group of individuals which have complementary abilities and are responsible for achieving their common goals [12]. Teamwork is related to the degree of cooperation between the members of the team involved in the process. Team members have their own behaviour patterns, different expectations and understanding of processes and products. Key part of each production development process is to achieve a common understanding of the objectives, despite individual mental models.

During the product and production development process, teams have relatively stable structure and usually work together on several projects [16]. It is common for each team member to be responsible for specific tasks depending on their competence. Although engineers work individually most of the time [16], the need for communication and interaction is continuous. The communicated information are influenced by their organizational and social context thus the communication embraces different contexts of engineering activities such as stakeholder, employee and project issues [17].

In research studies related to the analysis of individual and team work often quite rough and vague measures are used, thereby preventing simultaneous analysis of different production development aspects. Hence, as part of this research paper, analysis of different aspects of individual and team work has been done by analysing how much time individuals spent on different activities, how they communicated, within what context and in what manner. The work sampling approach provided insight into how individuals and team as a whole conduct their activities.

The best-known application of work sampling in the development context is the study conducted by Robinson in a blue-chip international manufacturing engineering organization [18]. He studied the behaviour of engineers across the organization in terms of information use and time spent during the development process [18]. Furthermore, the study by Škec *et al.* [19] represents the applications of here described work sampling approach in the context of product development, within an SME whose activities are focused on the design of systems for the generation, distribution and transformation of electrical energy.

In this paper, the work sampling is applied for a team in the production office context, to measure the timeshare of development-related activities of team members. It is argued that the possession of such type of objectivized data about the conducted development process can support the decision-making of project managers when they are confronted with a task of team composition or team member allocation. The self-reporting approach to work sampling overcomes some of the inherent drawbacks of design ethnography methods (e.g. significant effort because research subject is followed personally) and offers new opportunities for a simplified and more accurate data collection process. Sampling of work activities in such way offers possibility to explore multiple aspects of working content and context. By analysing collected data, more embrative picture of the individual and team work could be obtained.

Discussion with supplier representatives within the automotive industry added further understanding needed to build the case study, such as organization's contextual information, project types and project-based team composition strategies.

2.2 Adaptation of the work sampling approach

Before applying it in a case study, the work sampling approach had to be adapted to the specific context and embedded within a tool that is practical for the study participants to use. A series of menus and menu items were developed to include the aspects of individual and team work identified in production development within automotive industry and allow a predefined data entry. The menu structure will be only briefly explained. Comprehensive description of menus and menu items is available in Škec *et al.* [19]. The self-reporting menu structure (Table 1) includes several scenarios, based on the menu items selected in each menu.

Table 1 Menu structure of the work sampling application developed for the case study context

Activity type	Activity	Context	Party	Manner	Information transaction			
Teamwork	Discussion (informal)	Management activities	Planning	Designing the product	Electronics	Team member 1	Face-to-face	Giving information
			Resolving conflicts		Mechanical/Hardware	Telephone	Receiving information	
		Resource assignment	Software	Team member 2	Video conference			
		Negotiation		Team member 3	Email			
	Meeting (formal)	Evaluation activities	Analysis/Simulation	Designing the process	Manufacturing/Deploying	Team member 4	Engineering software tools	Processing information (group thinking)
			Decision making		Logistics/Installation	Team member X	Office software tools	
		FMEA	Maintenance/Serviceing	Team member X	ERP			
		Measurement/Testing		Disposal/Reusing	Internet			
	Presentation/Reporting	Definition activities	Conceptual/Design	Administrative	Customer	Supplier	PDM/PLM	Exchanging information
			Detailing/Coding				Knowledge base	
		Ideation/Improvement	People/Team members	Other-internal	Other-external	Paper misc	Requesting information	
		Documenting				Whiteboard/Smart board		
Prototype realization		Facilities/Infrastructure	Other-external	Other team manner	Searching for information			
Sales/Procurement								
User support	Other Teamwork context							
Individual technical work	Menu is bypassed	Management activities	Planning	Designing the product	Electronics	No one (item is automatically written in the database)	Email	Giving information
			Resolving conflicts		Mechanical/Hardware		Engineering software tools	Receiving information
		Resource assignment	Software	Team member 2	Office software tools			
		Negotiation		Team member 3	ERP			
	Menu is bypassed	Evaluation activities	Analysis/Simulation	Designing the process	Manufacturing/Deploying	Team member 4	PDM/PLM	Processing information
			Decision making		Logistics/Installation	Team member X	Internet	
		FMEA	Maintenance/Serviceing	Team member X	Knowledge base			
		Measurement/Testing		Disposal/Reusing	Paper misc			
	Monitoring/Reviewing	People/Team members	Other-internal	Other-external	Logbook	Requesting information		
	Conceptual/Design							
	Detailing/Coding	Facilities/Infrastructure	Other-external	Other individual technical manner	Calendar	Searching for information		
	Ideation/Improvement							
Documenting	Other individual context							
Individual administrative work	Menu is bypassed	Time booking	Administrative (item is automatically written in the database)	No one (item is automatically written in the database)	Email	Menu is bypassed		
		Arranging meeting			Office software tools			
		Arranging travel/accomodation			ERP			
		Traveling			Internet			
		Completing expense claim			Paper misc			
		Data entry			Logbook			
		Checking e-mails			Calendar			
		Other administration			Other individual admin. manner			
Break	Menu is bypassed	Menu is bypassed	Menu is bypassed	Menu is bypassed	Menu is bypassed	Menu is bypassed		

At the start of the self-report, the participant must select the *project* they are working on in the moment. This menu is followed by the selection of the *work type* which is either individual technical work, individual administrative work, teamwork, or break. Unless break was selected, the participants must also report the *activity type*. The types of activities derived from the work of Robinson [18] and were further developed based on the ontology of development activities [21] which provides researchers a consistent and coherent description of the interpretation of typical development activities. Completeness of activity type menu was ensured through an analysis of work activities provided by the HR department of the participating company.

For individual technical and team work, the participants must also report the *activity context*, based on a detailed classification of activities' technical context as provided in the ontology for engineering design by Ahmed and Štorga [22]. If the participant is engaged in teamwork, they must select the *party* involved. Apart from generic menu items such as customer and supplier, the menu is customized to contain the names of all team members allocated to the selected project.

Participants also need to select the *manner* in which the work is performed, ranging from communication means to computer-based tools. This menu is based on the work of Allard *et al.* [23] and McAlpine *et al.* [24]. Finally, the type of *information transaction* needs to be reported for the individual technical and team work. The types of information transaction derive from Cash [25].

Once created, the menus and the menu items were validated with the company representatives and the study participants. The menu items have been developed as highly abstract to enable applicability in different environments and different types of projects.

2.3 Development of a mobile application for work sampling

Once the work sampling method was adopted, a self-reporting mobile application had to be developed to serve as a tool for utilizing the approach. This step included both functional design and user experience design for the mobile application.

The architecture of the mobile application for work sampling has been designed to consist of the sequence of input screens with predefined menus, following Robinson's research [18] and using the analogy with the concept of a self-reporting electronic diary [26]. After work sampling application randomly emits an alarm, the user (study participant) is required to respond to application's notification which immediately redirects them to the first input screen of the application. Each input screen contains items of which one or more can be selected (based on the menu structure shown in Table 1). Such way of collecting simplifies and speeds up data entry.

Additionally, the administration interface was developed to allow customization of the work sampling sessions and real-time data access. The customization of the menu structure for particular study was done by importing contextual data, including ongoing projects and people.

2.4 Case study

The Case study was conducted in the organization which is Tier 1 development and manufacturing supplier for the automotive industry in EU. A team whose preoccupation are production ramp-up [27] and production planning and development [10] was selected for the study. Team's activities include establishment and improvement of manufacturing, logistics and procurement processes.

Two types of study preparation were performed: technical check of the application functionality and introductory workshops during which the work sampling application and the way it should be used were briefly explained. Study participants also received an application manual in which they could find instructions for using the application and thorough descriptions of each menu. Employees from the IT department were responsible for checking application's technical aspects. Researchers conducting the study were open for discussions during the work sampling period to clarify all misunderstandings. As the last step before session start, it was necessary that participants test the application for a one day period to better understand how to use it. This one day period was not included in the analysis. Once the participants got used to the data input, time required for data input significantly decreased to approximately 30 seconds per alarm.

The activities of 15 team members were sampled during 13 working days (two and a half weeks). Team members' field of expertise are as follows: 8 are from technical department, 5 from engineering sales/procurement and 2 from logistics. The sampled projects were at different phases implying different workload distribution. Alarms were randomly emitted 6-8 times per day with intervals of 30 to 90 minutes between two alarms. Such intervals were determined by a variation of stratified non-continuous random sampling [10, 28], where the working day is divided into several segments of different duration to reduce variance.

3. Results and discussion

The results are presented from several viewpoints. First is the analysis of the data collection process in terms of team members' responds to alarms. Following is the analysis of the work type and the occurrence of different types of activities. Finally, the analysis of team members' activity was coupled with the context, the manner and the nature of information transaction utilized, with a goal to obtain new insights for the sample points. Due to the limited period of 13 working days sampled in this study, the results cannot be generalized on organizational level, thus only the short-term socio-technical aspects of the project have been observed and discussed. Long-term insights and the effects of the proposed approach on the technical aspects of production development such as time, cost and quality, require conduction of longitudinal studies with a significantly longer work-sampling periods. To confirm the overall correctness and accuracy of results, a workshop with all participants was organized after the sampling session.

3.1 Data collection analysis

In total 1365 alarms were emitted during the work sampling session. Team members entered data on 1127 occasions meaning that the overall response rate was 82.6 %, which is higher than the response rate reported in Robinson's study (74.87 %) [10], but slightly lower than what was reported by Škec *et al.* for the product development context (87.9 %) [19]. This number of sample points enables detection of a task accounting for 5 % of the working time, with ± 20 % precision, and 90 % of confidence [19], according to work sampling calculations available in [11], [10]. The number of overall responds to alarms varied from 42 to 96 per each team member during the sampling session. Average number of alarms responded per team member was 75.1, indicating that the average number of alarms responded per day for individual team member was 5.78. The difference in the number of alarm responds is a result of the random number of alarms emitted for each team member (during one day) and lower response rate by some team members (Fig. 2).

To ensure that team members respond to alarms promptly, the percentage of answered alarms in the given time intervals was monitored. Fig. 3 shows the distribution of time elapsed between the moment of emitting the alarm and the moment of filling out the report for the given alarm.

In total 68.6 % of the alarms were responded in the period of first 30 minutes after alarm was emitted. Additional 10.6 % were responded in the interval from 30-60 minutes after the alarm. These response rates correspond to what has been reported in the study conducted in the product development context [19] and indicate team members' fast adaptation to the study requirements. Since team members entered data shortly after the alarm was emitted, it was possible to obtain data in real time and with less retrospective bias. Other self-reporting approaches such as interviews and surveys rely on memory to recall what was happening and in what manner [18].



Fig. 2 Number of responds to alarms during the work sampling period for each team member (TM)

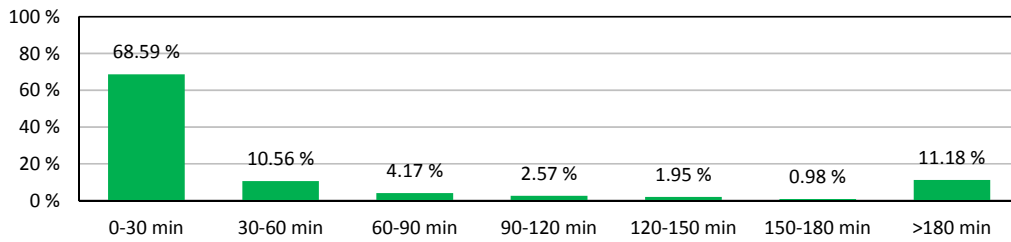


Fig. 3 Percentage of responds to alarms within particular periods of time after the alarm was emitted

Although the proposed approach allows simple data collection from team members on different locations, it still requires their additional effort as they have to input the report data. Moreover, every time team members were required to input data for a certain alarm, they were interrupted in their current execution of activity and had to again switch context from one activity (self-reporting) to another (current work activity). Because of these reasons, the motivation of team members could become an issue during long-term studies. Possible solutions could include various forms of extrinsic motivation and strong support from higher management.

3.2 Work type analysis

Analysis of work type indicated that some team members have higher proportions of *individual technical work* (e.g. Team member 6), while some have higher proportions of *teamwork* (e.g. Team member 8). One can also notice high proportion of *breaks* for certain team members such as Team member 4 (24 %) and Team member 9 (32 %) because of their absence from work during some days of the work sampling session (Fig. 4).

The results of work type analysis indicate significant proportion of *individual administrative work* among all team members. Based on the of individual work type profiles, it can be noticed that some team members were assigned more administrative tasks. Also, interviews conducted after the work sampling session showed that the reason for these results could be team members' perception of the administrative activities which were occasionally confused with routine tasks.

The proportion of teamwork activities (29.5 %) is higher than obtained in studies conducted by Škec *et al.* (14.8 %) [19] and Webster and Higgs (11.3 %) [29], but is lower than the 40.4 % of team activities in Robinson's [18] study. The proportion of team members' discussions is 18.0 % of the time, which is higher than 6.5 % obtained by Škec *et al.* [19], but again lower than the 26.3 % reported by Robinson [18]. Formal meetings have taken 18.0 % of the session time, while Robinson *et al.* [18] and Lowe *et al.* [30] reported 13.0 %, and Marsh reported 9.0 % [31]. Difference in these results arises from distinctive contexts and teams, but also due to different classification of activities proposed by the authors.

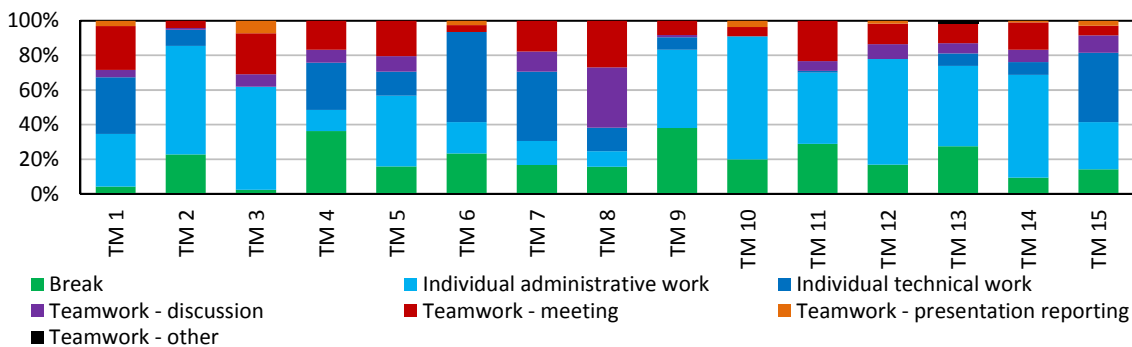


Fig. 4 Percentage of time spent in particular work type during the work sampling period for each team member

3.3 Activity type analysis

Deeper analysis of collected data was focused only on individual technical and team work activities to provide more details about the production development context. *Planning* and *sales/procurement* activities were the most frequent teamwork activities (Table 2), followed by *resolving conflicts* and *conceptualization/design* activities, which also took significant time proportion during the session. Individual technical activities with highest time percentages were *conceptualization/design*, *planning* and *detailing/coding*. During the sampled period, neither one team member reported *ideation/improvement* or *prototypes realization* activities as part of individual work. These two types of activity also had the lowest time proportion out of all teamwork activities.

Planning as the most frequently reported activity (24.20 %) could have been anticipated in a production development team. For comparison, the study conducted in the product development context reports only 3.25 % of time spent on the *planning* activity [19]. It is important to emphasize that *innovation/improvement* activities were reported only a few times during the sampling period. Interviews with the study participants showed that they had difficulties in identifying innovations during everyday activities, which could have caused the low percentage of innovation activity. Nevertheless, the results require further analysis to identify reasons for this behaviour.

As for the context of individual work, team members mostly reported working on *transport/installation* and *manufacturing/deploying* issues. Such results were expected taking into consideration team members' professional profiles and their backgrounds. *Manufacturing/deploying* was also the most reported context during formal meetings, followed by *people/team members*. Informal discussions were again related to *manufacturing/deploying* aspect of the production development. It is possible to notice significant percentage of time spent on administrative activities as part of both individual and team work. Proportions of the time spent engaged in individual technical and team work, coupled with the production development context are presented in Table 3.

As expected, the overall proportion of *process design* activities is significantly higher than what has been reported for the product development context by Škec *et al.* [19] (22.32 % to 8.58 %), and respectively the proportion of *product design* activities is lower (8.37 % to 76.78 %). Furthermore, the time spent on issues related to *people/team members* is higher (5.02 % compared to 1.87 % in [19]), which can be related to a generally higher proportion of teamwork.

Table 2 Percentage of production development activities within individual technical work and teamwork

Activity type	Individual technical work (%)	Teamwork (%)	Overall (%)
Planning	16.42	30.00	24.20
Sales/procurement	7.46	15.19	11.89
Conceptualization/design	16.92	5.56	10.40
Other teamwork	-	12.59	7.22
Other individual	15.42	-	6.58
Resolving conflicts	3.98	6.67	5.52
Analysis/simulation	6.47	4.44	5.31
Documenting	8.46	2.59	5.10
FMEA	6.47	4.07	5.10
Detailing/coding	9.95	0.00	4.25
Negotiation	2.49	5.56	4.25
Decision making	1.49	4.81	3.40
User support	1.49	3.33	2.55
Resource assignment	1.00	1.85	1.49
Monitoring/testing	0.50	1.48	1.06
Measurement/testing	1.49	0.74	1.06
Innovation/improvement	0.00	0.74	0.42
Prototypes realization	0.00	0.37	0.21

Table 3 Percentage of the activities conducted in particular context

Production development context		Teamwork				Overall (%)	Individ. work (%)	Overall (%)
		Discussion (%)	Meeting (%)	Present./ Report. (%)	Other (%)			
Designing the product	Electronics	0.22	0.33	-	-	0.56	0.45	1.00
	Mechanical/Hardware	0.45	1.90	0.11	-	2.46	1.56	4.02
	Software	0.33	1.12	-	-	1.45	1.90	3.35
Designing the process	Disposal/Reusing	-	-	0.11	-	0.11	-	0.11
	Maintenance/Servicing	0.89	0.45	-	-	1.34	0.56	1.90
	Manufacturing/Deploying	2.90	3.35	0.22	-	6.47	4.02	10.49
	Transport/Installation	1.00	1.12	0.11	-	2.23	7.59	9.82
People/Team members		1.12	3.24	0.22	-	4.58	0.45	5.02
Facilities/Infrastructure		0.22	0.67	0.11	-	1.00	0.22	1.23
Administrative		1.23	2.12	0.45	-	3.79	48.33	52.12
Other		1.45	3.68	0.22	0.11	5.47	5.47	10.94
Overall		9.82	17.97	1.56	0.11	29.46	70.54	100.00

3.4 Analysis of activity in a particular manner

Individual technical work and teamwork were conducted in various manners and using different resources during the work sampling period (Table 4). Individual technical work was mostly conducted using the *office software*, *engineering software* and *email*. On the other hand, during teamwork, team members mostly re-ported the use of *face-to-face communication*, *telephone* and *email*.

Extensive use of office software can be explained with a high proportion of administrative work, while engineering software is required for conducting the core production development activities. Robinson reported in his study that half of the activities were carried out using computer tools [18]. Within the individual work context, the presented results are similar. And while in the product development context [19] most of individual work was carried out in engineering software tools, in production development the office software tools are dominant.

Similar as reported in [25] and [19], team activities were mostly carried out face-to-face. This manner of communication is expected for collocated teams. On several occasions (e.g. [32], [33]), researchers emphasized importance of email communication in engineering context. However, within the presented study and similar to Škec *et al.* [19] emails were used rarely as part of teamwork because of the team collocation.

Table 4 Percentage of the activities conducted in particular manner

Manner	Individual technical work (%)	Teamwork (%)	Overall (%)
Face-to-face	-	84.39	48.40
Office software tools	43.50	1.49	19.40
Engineering software tools	22.50	0.00	9.59
Email	18.00	2.23	8.96
Telephone	-	7.81	4.48
Other manner - solo technical	7.50	-	3.20
ERP	3.00	0.37	1.49
Internet	2.00	0.00	0.85
Whiteboard/Smartboard	-	1.49	0.85
Calendar	1.50	-	0.64
Video conference	-	1.12	0.64
Other manner - team	-	1.12	0.64
Knowledge base	1.00	0.00	0.43
Paper misc.	1.00	0.00	0.43

3.5 Analysis of information transaction

As a part of individual technical work, team members reported *information processing* as the primary type of information transaction. Second most frequent information transaction activity was *giving information* (unidirectional). During teamwork team members mostly spent time on *information exchange* (bidirectional) and *information processing* (group thinking) (Fig. 5).

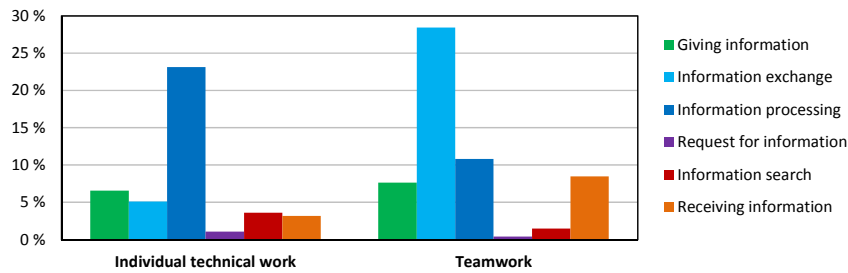


Fig. 5 Percentage of activities with a particular type of information transaction

The proportions of time that team members spent engaged in different type of activities with-in individual technical and teamwork in combination with the type of information transaction happening within the particular activity, are shown in Table 5.

The proportion of *receiving information* transactions was highest during *evaluation* activities (*analysis/simulation*) as part of individual technical work, and during *planning* as part of teamwork. *Information processing* in individual technical work is mostly present during *definition* activities (*conceptualization/design* and *detailing/coding*), while in teamwork this is the case during the *management* activities (*planning*). *Information search* is intensive during "other" individual technical work, while *requesting information* was reported for only 1.49 % of individual technical and team work during the sampling session. *Information exchange* had a significantly important role during teamwork activities such as *sales/procurement*, *resolving conflicts* and *planning*.

Table 5 Work type versus information transaction nature of activities

Activity type	Giving info. (%)	Info. exchange (%)	Info. process. (%)	Request. info (%)	Info. search (%)	Receiving info (%)	Overall (%)
Teamwork	7.64	28.45	10.83	0.42	1.49	8.49	57.32
Evaluation activities							
Analysis/Simulation	-	1.91	0.21	-	-	0.42	2.55
Decision making	0.42	1.27	-	-	-	1.06	2.76
FMEA	0.42	1.27	0.21	-	-	0.42	2.34
Measurement/Testing	-	0.42	-	-	-	-	0.42
Monitoring/Testing	-	0.42	-	-	-	0.42	0.85
Definition activities							
Conceptualization/Design	0.21	1.06	1.27	0.21	-	0.42	3.18
Detailing/Coding	-	-	0.42	-	-	-	0.42
Documenting	0.21	0.85	0.21	-	-	0.21	1.49
Manag. activities							
Planning	2.76	7.43	5.10	0.21	0.21	1.49	17.20
Resolving conflicts	0.21	2.34	0.21	-	-	1.06	3.82
Resource assignment	-	0.42	0.21	-	0.21	0.21	1.06
Negotiation	0.64	1.49	0.85	-	0.21	-	3.18
Other							
Prototypes realization	0.21	-	-	-	-	-	0.21
Sale/Procurement	1.27	4.46	1.91	-	0.21	0.85	8.70
User support	0.21	1.70	-	-	-	-	1.91
Other teamwork	1.06	3.40	0.21	-	0.64	1.91	7.22
Individual technical work	6.58	5.10	23.14	1.06	3.61	3.18	42.68
Evaluation activities							
Analysis/Simulation	0.21	-	1.91	-	-	0.64	2.76
Decision making	0.21	0.21	0.21	-	-	-	0.64
FMEA	-	0.21	1.49	-	0.64	0.42	2.76
Measurement/Testing	-	0.21	0.42	-	-	-	0.64
Monitoring/Testing	0.21	-	-	-	-	-	0.21
Definition activities							
Conceptualization/Design	1.06	0.21	5.73	-	-	0.21	7.22
Detailing/Coding	0.21	-	4.03	-	-	-	4.25
Documenting	0.42	0.64	2.12	-	0.21	0.21	3.61
Manag. activities							
Planning	1.91	2.12	2.12	0.21	0.21	0.42	7.01
Resolving conflicts	0.21	0.85	0.64	-	-	-	1.70
Resource assignment	-	-	0.21	-	-	0.21	0.42
Negotiation	-	0.42	0.21	-	0.21	0.21	1.06
Other							
Sale/Procurement	0.64	0.21	1.49	0.42	0.21	0.21	3.18
User support	0.42	-	0.21	-	-	-	0.64
Other individual	1.06	-	2.34	0.42	2.12	0.64	6.58
Grand total	14.23	33.55	33.97	1.49	5.10	11.68	100.00

4. Conclusions and future directions

In here presented study, a self-reporting work sampling approach was used to observe the activity of individuals and teams in production development context. Work sampling approach in form of a mobile phone application provides new opportunities for collecting self-reporting data. In comparison to wearable recording equipment and tracking software [9], work sampling application requires less data coding which leads to better understanding and interpretation of collected data. This is of great importance for research studies conducted in real organizational settings, since data interpretation is context-dependent and relies on the project manager's expertise.

The study reveals specific aspects of individual and team activity in production development, such as context, content, type and manner. Analysis and interpretation of the obtained data provide added value to project managers in form of insights into the activity of development teams, including resources they use and how they collaborate. By combining different facets of knowledge about the development activities, project managers can tailor workloads of team members and modify team composition to improve collaboration, coordination and information exchange. Moreover, the use of the self-reporting approach can eliminate the need for employees to compile daily, weekly or monthly work reports, thus reducing time spent on administrative work and improving satisfaction. These benefits suggest that implementing the approach can correspond to the introduction of organizational and administrative innovation in the company [6].

The proposed approach doesn't require researchers to be present at the workplace during the data collection procedure, since there is no need for individual observation of each team member. Such less intrusive approach is a prerequisite to conduct data collection in the real organizational settings. However, the approach requires a significant amount of preparation efforts, such as menu creation, application distribution and installation, and introductory workshops. Regardless of researchers' absence, the proposed approach as such still has significant biases since the approach is based on self-reporting. Team members are prone to entry biased data to appear "better" than the others [34]. For that reason, it is important to emphasize the purpose of the study in the introductory workshops to decrease animosity towards this type of studies. Bias could be also caused by emotional state of each team member during the session intervals.

Using the proposed methodology for longitudinal studies, it is possible to compare activity execution by different development teams and/or organizations. Such insights could be used to understand working routines and to modify existing practices related to team composition, resource planning, knowledge needs, and activity execution. Project managers could also use the data to determine project archetypes and adjust their management accordingly. For routine projects, the insights can reveal possible deviations from previously managed projects. The causes for these deviations could be identified via multi-perspective data collection approach, in which the work sampling insights can be coupled with other methods, e.g. PFMEA [35]. Furthermore, longitudinal studies can reveal the long-term effects that the proposed approach has on production development, such as the influence on development costs and efficiency. Further research will include tailoring of the proposed methodology for understanding of project health in terms of the socio-technical aspects, and identification of the production development risks on organizational level.

Acknowledgement

This paper reports on work funded by Ministry of Science and Education of the Republic of Croatia, and Croatian Science Foundation MInMED project (www.minmed.org).

References

- [1] Bellgran, M., Säfsten, K. (2010). *Production development, design and operation of production systems*, Springer-Verlag London, doi: [10.1007/978-1-84882-495-9](https://doi.org/10.1007/978-1-84882-495-9).
- [2] Fogliatto, F.S., da Silveira, G.J.C., Borenstein, D. (2012). The mass customization decade: An updated review of the literature, *International Journal of Production Economics*. Vol. 138, No. 1, 14-25, doi: [10.1016/j.ijpe.2012.03.002](https://doi.org/10.1016/j.ijpe.2012.03.002).
- [3] Ciravegna, L., Romano, P., Pilkington, A. (2013). Outsourcing practices in automotive supply networks: An exploratory study of full service vehicle suppliers, *International Journal of Production Research*, Vol. 51, No. 8, 2478-2490, doi: [10.1080/00207543.2012.746797](https://doi.org/10.1080/00207543.2012.746797).
- [4] Sharafi, A., Wolfenstetter, T., Wolf, P., Krcmar, H. (2010). Comparing product development models to identify process coverage and current gaps: A literature review, In: *Proc 2010 IEEE International Conference on Industrial Engineering and Engineering Management*, Macao, China, 1732-1736, doi: [10.1109/IEEM.2010.5674575](https://doi.org/10.1109/IEEM.2010.5674575).
- [5] Naveh, E. (2005). The effect of integrated product development on efficiency and innovation, *International Journal of Production Research*, Vol. 43, No. 13, 2789-2808, doi: [10.1080/00207540500031873](https://doi.org/10.1080/00207540500031873).
- [6] Koren, R., Palčič, I. (2015). The impact of technical and organisational innovation concepts on product characteristics, *Advances in Production Engineering & Management*, Vol. 10, No. 1, 27-39, doi: [10.14743/apem2015.1.190](https://doi.org/10.14743/apem2015.1.190).
- [7] Thamhain, H. (2013). Managing risks in complex projects, *Project Management Journal*, Vol. 44, No. 2, 20-35, doi: [10.1002/pmj.21325](https://doi.org/10.1002/pmj.21325).
- [8] Cicmil, S., Williams, T., Thomas, J., Hodgson, D. (2006). Rethinking Project Management; Researching the actuality of projects, *International Journal of Project Management*, Vol. 24, No. 8, 675-686, doi: [10.1016/j.ijproman.2006.08.006](https://doi.org/10.1016/j.ijproman.2006.08.006).
- [9] Thoring, K., Mueller, R.M., Badke-Schaub, P. (2015). Technology-supported design research, In: *Proceedings of the 20th International Conference on Engineering Design (ICED 15), Vol 11: Human Behaviour in Design, Design Education*, Milan, Italy, 31-40.
- [10] Matias, A.C. (2001). Work measurement: principles and techniques, In: Salvendy, G. (ed.), *Handbook of industrial engineering: technology and operations management: Third edition*, John Wiley & Sons, Hoboken, New York, USA, 1409-1462, doi: [10.1002/9780470172339.ch54](https://doi.org/10.1002/9780470172339.ch54).
- [11] Robinson, M.A. (2010). Work sampling: Methodological advances and new applications, *Human Factors and Ergonomics in Manufacturing & Service Industries*, Vol. 20, No. 1, 42-60, doi: [10.1002/hfm.20186](https://doi.org/10.1002/hfm.20186).
- [12] Kušar, J., Rihar, L., Gorenc, S., Starbek, M. (2012). Teamwork in the simultaneous product realisation, *Strojniški vestnik – Journal of Mechanical Engineering*, Vol. 58, No. 9, 534-544, doi: [10.5545/sv-jme.2012.420](https://doi.org/10.5545/sv-jme.2012.420).
- [13] Rösiö, C., Bruch, J., Johansson, A. (2015). Early production involvement in new product development, In: *POMS 26th Annual Conference*, Washington DC, USA.
- [14] Lee, J.Y., Swink, M., Pandejpong, T. (2017). Team diversity and manufacturing process innovation performance: The moderating role of technology maturity, *International Journal of Production Research*, Vol. 55, No. 17, 4912-4930, doi: [10.1080/00207543.2016.1272765](https://doi.org/10.1080/00207543.2016.1272765).
- [15] Feng, B., Jiang, Z.-Z., Fan, Z.-P., Fu, N. (2010). A method for member selection of cross-functional teams using the individual and collaborative performances, *European Journal of Operational Research*, Vol. 203, No. 3, 652-661, doi: [10.1016/j.ejor.2009.08.017](https://doi.org/10.1016/j.ejor.2009.08.017).
- [16] Badke-Schaub, P. (1999). Group effectiveness in design practice: Analysis and training by a critical-situation-approach, *Psychologische Beiträge*, Vol. 41, No. 3, 338-355.
- [17] Pavković, N., Štorga, M., Bojčetić, N., Marjanović, D. (2013). Facilitating design communication through engineering information traceability, *Artificial Intelligence for Engineering Design, Analysis and Manufacturing*, Vol. 27, No. 2, 105-119, doi: [10.1017/S0890060413000012](https://doi.org/10.1017/S0890060413000012).
- [18] Robinson, M.A. (2012). How design engineers spend their time: Job content and task satisfaction, *Design Studies*, Vol. 33, No. 4, 391-425, doi: [10.1016/j.destud.2012.03.002](https://doi.org/10.1016/j.destud.2012.03.002).
- [19] Škec, S., Štorga, M., Tečec Ribarić, Z. (2016). Work sampling of product development activities, *Tehnički vjesnik – Technical Gazette*, Vol. 23, No. 6, 1547-1554, doi: [10.17559/tv-20150606151030](https://doi.org/10.17559/tv-20150606151030).
- [20] Kirwan, B., Ainsworth, L.K. (1992). *A guide to task analysis: The task analysis working group*, CRC Press, London, UK, doi: [10.1201/b16826](https://doi.org/10.1201/b16826).
- [21] Sim, S.K., Duffy, A.H.B. (2003). Towards an ontology of generic engineering design activities, *Research in Engineering Design*, Vol. 14, No. 4, 200-223, doi: [10.1007/s00163-003-0037-1](https://doi.org/10.1007/s00163-003-0037-1).
- [22] Ahmed, S., Štorga, M. (2009). Merged ontology for engineering design: Contrasting empirical and theoretical approaches to develop engineering ontologies, *Artificial Intelligence for Engineering Design, Analysis and Manufacturing*, Vol. 23, No. 4, 391-407, doi: [10.1017/s0890060409000146](https://doi.org/10.1017/s0890060409000146).
- [23] Allard, S., Levine, K.J., Tenopir, C. (2009). Design engineers and technical professionals at work: Observing information usage in the workplace, *Journal of the American Society for Information Science and Technology*, Vol. 60, No. 3, 443-454, doi: [10.1002/asi.21004](https://doi.org/10.1002/asi.21004).
- [24] McAlpine, H., Cash, P., Storton, A., Culley, S. (2011). A technology selection process for the optimal capture of design information, In: *Proceedings of the 3rd International Conference on Research into Design Engineering (ICORD 11)*, Bangalore, India, 11-18.
- [25] Cash, P. (2012). *Characterising the relationship between practice and laboratory-based studies of designers for critical design situations*, Ph.D. thesis, University of Bath, UK.
- [26] Škec, S., Štorga, M., Tečec Ribarić, Z., Marjanović, D. (2015). Work sampling approach for measuring intellectual capital elements in product development context, In: *Proceedings of the 20th International Conference on Engineering Design (ICED 15) Vol 3: Organisation and Management*, Milan, Italy, 457-466.

- [27] Surbier, L., Alpan, G., Blanco, E. (2014). A comparative study on production ramp-up: State-of-the-art and new challenges, *Production Planning & Control, The Management of Operations*, Vol. 25, No. 15, 1264-1286, [doi: 10.1080/09537287.2013.817624](https://doi.org/10.1080/09537287.2013.817624).
- [28] Pape, E.S. (1988). Work sampling, In: Gael, S. (ed.), *The Job Analysis Handbook for Business, Industry, and Government*, John Wiley & Sons, New York, USA, 518-535.
- [29] Webster, J., Higgs, P. (1973). An analysis of drawing office activities, *Building Services Engineer*, Vol. 40, 246-257.
- [30] Lowe, A., McMahon, C., Culley, S. (2004). Information access, storage and use by engineering designers, part 1, *The Journal of the Institution of Engineering Designers*, Vol. 30, No. 2, 30-32.
- [31] Marsh, J.R. (1997). *The capture and utilisation of experience in engineering design*, Ph.D. thesis, University of Cambridge, UK.
- [32] Gopsill, J., Jones, S., Snider, C., Shi, L., McMahon, C.A., Hicks, B.J. (2014). Understanding the engineering design process through the evolution of engineering digital objects, In: *Proceedings of the 13th International Design Conference (DESIGN 2014)*, Dubrovnik, Croatia, 1773-1784.
- [33] Wasiak, J.O.A. (2010). *Content based approach for investigating the role and use of e-mail in engineering design projects*, Ph.D. thesis, University of Bath, UK.
- [34] Donaldson, S.I., Grant-Vallone, E.J. (2002). Understanding self-report bias in organizational behavior research, *Journal of Business and Psychology*, Vol. 17, No. 2, 245-260, [doi: 10.1023/A:1019637632584](https://doi.org/10.1023/A:1019637632584).
- [35] Banduka, N., Veža, I., Bilić, B. (2016). An integrated lean approach to process failure mode and effect analysis (PFMEA): A case study from automotive industry, *Advances in Production Engineering & Management*, Vol. 11, No. 4, 355-365, [doi: 10.14743/apem2016.4.233](https://doi.org/10.14743/apem2016.4.233).

An overview and evaluation of quality-improvement methods from the manufacturing and supply-chain perspective

Radej, B.^{a,*}, Drnovšek, J.^a, Begeš, G.^a

^aUniversity of Ljubljana, Faculty of Electrical Engineering, Laboratory of Metrology and Quality, Slovenia

ABSTRACT

In recent years, besides high productivity of the manufacturing process, quality issues (including safety requirements and cost efficiency) have both become major market drivers. In order to meet all the above objectives, so as to achieve competitive advantages, a number of quality techniques need to be implemented within the manufacturing process. Starting from the general manufacturing model and presenting a supply-chain philosophy, this paper provides an overview of the quality tools and methods such as quality techniques and links to manufacturing process quality and manufacturing cost-effectiveness; it focuses on manufacturing processes and perceived quality problems associated with the supplier's quality issues. Additionally, the impact of the component supplier on the overall quality of the final product needs to be distinguished from the impact of the manufacturing process. Based on the model of the general manufacturing process the authors propose methods of effective deployment for the most common quality methods and tools within different manufacturing areas. In the discussion the authors propose certain quality techniques to improve the key performance indicators (KPI) within the manufacturing process.

© 2017 PEI, University of Maribor. All rights reserved.

ARTICLE INFO

Keywords:

Manufacturing
Supply chain
Quality methods
Quality tools
Quality function deployment (QFD)

*Corresponding author:

blaz.radej@gmail.com
(Radej, B.)

Article history:

Received 29 May 2017
Revised 25 September 2017
Accepted 22 October 2017

1. Introduction

Customers define the functional requirements of products, while manufacturers need to respond appropriately and provide the market with products that customers will accept [1]. Customer requirements or trends in the market change quickly; therefore, manufacturers are forced to reorganize internal processes and quickly respond to the changing needs of the market [2]. This study shows that supplier management is essential to ensure product/service quality [3]. To achieve stability in the relationship, companies should choose suppliers based on their quality and reliability, encourage their participation in the design of products and try to improve the suppliers' awareness of the importance of quality. Quality assurance is one of the most essential processes in the supply chain; therefore, specific quality methods and tools need to be employed. Since there are many different methods and tools available, the characteristics need to be assessed, benefits and weaknesses need to be exposed, and optimal application areas have to be defined.

2. Quality assurance and manufacturing processes

A manufacturer can only be effective if the level of quality perceived by the buyers of its products is achieved. Since all production processes within manufacturing companies are supported by supply-chain management, it is crucial to understand the quality of the supply-chain network. Suppliers have taken on the responsibility to constantly ensure an adequate level of quality, which in turn has resulted in an overall increase in the reliability of products [4, 5].

2.1 General manufacturing model

A supply-chain network is supplying material components to a manufacturing company, which is converting them into final products – the final products are then sold to the final customer. An on-going selling process is only possible if the manufacturing company is able to produce products that are fulfilling requirements related to quality and functionality, defined both by the customer and local legislation [5]. Quality supervision is carried out by the buyers of components (manufacturing companies), which by using the (un)announced audits of processes and products have overseen the work of suppliers and therefore provided an appropriate level of product quality, which is essential for the satisfaction of end customers. Some manufacturers, despite the implemented ISO standards, started to demand that their component suppliers comply with specific quality requirements, which they define additionally by themselves. This requirement stems from the conviction of manufacturers that by defining and realizing specific quality requirements they will, to the greatest extent, meet the expectations of the customer for their products [7]. Globalization has resulted in the best tools and methods for the optimization of business processes, tools which have been refined and positively proven in various parts of the world [8]. With the aim of maximizing the profits of the business, there is a strong motivation for the manufacturer to employ the cost-effective implementation of internal company processes [9].

The recommended actions to improve the level of manufacturing quality [10] are as follows:

- collect all the necessary information about the cost of poor quality and display it in a transparent manner,
- define effective measures to improve each individual cost and determine the people responsible and the dates of implementation,
- regularly and promptly communicate information about the cost of poor quality and improvement actions to the employees,
- modify processes to prevent the detected problems from repeating and continuously analyse the situation of low-quality costs and implement improvement measures,
- motivate employees in the company so that they, on their own initiative, contribute to the implementation of preventive measures in the company processes.

Taguchi [11] summarized the costs of poor quality with a sketch of an iceberg, the visible part of which is obvious, while the hidden part becomes visible only after a thorough analysis. *Visible part*: administrative costs of a customer-complaints procedure, costs of claimed product's testing, costs of claimed product's rework, and costs of claimed product's scrap. *Hidden part*: costs of product's special freight, costs of labour overtime, costs of the subsequent development of non-conforming products; costs of the loss of production capacities, costs of sorting claimed products, and costs of the loss of the customer.

Based on the findings above we present a general manufacturing process model where the materials are provided by a supply-chain network (Fig. 1, left-hand side) to the manufacturing company (Fig. 1, in the middle), which is manufacturing the final product for an end customer (Fig. 1, right-hand side). The model emphasizes the importance of quality checks, which are crucial to achieving the required quality level. Quality checks are performed internally through the company's internal quality audits and/or externally through quality audits performed by local authorities and/or customer representatives.

The following two quality-assurance goals are taken into consideration:

- The first goal is to ensure internal quality standards: blue lightning icons are indicating the internal quality checks, which are independently executed within the supply-chain network and the manufacturing company,
- The second goal is to ensure compliance with the customer and legal requirements: the red loop icon is indicating an external quality check within the supply-chain network, executed by the manufacturing company.

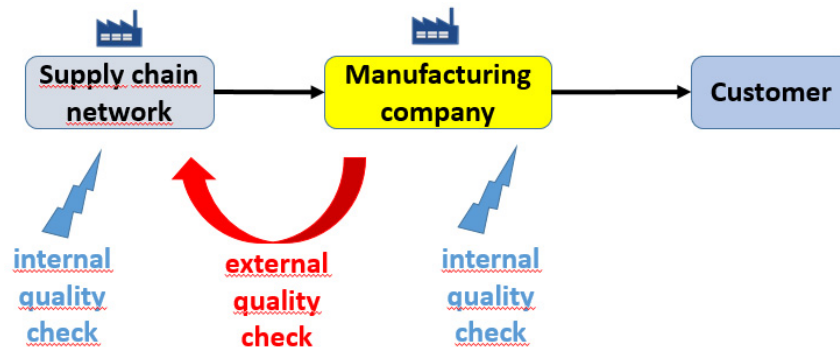


Fig. 1 A general manufacturing model

2.2 Quality assurance within a supply chain

Manufacturing companies have a tendency to deliver products with technical specifications that are defined by a customer. This is only possible within a faultless manufacturing process, where constant monitoring over the manufacturing parameters is applied. The same philosophy is valid for a supply-chain network consisting of multiple suppliers (*tier one* and *tier two*), which are delivering components in the following sequence: tier two is supplying tier one, while tier one is supplying the manufacturer [4, 6, 13].

There is a material stream between the tier suppliers and the manufacturing company (Fig. 2), where quality-performance monitoring has to be applied in order to ensure the required level of the component and consequently the final product quality [6].

Market requirements are met when an adequate quality level is integrated and the quality traceability is ensured in the manufacturing process, which needs to produce products with an acceptable cost. This known fact cannot be linked just to the manufacturer's processes, but to the supplier processes as well – they both need to ensure that the quality standards are met, otherwise the products will fail on the market. The agreed properties of the final product can only be achieved if the supplier's component with the proper quality is used in a well-designed (also in relation to the supplier's component) manufacturing process. Due to the fact that the majority of manufacturers outsource component production, many suppliers are forced to invest in methods and systems to improve the quality of their production, which also includes a traceability system that provides an insight into the manufacturing history of each individual component. Quite often the production facilities are arranged at different locations in the factories – subassemblies and manufacturing processes are assigned to certain production checks, named *final quality control*, which are providing the digital data by means of which the history of production for each product can be determined in the control system of production [14-16].

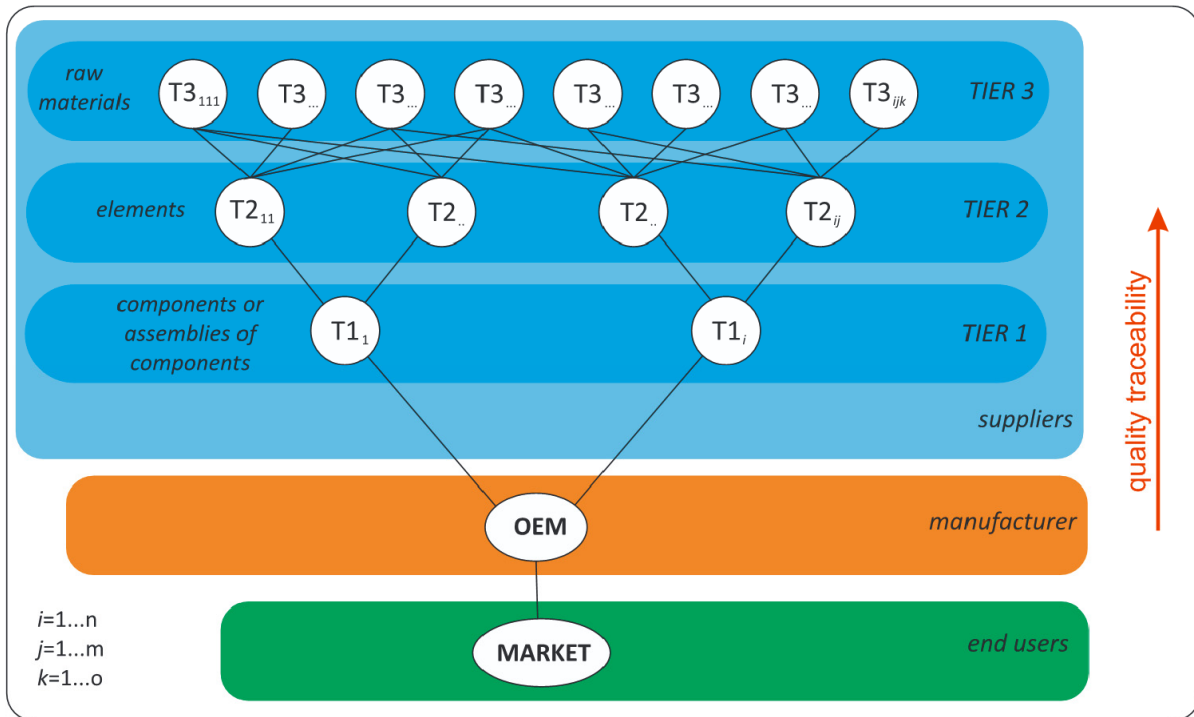


Fig. 2 An example of a supply chain [6]

3. Evaluation of common quality methods and tools

The concept of providing quality products includes not only the fulfilment of customer needs, but also the ability to maintain and service those products at low cost. The quality-assurance system was originally developed by the Toyota Motor Corporation and was later named the Toyota Production System. The high level of quality of their vehicles was achieved through the standardization of processes and the establishment of effective communications within the departments of the company. The activities of the staff were focused on obtaining information by audits, inspections, tests and analyses of a variety of development and production processes. Due to a decrease in the value of stocks of materials Toyota needed to ensure high flexibility in manufacturing, which followed the volume of vehicle sales, while other car manufacturers produced vehicles on stock, but then subsequently failed to sell them. The methodology of obtaining information through assessment, testing and inspection, and the creation of flexible production, was later named lean production [17].

3.1 Quality tools

The seven basic quality tools were defined by Kaoru Ishikawa and used for problem-solving purposes. Ishikawa is of opinion that 90 % of all issues could be solved using seven quality tools, which are presented in Table 1 [18, 19].

The characteristics of all seven tools are presented, and the strengths and weaknesses are highlighted. Based on a general manufacturing model, presented in Fig. 1, potential manufacturing areas are presented.

Table 1 Seven quality tools [4, 7, 13, 17, 19]

Quality tool	Characteristics	Strengths	Weaknesses	Areas of application
Cause-and-effect diagram	identifies the different types of possible causes that have led to a specific problem or effect	<ul style="list-style-type: none"> visualizes relationships between causes and effects visualizes dependent relationships 	<ul style="list-style-type: none"> the tool is not defining a proper solution (causes are only transparently presented) the probability level of the shown causes is always presented as equal 	Supply-chain network, manufacturing company
Flow chart	workflow mapping by showing the order that activities and decisions occur	<ul style="list-style-type: none"> problem can be effectively analysed (cost reduction) 	<ul style="list-style-type: none"> if alterations are required the flowchart might require re-drawing completely (waste of time) 	manufacturing company
Control table	pre-prepared table for data collection and analysis	<ul style="list-style-type: none"> structural presentation of data 	<ul style="list-style-type: none"> additional data processing is needed 	Supply-chain network, manufacturing company
Control chart	provides a graphical representation of the trend of the observed process and includes upper and lower limits of values	<ul style="list-style-type: none"> good visualization values of the control limits are added and mean line 	<ul style="list-style-type: none"> instructions are needed prior to interpretation of the results 	Supply-chain network, manufacturing company
Histogram	visualizes the distribution of the process, or the frequency of occurrence of each value of the process	<ul style="list-style-type: none"> data can be easily read works well with large ranges of information 	<ul style="list-style-type: none"> inconvenient when comparing multiple categories 	Supply-chain network, manufacturing company
Pareto analysis	diagram shows the causes ranked from most frequent to least frequent; this classification allows a focus on the main causes	<ul style="list-style-type: none"> organizational efficiency improved decision making 	<ul style="list-style-type: none"> focus on the past inaccurate problem scoring 	Supply-chain network, manufacturing company
Scatter plot	visualizes the interdependence of variables and defines the relationship between the dependent and independent variables	<ul style="list-style-type: none"> ability to show whether correlations between variables are positive or negative; linear or non-linear; high, low or n/a very convenient when identification of matching of different statistical data is needed 	<ul style="list-style-type: none"> the tool is not appropriate for observing more than two variables discretization of values 	Supply-chain network, manufacturing company

3.2 Quality-assurance methods

Quality management within the industry is not effective without an appropriate knowledge of quality methods. Despite the fact that many different quality-assurance methods are applied in many different industries, Table 2 represents six quality-assurance methods that are the most commonly used during the optimization of production processes [7, 20].

Table 2 Most commonly used quality-assurance methods [4, 7, 11, 17, 19]

Quality Method	Characteristics	Strengths	Weaknesses	Areas of application
Quality Function Deployment (QFD)	identifies the customers' needs and expectations, and then defines the correct responses to them.	<ul style="list-style-type: none"> • higher quality • lower development costs 	<ul style="list-style-type: none"> • not universal problem-solving method • time consuming 	manufacturing company
Statistical Process Control (SPC)	enables understanding of machine or process capability during the production process	<ul style="list-style-type: none"> • early detection and prevention of problems • improves productivity • 	<ul style="list-style-type: none"> • time consuming • it does not show by how much the rejected products are defective 	Supply-chain network, manufacturing company
Failure Modes and Effect Analysis (FMEA)	step-by-step approach for identification of possible failures	<ul style="list-style-type: none"> • a very structured and reliable method • the concept and application are very easy to learn 	<ul style="list-style-type: none"> • is tedious and time consuming • not suitable for multiple features 	Supply-chain network, manufacturing company
Plan-Do-Check-Act (PDCA)	an iterative improvement process and is run in repeating cycles	<ul style="list-style-type: none"> • can be widely applied • iterative process allows continuous delivery of improvements while moving towards the end goal 	<ul style="list-style-type: none"> • does not give specific details about how to analyse/resolve problem • waiting time of 1st iteration is needed to address the impact of a problem 	Supply-chain network, manufacturing company
Poka Yoke	Mistake proofing methodology	<ul style="list-style-type: none"> • error prevention • solutions can be implemented at low cost 	<ul style="list-style-type: none"> • requires knowledge of utilizing instrumentation and technology 	Supply-chain network, manufacturing company
5 S	Workplace organization method	<ul style="list-style-type: none"> • productivity increase • product quality increase 	<ul style="list-style-type: none"> • misunderstanding of what 5S accomplishes • lack of management support 	Supply-chain network, manufacturing company

Management in an average production-oriented company has a tendency to set highly positioned quality goals that should be based on efficient manufacturing processes. Despite the fact that quality tools (Table 1) and methods (Table 2) are not presenting any novelty in manufacturing industry, a proper and detailed root-cause analysis of a problem has to be made in order to choose a corresponding quality tool and/or method that leads to a company's performance improvement.

The reviewed literature states that manufacturing-industry practice is optimizing its internal processes by the application of FMEA, PDCA and Poka-Yoke, while product quality is many times optimised by the application of QFD and Cause-and-Effect diagrams [7]. The benefits of QFD and PDCA are presented in the following paragraphs.

The applicability of a PDCA methodology in manufacturing processes

The classic PDCA method includes four elements of process control: planning (preparation of the quality-assurance plan), execution (integration of improvement measures), checking (control of effects) and action (implementation of measures according to the determined deviations in the control of effects) [10, 22]. The classic PDCA method excludes performance monitoring to ensure the on-going effectiveness of change. Andersen *et al.* [11] state that the users of the classic PDCA method are not experienced enough to use it in an effective way, and therefore they propose an improved type of PDCA method, which includes the elements shown in Fig. 3: characterization and research into the problem, analysing the situation, preparation of measures to improve, a critical assessment of the reasonableness of the measures, implementation of the measures, and checking the effects of the implemented measures for improvement.

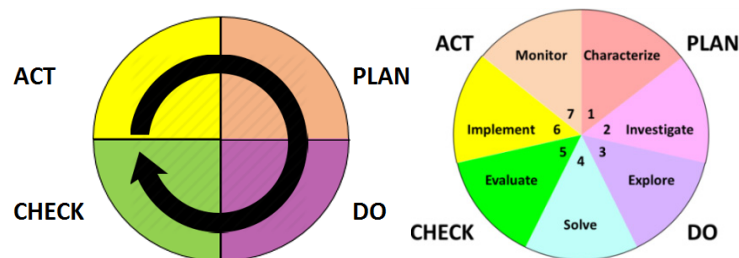


Fig. 3 Classic PDCA method (left) vs. improved PDCA method (right) [10, 11]

In order to prove the efficiency of both the classic and improved PDCA methods one typical automotive supplier manufacturing company was chosen as the unit of analysis. The company faced an increased rate of scrapped products on one of its biggest assembly lines, where counter measures to increase product quality represented a top priority. The management of the company defined a 4-weeks time frame to resolve quality issues and gave approval for the parallel application of both PDCA methods. The initial scrap rate was 320 products with unacceptable quality, while the target scrap rate, defined by the management, was 40 products with unacceptable quality.

After the 4 weeks of parallel testing was over, the results were analysed and are presented in table 3. The use of the classic PDCA method resulted in a 44 % decrease of products with unacceptable quality, while the improved PDCA method eliminated products with unacceptable quality.

A reduction* of 100 % is achieved by using the error prevention Poka-Yoke method, proposed by the improved PDCA method. However, we cannot generalize the statement that the use of the improved PDCA method will always eliminate products with unacceptable quality. Based on a parallel comparison of PDCA methods, shown above, the same procedure could be applied for other quality tools and methods.

Table 3 Analysis of parallel application

	Classic PDCA method	Improved PDCA method
Needed time for implementation	low	high
Implementation complexity	low	high
Level of structured approach	unstructured	structured
Problem-solving mind-set alteration	low	high
Problem-solving efficiency	low	high
Scrap reduction*	44 %	100 %

The applicability of the QFD methodology in manufacturing processes

The question is, what goals does a company envisage to satisfy or merely please its customers? The answer to this question is the QFD method, which represents a quality system focused on the customer (Fig. 4). The method initially identifies the customers' needs and expectations, and then defines the correct responses to them. QFD is a method enabling companies to achieve the optimal satisfaction of its customers [17].

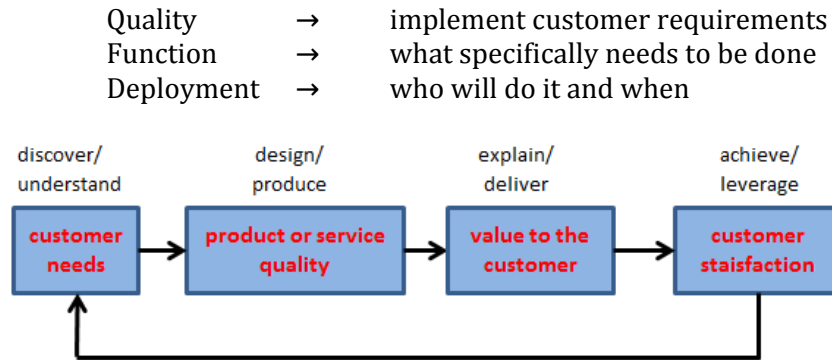


Fig. 4 Process display of the QFD method [35]

The QFD method represents a process that allows the identification of customer requirements, understanding markets and knowledge of different customer segments. The conditions for the successful implementation of the QFD method are a thorough knowledge of the requirements of each customer segment, how important the customer's benefit is and how effectively these requirements are met by existing suppliers of products/services [23, 35]. If these conditions are not met, the customer requirements are obviously unknown and, consequently, products/services cannot be consistently delivered to the market and would prevent customers from being generally satisfied [36]. The QFD method is therefore a quality-assurance system with the aim of maximizing the customer's satisfaction. It focuses on providing value in a product that delivers both spoken and unspoken customer requirements or expectations. These requirements are translated into the (development and production) activities of the producer. The QFD method allows cross-referencing of the product's producer with its competition by helping the company to direct further steps in the direction that will help increase competitive advantage [23, 34].

3.3 Influence of the quality of the manufacturing processes on manufacturing cost efficiency

The purpose of this section is to highlight the connection between the high-quality manufacturing processes and the cost efficiency of the manufacturing process. Companies are aiming to develop high-quality manufacturing processes, which are in turn enabling higher profits for the company. For that reason there is a need to reliably assess the manufacturing cost efficiency. There are various authors expressing different innovative approaches related to the measurement and improvement of process efficiency. According to Hendricks *et al.* [32], product quality is crucial to the success of any company – as evidenced by the statement that the companies that are winning awards for outstanding quality, achieve higher profits and a higher value of their shares on the stock market.

Process control is very important for improving the efficiency of production processes. Each serial production is designed in such a way that it can be effectively monitored, which can be done through constant control of important parameters, whereby it is necessary to effectively respond to any perceived deviation from the nominal value. The efficiency of the manufacturing processes is closely associated with productivity processes – it is important to ensure a continuous production process with or without the shortest-possible standstill and with zero or minimum poor-quality products [24]. Hanenkamp [25] describes a method for the control of production processes, described as "Overall Equipment Efficiency" (OEE), which uses the relative value to define the level of availability of machinery and equipment, quantity and the degree of product quality, with Eq. 1:

$$OEE = availability \times performance \times quality \tag{1}$$

The *availability* rate is the ratio between the available working time of the machinery and equipment and their actual working time; the *productivity* rate is the ratio between the available

working time of the employees and their actual working time; the *quality* level is the ratio of the quantity of poor-quality products and the total quantity of manufactured products.

Involving employees in a process-performance measurement (OEE, productivity, etc.) is very important. The productivity of companies is affected by the use of the 5S method, described as a method for organizing and standardizing workplaces within the company. An appropriately structured workplace motivates employees, both production workers and management, improves occupational safety, the productivity of the process and evokes a sense of responsibility among the employees [24-28].

Several authors [25, 28-30] also mention the Shop Floor Management method (SFM), the main advantage of which is a systematic, process-oriented industrial way of solving problems. The SFM method pursues three objectives: *gemba* (real venue, for example, assembly line), *genbutsu* (detailed knowledge of the affected process, e.g., increased scrap) and *genjitsu* (definition and implementation of corrective actions that will improve the current issue). Tanco *et al.* [31] propose a methodology to measure the impact of SFM on defect-free production, which can be summarised in the following steps: a) choose an adequate response (the impact of SFM should be measured in different ways: firstly, as the impact on defect-free cars and then in the last quality-control stage), b) gather significant data (to carry out a relevant statistical analysis, a significant amount of data must be gathered to give certainty to results), c) analyse several factors (production level, week day, shifts, quality level), d) draw conclusions and recommendations.

Jingshan *et al.* [33] speak about the certain demise of a company, if the company is only partially focused on improving the level of quality. They point out that product quality is not just vital for the profitability of the company, but also for its existence. Manufacturers want to cooperate with fewer suppliers, but the latter need to be large and strong enough for all the customer's requirements. This is due to the fact that the typical construction of products requires a large number of components; therefore, it makes sense that as many components as possible are supplied by one or a few suppliers. There is a risk that the parts purchased from a large number of suppliers would not be compatible [17]. Production-oriented companies implement operational processes by attempting to minimize resource consumption, in addition to realizing planned quantities of products that meet customer requirements regarding quality [36].

Hanenkamp [25] emphasizes the importance of using the SFM method in manufacturing processes, which results in improved productivity, a reduced rate of customer complaints and higher profitability of the company.

Manufacturing efficiency is of huge importance within every company. It is important to ensure a continuous manufacturing process with the shortest possible standstill and with the minimum number of poor-quality products. Therefore, manufacturing processes are cost efficient only if there is a reliable performance measurement integrated (established by SFM method) and if the mind-set of the employees is accepting the importance of quality (quality methods and tools). Fig. 5 illustrates major contributors to the improved cost efficiency of manufacturing processes, where the value of each contributor is assessed based on the available literature [24, 25, 28-30, 32, 33, 36].

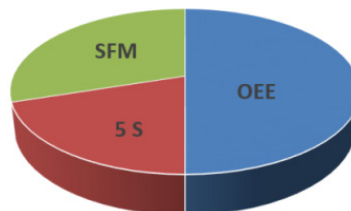


Fig. 5 Major contributors to cost efficiency [24, 25, 28-30, 32, 33, 36]

4. Discussion

The future of component suppliers will be financially successful only if they reduce the cost of doing business and start to produce products that can be sold to different customers, even beyond their core sector. Productivity and scrap levels impact on the operating costs, notes Hanenkamp [25], who recommends the use of methodologies for measuring the OEE. From the manufacturer’s point of view the measurement of productivity and OEE is important because it exposes process deviations in real time and enables opportunities for process improvements.

Based on a literature review we see that not all quality methods and tools can be equally implemented in all company departments. The classification of quality methods and tools into different manufacturing departments is divided into three main pillars, seen Table 4. We identified the prime responsibility and initiatives for a particular pillar in terms of quality deployment.

Table 4 A proposal for quality methods and tools deployment within company departments

		Pillars			
		Research and Development dept.	Production dept.	Customer support and service dept.	
Quality dpt.	Quality methods	QFD	yes	no	no
		SPC	no	yes	yes
		FMEA	yes	yes	yes
		PDCA	no	yes	yes
		Poka-Yoke	no	yes	no
		5 S	no	yes	no
	Quality tools	Cause and effect diagram	no	no	yes
		Flow chart	yes	yes	yes
		Control table	yes	yes	yes
		Control chart	no	yes	yes
		Histogram	no	yes	yes
		Pareto diagram	yes	yes	yes
		Scatter plot	yes	yes	yes

In Table 4, a horizontal line indicates a quality department that represents cross cutting through all three pillars: the research and development department, the production department and customer support and service department.

From the manufacturing point of view and based on manufacturing experiences we present some examples where the application of certain quality techniques (combination of tools and methods, presented in Table 3) can be implemented:

- unacceptable low level of first pass yield within the manufacturing process is increased by the application of SPC, FMEA, Cause-and-effect diagram and Histogram,
- increased number of scrapped components within the manufacturing process is usually decreased by the application of PDCA, 5 S, Control Table and Pareto diagram,
- a large number of customer claims related to the technical properties of the product are solved by the application of QFD, FMEA, Histogram and Pareto diagram.

Also other combinations/techniques of quality methods and tools are possible, depending on the manufacturing processes. Generic flowchart, presented in Fig. 6, introduces correlations between KPIs and quality techniques, whose application would resolve the deviations of the KPI.

Based on manufacturing practice we are able to identify that the increased scrap rate, caused by poor product design, is resulting in a lower product yield and a lower OEE of production line, while the increased scrap rate, caused by poor process design, is again resulting equally in a lower OEE of production line. The correlation between product and process improvement is therefore mutual, as the improvement of the product will directly improve processes and vice versa.

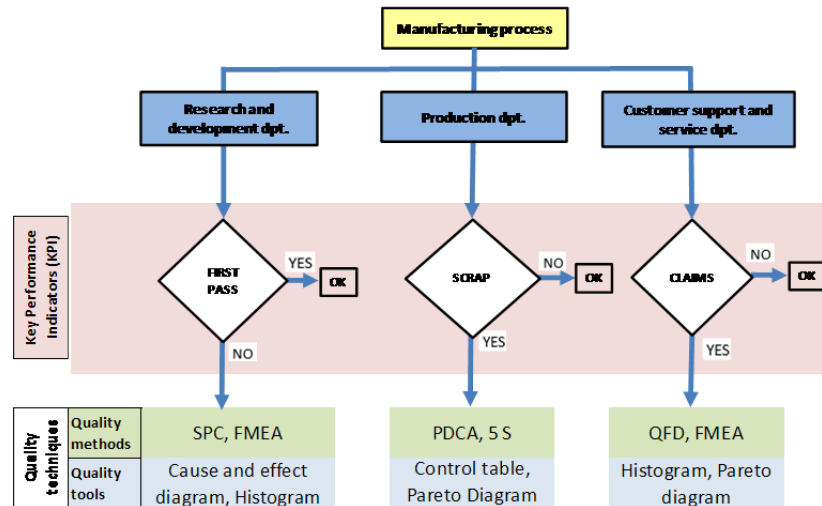


Fig. 6 Application techniques of quality methods and tools

Based on manufacturing practice we are able to identify that the increased scrap rate, caused by poor product design, is resulting in a lower product yield and a lower OEE of production line, while the increased scrap rate, caused by poor process design, is again resulting equally in a lower OEE of production line. The correlation between product and process improvement is therefore mutual, as the improvement of the product will directly improve processes and vice versa.

The increased complexity of the manufacturing processes is demanding an effective approach to resolve issues that are connected to poor quality in manufacturing. For that reason the following questions arise:

- How do we identify critical production processes and which methods should we use to improve OEE?
- How do we inspire employees in the company to adopt new quality methods and tools to improve the manufacturing efficiency?
- How do we use the QFD and new PDCA methods to fulfil the customer's expectations, assuming that mass production of the product is already in progress?

Although the most critical manufacturing processes can be detected using the SPC method and control chart tool, we are of the opinion that the application of the SFM method delivers better results through the identification and implementation of corrective actions that will improve the current issue, which will result in improved OEE. In addition, the SFM method motivates employees and their leaders through its systematic approach, where quality techniques need to be applied to every single quality issue.

Based on manufacturing experiences, where customer satisfaction with a product always plays a big role in a company, we propose the use of the QFD method, which successfully translates customer requirements into product specification. During the mass production of those products there are various manufacturing issues, related to the quality of the product, which can be solved by the use of the new PDCA method.

5. Conclusion

In today's highly competitive environment supplier quality is a very important operational issue for a modern, successful, and profitable production system. Confidence in a supplier's ability to deliver a component as part of the final product that will fulfil customer's needs can be achievable through the efficient quality traceability from the manufacturer to the suppliers.

This paper initially describes quality challenges within manufacturing processes, which is achieved through the integration of the quality tool and methods. The strengths and weaknesses of various quality methods and tools are revealed and potential applications in manufacturing

fields are presented. The parallel application of two quality methods on a manufacturing process was performed, while the positive effect of the usage is proved with a decrease of 44 % (first method) and 100 % (second method) of products with unacceptable quality.

The concepts of high OEE and high manufacturing quality are shown to be very important to secure a positive financial future for the company. Therefore, this article as a review of common quality tools and methods serves as an incentive for the definition of a new approach to the improvement of OEE, the reduction in the rate of complaints and the procedures for a faster and more efficient response to deviations within production processes.

Based on a general manufacturing model we propose a generic flow chart that identifies quality techniques for a particular KPI within the manufacturing process. Manufacturing processes are cost efficient only if there is a reliable performance measurement integrated and if the mindset of employees is willing to accept the importance of quality; therefore, we can also conclude that the use of methods and tools (QFD, 5 S, PDCA and SFM) significantly improves the efficiency of the processes.

This paper should serve as a basis for carrying out detailed analyses of manufacturing processes before and after the implementation of the above-described quality techniques. Consequently, manufacturing managers could motivate their staff to implement the above-described quality-assessment techniques more effectively.

Acknowledgment

We sincerely thank the reviewers of this journal for their insightful comments which helped us improve the quality of this paper. Authors are expressing their gratitude to Faculty of Electrical Engineering, Laboratory of Metrology and Quality for their financial support.

References

- [1] Tang, D. (2005). Partnership development between product customer and tool and die supplier, *Proceedings of the Institution of Mechanical Engineers, Part B: Journal of Engineering Manufacture*, Vol. 219, No. 4, 365-376, [doi: 10.1243/095440505X32265](https://doi.org/10.1243/095440505X32265).
- [2] Hirsh, E., Kakkar, A., Singh, A., Wilk, R. (2015). Auto industry trends; Industry perspectives, PriceWaterhouse-Coopers International Limited, from <http://www.strategyand.pwc.com/perspectives/2015-auto-trends>, accessed August 28, 2016.
- [3] Perez-Arostegui, M.N., Benitez-Amado, J., Huertas-Perez, J.-F. (2012). In search of loyalty: An analysis of the determinants of buyer-supplier relationship stability under a quality management approach, *Total Quality Management & Business Excellence*, Vol. 23, No. 5-6, 703-717, [doi: 10.1080/14783363.2012.669999](https://doi.org/10.1080/14783363.2012.669999).
- [4] Stylidis, K., Wickman, C., Söderberg, R. (2015). Defining perceived quality in the automotive industry: An engineering approach, *Procedia CIRP*, Vol. 36, 165-170, [doi: 10.1016/j.procir.2015.01.076](https://doi.org/10.1016/j.procir.2015.01.076).
- [5] Wang, F.-K., Du, T., Li, E. (2004). Applying six-sigma to supplier development, *Total Quality Management & Business Excellence*, Vol. 15, No. 9-10, 1217-1229, [doi: 10.1080/1478336042000255596](https://doi.org/10.1080/1478336042000255596).
- [6] Pavlínek P., Janák L. (2007). Regional restructuring of the Škoda auto supplier network in the Czech Republic, *European Urban and Regional Studies*, Vol. 14, No. 2, 133-155, [doi: 10.1177/0969776407076101](https://doi.org/10.1177/0969776407076101).
- [7] Goicoechea, I., Fenollera, M. (2012). Quality management in the automotive industry, In: Katalinic, B., *DAAAM International Scientific Book 2012*, DAAAM International Vienna, Austria, 619-632, [doi: 10.2507/daaam.scibook.2012.51](https://doi.org/10.2507/daaam.scibook.2012.51).
- [8] Šurinová, Y. (2013). Review of special standards in quality management systems audits in automotive production, , *Research Papers Faculty of Materials Science and Technology Slovak University of Technology, The Journal of Slovak University of Technology* Vol. 21, No. 33, 21-30, [doi: 10.2478/rput-2013-0036](https://doi.org/10.2478/rput-2013-0036).
- [9] Chang, S.-C., Pan, L.-Y., Yu, H.-C. (2008). The competitive advantages of Quanta computer – The world's leading notebook PC manufacturer in Taiwan, *Total Quality Management & Business Excellence*, Vol. 19, No. 9, 939-948, [doi: 10.1080/14783360802224602](https://doi.org/10.1080/14783360802224602).
- [10] Teli, S.N., Majali, V.S., Bhushi, U.M., Gaikwad, L.M., Surange, V.G. (2013). Cost of poor quality analysis for automobile industry: A case study, *Journal of The Institution of Engineers (India): Series C*, Vol. 94, No. 4, 373-384.
- [11] Andersen, B., Sorqvist, L., Saraiva, P., Watson, G. (2015). Structured improvement for the 21st century: A new model from Europe, In: *World Quality Forum – International academy for quality*, Budapest, Hungary, from <http://eoq.hu/iaq/andersen.pdf>, accessed September 25, 2017.
- [12] Taguchi, G., Chowdhury, S., Wu, Y. (2004). *Taguchi's quality engineering handbook*, John Wiley & Sons, New York, USA, [doi: 10.1002/9780470258354.ch17](https://doi.org/10.1002/9780470258354.ch17).
- [13] Omega, R.S., Noel, V.M., Masbad, J.G., Ocampo, L.A. (2016). Modelling supply risks in interdependent manufacturing systems: A case study, *Advances in Production Engineering & Management*, Vol. 11, No. 2, 115-125, [doi: 10.14743/apem2016.2.2014](https://doi.org/10.14743/apem2016.2.2014).

- [14] Cho, H. (2014). Traceability-driven system development and its application to automotive system development, In: *21st Asia-Pacific Software Engineering Conference*, Jeju, South Korea, 143-146, doi: [10.1109/APSEC.2014.30](https://doi.org/10.1109/APSEC.2014.30).
- [15] Doran, D., Roome, R. (2003). An evaluation of value-transfer within a modular supply chain, *Proceedings of the Institution of Mechanical Engineers, Part D: Journal of Automobile Engineering*, Vol. 217, No. 7, 521-527, doi: [10.1243/095440703322114906](https://doi.org/10.1243/095440703322114906).
- [16] Doran, D., Hill, A. (2008). A review of modular strategies and architecture within manufacturing operations, *Proceedings of the Institution of Mechanical Engineers, Part D: Journal of Automobile Engineering*, Vol. 223, No. 1, 65-75, doi: [10.1243/09544070JAUTO822](https://doi.org/10.1243/09544070JAUTO822).
- [17] Juran, J.M., Godfrey, A.B. (1998). *Juran's quality handbook: Fifth Edition*, McGraw Hill, New York, USA.
- [18] McQuater, R.E., Scurr, C.H., Dale, B.G., Hillman, P.G. (1995). Using quality tools and techniques successfully, *The TQM magazine*, Vol. 7, No. 6, 37-42, doi: [10.1108/09544789510103761](https://doi.org/10.1108/09544789510103761).
- [19] Bird, D. Dale, B.G. (1995). The use of statistical process control in the manufacture of high-integrity products, *Proceedings of the Institution of Mechanical Engineers, Part D: Journal of Automobile Engineering*, Vol. 209, No. 1, 25-31, doi: [10.1243/PIME PROC 1995 209 180 02](https://doi.org/10.1243/PIME PROC 1995 209 180 02).
- [20] Abdulaziz, A.-I. (2014). Quality management and its role in improving service quality in public sector, *Journal of Business and Management Sciences*, Vol. 2, No. 6, 123-147, doi: [10.12691/jbms-2-6-1](https://doi.org/10.12691/jbms-2-6-1).
- [21] Poksinska, B., Dahlgard, J.J., Antoni, M. (2002). The state of ISO 9000 certification: A study of Swedish organizations, *The TQM Magazine*, Vol. 14, No. 5, 297-306, doi: [10.1108/09544780210439734](https://doi.org/10.1108/09544780210439734).
- [22] Banduka, N., Veža, I., Bilić, B. (2016). An integrated lean approach to process failure mode and effect analysis (PFMEA): A case study from automotive industry, *Advances in Production Engineering & Management*, Vol. 11, No. 4, 355-365, doi: [10.14743/apem2016.4.233](https://doi.org/10.14743/apem2016.4.233).
- [23] Chao, L.P, Ishii, K. (2004). Project quality function deployment, *International Journal of Quality & Reliability Management*, Vol. 21, No. 9, 938-958, doi: [10.1108/02656710410561763](https://doi.org/10.1108/02656710410561763).
- [24] Coetzee, R., van der Merwe, K., van Dyk, L. (2016). Lean implementation strategies: How are the Toyota way principles addressed? *The South African Journal of Industrial Engineering*, Vol. 27, No. 3, 79-91, doi: [10.7166/27-3-1641](https://doi.org/10.7166/27-3-1641).
- [25] Hanenkamp, N. (2013). The process model for shop floor management implementation, *Advances in Industrial Engineering and Management*, Vol. 2, No. 1, 40-46.
- [26] Chang, H.H. (2006). An empirical evaluation of performance measurement system for total quality management, *Total Quality Management & Business Excellence*, Vol. 17, No. 8, 1093-1109, doi: [10.1080/14783360600941795](https://doi.org/10.1080/14783360600941795).
- [27] Soliman, M.H.A. (2017). Why continuous improvement programs fail in the egyptian manufacturing organizations? A research study of the evidence, *American Journal of Industrial and Business Management*, Vol. 7, No. 3, 202-222, doi: [10.4236/ajibm.2017.73016](https://doi.org/10.4236/ajibm.2017.73016).
- [28] Jasti, N.V.K., Kodali, R. (2015). Lean production: Literature review and trends, *International Journal of Production Research*, Vol. 53., No. 3, 867-885, doi: [10.1080/00207543.2014.937508](https://doi.org/10.1080/00207543.2014.937508).
- [29] Kayis, B., Kara, S. (2005). The supplier and customer contribution to manufacturing flexibility: Australian manufacturing industry's perspective, *Journal of Manufacturing Technology Management*, Vol. 16, No. 7, 733-752, doi: [10.1108/17410380510626169](https://doi.org/10.1108/17410380510626169).
- [30] Lee, S.-D., Kim, S.-L. (2010). Characterization and development of the ideal pedal force, pedal travel, and response time in the brake system for the translation of the voice of the customer to engineering specifications, *Proceedings of the Institution of Mechanical Engineers, Part D: Journal of Automobile Engineering*, Vol. 224, No. 11, 1433-1450, doi: [10.1243/09544070JAUTO1585](https://doi.org/10.1243/09544070JAUTO1585).
- [31] Tanco, M., Mateo, R., Santos, J., Jaca, C., Viles, E. (2012). On the relationship between continuous improvement programmes and their effect on quality defects: An automotive case study, *Total Quality Management & Business Excellence*, Vol. 23, No. 3-4, 277-290, doi: [10.1080/14783363.2011.637779](https://doi.org/10.1080/14783363.2011.637779).
- [32] Hendricks, K.B., Singhal, V.R. (1997). Does implementing an effective TQM program actually improve operating performance? Empirical evidence from firms that have won quality awards, *Management Science*, Vol. 43, No. 9, 1258-1274, doi: [10.1287/mnsc.43.9.1258](https://doi.org/10.1287/mnsc.43.9.1258).
- [33] Li, J., Blumenfeld, D.E., Marin, S.P. (2008). Production system design for quality robustness, *IEEE Transactions*, Vol. 40, No. 3, 162-176, doi: [10.1080/07408170601013661](https://doi.org/10.1080/07408170601013661).
- [34] Akao, Y., Mazur, G.H. (2003). The leading edge in QFD: Past, present and future, *International Journal of Quality & Reliability Management*, Vol. 20, No. 1, 20-35, doi: [10.1108/02656710310453791](https://doi.org/10.1108/02656710310453791).
- [35] Miller, K., Brand, C., Heathcote, N., Rutter, B. (2005). Quality function deployment and its application to automotive door design, *Proceedings of the Institution of Mechanical Engineers, Part D: Journal of Automobile Engineering*, Vol. 219, No.12, 1481-1493, doi: [10.1243/095440705X35053](https://doi.org/10.1243/095440705X35053).
- [36] Popovic, P, Ivanovic, G., Mitrovic, R., Subic, A. (2012). Design for reliability of a vehicle transmission system, *Proceedings of the Institution of Mechanical Engineers, Part D: Journal of Automobile Engineering*, Vol. 226, No. 2, 194-209, doi: [10.1177/0954407011416175](https://doi.org/10.1177/0954407011416175).
- [37] Mourtzis, D., Vlachou, E., Milas, N., Xanthopoulos, N. (2016). A cloud-based approach for maintenance of machine tools and equipment based on shop-floor monitoring, *Procedia CIRP*, Vol. 41, 655-660, doi: [10.1016/j.procir.2015.12.069](https://doi.org/10.1016/j.procir.2015.12.069).
- [38] Lee, S. (2008). Principal component analysis of vehicle acceleration gain and translation of voice of the customer, *Proceedings of the Institution of Mechanical Engineers, Part D: Journal of Automobile Engineering*, Vol. 222, No. 2, 191-203, doi: [10.1243/09544070JAUTO351](https://doi.org/10.1243/09544070JAUTO351).

Vehicle routing optimization with multiple fuzzy time windows based on improved wolf pack algorithm

Cao, Q.K.^a, Yang, K.W.^a, Ren, X.Y.^{a,*}

^aSchool of Management Engineering and Business, Hebei University of Engineering, Handan, Hebei, P.R. China

ABSTRACT

The vehicle routing problem with multiple fuzzy time windows is investigated in this paper. The dynamic change of traffic flow and the fuzzy time window of customers are considered. A multi fuzzy time window vehicle routing model based on time-varying traffic flow is proposed, and the objective function is to minimize the total cost of distribution and maximize customer satisfaction. According to the basic principle of wolf pack algorithm, in order to promote the exchange of information between the artificial wolves, improve the wolves' grasp of the global information and enhance the exploring ability of wolves, a drift operator and wave operator were introduced into scouting behaviors and summing behaviors. An adaptive dynamic adjustment factor strategy was proposed for beleaguering behaviors, the exploitation ability of the algorithm strengthened constantly. Thus the convergence rate of algorithm was enhanced. We further do simulation on an example, and compare the results obtained by wolf pack algorithm and ant genetic algorithm. The results show that use improved wolf pack algorithm to solve vehicle routing problem with multiple fuzzy time windows has the advantages of small number of iterations and high efficiency, it can converge to the global optimal solution in a short time. The improved wolf pack algorithm is an efficient algorithm for solving vehicle routing problem with multiple fuzzy time windows.

© 2017 PEI, University of Maribor. All rights reserved.

ARTICLE INFO

Keywords:
Vehicle routing
Traffic flow
Multi fuzzy time windows
Wolf pack algorithm
Customer satisfaction

**Corresponding author:*
boyrenxy@126.com
(Ren, X.Y.)

Article history:
Received 3 July 2017
Revised 12 October 2017
Accepted 8 November 2017

1. Introduction

With the development of the times, more and more attention has been paid to logistics, which has become one of the most important competitive fields. Whether the logistics distribution scheme is reasonable or not directly affects the enterprise's cost, service quality, efficiency and comprehensive competitiveness. In this paper, through the study of vehicle routing problem, choose a reasonable vehicle delivery path, in order to achieve the enterprise's distribution costs at least, customer satisfaction is the biggest, improve the enterprise's comprehensive competitiveness.

Dantzig and Ramser proposed vehicle routing problem in 1959 [1]. Many scholars have studied its optimization, and obtained rich research results in the fields of transportation [2], logistics [3], interference management [4].

The vehicle routing problem with time windows (VRPMTW) is generated in the traditional vehicle routing problem considering the time window requirements of customers. Most of the researches focus on hard time windows, soft time windows and fuzzy time windows, Cordeau (2001), Qureshi (2009), Hong (2012), He (2013), Meng Xianghu (2014) gave the methods for solving such problems: dynamic programming algorithm, branch and bound method, improved

large neighbourhood search algorithm, column generation algorithm and quantum ant colony algorithm [5-9]. On the basis of the above research results, in the distribution of fresh agricultural products, Shao (2015) *et al.* reflected the customer satisfaction by fuzzy membership function which is represented by the time window [10]. Li (2015) *et al.* researched the vehicle routing problem with multiple time windows, considered multiple hard time windows and the capacity of the distribution vehicle, designed a intelligent water drop algorithm to solve the problem [11]. In the study of fuzzy time windows, Yan (2016) *et al.* dealt with the multiple time windows as fuzzy variables, applied particle swarm optimization (PSO) algorithm solve the vehicle routing problem with multiple fuzzy time windows, compared with the VRPMTW model, the model is more close to the needs of customers in real life [12].

Vehicle routing problem based on time varying traffic flow is that when formulate vehicle distribution routes, based on the constraints of the basic transportation scheduling to consider the changing road traffic flow. In the classical research results, the vehicle speed is assumed to be a constant value, but in real life, vehicles are affected by changing traffic flow, and the driving speed is not constant. Van Woensel (2008) *et al.* solved the vehicle routing problem with dynamic traffic time considering potential traffic congestion, considered the traffic jam can shorten the total travel time in the optimization process effectively, optimized the departure time of the vehicle [13]. Kritzingner (2012) *et al.* considered the traffic information in real life into the vehicle routing problem, used the Dijkstra algorithm and a variable neighbourhood search algorithm to solve the problem [14]. Kok (2012) *et al.* considered the influence of traffic jam in vehicle routing, respond to the actual situation of traffic congestion in the speed model [15]. Li (2012) *et al.* proposed a method of cross-time processing, which can deduce the corresponding vehicle travel time directly [16].

Vehicle routing problem with time window in time-varying traffic flow considered the two constraints of customer time window and time-varying traffic flow at the same time, closer to real life, and some achievements have been made in the optimization of cold chain transportation and transportation of dangerous chemicals. Tagmouti (2007), Woensel (2008) *et al.*, Donati (2008) *et al.*, Zhu (2014) and Lin (2014) gave the algorithm column for solving the problem is that generation algorithm, queuing theory, multi ant colony system and tabu search algorithm [17-19]. Xiang (2008) *et al.* researched the scheduled delivery service problem under time-varying constraints [20]. Shi (2013) *et al.* analyzed the travel time based on time-varying characteristics of distribution roads, designed the satisfaction function according to the service time window [21]. Zhu (2016) *et al.* took transportation time and risk as multiple objectives, considered the time-varying transportation time and risk, the service time window constraint of the road node, the mathematical model of the problem is established, designed ant colony algorithm to solve it [22].

In summary, scholars at home and abroad have a deep research on vehicle routing problem with traffic flow and time window constraints, it was also a very useful attempt, the theory, model and algorithm have achieved abundant results. However, the vehicle speed is affected by the dynamic traffic flow in real life, and customers usually have multiple fuzzy time windows, therefore, the study of vehicle routing problem with multiple fuzzy time windows based on time-varying traffic flow is more in line with the actual situation, and the problem has not been studied at present. This paper aims at the dynamic changes of traffic flow in real life and customer acceptance of the delivery service period is not unique, a vehicle routing model with multiple fuzzy time windows based on time-varying traffic flow is constructed, design an improved wolf pack algorithm to solve the problem.

2. Problem description and definition of the model

This paper takes into account the different speed during different time periods in delivery process, deal multiple time windows with fuzzy, establish the membership function of service start time to quantify customer satisfaction, and the objective is to minimize total delivery cost and maximize customer satisfaction, construct a vehicle routing model with multiple fuzzy time windows based on time-varying traffic flow.

2.1 Problem description

A vehicle routing problem with multiple fuzzy time windows based on time-varying traffic flow is described as: a distribution center has m cars and serve n clients, customer i has W_i fuzzy time windows; the coordinates, requirement of n clients and the capacity of m cars are known, vehicles of the same type will start from the distribution center, select a time window for the customer's delivery service, return to the distribution center after all delivery tasks have been completed; the distribution center has sufficient stock, not to consider the shortage situation; at different times of the day, the corresponding driving speed is also different; the fixed cost per vehicle and the cost of travelling per unit distance are known throughout the delivery schedule; the time to service each customer point is known; the total travel distance (time) of each vehicle is within the limits, and the path is rationally planned to obtain the optimal objective function.

2.2 Model definition

$G = (L, A)$: represents the relation between the location of the distribution center and the point of delivery, the path and the spatial temporal distance between each other;

$A = \{a_{i,j} | i \neq j \wedge i, j \in L\}$: represents the route between two delivery points or distribution points and distribution centers;

$L = \{1, 2, \dots, n\}$: represents customer set for distribution;

$K = \{1, 2, \dots, m\}$: represents distribution vehicle set;

Q_k : represents capacity of vehicle k ;

$d_{i,j}$: represents distance from point i to point j ;

D_k : represents the total distance (time) value of the vehicle k during the distribution process;

c : represents the fixed cost of delivering a vehicle;

$c_{i,j}$: represents the cost of delivery per unit distance;

t_i : represents the time when the vehicle started serving customer i ;

s_i : represents the time of service client i ;

t_{ij} : represents the time from customer i to customer j ;

q_i : represents the requirements of customer i ;

W_i : represents the number of time windows for client i ;

$[a_i^\alpha, b_i^\alpha]$: represents that the customer i expects to be served at the α time window, a_i^α represents the earliest service time to start, b_i^α represents the latest service time;

$[E_i^\alpha, L_i^\alpha]$: represents the α fuzzy time window that the client has, E_i^α represents the earliest service time that can be tolerated, L_i^α represents the latest service time that the customer i can tolerate. Introducing decision variables.

$$\begin{aligned}
 x_{ijk} &= \begin{cases} 1, & \text{vehicle } k \text{ access } i \text{ from } j \\ 0, & \text{else} \end{cases} \\
 y_i^\alpha &= \begin{cases} 1, & \text{service the } \alpha \text{ window of the client } i \\ 0, & \text{else} \end{cases}
 \end{aligned} \tag{1}$$

In this paper, we use trapezoidal fuzzy time window from literature [12], the satisfaction of customer i is defined by the service start time membership function, $\mu_i(t_i)$ as shown in Eq. 2.

$$\mu_i = \begin{cases} 0, & t_i < E_i^\alpha \\ (t_i - E_i^\alpha)/(a_i^\alpha - E_i^\alpha), & E_i^\alpha < t_i < a_i^\alpha \\ 1, & a_i^\alpha < t_i < b_i^\alpha \\ (L_i^\alpha - t_i)/(L_i^\alpha - b_i^\alpha), & b_i^\alpha < t_i < L_i^\alpha \\ 0, & t_i > L_i^\alpha \end{cases} \tag{2}$$

The characteristics of traffic flow are expressed by driving speed, the road traffic flow corresponding to the day is divided into three sections: congestion time, general time and unblocked time, the vehicle speed distribution function is as follows:

$$f(v(t)) = \begin{cases} \frac{1}{\sqrt{2\pi}v(t)\sigma} e^{-\frac{(\ln v(t)-\mu)^2}{2\sigma^2}}, v \in [v_{min}, v_{max}], t \in tw_1 \\ \frac{1}{\sqrt{2\pi}\sigma} e^{-\frac{(v(t)-\mu)^2}{2\sigma^2}}, v \in [v_{min}, v_{max}], t \in tw_2, tw_3 \end{cases} \quad (3)$$

$$\mu = \begin{cases} \lambda_1, t \in tw_1 \\ \lambda_2, t \in tw_2 \\ \lambda_3, t \in tw_3 \end{cases}, \sigma_v = \begin{cases} \sigma_{v1}, t \in tw_1 \\ \sigma_{v2}, t \in tw_2 \\ \sigma_{v3}, t \in tw_3 \end{cases} \quad (4)$$

Symbols tw_1, tw_2, tw_3 represent three time periods: unblocked time section, general time section and congestion time section, $\lambda_1, \lambda_2, \lambda_3$ represent the speed expectations of the vehicle in these three time periods, $\sigma_{v1}, \sigma_{v2}, \sigma_{v3}$ represent the standard deviation of speed in these three time periods.

When the vehicle speed is in the unblocked period, it obeys the logarithmic distribution:

$$\ln v(t) \sim N(\mu, \sigma^2)$$

$$E(v(t)) = \lambda_1 e^{(\mu + \frac{\sigma^2}{2})}, \text{ var}(v(t)) = \sigma_{v1} = (e^{2\mu + \sigma^2})(e^{\sigma^2} - 1) \quad (5)$$

When the vehicle speed is in the normal time period and the peak time period, it obeys normal distribution, that is $v(t) \sim N(\mu, \sigma^2)$, so that:

$$E(v(t)) = \mu, \text{ var}(v(t)) = \sigma \quad (6)$$

Vehicle routing model with multiple fuzzy time windows based on time varying traffic flow:

Objective functions:

$$\max Z_1 = \frac{1}{n} \sum_{i \in N} \mu_i(t_i) \quad (7)$$

$$\min Z_2 = C + \sum_{m=1}^M \sum_{i=0}^N \sum_{j=0}^N c_{ij} \cdot x_{ijk} \quad (8)$$

Constraint conditions:

$$\sum_{i=1}^n \left(q_i \sum_{j=0}^n x_{ijk} \right) \leq Q_k, \forall k \in K \quad (9)$$

$$\sum_{i=0}^n \sum_{j=1}^{n+1} d_{ij} x_{ijk} \leq D_k \quad (10)$$

$$\sum_{i=1}^n \sum_{k=1}^m x_{ijk} = 1, \forall j \in L \quad (11)$$

$$\sum_{i,j \in S \times S} x_{ijk} \leq |S| - 1, S \subseteq L; \forall k \in K \quad (12)$$

$$L_i^\alpha \leq E_i^{\alpha+1}, \forall i \subseteq L; \alpha \in \{1, 2, \dots, W_i - 1\} \quad (13)$$

$$t_j \geq \max \left\{ \sum_{\alpha=1}^{w_i} y_i^\alpha E_i^\alpha, (t_i + s_i + t_{ij})x_{ijk} \right\}, \forall i, j \in L; \forall k \in K \quad (14)$$

$$t_j \leq \sum_{\alpha=1}^{w_i} y_j^\alpha L_j^\alpha, \forall j \in L \quad (15)$$

$$\sum_{\alpha=1}^{w_i} y_i^\alpha = 1, \forall i \in L \quad (16)$$

$$\ln v(t) \sim N(\overline{v(t)}, \sigma_v), t \in tw_1$$

$$v(t) \sim N(\overline{v(t)}, \sigma_v), t \in tw_2, tw_3$$

$$\overline{v(t)} = \begin{cases} \lambda_1, tw_1 \\ \lambda_2, tw_2 \\ \lambda_3, tw_3 \end{cases}, \sigma_v = \begin{cases} \sigma_{v1}, tw_1 \\ \sigma_{v2}, tw_2 \\ \sigma_{v3}, tw_3 \end{cases}$$

$$t_{ij} = \frac{s_{ij}}{v(t)}, i \in [0, N + M], j \in [0, N + M] \quad (17)$$

$$x_{ijk} = 0 \text{ or } 1, \forall i, j, k \quad (18)$$

$$y_i^\alpha = 0 \text{ or } 1, \forall i \in L; \alpha \in \{1, 2, \dots, W_i\} \quad (19)$$

Function (Eq. 7) is maximize average customer satisfaction; function (Eq. 8) is minimum distribution cost. Constraint condition (Eq. 9) ensure that each vehicle does not exceed the maximum load capacity. Constraint condition (Eq. 10) represents the total travel distance (time) of any distribution vehicle is within the limit. Constraint condition (Eq. 11) ensure that each customer is only served by one car. Constraint condition (Eq. 12) represents a cancellation loop. Constraint condition (Eq. 13) represents the travel time from the customer point i to the customer point j is related to the distribution of traffic flow on the road, and the delivery time is affected by vehicle speed. Constraint conditions (Eq. 14) and (Eq. 15) represent customers are served within the time window. Constraint condition (Eq. 16) represents that each client is only served at one of the time windows. Constraint condition (Eq. 17) represents that a mathematical expectation that corresponds to the speed of the vehicle at different times of the day. Constraint conditions (Eq. 18) and (Eq. 19) represent the range of variables.

3. Improved wolf swarm algorithm

Wolf Colony Algorithm (WCA) is a new intelligent optimization algorithm proposed in 2011, as soon as the algorithm was put forward, it attracted the attention of scholars at home and abroad. Wu Husheng (2013) *et al.* proposed Wolf Pack Algorithm (WPA) based on the characteristics of cooperative hunting of wolves, which is different from WCA algorithm [23]. After several years of research and exploration, the WPA has been applied to the TSP problem, vehicle routing problem and other fields successfully [24, 25].

3.1 Migration modes with drift operators and wave operators

In order to strengthen the information interaction between wolves, this paper adds the drift operator and wave operator to search the whole search space comprehensively, such as Eq. 20:

$$v_{i,d} = x_{i,d} + \varphi_{i,d}(x_{i,d} - x_{k,d}) + \phi_{i,d}(x_{g,d} - x_{k,d}) \quad (20)$$

$\phi_{i,d}$ is random number within the interval $[0,1]$, $\varphi_{i,d}$ is random number within the interval $[-1,1]$, $x_{g,d}$ represents optimum solution in explore wolf's individual history, $\phi_{i,d}$ is drift coefficient, $(x_{g,d} - x_{i,d})$ is drift direction, $\varphi_{i,d}(x_{i,d} - x_{k,d})$ is fluctuation term, $\varphi_{i,d}$ is fluctuation coefficient.

3.2 Summoning behavior with drift operators and wave operators

In order to improve the ability of information interaction in the process of fierce wolf raid, in this paper, the wolf executes each round of search, and then search again with formula (21). Select the strongest scent of prey and advance in the direction of the smell concentration in the current position, update fierce wolf position, select the maximum smell concentration wolf as leader wolf.

3.3 Self-adaption dynamic adjustment factor strategy

The siege behavior requires the fierce wolf to have stronger local searching ability, in order to enhance exploit capacity of fierce wolf, this paper introduce the adaptive adjustment factor strategy, as shown in Eqs. 21 to 24.

$$v_{ij} = t_1 \cdot x_{ij} + t_2 \cdot \varphi_{ij}(x_{ij} - x_{kj}) \quad (21)$$

$$\varphi_{ij} = (rand - 0.5) \cdot 2 \quad (22)$$

$$t_1 = m(w_2 - \left(\frac{iter}{max\ cycle}\right)^\alpha (w_2 - w_1)) \quad (23)$$

$$t_2 = m(w_4 - \left(\frac{iter}{max\ cycle}\right)^\beta (w_4 - w_3)) \quad (24)$$

t_1 represents memory factor, is the record of the historical position of the proportion, the greater the value, the better the global optimization ability, the change is shown in Eq. 23; t_2 represents relationship factors of information sharing between food sources and adjacent food sources, its change is shown in Eq. 24.

In formula, w_1, w_2, w_3, w_4 is constants, simultaneous satisfaction $w_2 > w_1, w_4 > w_3$, and its range of value is in the range $[0.1,1.5]$. t_1 is reduced from w_2 to w_1 , is from the global search gradually refined to local search, α usually less than 1, but the numerical value is too small is not conducive to global convergence, so the range of numerical value is in $[0.6,1]$. t_2 is reduced from w_3 to w_4 , usually, $\beta > 1$, but the fierce wolf can easily cross the global optimal solution when the numerical value is too large, so the range of numerical value is in $[1,1.3]$. m is a constant, it is based on the comparison between the food source and the food source in the neighborhood, when the neighborhood food source position is better than the current food source, the neighborhood tends to search and share information, value $m = 1.5$, otherwise $m = 0.6$.

3.4 Algorithm flow

The improved WPA solves the flow chart of the multi time vehicle path model based on time varying traffic flow, as shown in Fig 1.

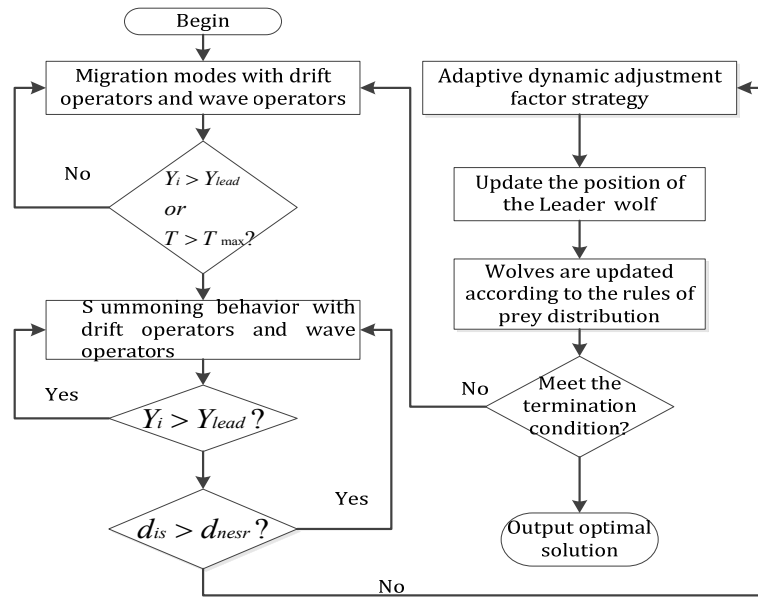


Fig 1 algorithm flow chart

4. Results and discussion

Multiple fuzzy time windows vehicle routing problem for time-varying traffic flow, considers the time-varying traffic flow and fuzzy time windows at the same time. At present, there is no common standard test data internationally, referring to the literature [11], the simulation data are designed as follows. A distribution center services for 20 clients, each client has 2 time windows, the distribution center has N delivery vehicles, it's a single model, the maximum capacity of each car is 45 t, the delivery cost of the distribution vehicle is 6 yuan per kilometer, the fixed cost of each car is 150 yuan, customer coordinates, customer requirements, service times, and time windows are shown in Table 1. It is assumed that the delivery vehicle will work from 7:00 to 20:00 a day, affected by traffic flow at different times, the corresponding distribution vehicles have different running speeds, based on the actual situation to do the relevant design, as shown in Table 2.

Table 1 Customer information

Customer	q_i	s_i	Coordinate	E_i^1	a_i^1	b_i^1	L_i^1	E_i^2	a_i^2	b_i^2	L_i^2
1	2	0.2	(1,5)	23.0	0.0	1.0	3.0	2.7	4.0	5.0	6.6
2	3	0.2	(22,10)	22.5	0.5	1.5	2.0	2.4	3.0	4.0	5.6
3	4	0.3	(12,20)	22.5	0.5	2.0	2.2	2.6	3.0	4.0	5.6
4	3	0.2	(6,28)	23.0	0.5	1.5	2.5	2.2	3.0	4.0	5.6
5	5	0.3	(10,2)	22.5	0.0	1.0	2.4	2.2	3.0	4.0	5.6
6	7	0.4	(8,15)	22.5	0.5	1.0	1.4	1.4	2.0	3.0	4.6
7	6	0.4	(-10,20)	22.5	0.5	1.5	1.5	2.0	2.5	3.5	5.1
8	4	0.3	(-15,6)	22.5	0.5	2.0	2.0	2.4	3.0	4.0	5.6
9	6	0.4	(-18,25)	22.5	0.5	1.5	1.8	1.8	2.0	3.0	4.6
10	6	0.4	(-22,5)	23.0	0.5	1.0	1.4	1.4	2.0	4.0	5.6
11	7	0.4	(-15,-5)	23.0	0.5	1.5	2.5	2.4	3.0	4.0	5.6
12	10	0.5	(-17,-12)	23.0	0.5	1.0	1.8	1.7	3.0	4.0	5.6
13	5	0.3	(-10,-25)	22.5	0.5	1.0	1.5	1.4	1.5	3.0	4.6
14	7	0.4	(-5,-15)	23.0	0.5	1.0	1.5	1.4	2.0	3.0	4.6
15	11	0.5	(2,-35)	23.5	1.0	3.0	3.5	3.6	4.0	5.0	6.6
16	12	0.5	(3,-15)	23.5	0.5	1.5	2.5	2.2	3.0	4.0	5.6
17	4	0.3	(5,-10)	22.5	0.0	1.0	2.5	2.6	4.0	5.0	6.6
18	5	0.3	(12,-35)	23.0	0.5	1.5	1.8	1.9	2.0	4.0	5.6
19	10	0.5	(23,-20)	23.6	1.0	2.0	2.3	2.4	3.0	5.0	6.6
20	12	0.5	(16,-12)	23.0	0.5	1.0	2.0	2.1	3.0	5.0	6.6

Table 2 Vehicle speed

Congestion situation	Specific time	Running speed
Expedite time	7:00-7:20	55
	19:00-20:00	
General time	9:00-12:00	45
	13:00-17:00	
Congestion time	7:20-9:00	35
	12:00-13:00 17:00-19:00	

Authors through a large number of experiments to verify that α (i.e., exploring wolf scaling factor) and β (i.e., update scaling factor) in WPA not as sensitive as other intelligent algorithms, random selection is only required within the bounds; ω (the distance determination factor) is an important parameter to control the artificial wolf from the raid state to siege behavior, with the increase of ω , determine the distance decreases, the artificial fierce wolf into siege behavior in the distance near the position of the leader wolf, improve the convergence speed of the algorithm, reduce iterations, but the value of ω is too large, the artificial wolf is difficult to move into the siege, which leads to an increase in iterations; S (the step size factor) shows the fine degree of searching the optimal solution for the wolf in the solution space, with the increase of S , the search precision is increased, and the average iteration number of the algorithm is also increased, if the S exceeds a certain range, the convergence accuracy of the algorithm will decrease and the optimization results will be poor.

According to references [23-26], this paper sets up the running parameters of the improved WPA: experimental setting maximum iterations is 100, maximum number of trips is 15, initial wolf size is 200, $\alpha = 4, \beta = 6, S = 22$; the average level of satisfaction is set to 0.75, the optimal experimental results obtained by the improved wolf pack algorithm are shown in Table 3, the optimal experimental result path is shown in Fig 2.

For further analysis the improved WPA, the calculation results are compared with the results of genetic algorithm, the selected algorithm parameters are as follows: population size is 30, crossover rate is 0.6, mutation rate is 0.05. Each algorithm is calculated with the same constraints and computer configuration, run 100 times separately.

Table 3 Optimal experimental results

Vehicle	Route	Travel distance (km)	Customer satisfaction	Loading capacity (t)	Distribution cost (yuan)
1	0-17-16-14-13-12-0	71.32	0.75	38	577.92
2	0-7-9-10-8-11-0	86.07	0.77	29	666.42
3	0-20-19-18-15-0	94.29	0.76	38	715.74
4	0-5-2-6-3-4-1-0	84.53	0.78	24	657.18

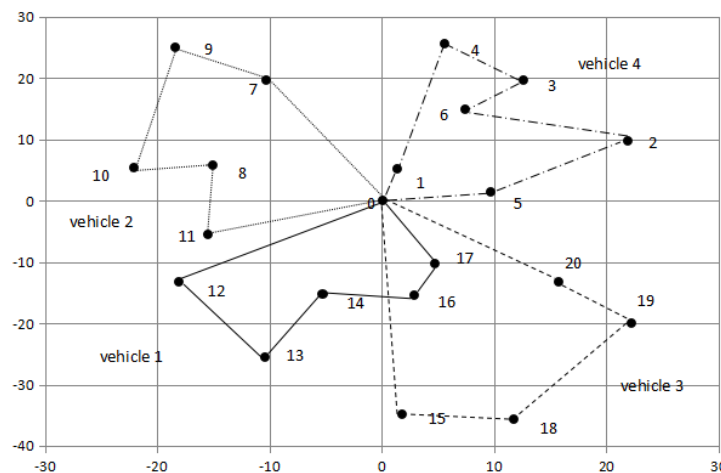


Fig 2 Optimal experimental result path chart

The experimental comparison results are shown in Table 4, the improved WPA has the best path, the shorter total travel distance and the lower total distribution cost, average customer satisfaction is higher; The Table 4 shows that the improved WPA does not increase the computational time on the basis of performance improvement, and is an efficient improved wolf swarm algorithm.

The convergence of the optimal solution is shown in Fig 3. These results show that the improved WPA has the advantages of small number of iterations and high efficiency. It can converge to the global optimal solution in a short period of time.

Table 4 Experimental results of improved WPA and genetic algorithm

Algorithm	Vehicle route	Total travel distance (km)	Total distribution cost (yuan)	Average customer satisfaction	Average computational time (s)
Improved WPA	0-17-16-14-13-12-0	336.21	2617.26	0.77	10.39
	0-7-9-10-8-11-0				
	0-20-19-18-15-0				
	0-5-2-6-3-4-1-0				
Genetic algorithm	0-8-10-11-12-0	343.033	2658.17	0.76	11.87
	0-1-5-2-6-3-4-7-9-0				
	0-20-19-18-15-0				
	0-17-16-13-14-0				

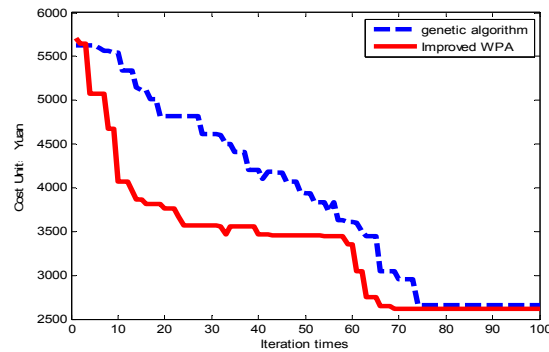


Fig 3 Convergence of the optimal solution

5. Conclusion

This paper considers the time-varying speed in real life and the fuzzy time window of customers, a vehicle routing model with multiple fuzzy time windows based on time-varying traffic flow is constructed. The drift operator and wave operator are introduced in the migration and wave operators, in order to enhance the exploit capacity of the wolf, an adaptive dynamic adjustment factor is introduced, design an improved WPA and give the algorithm steps. Through simulation analysis, the improved wolf pack algorithm is compared with genetic algorithm, it shows that the algorithm can obtain the optimal solution, and the efficiency of the solution has been improved, can reduce the total distance travelled more effectively, reduce distribution costs and improve customer satisfaction.

Therefore, the improved WPA increase exchanges of information between the artificial wolf, enhance the wolves grasp of global information, the exploration ability and exploitation ability. WPA is a swarm intelligence optimization algorithm to solve multi fuzzy vehicle routing problem with time window. WPA is a new swarm intelligence algorithm. How to combine the WPA with other intelligent algorithms to solve the problem more efficiently is the next step.

Meanwhile, the uncertainties faced in reality are even more complex, for example, changes in customer demand, sudden vehicle failure, customer cancellations, changes in customer's time window, bad weather, etc. In the future, such extensions can study in depth.

Acknowledgement

The research of this paper is made possible by the generous support from National Natural Science Foundation of China (61375003), Social Science Foundation of Hebei Province (HB16GL026; HB17GL022), Research Projects of Innovative Talents Training Fund of Hebei Province (A2016001120). Project of Scientific Research Project of Hebei Provincial Education Department (SD161009).

References

- [1] Dantzig, G.B., Ramser, J.H. (1959). The truck dispatching problem, *Management Science*, Vol. 6, No. 1, 80-91, doi: [10.1287/mnsc.6.1.80](https://doi.org/10.1287/mnsc.6.1.80).
- [2] Lu, X.C., Chen, Q.B., Zhang, Z.J. (2014). The electric vehicle routing optimizing algorithm and the charging stations' layout analysis in Beijing, *International Journal of Simulation Modelling*, Vol. 13, No. 1, 116-127, doi: [10.2507/IJSIMM13\(1\)CO4](https://doi.org/10.2507/IJSIMM13(1)CO4).
- [3] Cao, Q.-K., Liu, X.-Y., Ren, X.-Y. (2015). Vehicle scheduling problem based on plant growth simulation algorithm, *Systems Engineering – Theory & Practice*, Vol. 35, No. 6, 1449-1456, doi: [10.12011/1000-6788\(2015\)6-1449](https://doi.org/10.12011/1000-6788(2015)6-1449).
- [4] Wang, X., Ruan, J., Sun, Z., Cao, H. (2013). Disruption recovery model for vehicle routing problem with backhaul, *Journal of Systems Engineering*, Vol. 28, No. 5, 608-616.
- [5] Cordeau, J.-F., Laporte, G., Mercier, A. (2001). A unified tabu search heuristics for vehicle routing problems with time windows, *Journal of the Operational Research Society*, Vol. 52, No. 8, 928-936, doi: [10.1057/palgrave.jors.2601163](https://doi.org/10.1057/palgrave.jors.2601163).
- [6] Qureshi, A.G., Taniguchi, E., Yamada, T. (2009). An exact solution approach for vehicle routing and scheduling problems with soft time windows, *Transportation Research Part E: Logistics & Transportation Review*, Vol. 45, No. 6, 960-977, doi: [org/10.1016/j.tre.2009.04.007](https://doi.org/10.1016/j.tre.2009.04.007).
- [7] Hong, L. (2012). An improved LNS algorithm for real-time vehicle routing problem with time windows, *Computers & Operations Research*, Vol. 39, No. 2, 151-163, doi: [org/10.1016/j.cor.2011.03.006](https://doi.org/10.1016/j.cor.2011.03.006).
- [8] He, X.-F., Ma, L. (2013). Quantum-inspired ant colony algorithm for vehicle routing problem with time windows, *Systems Engineering – Theory & Practice*, Vol. 33, No. 5, 1255-1261, doi: [10.3969/j.issn.1000-6788.2013.05.021](https://doi.org/10.3969/j.issn.1000-6788.2013.05.021).
- [9] Meng, X.-H., Hu, R., Qian, B. (2014). Effective hybrid population-based incremental learning algorithm for vehicle routing problem with time windows, *Systems Engineering – Theory & Practice*, Vol. 34, No. 10, 2701-2709, doi: [10.12011/1000-6788\(2014\)10-2701](https://doi.org/10.12011/1000-6788(2014)10-2701).
- [10] Shao, J.-P., Cao, Q., Shen, M., Sun, Y. (2015). Research on multi-objective optimization for fresh agricultural products VRP problem, *Industrial Engineering and Management*, Vol. 20, No. 1, 122-127, doi: [10.3969/j.issn.1007-5429.2015.01.019](https://doi.org/10.3969/j.issn.1007-5429.2015.01.019).
- [11] Li, Z.P., Zhao, F., Liu, H.D. (2015). Intelligent water drops algorithm for vehicle routing problem with multiple time windows, *Operations Research and Management Science*, Vol. 24, No. 6, 1-10.
- [12] Yan, F., Wang, Y. (2016). Modeling and solution of vehicle routing problem with multiple fuzzy time windows, *Journal of Transportation Systems Engineering and Information Technology*, Vol. 16, No. 6, 182-188, doi: [10.3969/j.issn.1009-6744.2016.06.028](https://doi.org/10.3969/j.issn.1009-6744.2016.06.028).
- [13] Van Woensel, T., Kerbache, L., Peremans, H., Vandaele, N. (2008). Vehicle routing with dynamic travel times: A queueing approach, *European Journal of Operational Research*, Vol. 186, No. 3, 990-1007, doi: [10.1016/j.ejor.2007.03.012](https://doi.org/10.1016/j.ejor.2007.03.012).
- [14] Kritzingner, S., Doerner, K.F., Hartl, R.F., Kiechle, G.ÿ., Stadler, H., Manohar, S.S. (2012). *Using traffic information for time-dependent vehicle routing*, *Procedia – Social and Behavioral Sciences*, Vol. 39, 217-229, doi: [10.1016/j.sbspro.2012.03.103](https://doi.org/10.1016/j.sbspro.2012.03.103).
- [15] Kok, A.L., Hans, E.W., Schutten, J.M.J. (2012). Vehicle routing under time-dependent travel times: The impact of congestion avoidance, *Computers & Operations Research*, Vol. 39, No. 5, 910-918, doi: [10.1016/j.cor.2011.05.027](https://doi.org/10.1016/j.cor.2011.05.027).
- [16] Li, Y., Li, J., Gao, Z. (2012). Dynamic programming heuristics for solving time dependent vehicle routing problem, *Systems Engineering – Theory & Practice*, Vol. 32, No. 8, 1712-1718, doi: [10.3969/j.issn.1000-6788.2012.08.010](https://doi.org/10.3969/j.issn.1000-6788.2012.08.010).
- [17] Tagmouti, M., Gendreau, M., Potvin, J.-Y. (2007). Arc routing problems with time-dependent service costs, *European Journal of Operational Research*, Vol. 181, No. 1, 30-39, doi: [10.1016/j.ejor.2006.06.028](https://doi.org/10.1016/j.ejor.2006.06.028).
- [18] Van Woensel, T., Kerbache, L., Peremans, H., Vandaele, N. (2008). Vehicle routing with dynamic travel times: a queueing approach, *European Journal of Operational Research*, Vol. 186, No. 3, 990-1007, doi: [10.1016/j.ejor.2007.03.012](https://doi.org/10.1016/j.ejor.2007.03.012).
- [19] Donati, A.V., Montemanni, R., Casagrande, N., Rizzoli, A.E., Gambardella, L.M. (2008). Time dependent vehicle routing problem with a multi ant colony system, *European Journal of Operational Research*, Vol. 185, No. 3, 1174-1191, doi: [10.1016/j.ejor.2006.06.047](https://doi.org/10.1016/j.ejor.2006.06.047).
- [20] Xiang, Z., Chu, C., Chen, H. (2008). The study of a dynamic dial-a-ride problem under time-dependent and stochastic environments, *European Journal of Operational Research*, Vol. 185, No. 2, 534-551, doi: [10.1016/j.ejor.2007.01.007](https://doi.org/10.1016/j.ejor.2007.01.007).
- [21] Shi, Z., Fu, Z. (2013). Distribution location routing optimization problem of food cold chain with time window in time varying network, *Application Research of Computers*, Vol. 30, No. 1, 183-188, doi: [10.3969/j.issn.1001-3695.2013.01.047](https://doi.org/10.3969/j.issn.1001-3695.2013.01.047).

- [22] Zhu, T., Wang, X.L., Zhao, L.J. (2016). Path selection of hazardous materials road transportation with time window and multi-objectives, *Industrial Engineering Journal*, Vol. 19, No. 2, 62-67, [doi: 10.3969/j.issn.1007-7375.2016.02.010](https://doi.org/10.3969/j.issn.1007-7375.2016.02.010).
- [23] Wu, H.S., Zhang, F.M., Wu, L.S. (2013). New swarm intelligence algorithm-wolf pack algorithm, *Systems Engineering and Electronics*, Vol. 35, No. 11, 2430-2438.
- [24] Wu, H.-S., Zhang, F.-M., Li, H., Liang, X.-L. (2015). Discrete wolf pack algorithm for traveling salesman problem, *Control and Decision*, Vol. 30, No. 10, 1861-1867, [doi: 10.13195/j.kzyjc.2014.1055](https://doi.org/10.13195/j.kzyjc.2014.1055).
- [25] Ye, Y., Zhang, H.Z. (2017). Wolf pack algorithm for multi-depot vehicle routing problem, *Application Research of Computers*, Vol. 34, No. 9, 2590-2593.
- [26] Li, G., Wei, Z., Xu, L. (2015). Wolf pack algorithm based on modified search strategy, *Journal of Computer Applications*, Vol. 35, No. 6, 1633-1636, [doi: 10.11772/j.issn.1001-9081.2015.06.1633](https://doi.org/10.11772/j.issn.1001-9081.2015.06.1633).

Laser drilling of alumina ceramics using solid state Nd:YAG laser and QCW fiber laser: Effect of process parameters on the hole geometry

Rihakova, L.^{a,*}, Chmelickova, H.^b

^aRegional Centre of Advanced Technologies and Materials, Joint Laboratory of Optics of Palacký University and Institute of Physics CAS, Faculty of Science, Palacký University, Olomouc, Czech Republic

^bJoint Laboratory of Optics of Palacký University and Institute of Physics CAS, Faculty of Science, Palacký University, Olomouc, Czech Republic

ABSTRACT

Nowadays a lot of lasers working at different parameters could be used for machining of a wide spectrum of materials. One of these materials is alumina ceramic as it is hard to machine using conventional methods due to high hardness and brittleness. In this paper the percussion drilling of alumina ceramics was performed by Nd:YAG laser and quasi-continuous-wave fiber laser. Effects of laser wavelength, pulse energy, pulse length and number of pulses were examined and the comparison of produced holes geometry was reported. The results show that it is possible to control the holes dimensions by changing lasers and parameters. Fiber laser provides generation of narrower holes due to its small spot and better beam quality together with high power densities. Shorter pulses 0.5 ms, high peak power 1 kW and energy density around 10 kJ/cm² are satisfactory for drilling, as they assured good holes circularity and less amount of melt. For Nd:YAG laser it was found that both entrance and exit holes diameters go up proportionally with the pulse length and pulse energy. The optimum parameters for this laser were pulse length 1 ms as good circularity and less amount of dross was obtained, and energy densities around 1 kJ/cm² leading to formation of hole with better quality. Moreover, higher number of pulses improves holes circularity.

© 2017 PEI, University of Maribor. All rights reserved.

ARTICLE INFO

Keywords:

Alumina ceramics
Laser drilling
Solid state Nd:YAG laser
QCW fiber laser
Hole geometry

*Corresponding author:

lenka.rihakova@upol.cz
(Rihakova, L.)

Article history:

Received 17 July 2017
Revised 10 October 2017
Accepted 26 October 2017

1. Introduction

Technical ceramic such as Al₂O₃ can be found in many fields of human activity. It is used for example in microelectronics as thin film substrate in circuit boards, in automobile engines, telecommunication or mechanical engineering for producing valves, seals and pump impellers. Significant exploitation of ceramic is also in medicine as orthopedic implants are made from it. Due to its characteristic properties, like high hardness and brittleness, high thermal conductivity and wear, and chemical resistance, it is hard to machine it by conventional methods. Fortunately, laser machining brings several advantages including high precision and process control together with reduction of mechanical stress. Moreover, laser treatment ensures low heat input to the material thus the heat affected zone around the interaction area is limited [1-4].

Laser machining ceramics is the actual issue for many applications including cutting, drilling and scribing. Lots of laser parameters, mainly pulse length, peak power, pulse energy, pulse frequency and focus position are involved in laser drilling [5-7]. The previous papers are mostly

devoted to the study of the effect of the laser parameters on the drilled holes and their characteristics involving taper, recast, spatter and micro-cracks. For every specific application, it is important to find the optimum parameters to achieve required holes geometry and quality. For example, Sibaliya *et al.* 2011 studied the process of Nd:YAG laser drilling of Ni-based superalloy Nimonic 263 sheets and developed a hybrid strategy that is able to find optimum process parameters and fulfill the specific demands for seven characteristics of the drilled holes including holes diameter, circularity, aspect ratio, taper and spatter [8].

In literature there are reports that concern experimental and theoretical investigation of the laser drilling process of alumina ceramics. Kacar *et al.* 2009 [9] inspected the dependence of the hole diameter on the laser peak power using Nd:YAG laser. They ascertained that the holes diameter increases with increasing peak power. Nedialkov *et al.* 2003 [10] compared the process of ceramic drilling using fundamental, second and third harmonics of Nd:YAG laser experimentally and theoretically. Another theoretical model for predicting the holes circularity was presented in Bharatish *et al.* 2013 [11]. Hanon *et al.* 2012 [6] examined and simulated the influence of laser parameters on geometrical and microstructural hole properties. They also compared the experimental and simulation results to assess the differences in the holes dimensions. Although many researches have been held, several problems concerning laser drilling, such as sample cracking or melt deposition need to be figured out.

Thermal effects can be strongly reduced using short pulses, but processing speeds have to be lowered [12]. A new generation of quasi-continuous-wave (QCW) ytterbium fiber lasers emitting at wavelength of 1070 nm, with unique properties including high pulse energy and high average and peak power together with excellent beam quality can bring an improvement. Extreme high-power densities allow high quality and rapid machining of ceramic materials. Fiber lasers also offer the possibility to machine structures with dimensions smaller than 100 μm due to low beam parameter product [13].

In this paper laser drilling of alumina ceramics was carried out using two different lasers, with the aim of creating high quality holes. For this reason the effect of drilling parameters (pulse energy, pulse length, number of pulses) on the holes characteristics is examined and optimum parameters are determined. The holes and their dimensions were characterized by scanning confocal microscopy.

2. Materials and methods

The first laser source was flash lamp pumped Nd:YAG laser LASAG KLS 246-102 emitting at wavelength of 1064 nm. We can obtain laser spot in focus plane 0.6 mm allowing maximum power 150 W. Firstly, fixed parameters during the process were frequency 20 Hz and pulse length 0.5 ms. The pulse energy in the range 0.7-2.7 J was adjusted by setting the flash lamp charging voltage (220-350 V) to investigate the effect of pulse energy on the holes geometry. Simultaneously the dependence on the number of pulses (20-180 pulses) was examined as well. During the second experiment, the effect of pulse length, pulse energy and number of pulses (80-120) was tested. The pulse length was increased from 0.6 ms to 1 ms with the increment 0.1 ms, namely for each value from the interval of flash lamp voltages (250-300 V, Table 1).

The second laser was QCW ytterbium fiber laser YLR-150/1500-QCW (IPG) with a multi-mode core fiber that can work at pulse mode providing various pulse lengths and high peak powers, as well as at continuous-wave mode providing high average powers. QCW mode was used for drilling enabling a maximum peak power of 1.5 kW. High beam quality and small spot size allow achieving high power densities for precise process. During drilling the pulse frequency was set to 50 Hz and the influence of pulse length (0.5-1 ms, with the increment 0.1 ms) and pulse energy (0.34-1.54 J) on the hole characteristics were evaluated (Table 2).

Table 1 Process parameters for drilling alumina ceramics using Nd:YAG laser

Voltage (V)	Pulse length (ms)	Pulse energy (J)	Energy density (kJ/cm^2)	Average power (W)	Peak power (kW)	Power density (MW/cm^2)
250-300	0.6-1.0	1.37-4.00	0.48-1.42	27.4-80.0	2.28-4.00	0.81-1.42

Table 2 Process parameters for drilling alumina ceramics using QCW fiber laser

Pulse length (ms)	Pulse energy (J)	Energy density (kJ/cm ²)	Average power (W)	Peak power (W)	Power density (MW/cm ²)
0.5-1.0	0.34-1.54	4.36-19.63	17.13-77.05	685-1540	8.71-19.63

For experimental studies alumina ceramic (Al₂O₃, purity 96 %) plates with thickness 2 mm were used. Before starting experiments, the sample surface was cleaned by acetone to remove oil and dust residues. Tests were performed at ambient temperature in air with the aid of compressed air supplied at pressure of 2 bars. Holes diameters and depths were measured with the help of scanning confocal microscope OLYMPUS LEXT 3100. Measurements of dimensions and 3D reconstructions of the irradiated surfaces were provided by attached software.

3. Results and discussion

Laser drilling is a complex process, dependent on several laser parameters. Therefore, there could be problems with melt produced during the drilling. The shape of the hole is affected by melt expulsion and irregular or incomplete expulsion causes formation of recast layer and can even close the hole. In this paper modifications of the holes geometry are analysed under several process conditions. The effects of the wavelength, pulse energy, pulse, length, peak power and number of pulses on the holes characteristics were investigated.

3.1 Ceramics drilling using Nd:YAG laser

Dependence of the entrance holes diameter drilled in alumina ceramics on the pulse energy for three selected number of pulses is presented in Fig. 1. As one can see, the entrance holes diameter increases with increasing value of pulse energy. The lowest value of pulse energy capable of machining a hole through the entire sample thickness was 1.47 J. For lower values an interaction between laser radiation and the alumina ceramic surface was not observed. The graph also shows that the number of pulses is not a decisive parameter as its influence on the holes diameter was not significantly proved, in contrast with Hanon *et al.* 2012 [6] who claimed that the proportions of the holes were strictly influenced by the number of pulses. By setting different values of pulse energy the required holes with entrance diameters between 374 µm and 537 µm were created. The exit holes diameters did not exhibit clear dependence on pulse energy and their dimensions were between 200 µm and 300 µm.

Fig. 2 depicts the created entrance and exit holes using laser radiation with pulse energy 1.47 J, and number of pulses 20 and 160. The recast layer produced after re-solidification of the melt phase formed during the drilling encloses the hole. Furthermore, a part of the melt material can be observed also on the edges of the exit hole created by low number of pulses. This phenomenon arises from the melt expulsion from the cavity. However, more pulses cleanse the cavity and drops of melt disappear from the exit hole. Thus, the increase in the number of pulses does not significantly affect the holes diameter but can affect the amount of the recast material. Fig. 2 also shows that the entrance holes are quite circular, while the exit ones have non-circular, irregular shape. However, circularity of exit holes could be improved by increasing the number of pulses. Thus, according to our results it is important to set suitable parameters that are in our case pulse energy at least 1.47 J and number of pulses 100.

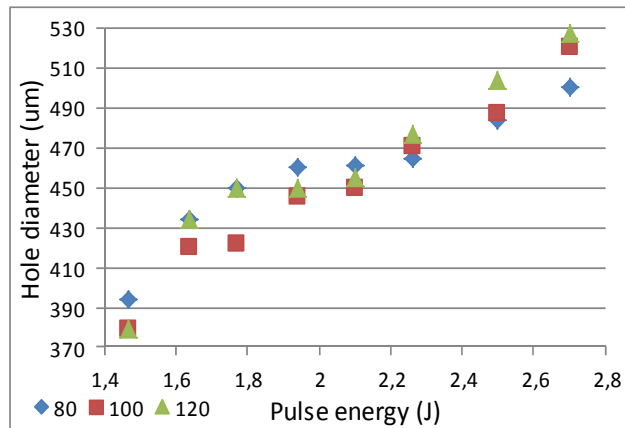


Fig. 1 The diameter of the holes drilled in alumina ceramics by Nd:YAG laser in dependence on pulse energy for number of pulses 80, 100 and 120 by keeping frequency 20 Hz and pulse length 0.5 ms.

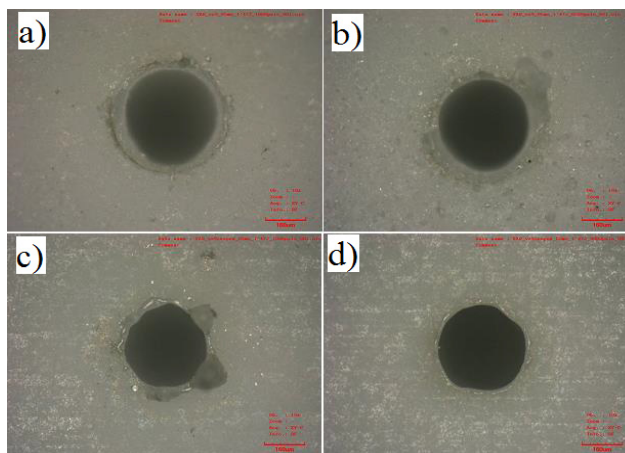


Fig. 2 Images of holes in alumina ceramics drilled by Nd:YAG laser obtained at process parameters of pulse length 0.5 ms, frequency 20 Hz and pulse energy 1.47 J: a) entrance, 20 pulses, b) entrance, 160 pulses, c) exit, 20 pulses, d) exit, 160 pulses. Magnification 240x, red scale 160 µm.

The study of the holes characteristics and geometry gave us the information about the influence of number of pulses and pulse energy on the drilling of alumina ceramics. After that a second experiment was held. At first, the holes diameter was investigated by increasing pulse length at six different charging voltages of the flash lamp. Corresponding pulse energies are given in Table 1. The entrance holes diameter as a function of pulse length for different charging voltages is shown in Fig. 3. The holes diameter goes up with increasing pulse length, and higher charging voltage also leads to the rise of the holes diameter for each pulse length. Thus, for one value of pulse length higher charging voltage causing higher power leads to the rise of the holes diameter. Consequently, with given laser configuration and theoretical spot diameter it was possible to achieve desired holes formation with diameters in the range from 350 µm to 600 µm by controlling the laser parameters. Similar results presented Kacar *et al.* 2009 [9] and Hanon *et al.* 2012 [6] who determined that holes diameter increased with pulse length and peak power. In addition, similar results can be obtained also for different materials. Petronic *et al.* 2010 drilled Ni-based superalloy NIMONIC 263 with two different thicknesses and reported that the diameter increases with increasing pulse length and decreases with increasing frequency [14].

Images of the holes generated by Nd:YAG laser using charging voltages of flash lamp 250 V and 280 V are displayed in Fig. 4 and Fig. 5. Each figure includes entrance and exit holes created by laser radiation with different pulse lengths. These figures confirm that increase in the pulse length and thus also pulse energy leads to enlarging of the hole. Longer pulse lengths also improve the exit holes quality as the hole is becoming more circular. From Fig. 4 and Fig. 5 it is evident that re-solidification of the melt occurred around the holes entrance. Drops of melt are also

visible at the edge of exit holes. Some holes could be even partially closed by the re-solidified melt (Fig. 4b). This phenomenon has its origin in the melt erosion of the holes sidewalls induced by the high pressure of vapour located nearby the material surface within irradiation that press the melted material up and away from the hole [15]. However, these imperfections can be reduced by using longer pulses and higher energies. From our observations it can be concluded that relatively long pulses (1 ms) with pulse energy 3,4 J and energy densities above 1 kJ/cm² are the right parameters for alumina drilling by Nd:YAG laser.

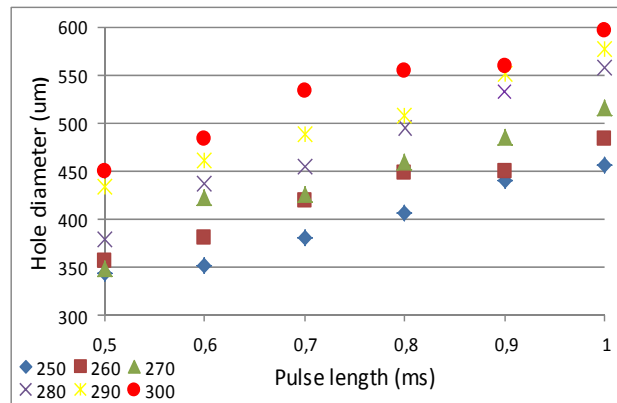


Fig. 3 The entrance diameter of the holes drilled in alumina ceramics by Nd:YAG laser in dependence on pulse length for six charging voltages in the range from 250 V to 300 V by keeping frequency 20 Hz

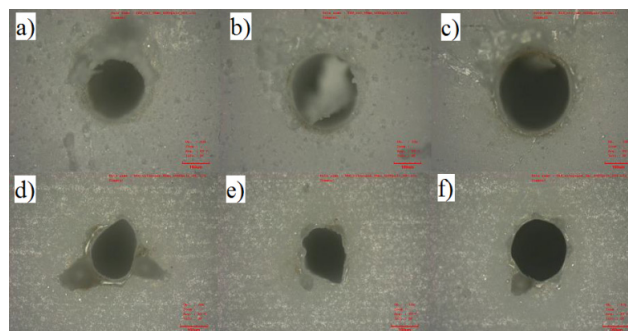


Fig. 4 Images of the holes in alumina ceramics drilled by Nd:YAG laser obtained at process parameters of frequency 20 Hz, charging voltage 250 V and number of pulses 120: a) pulse length 0.6 ms, pulse energy 1.37 J, entrance, b) pulse length 0.8 ms, pulse energy 1.9 J, entrance c) pulse length 1 ms, pulse energy 2.4 J, entrance, d) pulse length 0.6 ms, pulse energy 1.37 J, exit, e) pulse length 0.8 ms, pulse energy 1.9 J, exit, f) pulse length 1 ms, pulse energy 2.4 J, exit. Magnification 240x, red scale 160 µm.

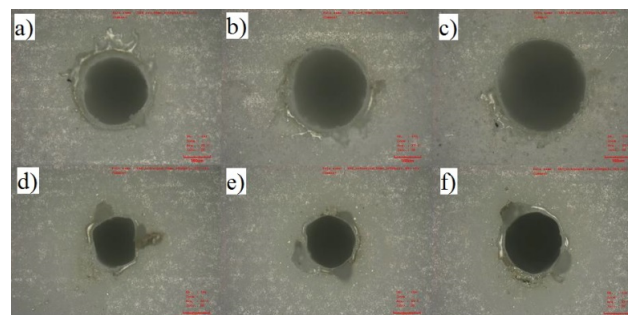


Fig. 5 Images of the holes in alumina ceramics drilled by Nd:YAG laser obtained at process parameters of frequency 20 Hz, charging voltage 280 V and number of pulses 120: a) pulse length 0.6 ms, pulse energy 1.84 J, entrance, b) pulse length 0.8 ms, pulse energy 2.64 J, entrance c) pulse length 1 ms, pulse energy 3.4 J, entrance, d) pulse length 0.6 ms, pulse energy 1.84 J, exit, e) pulse length 0.8 ms, pulse energy 2.64 J, exit, f) pulse length 1 ms, pulse energy 3.4 J, exit. Magnification 240x, red scale 160 µm.

3.2 Ceramics drilling using QCW fiber laser

QCW fiber laser was the second laser used to drill alumina ceramics. The holes diameter was investigated in dependence on pulse energy, peak power, pulse length and number of pulses. The dependence of the holes diameter on pulse length is depicted in Fig. 6. It is evident that the holes diameter is lowest for pulse length 0.8 ms. The figure also shows that the hole diameter goes up with increasing peak power for each pulse length. In order to get more information about the holes, the entrance and exit diameters were examined in dependence on pulse energy. It was observed that the exit diameter increases with increasing pulse energy although it was always smaller than the entrance one. Furthermore, a rise of the entrance diameter is detected with increasing pulse energy for each analysed pulse length. Thus, using different parameters it is possible to create holes with entrance diameters in the range from 133 μm to 266 μm .

Images of the entrance and exit holes drilled by laser radiation with pulse lengths 0.6 ms and 1 ms are displayed in Fig. 7 and Fig. 8. Each figure is specific for certain pulse length and increasing series of peak powers. The entrance holes are quite circular, but a small amount of the melt is visible around the holes. On the contrary, the exit holes are not circular and the melt is evident there too. The entrance and exit holes circularity can be improved using higher peak powers, as they deliver high energy radiation that transports the melted material further from the hole and does not allow it to accumulate. It can be said that the amount of melt presented at the edges of entrance and exit holes is lowered for higher peak powers too, since the increase in laser power leads to increase in thermal energy which causes better material removal in the whole cross-section of the hole. This explanation is in concordance with the results acquired also by Biswas *et al.* 2010 [16] and Bharatish *et al.* 2013 [11]. Therefore, according to these statements and our observations high peak powers at least 1 kW are adequate for alumina drilling by fiber laser. In addition, the amount of the melt is also reduced for shorter pulses so pulses 0.5 ms and 0.6 ms are optimum pulse lengths. Mutlu *et al.* 2009 [17] and Ng and Li 2001 [7] who studied the drilling of ceramic samples and the effect of laser parameters on the process also reported similar results. For example Ng and Li suggested that the holes circularity was the best when drilling was performed at shorter pulse length and higher peak power.

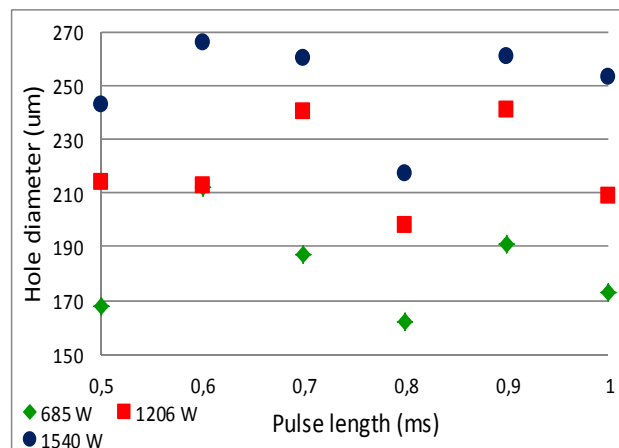


Fig. 6 The entrance diameter of the holes drilled in alumina ceramics by QCW fiber laser in dependence on pulse length for three peak powers by keeping frequency 50 Hz and number of pulses 100

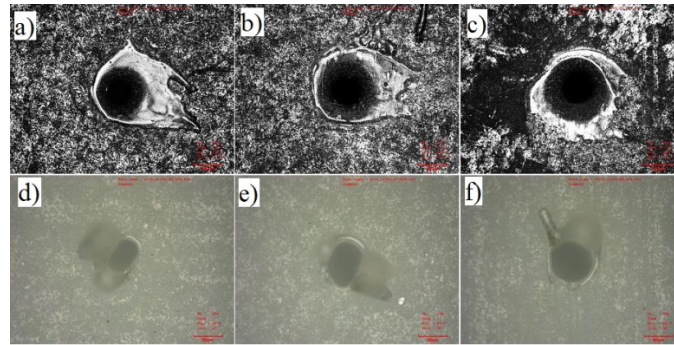


Fig. 7 Images of entrance and exit holes in alumina ceramics drilled by QCW laser obtained at process parameters of pulse length 0.6 ms, frequency 50 Hz: a) peak power 685 W, pulse energy 0.41 J, entrance, b) peak power 1027 W, pulse energy 0.62 J, entrance, c) peak power 1374 W, pulse energy 0.82 J, entrance, d) peak power 685 W, pulse energy 0.41 J, exit, e) peak power 1027 W, pulse energy 0.62 J, exit, f) peak power 1374 W, pulse energy 0.82 J, exit. Magnification 240x, red scale 160 μm .

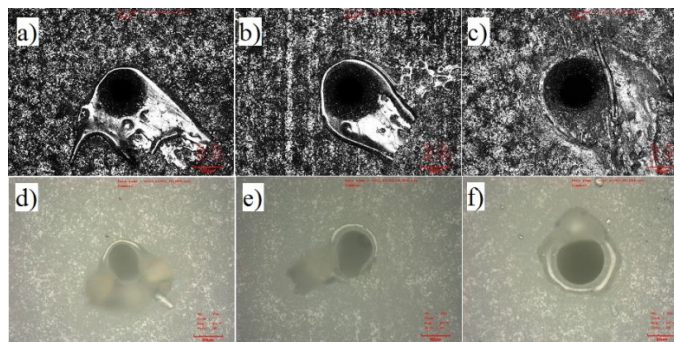


Fig. 8 Images of entrance and exit holes in alumina ceramics drilled by QCW laser and obtained at process parameters of pulse length 1 ms, frequency 50 Hz: a) peak power 685 W, pulse energy 0.68 J, entrance, b) peak power 1027 W, pulse energy 1.02 J, entrance, c) peak power 1374 W, pulse energy 1.37 J, entrance, d) peak power 685 W, pulse energy 0.68 J, exit, e) peak power 1027 W, pulse energy 1.02 J, exit, f) peak power 1374 W, pulse energy 1.37 J, exit. Magnification 240x, red scale 160 μm .

Using Nd:YAG and QCW fiber laser complete holes were drilled by setting a large range of lasers parameters. A gradual increase of the holes diameter was detected due to increasing energy applied to the sample surface. The holes diameters also seem to be dependent on the pulse length and peak power whereas the hole circularity can be improved using high number of pulses. Our results can be useful for practitioners in industry. According to their specific requirements for the drilled holes dimensions and quality they can choose optimum parameters suitable for given application. If the smaller diameter and the high circularity are needed, the short pulses and high peak powers of QCW fiber laser should be settled. If the larger diameter and good circularity are requested, Nd:YAG laser with longer pulse lengths and energy density above 1 kJ/cm^2 should be used.

4. Conclusion

In this paper drilling of 2 mm thick alumina ceramics was studied in dependence on laser wavelength, pulse energy, peak power and number of pulses. The process was performed using Nd:YAG and QCW fiber laser. The laser drilled holes characteristics (holes dimensions, circularity) were analysed and the influence of process parameters was determined. Created holes and their geometry were observed and evaluated using scanning confocal microscope.

Both lasers ensure formation of complete holes in most cases with recast layer surrounding the entrance hole. Drops of melt are visible at the edges of the exit hole as a result of incomplete ejection of the material from the cavity, which remains attached to the hole margins. Analysis of the holes reveals that the entrance diameter was always larger than exit, thus the holes were positively tapered. The entrance holes were also wider than the laser spot diameter.

The results show that it is possible to control the holes dimensions by changing lasers and their parameters. It was possible to create holes with diameters in the range from 350 μm to 600 μm using Nd:YAG laser and from 133 μm to 266 μm using fiber laser. It is obvious that fiber laser ensures formation of narrower holes due to its small spot and better beam quality together with high power and energy densities. The holes diameter can be also controlled by setting the laser parameters, e. g. pulse length pulse energy and peak power. Both entrance and exit holes diameters go up proportionally with the pulse length and pulse energy for Nd:YAG laser. Consequently, the optimum parameters for this laser were selected relatively longer pulse (1ms) as good circularity, and less amount of dross was obtained, and higher energies with corresponding energy densities around 1 kJ/cm^2 leading to formation of hole with better quality using these parameters. We can also conclude that a bigger number of pulses ensures getting better holes circularity. On the other hand, for fiber laser it was detected that relatively shorter pulses (0.5 ms and 0.6 ms), high peak power (1 kW) and high energy density (around 10 kJ/cm^2) are satisfactory for drilling as they assured good holes circularity and less amount of melt.

Acknowledgement

The authors gratefully acknowledge the support by the projects LO1305 and LTT17006 of the Ministry of Education, Youth and Sports of the Czech Republic and the project IGA_PrF_2017_005.

References

- [1] Preusch, F., Adelman, B., Hellmann, R. (2014). Micromachining of AlN and Al₂O₃ using fiber laser, *Micromachines*, Vol. 5, No. 4, 1051-1060, doi: [10.3390/mi5041051](https://doi.org/10.3390/mi5041051).
- [2] Samant, A.N., Dahotre, N.B. (2008). Computational predictions in single-dimensional laser machining of alumina, *International Journal of Machine Tools and Manufacture*, Vol. 48, No. 12-13, 1345-1353, doi: [10.1016/j.ijmactools.2008.05.004](https://doi.org/10.1016/j.ijmactools.2008.05.004).
- [3] Kim, S.H., Sohn, I.-B., Jeong, S. (2009). Ablation characteristics of aluminum oxide and nitride ceramics during femtosecond laser micromachining, *Applied Surface Science*, Vol. 255, No. 24, 9717-9720, doi: [10.1016/j.apsusc.2009.04.058](https://doi.org/10.1016/j.apsusc.2009.04.058).
- [4] Chang, C.-W., Kuo, C.-P. (2007). An investigation of laser-assisted machining of Al₂O₃ ceramics planning, *International Journal of Machine Tools and Manufacture*, Vol. 47, No. 3-4, 452-461, doi: [10.1016/j.ijmactools.2006.06.010](https://doi.org/10.1016/j.ijmactools.2006.06.010).
- [5] Saloniitis, K., Stournaras, A., Tsoukantas, G., Stavropoulos, P., Chryssolouris, G. (2007). A theoretical and experimental investigation on limitations of pulsed laser drilling, *Journal of Materials Processing Technology*, Vol. 183, No. 1, 96-103, doi: [10.1016/j.jmatprotec.2006.09.031](https://doi.org/10.1016/j.jmatprotec.2006.09.031).
- [6] Hanon, M.M., Akman, E., Genc Oztoprak, B., Gunes, M., Taha, Z.A., Hajim, K.I., Kacar, E., Gundogdu, O., Demir, A. (2012). Experimental and theoretical investigation of the drilling of alumina ceramic using Nd: YAG pulsed laser, *Optics & Laser Technology*, Vol. 44, No. 4, 913-922, doi: [10.1016/j.optlastec.2011.11.010](https://doi.org/10.1016/j.optlastec.2011.11.010).
- [7] Ng, G.K.L., Li, L. (2001). The effect of laser peak power and pulse width on the hole geometry repeatability in laser percussion drilling, *Optics & Laser Technology*, Vol. 33, No. 6, 393-402, doi: [10.1016/S0030-3992\(01\)00048-2](https://doi.org/10.1016/S0030-3992(01)00048-2).
- [8] Sibalija, T.V., Petronic, S.Z., Majstorovic, V.D., Prokic-Cvetkovic, R., Milosavljevic, A. (2011). Multi-response design of Nd: YAG laser drilling of Ni-based superalloy sheets using Taguchi's quality loss function, multivariate statistical methods and artificial intelligence, *The International Journal of Advanced Manufacturing Technology*, Vol. 54, No. 5-8, 537-552, doi: [10.1007/s00170-010-2945-3](https://doi.org/10.1007/s00170-010-2945-3).
- [9] Kacar, E., Mutlu, M., Akman, E., Demir, A., Candan, L., Canel, T., Gunay, V., Sinmazcelik, T. (2009). Characterization of the drilling alumina ceramic using Nd: YAG pulsed laser, *Journal of Materials Processing Technology*, Vol. 209, No. 4, 2008-2014, doi: [10.1016/j.jmatprotec.2008.04.049](https://doi.org/10.1016/j.jmatprotec.2008.04.049).
- [10] Nedialkov, N.N., Atanasov, P.A., Sawczak, M., Sliwinski, G. (2003). Ablation of ceramics with ultraviolet, visible and infrared nanosecond laser pulses, In: *Proceedings of XIV International Symposium on Gas Flow, Chemical Lasers, and High-Power Lasers*, Wroclow, Poland, 703-708, doi: [10.1117/12.515847](https://doi.org/10.1117/12.515847).
- [11] Bharatish, A., Narasimha Murthy, H.N., Anand, B., Madhusoodana, C.D., Praveena, G.S., Krishna, M. (2013). Characterization of the hole circularity and heat affected zone in pulsed CO₂ laser drilling of alumina ceramics, *Optics & Laser Technology*, Vol. 53, 22-32, doi: [10.1016/j.optlastec.2013.04.010](https://doi.org/10.1016/j.optlastec.2013.04.010).
- [12] Kononenko, T.V., Garnov, S.V., Klimentov, S.M., Konov, V.I., Loubnin, E.N., Dausinger, F., Raiber, A., Taut, C. (1997). Laser ablation of metals and ceramics in picosecond-nanosecond pulse width in the presence of different ambient atmospheres, *Applied Surface Science*, Vol. 109-110, 48-51, doi: [10.1016/S0169-4332\(96\)00905-1](https://doi.org/10.1016/S0169-4332(96)00905-1).
- [13] Mendes, M., Sarrafi, R., Schoenly, J., Vangemert, R. (2015). Fiber laser micromachining in high-volume manufacturing, In: *Proceedings of LPM2014 - the 15th International Symposium on Laser Precision Microfabrication*, Vilnius, Lithuania.

- [14] Petronić, S., Milosavljević, A., Radaković, Z., Drobnjak, P., Grujić, I. (2010). Analysis of geometrical characteristics of pulsed Nd: YAG laser drilled holes in superalloy NIMONIC 263 sheets, *Tehnički Vjesnik – Technical Gazette*, Vol. 17, No. 1, 61-66.
- [15] Tunna, L., O'Neill, W., Khan, A., Sutcliffe, C. (2005). Analysis of laser micro drilled holes through aluminium for micro-manufacturing applications, *Optics and Lasers in Engineering*, Vol. 43, No. 9, 937-950, [doi: 10.1016/j.optlaseng.2004.11.001](https://doi.org/10.1016/j.optlaseng.2004.11.001).
- [16] Biswas, R., Kuar, A.S., Biswas, S.K., Mitra, S. (2010). Characterization of hole circularity in pulsed Nd: YAG laser micro-drilling of TiN-Al₂O₃ composites, *The International Journal of Advanced Manufacturing Technology*, Vol. 51, No. 9-12, 983-994, [doi: 10.1007/s00170-010-2691-6](https://doi.org/10.1007/s00170-010-2691-6).
- [17] Mutlu, M., Kacar, E., Akman, E., Akkan, C.K., Demir, P., Demir, A. (2009). Effects of the laser wavelength on drilling process of ceramic using Nd: YAG laser, *Journal of Laser Micro/Nanoengineering*, Vol. 4, No. 2, 84-88, [doi: 10.2961/jlmn.2009.02.0002](https://doi.org/10.2961/jlmn.2009.02.0002).

Calendar of events

- 14th International Conference on Functional Energy Materials, Dallas, Texas, USA, December 6-7, 2017.
- IEEE International Conference on Industrial Engineering and Engineering Management, Singapore, December 10-13, 2017.
- The 7th Advanced Functional Materials and Devices – SCOPUS, EI Compendex, Havana, Cuba, December 13-15, 2017.
- 11th International Conference on Data Mining, Computers, Communication & Industrial Applications, Kuala Lumpur, Malaysia, December 14-15, 2017.
- 10th International Conference on Advances in Mechanical Design and Manufacturing, Giza, Egypt, December 18-20, 2017.
- 8th International Conference on Innovative Trends in Engineering, Technology, Computers and Applied Sciences Conference, Tokyo, Japan, December 23-24, 2017.
- 9th International Conference on Mechatronics and Manufacturing, Phuket Island, Thailand, January 27-29, 2018.
- The 7th International Conference on Manufacturing Engineering and Process, Barcelona, Spain, February 5-7, 2018.
- 9th International Conference on Mechanical and Intelligent Manufacturing Technologies, February 10-13, 2018, Cape Town, South Africa.
- International Conference on Robotics and Intelligent System, Amsterdam, Netherlands, February 21-23, 2018.
- 7th International Conference on Industrial Technology and Management, Oxford, UK, March 7-9, 2018.
- The 8th International Conference on Key Engineering Materials, Osaka, Japan, March 16-18, 2018.
- 2nd International Conference on 3D Printing Technology and Innovations, London, UK, March 19-20, 2018.
- The 2018 International Conference on Robotics and Intelligent Control, Nagoya, Japan, April 27-30, 2018.
- 2018 The 5th International Conference on Manufacturing and Industrial Technologies, Hefei, China, May 18-21, 2018.
- The 3rd International Conference on Advanced Functional Materials, San Francisco, USA, August 3-5, 2018.
- 3rd International Conference on Material Engineering and Smart Materials, Okinawa, Japan, August 11-13, 2018.

This page intentionally left blank.

Notes for contributors

General

Articles submitted to the *APEM journal* should be original and unpublished contributions and should not be under consideration for any other publication at the same time. Manuscript should be written in English. Responsibility for the contents of the paper rests upon the authors and not upon the editors or the publisher. Authors of submitted papers automatically accept a copyright transfer to *Production Engineering Institute, University of Maribor*. For most up-to-date information on publishing procedure please see the *APEM journal* homepage apem-journal.org.

Submission of papers

A submission must include the corresponding author's complete name, affiliation, address, phone and fax numbers, and e-mail address. All papers for consideration by *Advances in Production Engineering & Management* should be submitted by e-mail to the journal Editor-in-Chief:

Miran Brezocnik, Editor-in-Chief
UNIVERSITY OF MARIBOR
Faculty of Mechanical Engineering
Production Engineering Institute
Smetanova ulica 17, SI – 2000 Maribor
Slovenia, European Union
E-mail: editor@apem-journal.org

Manuscript preparation

Manuscript should be prepared in *Microsoft Word 2007* (or higher version) word processor. *Word .docx* format is required. Papers on A4 format, single-spaced, typed in one column, using body text font size of 11 pt, should not exceed 12 pages, including abstract, keywords, body text, figures, tables, acknowledgements (if any), references, and appendices (if any). The title of the paper, authors' names, affiliations and headings of the body text should be in *Calibri* font. Body text, figures and tables captions have to be written in *Cambria* font. Mathematical equations and expressions must be set in *Microsoft Word Equation Editor* and written in *Cambria Math* font. For detail instructions on manuscript preparation please see instruction for authors in the *APEM journal* homepage apem-journal.org.

The review process

Every manuscript submitted for possible publication in the *APEM journal* is first briefly reviewed by the editor for general suitability for the journal. Notification of successful submission is sent. After initial screening, and checking by a special plagiarism detection tool, the manuscript is passed on to at least two referees. A double-blind peer review process ensures the content's validity and relevance. Optionally, authors are invited to suggest up to three well-respected experts in the field discussed in the article who might act as reviewers. The review process can take up to eight weeks. Based on the comments of the referees, the editor will take a decision about the paper. The following decisions can be made: accepting the paper, reconsidering the paper after changes, or rejecting the paper. Accepted papers may not be offered elsewhere for publication. The editor may, in some circumstances, vary this process at his discretion.

Proofs

Proofs will be sent to the corresponding author and should be returned within 3 days of receipt. Corrections should be restricted to typesetting errors and minor changes.

Offprints

An e-offprint, i.e., a PDF version of the published article, will be sent by e-mail to the corresponding author. Additionally, one complete copy of the journal will be sent free of charge to the corresponding author of the published article.

APEM

journal

Advances in Production Engineering & Management

Production Engineering Institute (PEI)
University of Maribor
APEM homepage: apem-journal.org

Volume 12 | Number 4 | December 2017 | pp 301-424

Contents

Scope and topics	304
A general approach to optimize disassembly sequence planning based on disassembly network: A case study from automotive industry Yu, B.; Wu, E.; Chen, C.; Yang, Y.; Yao, B.Z.; Lin, Q.	305
An integrated generalized discriminant analysis method and chemical reaction support vector machine model (GDA-CRSVM) for bearing fault diagnosis Nguyen, V.H.; Cheng, J.S.; Thai, V.T.	321
Improving workforce scheduling using artificial neural networks model Simeunović, N.; Kamenko, I.; Bugarski, V.; Jovanović, M.; Lalić, B.	337
Infrared temperature measurement and increasing infrared measurement accuracy in the context of machining process Masoudi, S.; Gholami, M.A.; Janghorban Lariche, M.; Vafadar, A.	353
Container assignment optimization considering overlapping amount and operation distance in rail-road transshipment terminal Wang, L.; Zhu, X.; Xie, Z.	363
Work sampling for the production development: A case study of a supplier in European automotive industry Martinec, T.; Škec, S.; Savšek, T.; Perišić, M.M.	375
An overview and evaluation of quality-improvement methods from the manufacturing and supply-chain perspective Radej, B.; Drnovšek, J.; Begeš, G.	388
Vehicle routing optimization with multiple fuzzy time windows based on improved wolf pack algorithm Cao, Q.K.; Yang, K.W.; Ren, X.Y.	401
Laser drilling of alumina ceramics using solid state Nd:YAG laser and QCW fiber laser: Effect of process parameters on the hole geometry Rihakova, L.; Chmelickova, H.	412
Calendar of events	421
Notes for contributors	423

Copyright © 2017 PEI. All rights reserved.



apem-journal.org